

SoftMatterLecture

Frank Cichos, Ralf Seidel

2026-05-09

Abstract

Table of contents

Index	10
I Course Info	11
Course Information	12
Lecture Schedule	12
Exercise Schedule	12
Seminar Schedule	12
Instructors	13
Lectures	13
Seminar	13
Exercise	13
Resources	14
Books	15
Exercises and Exam	16
Exercises	16
Seminars	16
Exam	16
II Lecture 1	17
1 Introduction	18
2 Thermodynamics and Statistical Physics Revisited	19
2.2 Thermodynamics	19
2.2.1 Fundamental Quantities	19
2.2.2 Laws of Thermodynamics	21

III Lecture 2	23
3 Statistical Physics Definitions	24
3.3 Entropy	24
3.3.1 Entropy Definition by Boltzmann	24
3.3.2 Shannon Entropy	27
3.4 Boltzmann Distribution	29
3.4.1 Mean Energy	31
3.4.2 Free Energy	31
3.4.3 Deriving the Boltzmann Distribution	32
IV Lecture 3	36
4 Equipartition	37
4.1 When a Macrostate is a Microstate	43
5 Chemical Potential	45
5.1 Phase equilibria	47
5.2 Chemical equilibria	48
V Lecture 4	53
6 Osmotic Pressure	54
6.0.1 Shape of red blood cells	56
6.0.2 Reverse Osmosis	56
7 Gibbs Distribution	58
VI Lecture 5	61
8 Phase Transitions	62
8.1 Liquid-Liquid Unmixing	64
VII Lecture 6	72
9 Kinetics of Liquid–Liquid Unmixing	73
9.3.2 Spinodal decomposition	74
9.3.3 Nucleation	77

VIII Lecture 7	84
10 Solid–Liquid Phase Transitions	85
10.0.1 Kinetics of the Liquid–Solid Phase Transition	86
10.0.2 Heterogeneous Nucleation	92
10.0.3 Classification of phase transitions	97
11 Forces and Interactions in Soft Matter	100
11.1 Pairwise interaction energy	101
11.2 Cohesive energy of a liquid	101
11.3 Coulomb forces, charge–charge interactions	102
11.3.1 Charge–charge interactions	103
11.3.2 Born energy of solvation	104
11.3.3 Interactions involving polar molecules	107
11.3.4 Ion–dipole interaction	110
IX Lecture 8	114
12 Forces and Interactions in Soft Matter	115
12.0.4 Interactions involving polar molecules	115
12.0.5 Ion–Dipole interaction	119
12.0.6 Dipole-Dipole Interactions	123
12.0.7 Rotating Dipoles, angle averaged Potential	124
12.0.8 Dipole-Dipole interaction with rotating dipoles	125
12.0.9 Interactions involving polarizability	126
12.0.10 Ion-Induced Dipole Interaction	127
12.0.11 Polarizability of polar molecules	129
12.0.12 Dipole Induced Dipole	129
X Lecture 9	130
13 Electric Double Layer	131
13.1 Charges surfaces in solution, no salt	131
13.2 Poisson-Boltzmann equation	132
13.2.1 Example	135
XI Lecture 10	142
14 van der Waals Interactions	143
14.1 Dispersion Interaction	144

XII Lecture 11	150
15 van der Waals Interactions	151
15.1 McLachlan Theory	151
15.1.1 Frequency Dependent Polarizability	152
15.1.2 Optical Frequency Contribution	154
16 van der Waals Interaction	155
16.1 Interaction Between Macroscopic Bodies	155
16.2 Hamaker Constant	159
XIII Lecture 12	164
17 van der Waals Interaction	165
17.1 Lifshitz Theory	165
XIV Lecture 13	168
18 Depletion Forces	169
18.1 Depletion force between two plates	169
18.2 Depletion force between two spheres	173
18.3 General description	176
XV Lecture 14	178
19 Depletion Forces	179
19.1 Depletion force between two plates	179
19.2 Depletion force between two spheres	183
19.3 General description	186
20 Flows and Transport in Liquids	188
20.1 Translational Diffusion	188
20.1.1 Diffusion in External Potential - Smoluchowski Equation	191
20.1.2 Application: Fluorescence Recovery after Photobleaching	194
20.2 Rotational Diffusion	199
20.2.1 NMR Spectroscopy/Dielectric Relaxation	201

XVI Lecture 16	203
21 Brownian Motion	204
21.1 Langevin Theory	205
21.1.1 Langevin Equation	205
21.2 Fluctuation Dissipation Theorem	212
21.2.1 Damped Driven Harmonic Oscillator	212
XVII Lecture 17	217
22 Hydrodynamics	218
22.1 Navier Stokes Equation	219
22.1.1 Viscous Stress Tensor	223
22.1.2 Mechanical Stress Tensor	226
XVIII Lecture 18	228
23 Reynolds Number	229
23.1 Stokes Equation	232
23.2 Solutions of the Stokes Equation	232
23.2.1 Couette Flow - Shear Driven Flow	234
23.2.2 Poiseuille Flow - Pressure Driven Flow	236
24 Boundary Hydrodynamics	238
24.1 Thermo-osmosis	240
XIX Lecture 19	245
25 Electro-osmosis	246
26 Polymers	247
26.1 Freely Jointed Chain	247
26.1.1 Mean-squared end-to-end distance of a FJC	248
26.1.2 Distribution of the end-to-end distances	250
26.1.3 Radius of gyration	251
26.2 Force-extension behavior of a FJC	253
XX Lecture 20	254
27 Ideal Polymer Models	255
27.1 Freely Rotating Chain	256

27.2 Gaussian Chain	256
27.3 Wormlike Chain	259
XXI Lecture 22	265
28 Real Polymers	266
28.1 Mayer f-function and excluded volume	266
28.1.1 Interaction potential	267
28.1.2 Probability distribution	268
28.1.3 Mayer f-function	270
28.1.4 Polymer chain as a real gas	271
28.2 Non-spherical segments and Free energy of interaction of a real chain	273
28.3 Solvent Classification	275
28.4 Flory theory (in a good solvent)	275
28.5 Flory Theory (in all solvents)	278
28.6 Temperature dependence of the chain size	279
XXI Lecture 23	281
29 Scattering Techniques for Polymer Conformation	282
29.1 Form Factor	282
29.2 Radius of Gyration	285
29.3 Debye Function	286
30 Viscoelasticity	290
30.1 Models for Viscoelastic behavior	293
30.2 Maxwell Model	293
30.3 Kelvin-Voigt	293
30.4 Standard Model	294
XXII Lecture 24	295
31 Viscoelasticity	296
31.1 Maxwell Model	296
31.2 Stress Relaxation after Step Strain	297
31.2.1 Boltzmann Superposition	299
31.3 Steady Shear	300
31.4 Creep and Creep Recovery	301
31.4.1 Creep	301
31.4.2 Creep Recovery	304

31.5 Oscillatory Shear	305
31.5.1 Complex shear modulus of the Maxwell model	308
31.5.2 Complex shear modulus of the Kelvin-Voigt model	309
XXIV Lecture 25	311
32 Dynamics of Polymers	312
32.1 Diffusion of a Single Polymer Chain	312
32.1.1 Rouse Model	313
32.1.2 Zimm Model	314
32.2 Intrinsic viscosity of polymer solutions	315
32.2.1 Affine Deformation and Entropy	316
32.3 Relaxation Modes of a Polymer	320
32.3.1 Rouse modes	321
32.3.2 Zimm modes	325
XXV Lecture 26	329
33 Semidilute Polymer Solutions	330
33.0.1 Stress Relaxation	333
XXVI Lecture 27	335
34 Liquid Crystals	336
XXVII Lecture X	338
35 Forces and Interactions in Soft Matter	339
35.0.1 Coulomb forces, charge-charge interactions	340
35.0.2 van der Waals interactions	344
35.0.3 Depletion Forces	344
36 Flows and Transport in Liquids	348
36.0.1 Diffusion and Brownian Motion	348
36.0.2 Smoluchowski-diffusion in an external potential	350
36.0.3 Hydrodynamics	355

Index

Part I

Course Info

Course Information

Lecture Schedule

- Wednesday: 13:15 - 14:45 Uhr, SR 224
- Thursday: 09:15 - 10:45 Uhr, SR 224

Exercise Schedule

- Tuesday: 9:15 - 10:45 Uhr, SR 221 (Will start on **24. October 2023**)

Seminar Schedule

- Tuesday: 13:15 - 14:45 Uhr, SR 221 (Will start on **24. October 2023**)

The lectures will be supported by a seminar where current topics of soft matter are discussed by the students in the form of seminar talks.

Instructors

Lectures

Email: cichos@physik.uni-leipzig.de

- Prof. Dr. Frank Cichos

- Linnéstr. 5, 04103 Leipzig
- Office: 322
- Phone: +0341 97 32571

Seminar

Email: diptabrata.paul@physik.uni-leipzig.de

- Dr. Diptabrata Paul

- Linnéstr. 5, 04103 Leipzig
- Office: 178a
- Phone: +0341 97 32570

Exercise

Email: anton@physik.uni-leipzig.de

- Dr. Markus Anton

- Linnéstr. 5, 04103 Leipzig
- Office:
- Phone: +0341 97 32575

Resources

The script with the lecture contents will be published on this website. Additional information may also be found on the group's [Teaching Pages](#).

All exercise sheets will be available on the [Teaching Pages](#).

All literature for the seminar will be available on the [Teaching Pages](#).

The presentation for the seminars will be available [here](#).

Books

There are several books available on the topic of Soft Matter. Many set their own focus. Here is a list of books useful for the lecture.

- Jacob N. Israelachvili: **Intermolecular and Surface Forces: With Applications to Colloidal and Biological Systems** (Academic Press)
- Rob Phillips, Jane Kondev, Julie Theriot: **Physical Biology of the Cell** (Garland Science)
- Richard A.L. Jones: **Soft Condensed Matter** (Oxford University Press)
- Michael Rubinstein, Ralph H. Colby: **Polymer Physics** (Oxford University Press)
- Jonathan Howard: **Mechanics of Motor Proteins and the Cytoskeleton** (Sinauer Associates)
- M. Doi and S.F. Edwards: **The Theory of Polymer Dynamics** (Oxford Academic Press)
- P.G. de Gennes and J. Prost: **The Physics of Liquid Crystals** (Oxford Academic Press)

In addition, we will make current literature from different journals available.

Exercises and Exam

Exercises

The first exercise will take place on **October 24**.

The first exercise sheet will be published on **October 19 online**.

The solutions to the exercise sheets have to be handed in before the lecture on Tuesday in the following week.

For every solved problem, **1 point** can be obtained.

Seminars

The seminar will start on **October 24, 2023**.

The registration for your talk in the seminar starts on **October 11, 2023, at 1 pm**.

At this time, a link for the registration will be provided here on the website.

Exam

Prerequisite for the admission to the examination are **50%** of the total points.

Examination: **180 min** written (knowledge + problem solving).

The final grade will be calculated from **66%** of the exam mark + **33%** seminar talk mark.

Part II

Lecture 1

1 Introduction

[Lecture Slides](#)

2 Thermodynamics and Statistical Physics Revisited

2.2 Thermodynamics

2.2.1 Fundamental Quantities

We can define different thermodynamic systems depending on their ability to exchange energy and particles with the environment.

A system is called *isolated* if it can neither exchange energy nor particles with its environment. This ensemble of particles is also called *micro-canonical*. The energy in such a system can not fluctuate. It is a *closed system* if it can exchange energy with the surrounding, i.e., a heat bath keeping it at a constant temperature. The ensemble of particles in such a system corresponds to a *canonical* ensemble. Energy can fluctuate. In case the system can also exchange particles, it is called an *open system* or *grand-canonical* ensemble.

A thermodynamic system can be defined by **state variables** p , V and/or T . **State functions** are useful to formulate the laws of thermodynamics. A state function is independent of how one arrived at that particular state. They are most often used to characterize an equilibrium state.

Note: State Function and State Variables

- State function is a function of state variables that depends only on the state of the system.
- State variables characterize the state of a system and are independent of how the system got there.

We will refer to a number of state functions during the course. Here is a list of the most useful ones:

- **Internal energy** U (state function):

State function. The total energy contained in a thermodynamic system. It is the energy necessary to create the system with the major components kinetic energy and potential energy.

$$U = Q + W \quad (2.1)$$

The internal energy can be changed by supplying heat or doing work on the system such that

$$dU = dQ - pdV \quad (2.2)$$

- **Enthalpy H** (state function):

The enthalpy H of a system is measuring the internal energy plus the product of volume and pressure.

$$H = U + pV \quad (2.3)$$

The enthalpy is especially useful for a system at constant pressure $p = \text{const.}$, i.e., for processes where the volume can not be controlled.

$$dH = dU + pdV + Vdp = \delta Q + Vdp \quad (2.4)$$

In this case the change in enthalpy of a system corresponds to the exchanged heat.

- **Entropy S** (state function):

The change of entropy of a system is given by

$$dS = \frac{\delta Q}{T}, \quad (2.5)$$

where T denotes the temperature and δQ the heat exchanged in a reversible process.

- **Free Energy G or F** (state function):

Free energies are useful for systems which can exchange energy with the environment but not particles. In such non-isolated systems we define the

Gibbs Free Energy

$$G = H - TS \quad (2.6)$$

for a system with constant pressure and

Helmholtz Free Energy

$$F = U - TS \quad (2.7)$$

for a system with constant volume. Both quantities are used to indicate in which direction physical or chemical processes proceed. After we have written down the two first laws of thermodynamics, we will have a look at a specific example.

2.2.2 Laws of Thermodynamics

2.2.2.1 First Law of Thermodynamics

The internal energy U is connected to the first law of thermodynamics:

$$dU = \delta Q + \delta W = \delta Q - pdV \quad (2.8)$$

which states, that the energy contained in a system can be changed by providing heat or performing mechanical work on the system. Here δQ and δW are no state functions. They characterize a process of delivering heat or performing mechanical work.

Note: First Law of Thermodynamics

- The internal energy of a system can only be changed by exchanging heat with the environment or by doing mechanical work on it (energy cannot appear or disappear).

2.2.2.2 Second Law of Thermodynamics

While the internal energy U may be fixed (i.e., $dU = 0$), the system may exist in different configurations (see, for example, an ideal gas with different arrangements of molecules). Such an isolated system will always evolve such that the change in entropy is positive or zero ($dS \geq 0$). This is equivalent to the formulation that the entropy becomes maximized.

Note: Second Law of Thermodynamics

- When an isolated system is left alone long enough it evolves to thermal equilibrium whose entropy is at least as great as before ($dS > 0$).

Example: Closed System in Contact with Reservoir

Look at the above figure of the closed systems (inner part) inside a temperature bath (reservoir). If we apply the 2nd Law of thermodynamics to reservoir and system we write down

$$dS_{\text{tot}} = dS_R + dS_S \geq 0. \quad (2.9)$$

The system may exchange energy with the reservoir and, thus, according to the 1st Law of thermodynamics we have

$$dU_R = TdS_R - pdV_R \quad (2.10)$$

with T being the constant temperature of the reservoir. We may transform this equation and insert it into the 2nd law to obtain:

$$dS_S + \frac{dU_R}{T} + \frac{p}{T}dV_R \geq 0. \quad (2.11)$$

Using $dU_R = -dU_S$ and $dV_R = -dV_S$ we can transform the equation for constant pressure and temperature to

$$dG = d(U_S + pV_S - TS_S) \leq 0. \quad (2.12)$$

This indicates the direction in which a closed system, that can exchange energy with a bath, develops according to the 2nd Law of thermodynamics.

If we bring a small system into thermal contact with a reservoir, which is in equilibrium at temperature T , then the reservoir will stay in equilibrium at the same temperature, but the small system will come to a new equilibrium, which minimizes the free energy.

Thus, in equilibrium the free energy reaches a minimum value. Free energy minimization does two things at the same time: It tries to minimize the internal energy/enthalpy as well as to maximize the entropy (due to the negative sign in front of the entropy term) of a non-isolated object. The free energy minimum is, thus, the optimal balance between the two extrema.

Part III

Lecture 2

3 Statistical Physics Definitions

The field of statistical physics uses approaches of statistics and probability theory to address physical problems. It considers large populations and derives expressions for the ensemble (or the macrostate) of a system from the microscopic states in the system.

```
import numpy as np
import matplotlib.pyplot as plt
from scipy.special import factorial as fac

%matplotlib inline
%config InlineBackend.figure_format = 'retina'

plt.rcParams.update({'font.size': 12,
                    'axes.titlesize': 18,
                    'axes.labelsize': 16,
                    'axes.labelpad': 14,
                    'lines.linewidth': 1,
                    'lines.markersize': 10,
                    'xtick.labelsize' : 16,
                    'ytick.labelsize' : 16,
                    'xtick.top' : True,
                    'xtick.direction' : 'in',
                    'ytick.right' : True,
                    'ytick.direction' : 'in',})
```

3.3 Entropy

3.3.1 Entropy Definition by Boltzmann

The term of entropy becomes very important in that context. It measures the number of different ways a system can be rearranged to yield the same macrostate. It is, thus, an indicator for the microscopic degeneracy of a macrostate. In this context the definition of entropy by **Boltzmann** is well known, i.e.,

$$S = k_B \ln(W) \quad (3.1)$$

where W is the number of microstates corresponding to a system's macrostate with energy E . Here $k_B = 1.38064852 \times 10^{-23} \text{ m}^2 \text{ kg s}^{-2} \text{ K}^{-1}$ is the Boltzmann constant. Below are two examples of how to use the formula for the calculation of the entropy.

Example: Entropy of an N letter word

SMP	PMS	MSP	MPS	SPM
SSS	PPP	MMM	MMP	MMS
⋮				

Figure 3.1: letters

Consider the number of states W of a word with N letters of M different characters. The letter can be arranged in

$$W = M^N \quad (3.2)$$

different ways such that the entropy is given by

$$S = N k_B \ln(M) = k_B \sum_1^N \ln(M) \quad (3.3)$$

which just tells that entropy is an additive quantity.

Example: Arrangement of molecules along a chain

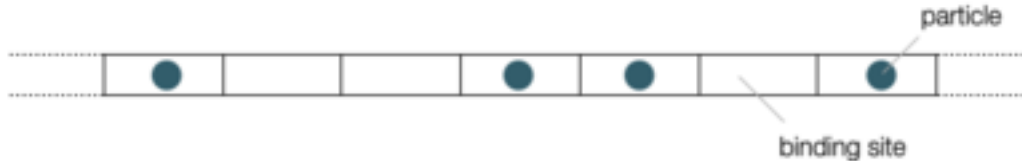


Figure 3.2: binding

We consider a linear molecules (perhaps a DNA) that has N binding sites for, e.g., proteins. N_p sites are occupied with a protein where the binding energy is equal for each site. The number of different ways in which the N_p proteins can be arranged on the N sites is given by the binomial coefficient

$$W(N_p; N) = \frac{N!}{N_p!(N - N_p)!}. \quad (3.4)$$

Therefore, the entropy is given by

$$S = k_B \ln \left(\frac{N!}{N_p!(N - N_p)!} \right) \quad (3.5)$$

which can be further simplified using the identity

$$\ln(N!) = \sum_{n=1}^N \ln(n) \quad (3.6)$$

and the *Stirling approximation*

$$\sum_{n=1}^N \ln(n) \approx \int_1^N \ln(x) dx \approx N \ln(N) - N. \quad (3.7)$$

This, finally, leads to

$$S = -k_B N [c \ln(c) + (1 - c) \ln(1 - c)] \quad (3.8)$$

with $c = N_p/N$ being the mean occupation of each site or the probability to find a state occupied.

Below you just find some Python code calculating the entropy as a function of “concentration” using the Stirling approximation and the original formula. You also recognize there, that the Stirling formula is not yet very good, since $N = 100$.

```
epsilon=1e-3
c=np.linspace(epsilon,1-epsilon,100);N=100
Np=np.arange(1,N)

def S(x):
    return(np.log(fac(N)/(fac(x)*fac(N-x))))
```

```

fig=plt.figure()
plt.ion()
plt.plot(c,-(c*np.log(c)+(1-c)*np.log(1-c)),'r-',label="Stirling")
plt.plot(Np/N,S(Np)/N,'k--',label="Original")
plt.xlabel("$c$")
plt.ylabel(r"$S [k_B]$")
plt.title("Accuracy of the Stirling Formula")
plt.tight_layout()
plt.legend()
plt.savefig("img/stirling.png")
plt.close(fig)

```

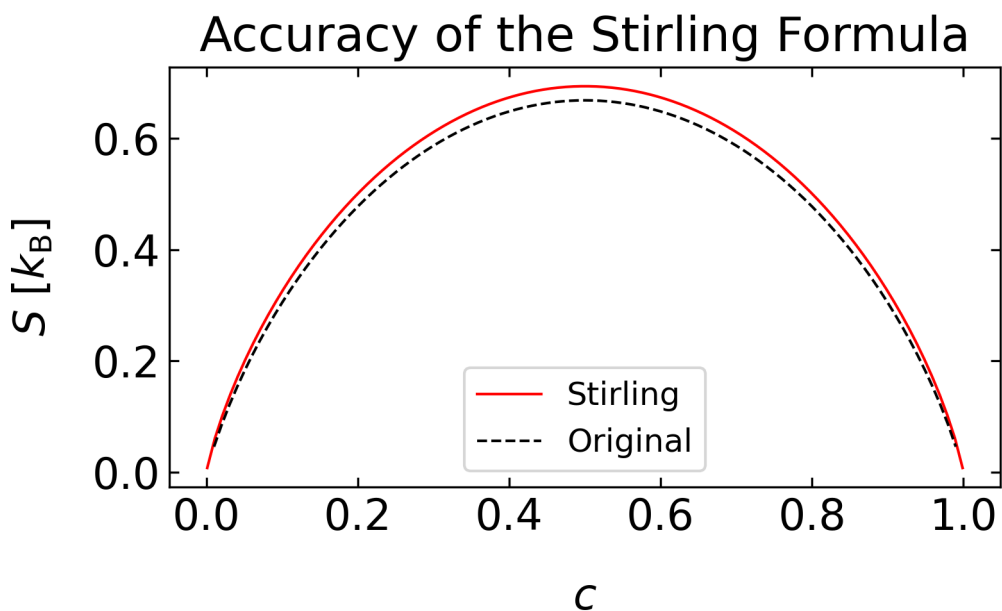


Figure 3.3: stirling

3.3.2 Shannon Entropy

A different access to entropy comes from the field of information theory and has been devised by Claude Shannon. Information theory is trying to mathematically assess the information content of a measurement facing uncertainty. It will turn out further below that this alternative description results in the Boltzmann distribution and effectively amounts to making a best guess about the probability distribution given some limited knowledge about the system such as the average energy.

The Shannon entropy is defined by

$$S(p_1, p_2, \dots, p_N) = S(\{p_i\}) = - \sum_{i=1}^N p_i \ln p_i \quad (3.9)$$

and relates to its thermodynamic version, the Gibbs entropy

$$S(\{p_i\}) = -k_B \sum_{i=1}^N p_i \ln p_i, \quad (3.10)$$

where p_i is the probability of the i th microstate (or outcome). The example below will show, that if only the normalization of the probability is known, maximization of the Shannon entropy will directly lead to an equal probability of events (uniform distribution). Later, we see that similar calculations can be done to yield the Boltzmann distribution.

Example: Uniform distribution

To figure out that the Shannon entropy is indeed delivering some useful measure, we will have a look at a measurement which has N outcomes (e.g., rolling a dice). We, of course, know that in this case all numbers of the dice have equal probability, but we can test this by maximizing the Shannon entropy as required by our thermodynamic considerations earlier.

To do so, we use the technique of Lagrange multipliers, which allows us to set a constraint while maximizing the entropy. This constraint is for this example, that

$$\sum_i^N p_i = 1 \quad (3.11)$$

i.e., that the probability is normalized to 1. With this constraint we maximize the entropy by adding an additional term with the constraint multiplied by the Lagrange multiplier λ :

$$S' = - \sum_i p_i \ln p_i - \lambda \left(\sum_i p_i - 1 \right). \quad (3.12)$$

We see, that if the probability is normalized to 1, we do not change the entropy. Our procedure is to find that set of probabilities p_i which maximizes this augmented entropy function.

The derivative of the augmented entropy with respect to λ yields the normalization condition, i.e.,

$$\frac{\partial S'}{\partial \lambda} = - \left(\sum_i p_i - 1 \right) \stackrel{!}{=} 0. \quad (3.13)$$

Differentiation with respect to the probabilities yields

$$\frac{\partial S'}{\partial p_i} = -\ln p_i - 1 - \lambda \stackrel{!}{=} 0 \quad (3.14)$$

which directly gives

$$p_i = e^{-1-\lambda}. \quad (3.15)$$

Together with the normalization condition we therefore obtain

$$\sum_{i=1}^N e^{-1-\lambda} = 1 \quad (3.16)$$

and since the exponent does not depend on i we find

$$e^{-1-\lambda} = \frac{1}{N} \quad (3.17)$$

or

$$p_i = \frac{1}{N} \quad (3.18)$$

which is the expected equal probability of finding one of the N outcomes.

3.4 Boltzmann Distribution

Our previous consideration of the state functions has shown, that thermal equilibrium is associated with a minimum in free energy. As the free energy consists of internal energy U (or enthalpy H) and an entropic term ($-TS$), we may understand this minimization as a competition between the minimization of the internal energy and a maximization of the entropy (since it is $-TS$). The figure below illustrates this competition for a gas in the gravity field.

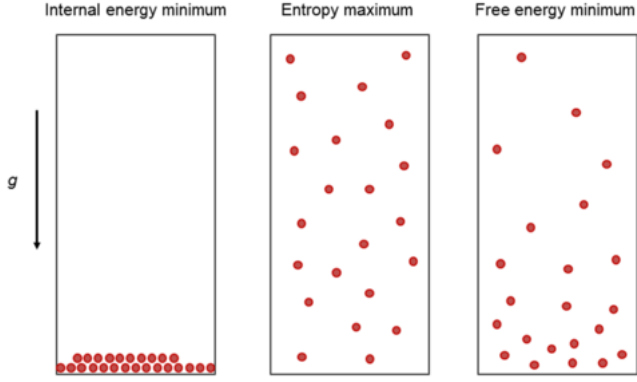


Figure 3.4: entropy

The internal energy minimization yields just a condensed layer at the bottom of the container, while the entropy maximization will try to spread the particles evenly (middle picture). The compromise of both at finite temperature is given by the **barometric height formula**, i.e.,

$$p(z) = p_0 \exp\left(-\frac{mgz}{k_B T}\right), \quad (3.19)$$

where $p(z)$ is the probability to find a particle at height z , m is the mass of a particle, g is the gravitational acceleration and p_0 is a normalization constant. The result actually gives a hint at some very fundamental distribution, which always provides the free energy minimum in thermal equilibrium. This distribution is the Boltzmann distribution.

The Boltzmann distribution is an approach of statistical physics to describe a thermodynamic system in equilibrium. The idea is hereby to deliver probability distributions for the probability of all different microstates. Key distinguishing feature of different microstates is their energy E_i (that was so far neglected in the examples above), where i indicates the i th microstate.

The Boltzmann distribution tells us precisely the probability of finding a given microstate with energy E_i : If a particle is in equilibrium with its environment then the probability of finding the particle in state i with energy E_i is

$$p(E_i) = \frac{1}{Z} \exp\left(-\frac{E_i}{k_B T}\right). \quad (3.20)$$

The normalization factor $1/Z$ contains the so-called partition function Z :

$$Z = \sum_i \exp\left(-\frac{E_i}{k_B T}\right) = \text{const.} \quad (3.21)$$

It ensures that the total probability to find a system in any of the states is

$$\sum_i p(E_i) = 1. \quad (3.22)$$

3.4.1 Mean Energy

The Boltzmann distribution is useful to calculate also expectation values, for example, of the total energy of the system (the mean energy $\langle E \rangle$).

The mean is defined by:

$$\langle E \rangle = \frac{1}{Z} \sum_{i=1}^N E_i \exp\left(-\frac{E_i}{k_B T}\right). \quad (3.23)$$

Abbreviating $\beta = (k_B T)^{-1}$ we find

$$\langle E \rangle = \frac{1}{Z} \sum_{i=1}^N \left(-\frac{\partial}{\partial \beta} \exp(-\beta E_i) \right), \quad (3.24)$$

where the sum is nothing else than the derivative of the partition function

$$\langle E \rangle = -\frac{1}{Z} \frac{\partial}{\partial \beta} Z \quad (3.25)$$

or just

$$\langle E \rangle = -\frac{\partial}{\partial \beta} \ln(Z). \quad (3.26)$$

3.4.2 Free Energy

Employ the Gibbs entropy $S = -k_B \sum_{i=1}^N p_i \ln p_i$ to find a relation between the free energy F (or G) and the partition function. Inserting the probability $p_i = Z^{-1} \exp(-\beta E_i)$ and doing some transformations yields

$$S = k_B (\ln(Z) + \beta \langle E \rangle). \quad (3.27)$$

Using

$$F = U - TS \quad (3.28)$$

for the free energy, we can insert the above result for the entropy and obtain

$$F = -k_B T \ln(Z) \quad (3.29)$$

(or G in the same way).

Note that this is the total energy and not the mean energy (internal, enthalpy or free energy) of the states in the system. The partition function thus allows us to calculate the free energy.

3.4.3 Deriving the Boltzmann Distribution

There are a number of ways to derive the Boltzmann distribution. We will have a quick look at a classical derivation of the Boltzmann distribution for a closed system, e.g., a system which is in contact with a reservoir as depicted below.

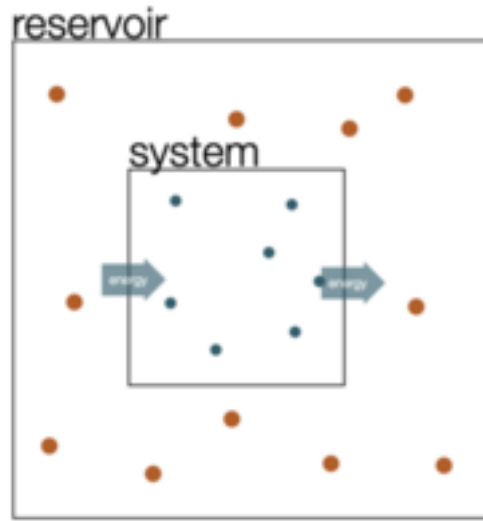


Figure 3.5: Test

System (index s) and reservoir (index r) have total energy $E_{\text{tot}} = E_r + E_s$. We assert now, that the probability to find the system in a specific microstate $p(E_s^{(i)})$ with the energy $E_s^{(i)}$ is directly proportional to the number of states available to the reservoir, when the system is in that state. The ratio of the probabilities of two states is then equal to the ratio of the number of states of the reservoir, i.e.,

$$\frac{p(E_s^{(1)})}{p(E_s^{(2)})} = \frac{W_r(E_{\text{tot}} - E_s^{(1)})}{W_r(E_{\text{tot}} - E_s^{(2)})}.$$

Here, the function $W_r(E_{\text{tot}} - E_s^{(1)})$ is the number of states available to the reservoir, when the system is having the energy $E_s^{(1)}$.

We can now rewrite the above equation in terms of the entropy using $W(S(E)) = \exp(S(E)/k_B)$ such that

$$\frac{W_r(E_{\text{tot}} - E_s^{(1)})}{W_r(E_{\text{tot}} - E_s^{(2)})} = \frac{\exp(S_r(E_{\text{tot}} - E_s^{(1)})/k_B)}{\exp(S_r(E_{\text{tot}} - E_s^{(2)})/k_B)}.$$

We may now expand the entropy to first order

$$S_r(E_{\text{tot}} - E_s) \approx S_r(E_{\text{tot}}) - \frac{\partial S_r}{\partial E} E_s$$

considering that E_s is only very tiny as compared to the total energy of the reservoir. Using the thermodynamic identity that

$$\frac{\partial S_r}{\partial E}|_{V,N} = \frac{1}{T}$$

we finally find

$$\frac{p(E_s^{(1)})}{p(E_s^{(2)})} = \frac{\exp(-E_s^{(1)}/k_B T)}{\exp(-E_s^{(2)}/k_B T)}$$

which corresponds to the ratio of two Boltzmann distributions

$$p(E_s^{(i)}) = \frac{1}{Z} \exp\left(-\frac{E_s^{(i)}}{k_B T}\right),$$

where Z is the previously mentioned normalization factor, which is called *partition function*.

Example: Barometric height formula

We have mentioned already the barometric height formula giving the probability of finding a particle at a height z . To derive that, we consider a constant gravitational force $F = -mg$ along the z -direction such that the potential energy is given by $E = mgz$, assuming that $E = 0$ at $z = 0$.

The probability for finding the particle at position z is therefore

$$p(z) = \frac{1}{Z} \exp\left(-\frac{mgz}{k_B T}\right) = \frac{1}{\langle z \rangle} \exp\left(-\frac{z}{\langle z \rangle}\right).$$

Normalization provides the value of the partition function

$$Z = \int_0^\infty \exp\left(-\frac{mgz}{k_B T}\right) dz = \frac{k_B T}{mg}.$$

We may further calculate the mean height, which is the sedimentation length in sedimentation problems:

$$\langle z \rangle = \frac{1}{Z} \int_0^\infty z \exp\left(-\frac{mgz}{k_B T}\right) dz = \frac{k_B T}{mg}$$

and the mean energy:

$$\langle E \rangle = -\frac{\partial}{\partial \beta} \ln(Z) = +\frac{\partial}{\partial \beta} \ln(\beta mg) = \frac{1}{\beta} = k_B T = mg\langle z \rangle.$$

Example: Boltzmann distribution is the maximum entropy distribution in which the average energy is prescribed as a constraint

We can also obtain the Boltzmann distribution from the Shannon entropy by constraining the Shannon entropy. With only the normalization as a constraint in entropy maximization, we obtained equally likely microstates. If we now constrain the mean energy $\langle E \rangle$ of the system, we obtain a distribution which maximizes the entropy under this condition. The mean energy is given by

$$\langle E \rangle = \sum_i E_i p_i, \quad (3.30)$$

such that we can add another constraint to our augmented entropy. We now have a Lagrange multiplier λ for the normalization of the probability and a second one β which is multiplied by the energy constraint.

$$S' = -\sum_i p_i \ln p_i - \lambda \left(\sum_i p_i - 1 \right) - \beta \left(\sum_i p_i E_i - \langle E \rangle \right). \quad (3.31)$$

Taking the derivative

$$\frac{\partial S'}{\partial p_i} = -\ln p_i - 1 - \lambda - \beta E_i \stackrel{!}{=} 0 \quad (3.32)$$

results in

$$p_i = e^{-1-\lambda-\beta E_i} \quad (3.33)$$

and together with the normalization condition $\sum p_i = 1$ finally

$$e^{-1-\lambda} = \frac{1}{\sum_i e^{-\beta E_i}}, \quad (3.34)$$

where we already recognized that we can replace the prefactor $e^{-1-\lambda}$ by $1/Z$ with Z being the partition function

$$Z = \sum_i e^{-\beta E_i}. \quad (3.35)$$

Overall this, therefore, leads to the Boltzmann distribution

$$p_i = \frac{e^{-\beta E_i}}{\sum_i e^{-\beta E_i}} \quad (3.36)$$

which is quite interesting. We have just fixed the mean energy of the system and maximized the entropy. The Boltzmann distribution is therefore the probability distribution which maximizes the entropy under as little as possible additional information (just the mean energy).

The only thing that is missing in the above formula is an expression for the value of β , the Lagrange multiplier. This can be obtained when knowing the mean energy. In thermal equilibrium, this mean energy can be obtained from the equipartition theorem.

Part IV

Lecture 3

4 Equipartition

In the previous section, we showed how the probability distribution for a system with average energy $\langle E \rangle$ could be guessed by using the principle of maximum entropy. However, to finish that calculation, we need to determine the meaning and significance of the Lagrange multiplier β . We can derive a value for β with the help of the equipartition theorem.

The equipartition theorem, also known as the law of equipartition, equipartition of energy or simply equipartition, states that every degree of freedom that appears only quadratically in the total energy has an average energy of $\frac{1}{2}k_B T$.

To obtain the Lagrange parameter we just consider one degree of freedom for a monoatomic gas. This degree of freedom is the kinetic energy of one atom along the x-direction, which is given by

$$E = \frac{p_x^2}{2m} \quad (4.1)$$

According to the Boltzmann distribution, the probability to find an atom with a certain momentum is given by

$$P(p_x) = \frac{e^{-\beta(p_x^2/2m)}}{\sum_{\text{states}} e^{-\beta(p_x^2/2m)}} \quad (4.2)$$

We can thus calculate the mean energy by summing up (or integrating when going to continuous states) over all possible momenta

$$\sum_{\text{states}} \rightarrow \int_{-\infty}^{\infty} dp_x \quad (4.3)$$

This yields

$$\int_{-\infty}^{\infty} e^{-\beta p_x^2/2m} dp_x = \sqrt{\frac{2m\pi}{\beta}} \quad (4.4)$$

To obtain the value of β we now constrain the mean energy to the value given by the equipartition principle

$$\langle E \rangle = \frac{1}{2} k_B T \quad (4.5)$$

This is the mean energy per degree of freedom. One can show that each degree of freedom, independent of the object (atom, colloid, parking car) is carrying this mean energy. It provides actually our measure of temperature.

Using the momentum to calculate the mean energy we write down

$$\langle E \rangle = \frac{\int_{-\infty}^{\infty} \frac{p_x^2}{2m} e^{-\beta(p_x^2/2m)} dp_x}{\sqrt{2m\pi/\beta}} \quad (4.6)$$

which can be slightly simplified

$$\langle E \rangle = \frac{\alpha^{3/2}}{\beta\sqrt{\pi}} \left(-\frac{\partial}{\partial \alpha} \right) \int_{-\infty}^{\infty} e^{-\alpha p_x^2} dp_x \quad (4.7)$$

and calculated via some tricks valid for integrals over Gaussian functions. This finally leads us to the result that the value of the Lagrangian multiplier must be

$$\beta = \frac{1}{k_B T} \quad (4.8)$$

A good example for a non-quadratic degree of freedom is the barometric height formula with a potential energy that is linear in position.

Equipartition is useful in many ways. The fundamental degrees of freedom, e.g. the vibrations of a single molecule are quadratic in the bond length. Similarly all rotational degrees of freedom are as well. Their occupation is determined by a Boltzmann distribution and readily visible in molecular spectra. On more macroscopic scales it is very useful in the field of force measurements using optical tweezers.

Example: Two-level-system

As another frequent application of Boltzmann's law are state populations of two state systems, as we find them frequently in physics, e.g., for spin systems. Such two-level spin systems are, for example, very important for nuclear magnetic resonance (NMR), which is an important tool to study the structure and dynamics of soft matter.

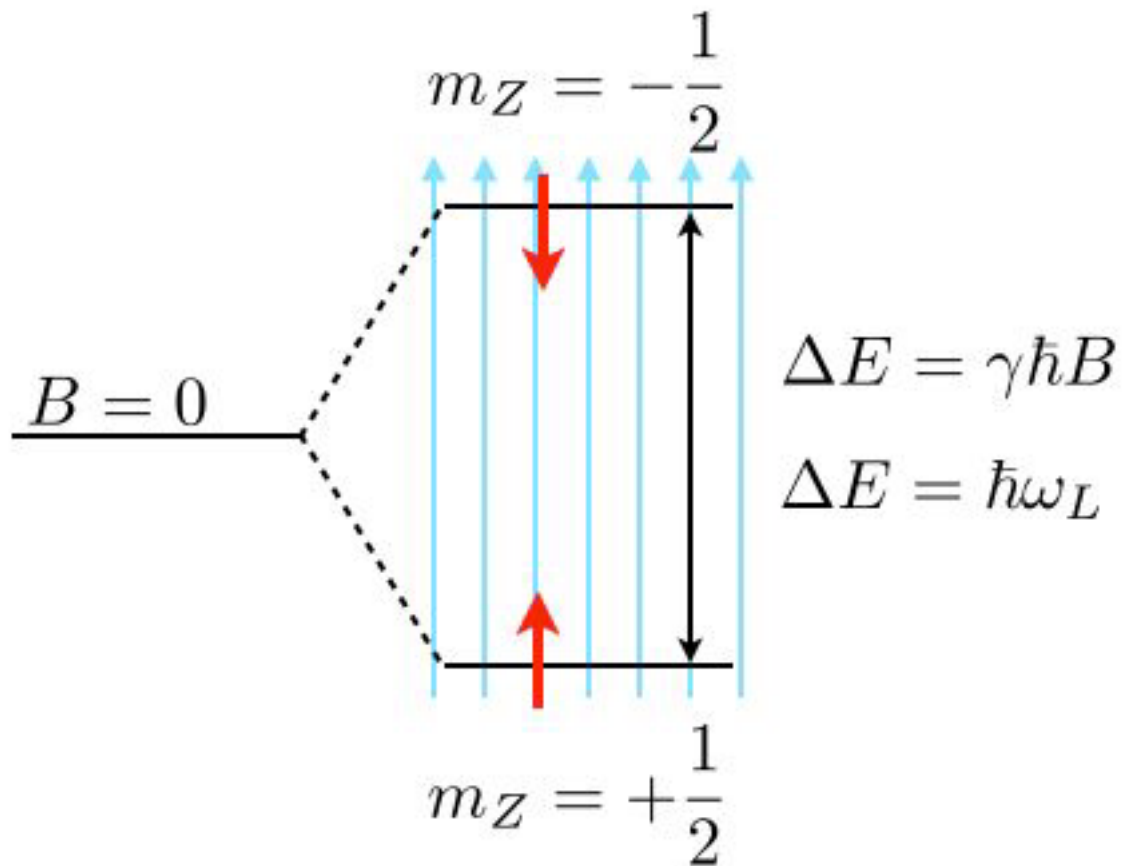


Figure 4.1: Two Level

Consider the image above, where a single energy level at zero magnetic field ($B = 0$) splits into two energy levels due to the interaction of a proton spin (red arrow) with the external magnetic field.

The magnetic moment of the proton spin may take two expectation values in the magnetic field, which are characterized by the magnetic quantum number $m_Z = \pm 1/2$. The magnetic moment projected along the magnetic field direction is then

$$\mu_Z = \gamma m_Z \hbar$$

and the energy of the states

$$E(m_Z) = -\mu_Z B = -\gamma m_Z \hbar B$$

with $\gamma = 2.675222005 \times 10^8 \text{ s}^{-1}\text{T}^{-1}$ being the gyromagnetic ratio of the proton. The energy difference for a nonzero magnetic field is therefore given by

$$\Delta E = \gamma\hbar B = \hbar\omega_L$$

which results for a magnetic field of $B = 1 \text{ T}$ in $\Delta E \approx 1.76 \times 10^{-7} \text{ eV}$ or a Larmor frequency of $\omega_L = 42 \text{ MHz}$. This energy difference is almost negligible as compared to the thermal energy at room temperature $k_B T = 2.6 \times 10^{-2} \text{ eV}$. Yet, this small energy difference is used to give the contrast in NMR and related techniques such as MRI.

Using the Boltzmann distribution we can now calculate the ratio of the population of spins in the lower or excited state

$$\frac{N_{-\frac{1}{2}}}{N_{+\frac{1}{2}}} = \exp\left(-\frac{\Delta E}{k_B T}\right)$$

which is very close to one:

$$\frac{N_{-\frac{1}{2}}}{N_{+\frac{1}{2}}} = 0.99999332.$$

If you now consider a volume of $V = 1 \text{ m}^3$ water, then you would roughly have about $N = 6.7 \times 10^{19}$ protons. This then means that the excess number of protons in the excited state is just $N_{+\frac{1}{2}} - N_{-\frac{1}{2}} = 4.5 \times 10^{12}$, which is extremely low. Thus, to detect something in NMR or MRI, a certain number of protons in the volume is required.

Example: Position of a Bead in an Optical Tweezer

In an optical tweezer, a polarizable object (e.g. a polymer bead) is held in the intensity gradient of a focused laser beam. The nearly Gaussian intensity distribution of a focused beam leads, in first approximation to a linear force a parabolic potential and can be employed to measure tiny forces.

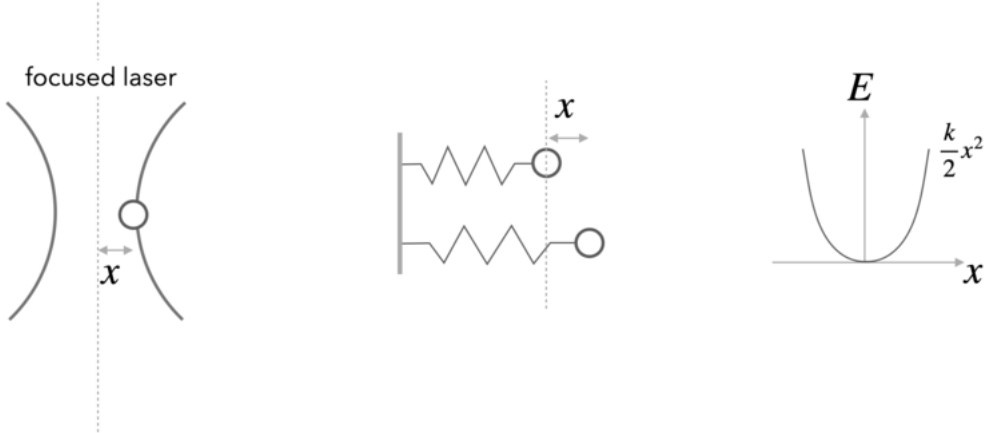


Figure 4.2: tweezers

For one dimension of the 3D optical potential it can thus be written as

$$F = -kx \quad (4.9)$$

and

$$E = \frac{1}{2}kx^2 \quad (4.10)$$

Using the Boltzmann distribution for the potential provides the probability distribution for finding the particle at a certain position x

$$p(x) = \frac{1}{Z} \exp\left(-\frac{kx^2}{2k_B T}\right) \quad (4.11)$$

which resembles a Gaussian distribution with a variance of

$$\sigma^2 = \langle x^2 \rangle = \frac{k_B T}{k} \quad (4.12)$$

We also readily recognize that the partition function Z is the normalization factor of the Gaussian

$$Z = \sqrt{2\pi}\sigma = \sqrt{2\pi \frac{k_B T}{k}} \quad (4.13)$$

The mean potential energy is then calculated by

$$\langle E \rangle = \int_{-\infty}^{\infty} E p(x) dx = \frac{1}{2} k \int_{-\infty}^{\infty} x^2 p(x) dx = \frac{1}{2} k \frac{k_B T}{k} = \frac{1}{2} k_B T \quad (4.14)$$

With the help of the variance of the distribution mentioned above, we also recognize that the trap stiffness can be obtained by dividing the thermal energy $k_B T$ by the variance of the positional fluctuations.

$$k = \frac{k_B T}{\langle x^2 \rangle} \quad (4.15)$$

which is very helpful for the experiment calibrating the trap stiffness for using the tweezers for force measurements. According to that you just have to observe the position of the trapped object in the potential and measure the variance.

We will deal with this relation later again in the section about the fluctuation dissipation relation.

The second degree of freedom of a particle in an optical tweezer is given by its velocity v . This is as well a quadratic degree in v , yet its measurement turns out to be tricky. As the particle is carrying out Brownian motion in the trap, its velocity is not given by the difference of positions divided by the difference in observation times. To measure the velocity accurately one has to go to very short times, when the particle is carrying out ballistic motion. This has been achieved only about 10 years ago, while the distribution connected to the velocities, the **Maxwell-Boltzmann distribution** is already known for a very long time.

Take some time to have a look at the Maxwell-Boltzmann distribution again.

We could now come back to our example with the Barometric height formula to check the equipartition for a system with a linear and not a quadratic dependence of the energy on the degree of freedom.

Example: Barometric height formula

We have already mentioned the barometric height formula giving the probability of finding a particle at a height z . To derive that, we consider a constant gravitational force $F = -mg$ along the z -direction such that the potential energy is given by $E = mgz$ assuming that $E = 0$ at $z = 0$.

The probability for finding the particle at position z is therefore

$$p(z) = \frac{1}{Z} \exp\left(-\frac{mgz}{k_B T}\right) = \frac{1}{\langle z \rangle} \exp\left(-\frac{z}{\langle z \rangle}\right).$$

Normalization provides the value of the partition function:

$$Z = \int_0^\infty \exp\left(-\frac{mgz}{k_B T}\right) dz = \frac{k_B T}{mg}.$$

We may further calculate the mean height, which is the sedimentation length in sedimentation problems:

$$\langle z \rangle = \frac{1}{Z} \int_0^\infty z \exp\left(-\frac{mgz}{k_B T}\right) dz = \frac{k_B T}{mg}$$

and the mean energy:

$$\langle E \rangle = -\frac{\partial}{\partial \beta} \ln(Z) = +\frac{\partial}{\partial \beta} \ln(\beta mg) = \frac{1}{\beta} = k_B T = mg\langle z \rangle.$$

4.1 When a Macrostate is a Microstate

In practice, we are often interested in the likelihood that the system is in a state that is described by some macroscopic parameter X that we can measure. For example, for a DNA molecule inside a cell, an interesting quantity, which can be measured using fluorescent markers, is the distance R between two sites on the DNA chain. Repeated measurements of R can be used to construct the probability distribution $p(R)$.

In general, the probability of the macrostate X is given by the sum of probabilities of all the microstates of the system that adopt the specified value X ,

$$p(X) = \sum_{i_X} p_i = \sum_{i_X} \frac{1}{Z} e^{-\beta E_i} \quad (4.16)$$

For the DNA example, the sum in the above equation would run over only those microstates i_X that have the prescribed distance between the two labeled sites on the polymer, e.g. $X = R$. Using the basic relation between the partition function and the free energy, $G = -k_B T \ln(Z)$, we can express the probability of the macrostate X as

$$p(X) = \frac{1}{Z} e^{-\beta G(X)} \quad (4.17)$$

where

$$G(X) = -k_B T \ln \left(\sum_{i_X} e^{-\beta E_i} \right) \quad (4.18)$$

is the free energy of the macrostate X . Note that the formula for $p(X)$ is identical to the Boltzmann formula for the probability of a microstate, with the energy of the microstate replaced by the free energy of the macrostate. Note that the sum on the right side of the last equation is not the partition function Z but that of the subensemble of microstates fulfilling the condition X , i.e. Z_X . Similarly, when writing down the states and weights for the macrostates X , the energy is replaced by the free energy, as shown in the figure below. In this sense, one person's macrostate is truly another person's microstate.

STATE	WEIGHT
X_1	$e^{-\beta e_1}$ $e^{-\beta e_2}$ $e^{-\beta e_3}$ \vdots $e^{-\beta e_{n_1}}$
X_2	$e^{-\beta e_{n_1+1}}$ \vdots $e^{-\beta e_{n_2}}$
X_3	$e^{-\beta e_{n_2+1}}$ \vdots $e^{-\beta e_{n_3}}$

STATE	WEIGHT
X_1	$e^{-\beta G(X_1)}$
X_2	$e^{-\beta G(X_2)}$
X_3	$e^{-\beta G(X_3)}$
\vdots	\vdots

Figure 4.3: micro_macro

5 Chemical Potential

So far, we have considered either isolated systems, meaning that no energy nor particle exchange is possible, and closed systems, which allow an exchange of energy with a reservoir (bath). We will now have a look at a system that also allows an exchange of particles with a reservoir. For these systems, we will define the **chemical potential** μ which we will identify as the **free energy change when adding one molecule of a given species to a thermodynamic system** at constant p and T .

We consider a system of two components A and B in contact with a heat bath and a diffusive equilibrium between A and B.



Figure 5.1: Chemical Potential

The total free energy of our system is then defined as

$$G = G_A + G_B. \quad (5.1)$$

The total number of particles in the system is also conserved and given by $N_{\text{tot}} = N_A + N_B$. In equilibrium we require the free energy of the system to be a minimum with respect to the particle number such that:

$$dG = \left. \frac{\partial G_A}{\partial N_A} \right|_{T,p} dN_A + \left. \frac{\partial G_B}{\partial N_B} \right|_{T,p} dN_B = \left. \frac{\partial G_A}{\partial N_A} \right|_{T,p} dN_A - \left. \frac{\partial G_B}{\partial N_B} \right|_{T,p} dN_A = 0. \quad (5.2)$$

with $dN_A = -dN_B$, since the total number of particles is conserved (i.e., $dN_{\text{tot}} = 0$):

$$\frac{dG_A}{dN_A} = \frac{dG_B}{dN_B}. \quad (5.3)$$

Apparently, in equilibrium the change in the free energy of system A needs to be the same of system B when exchanging particles at constant T, p .

Chemical Potential

We can define a quantity

$$\mu(T, p, N) = \left. \frac{dG}{dN} \right|_{T, P} \quad (5.4)$$

which is termed the **chemical potential**, which is the change in the free energy when adding a particle to the system. The chemical potential may be interpreted as the cost for adding one more particle (at constant T, p) to the system.

Note

- if $\mu_l < \mu_v$ at constant T, p , we can lower the free energy by moving a particle from v to l ,
- $\mu_l \neq \mu_v$ means non-equilibrium and particles will diffuse until $\mu_l = \mu_v$.

We will have a closer look at the chemical potential with an example below. The previous condition states that the chemical potential of the two systems is the same in equilibrium. The chemical potential is useful in many situations. For example, to determine

5.1 Phase equilibria

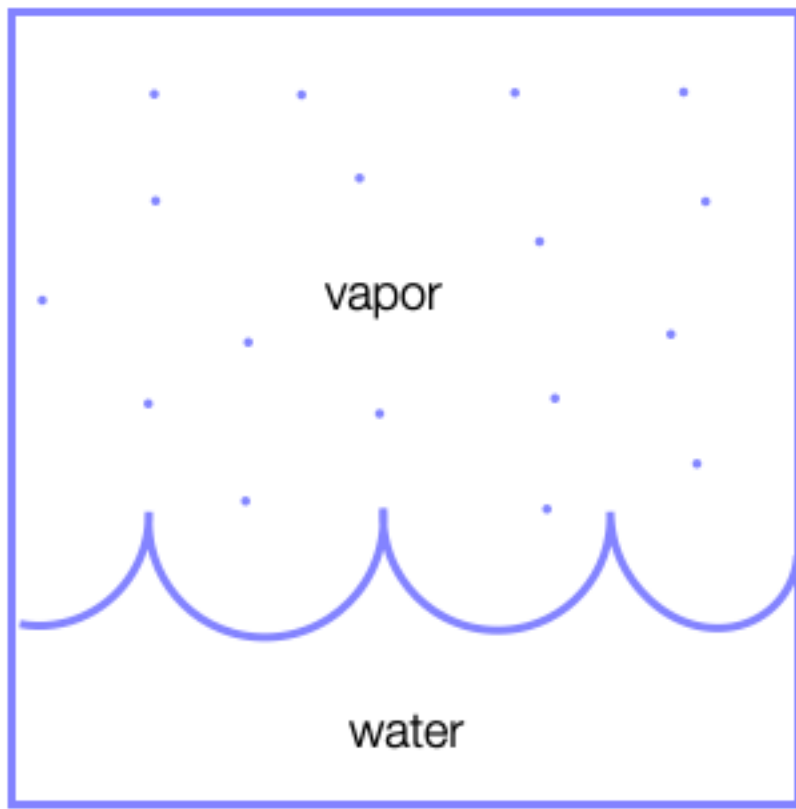


Figure 5.2: Phase equilibrium

In this case, we have a boundary between two phases (e.g., liquid and vapor) and particles of the vapour phase may join the liquid phase and vice versa. In this case, the number of vapor particles N_{vapor} and the number of liquid particles N_{liquid} is not fixed, but the total number of particles $N = N_{\text{vapor}} + N_{\text{liquid}}$ is.

5.2 Chemical equilibria

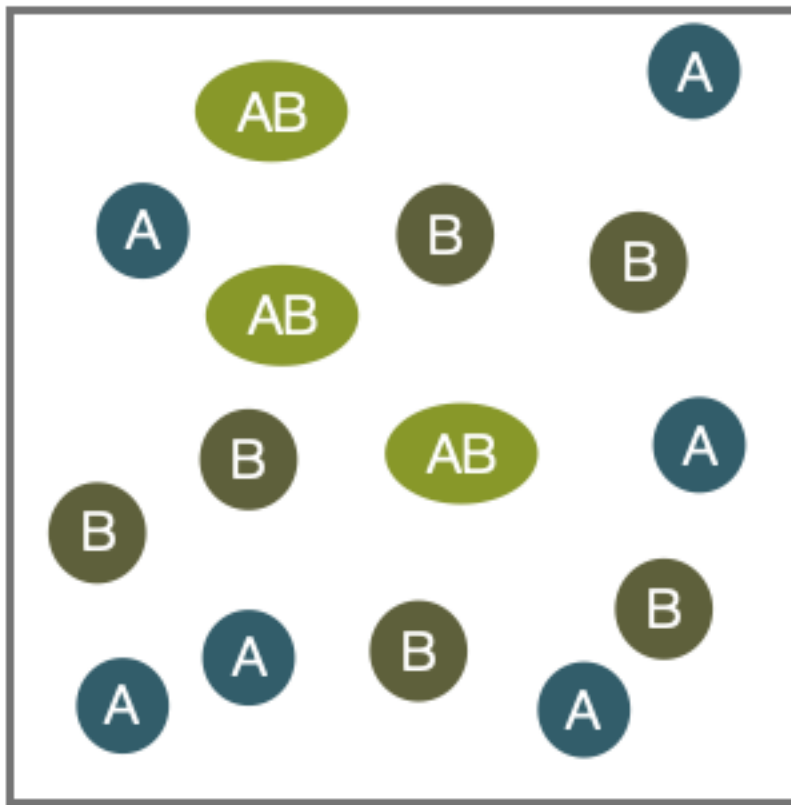


Figure 5.3: Chemical equilibrium

In the case of chemical equilibria, two species A and B may react to form a new species AB by a chemical reaction:



Here the individual numbers of particles N_A, N_B and N_{AB} are not fixed, but $N_A + N_{AB}$ and $N_B + N_{AB}$ are.

Example: Free energy of a dilute solution

We would like to calculate the free energy and the chemical potential for a dilute solution of some *solutes* in a solvent, which we just term H_2O . Actually, no additional information on the details of the solute and solvent are currently required, though if we want to have numbers, we would need to know which solute or solvent we are looking at.

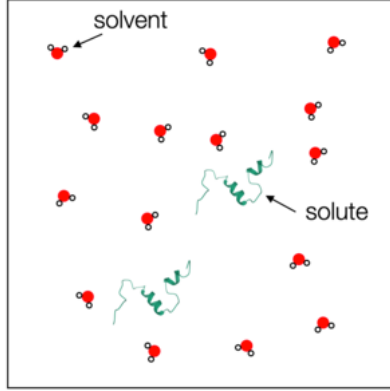


Figure 5.4: Solute Solvent

Suppose we have

- $N_{\text{H}_2\text{O}}$ solvent molecules (e.g., water),
- N_s solute molecules (e.g., proteins).

The solute chemical potential is defined by

$$\mu_s = \left(\frac{\partial G_{\text{tot}}}{\partial N_s} \right) \Big|_{p,T}$$

or intuitively as

$$\mu_s = G_{\text{tot}}(N_s + 1) - G_{\text{tot}}(N_s)$$

The total free energy G_{tot} consists of the enthalpy of forming the solvent molecules $N_{\text{H}_2\text{O}}\varepsilon_{\text{H}_2\text{O}}$ and the enthalpy of solvating the solute proteins $N_s\varepsilon_s$:

$$G_{\text{tot}} = N_{\text{H}_2\text{O}}\varepsilon_{\text{H}_2\text{O}} + N_s\varepsilon_s - TS_{\text{mix}}$$

The last term TS_{mix} denotes the entropy for mixing the solute and the solvent molecules. In the following, we are interested in the last term, which is the entropic contribution to the free energy containing the entropy of mixing solute and solvent.

The mixing entropy can be calculated by either the Gibbs definition

$$S_{\text{mix}} = -k_B \sum_i p_i \ln(p_i)$$

or the Boltzmann definition

$$S_{\text{mix}} = k_{\text{B}} \ln(W)$$

We will use the latter definition, including the number of possible configurations, to obtain the mixing entropy. If the total number of molecules in the volume is $N = N_{\text{H}_2\text{O}} + N_s$, we can write down the number of different ways to arrange the molecules as previously done. We obtain:

$$W(N_{\text{H}_2\text{O}}, N_s) = \frac{N!}{N_{\text{H}_2\text{O}}! N_s!}$$

As in our example with the DNA binding, we can apply the Stirling formula for large N and find:

$$S_{\text{mix}} = -k_{\text{B}} \left(N_{\text{H}_2\text{O}} \ln \left(\frac{N_{\text{H}_2\text{O}}}{N_{\text{H}_2\text{O}} + N_s} \right) + N_s \ln \left(\frac{N_s}{N_{\text{H}_2\text{O}} + N_s} \right) \right)$$

To really go in the dilute limit, the number of solute molecules should be much larger than the number of solvent molecules, i.e.,

$$\frac{N_s}{N_{\text{H}_2\text{O}}} \ll 1$$

which allows us to approximate the solution with

$$S_{\text{mix}} \approx -k_{\text{B}} \left(N_{\text{H}_2\text{O}} \ln \left(1 - \frac{N_s}{N_{\text{H}_2\text{O}}} \right) + N_s \ln \left(\frac{N_s}{N_{\text{H}_2\text{O}}} \right) \right)$$

employing the Taylor series expansion of $N_{\text{H}_2\text{O}}/(N_{\text{H}_2\text{O}} + N_s) = 1/(1 + N_s/N_{\text{H}_2\text{O}})$ at $N_s/N_{\text{H}_2\text{O}} \approx 0$.

Using

$$\ln(1 + \epsilon) \approx \epsilon$$

we may finally write

$$S_{\text{mix}} \approx -k_{\text{B}} \left(N_s \ln \left(\frac{N_s}{N_{\text{H}_2\text{O}}} \right) - N_s \right)$$

and the total free energy is then given by

$$G_{\text{tot}} = N_{\text{H}_2\text{O}} \varepsilon_{\text{H}_2\text{O}} + N_{\text{s}} \varepsilon_{\text{s}} + k_{\text{B}} T \left(N_{\text{s}} \ln \left(\frac{N_{\text{s}}}{N_{\text{H}_2\text{O}}} \right) - N_{\text{s}} \right)$$

We can now come back and calculate the chemical potential of the solute as noted above:

$$\mu_{\text{s}} = \varepsilon_{\text{s}} + k_{\text{B}} T \ln \left(\frac{N_{\text{s}}}{N_{\text{H}_2\text{O}}} \right)$$

As we rather work with concentrations than number of molecules we can use $c = N_{\text{s}}/V$ and $c_0 = c_{\text{H}_2\text{O}} = N_{\text{m}} \text{atm} \text{H}_2\text{O}/V$ to write

$$\mu_{\text{s}} = \varepsilon_{\text{s}} + k_{\text{B}} T \ln \left(\frac{c}{c_0} \right).$$

The value of c_0 thereby acts as a reference point, which is commonly chosen to be at $c_0 = 1 \text{ M}$. The value of ε_{s} is termed the standard chemical potential μ_{s}^0 . The standard chemical potential is measured at standard thermodynamic conditions, i.e., $p_0 = 101.3 \text{ kPa}$, $T = 293.15 \text{ K}$, and $c_0 = 1 \text{ M}$.

In a mixed system, we define the chemical potential of a component i as the sum of two components

$$\mu_i = \mu_i^0 + k_{\text{B}} T \ln \left(\frac{c_i}{c_{i,0}} \right). \quad (5.6)$$

- The standard chemical potential is a molecular property (see slides) that contains
 - the internal energy/enthalpy to create the molecule,
 - the conformational entropy of the molecule, and
 - the enthalpy and entropy contributions when bringing the molecule into contact with the solvent (solvation free energy).
- The logarithm term $k_{\text{B}} T \ln \left(\frac{c_i}{c_{i,0}} \right)$ is the pure mixing/dilution entropy reflecting the different abundance of solute and solvent due to the resulting numbers of microstates.

For a solvent we consequently write

$$\mu_{\text{H}_2\text{O}} = \frac{\partial G_{\text{tot}}}{\partial N_{\text{H}_2\text{O}}} \Big|_{T,p} = \mu_{\text{H}_2\text{O}}^0 - k_{\text{B}} T \left(\frac{c_{\text{s}}}{c_{\text{H}_2\text{O}}} \right)$$

Finally, a chemical potential may also be defined for gases, e.g., for the ideal gas:

$$\mu_{iG} = k_B T \ln \left(\frac{p}{p_0} \right)$$

which only has entropic contributions.

Example: Barometric height formula

We can have a look again at the barometric height formula using the framework of the chemical potential. Each height $[h, h + dh]$ is exchanging particles with other heights until the chemical potential in all regions is the same. We can thus write

$$\mu(h = 0) = \mu_0(h = 0) + k_B T \ln \left(\frac{n(h = 0)}{n_0} \right) \quad (5.7)$$

$$= \mu_0(h) + k_B T \ln \left(\frac{n(h)}{n_0} \right) \quad (5.8)$$

The standard chemical potential is just given by the potential energy, i.e.:

$$\mu_0(h) = mgh$$

and

$$\mu_0(h = 0) = 0$$

which then leads us to

$$-mgh = k_B T \left(\ln \left(\frac{n(h)}{n_0} \right) - \ln \left(\frac{n(h = 0)}{n_0} \right) \right). \quad (5.9)$$

This finally leads us to

$$\frac{n(h)}{n(h = 0)} = \exp \left(-\frac{mgh}{k_B T} \right) \quad (5.10)$$

which is, of course, the barometric height formula.

Part V

Lecture 4

6 Osmotic Pressure

The chemical potential as defined in the previous section also allows us to understand the osmotic pressure. Consider a volume that is separated into two equally sized parts by a semipermeable membrane. One of the compartments is filled with pure water, the other compartment contains a number of additional solute molecules. The solute molecules thereby cannot pass the membrane while the water can easily pass it.

The chemical potential of the water

$$\mu_{\text{H}_2\text{O}} = \frac{\partial G_{\text{tot}}}{\partial N_{\text{H}_2\text{O}}}$$

needs to be the same on both sides.

The chemical potential on the solute side is given by

$$\mu_{\text{H}_2\text{O}} = \mu_{\text{H}_2\text{O}}^o(T, p_2) - \frac{N_s}{N_{\text{H}_2\text{O}}} k_{\text{B}} T$$

and on the solvent side

$$\mu_{\text{H}_2\text{O}} = \mu_{\text{H}_2\text{O}}^o(T, p_1)$$

from which follows that

$$\mu_{\text{H}_2\text{O}}^o(T, p_1) = \mu_{\text{H}_2\text{O}}^o(T, p_2) - \frac{N_s}{N_{\text{H}_2\text{O}}} k_{\text{B}} T.$$

Here we have already assumed that on both sides of the membrane we have a different pressure ($p_1 \neq p_2$). If both pressures are only slightly different we can write

$$\mu_{\text{H}_2\text{O}}^o(T, p_2) \approx \mu_{\text{H}_2\text{O}}^o(T, p_1) + \left(\frac{\partial \mu_{\text{H}_2\text{O}}^o}{\partial p} \right) (p_2 - p_1)$$

which is just a Taylor expansion. It turns out, that the derivative

$$\frac{\partial \mu}{\partial p} = v$$

is nothing else than the volume occupied by one molecule. Inserting the Taylor expansion into the original equality of the chemical potentials, we find

$$p_2 - p_1 = \frac{N_s}{v N_{H_2O}} k_B T.$$

With $V = v N_{H_2O}$ as the total volume of water we have

$$\Pi = p_2 - p_1 = \frac{N_s}{V} k_B T = n_s k_B T$$

which is the van't Hoff formula for the **osmotic pressure**.

Osmotic Pressure

The van't Hoff formula for the osmotic pressure is

$$\Pi = n_s k_B T$$

where n is the number density of suspended objects and $k_B T$ is the thermal energy.

Note that the equation looks very much like the equation of state of the ideal gas, however, the pressure is not generated by the collisions of the solute molecules with the membrane. The pressure is generated by the water molecules which try to dilute the solute molecules.

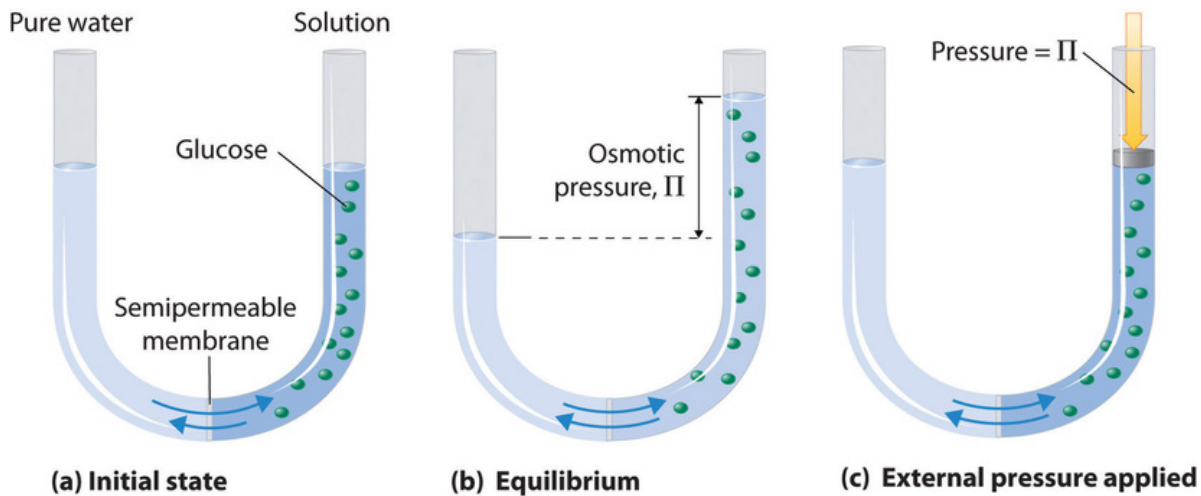


Figure 6.1: osmotic pressure

Image taken from [chemistry libre texts](#)

The concept of osmotic pressures play a very important role in soft matter physics, biology but also environmental science.

6.0.1 Shape of red blood cells

One particular and often mentioned example of the importance of osmotic pressure is the shape of red blood cells.

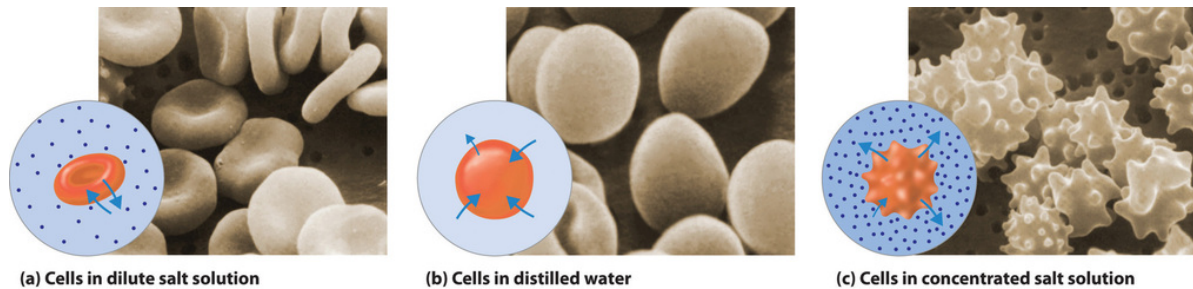


Figure 6.2: red_blood_cells

Image taken from [chemistry libre texts](#)

6.0.2 Reverse Osmosis

A second very important application for osmosis is actually reverse osmosis. Reverse osmosis is heavily employed for water desalination. Salt water is pumped through a membrane, which is selectively preventing ions from passing the membrane. Due to the osmotic pressure difference between the salt free and the salty regions, high pressures are required to pump the water through these membranes. Yet, the technical realizations of this method come close to the thermodynamic limit of this process.

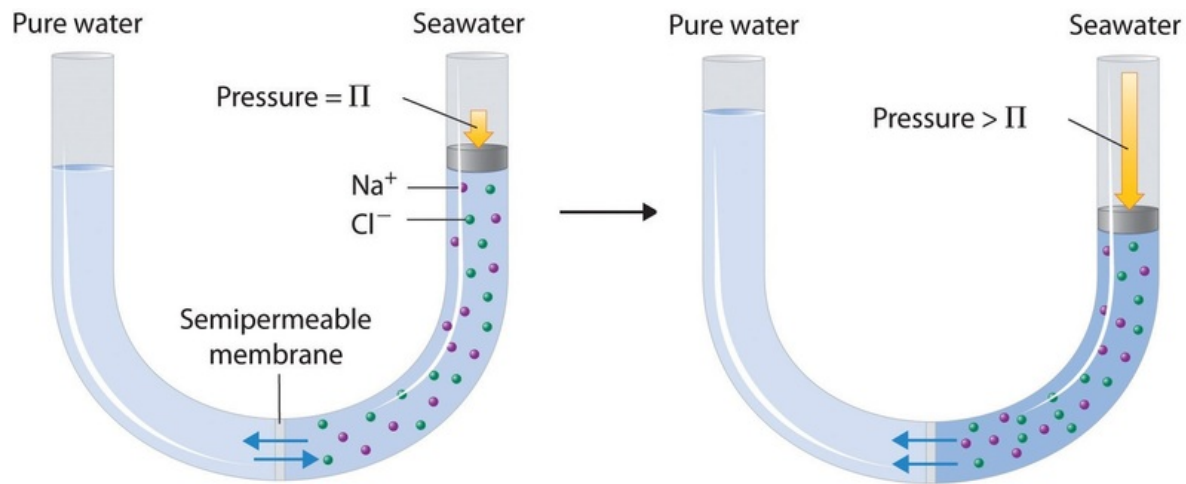


Figure 6.3: reverse osmosis

Image taken from [chemistry libre texts](#)

7 Gibbs Distribution

So far, we have considered closed systems and derived and studied the Boltzmann distribution. Now our systems are open and the particle number might change. The Boltzmann distribution is therefore not anymore sufficient to describe the probability to find a system with an energy E_s and a particle number N_s in contact with a reservoir. To derive a distribution for this new situation, we can use one of the ways, which also allowed the derivation of the Boltzmann distribution. This route is, again, considering the ratio of the probabilities of two arbitrary states of the system (index s) which is equal to the ratio of the numbers of possible states of the reservoir (index r):

$$\frac{p(E_s^{(1)}, N_s^{(1)})}{p(E_s^{(2)}, N_s^{(2)})} = \frac{W_r(E_{\text{tot}} - E_s^{(1)}, N_{\text{tot}}^{(1)})}{W_r(E_{\text{tot}} - E_s^{(2)}, N_{\text{tot}}^{(2)})} \quad (7.1)$$

Hereby, the $E_s^{(i)}, N_s^{(i)}$ denote the energy and the number of particles in the system in the i th state. W_r indicates the number of available states to the reservoir, when the system is in a specific energy state with a specific number of particles. Similar to the derivation of the Boltzmann distribution, we can now assert that the total number of available states of the system and the reservoir is given by

$$W_{\text{tot}}(E_{\text{tot}} - E_s^{(1)}, N_{\text{tot}} - N_s^{(1)}) = 1 \times W_r(E_{\text{tot}} - E_s^{(1)}, N_{\text{tot}} - N_s^{(1)}). \quad (7.2)$$

Note that the system is in exactly one state in this case. Utilizing again that $S = k_B \ln(W)$ or $W = \exp(S/k_B)$, we find

$$\frac{W_r^{(1)}}{W_r^{(2)}} = \frac{\exp(S_r^{(1)}/k_B)}{\exp(S_r^{(2)}/k_B)}. \quad (7.3)$$

Once more, we can use a first order expansion to get

$$S_r(E_{\text{tot}} - E_s, N_{\text{tot}} - N_s) \approx S_r(E_{\text{tot}}, N_{\text{tot}}) - \frac{\partial S_r}{\partial E} E_s - \frac{\partial S_r}{\partial N} E_{N_s}. \quad (7.4)$$

The partial derivatives can be converted with the help of the known thermodynamic relations

$$\left. \frac{\partial S_r}{\partial E} \right|_{V,N} = \frac{1}{T} \quad (7.5)$$

and

$$\left. \frac{\partial S_r}{\partial N} \right|_{V,E} = -\frac{\mu}{T} \quad (7.6)$$

which finally yields the Gibbs distribution:

Gibbs distribution

$$p(E_s^{(1)}, N_s^{(1)}) = \frac{1}{Z} \exp \left(-\frac{E_s^{(1)} - \mu N_s^{(1)}}{k_B T} \right) \quad (7.7)$$

with the **grand partition function**

$$Z = \sum_i \exp \left(-\frac{E_s^{(i)} - \mu N_s^{(i)}}{k_B T} \right). \quad (7.8)$$

Ligand Binding

As an example, we have a look at the binding of a ligand (green) to a receptor, which is indicated in the figure below.

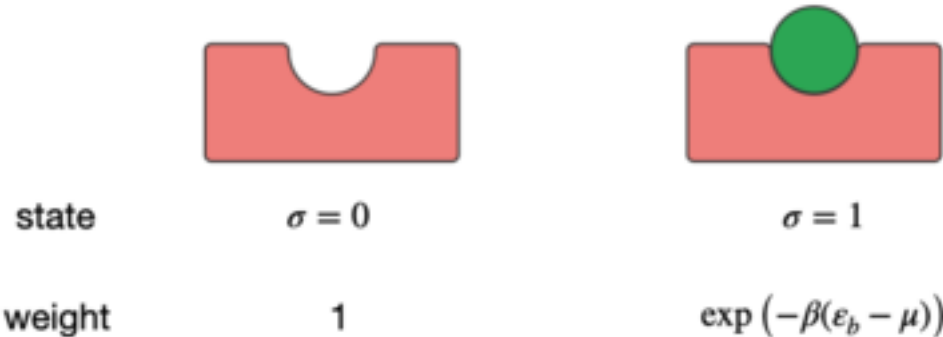


Figure 7.1: Two State Binding

The binding is reported by the variable σ , which can be either 0 or 1. The binding energy is therefore

$$E = \sigma \varepsilon_b$$

with $\varepsilon_b < 0$, since the ligand wants to bind. The grand partition function

$$Z = \sum_{\text{states}} \exp(-\beta(E_{\text{state}} - \mu N_{\text{state}})),$$

in which the chemical potential μ reflects the contact with the particle reservoir and $\beta = (k_B T)^{-1}$, can therefore be written as:

$$Z = \sum_{\sigma=0}^1 \exp(-\beta(\varepsilon_b \sigma - \mu \sigma)) = 1 + \exp(-\beta(\varepsilon_b - \mu)).$$

From that we can calculate the mean number of bounded ligands to be

$$\langle N \rangle = \frac{\exp(-\beta(\varepsilon_b - \mu))}{1 + \exp(-\beta(\varepsilon_b - \mu))}.$$

Using

$$\mu = \mu_0 + k_B T \ln \left(\frac{c}{c_0} \right)$$

we can finally write

$$\langle N \rangle = \frac{c/c_0 \exp(-\beta \Delta \varepsilon_b)}{1 + \frac{c}{c_0} \exp(-\beta \Delta \varepsilon_b)}$$

with $\Delta \varepsilon_b = \varepsilon_b - \mu_0$, which is the energy freed when taking the ligand from the solution and placing it at the acceptor.

Part VI

Lecture 5

8 Phase Transitions

The importance of looking at phase transitions resides in the multicomponent nature of soft matter and its interaction energy scales.

```
import numpy as np
from ipywidgets import interact, interactive, fixed, interact_manual
import ipywidgets as widgets
import matplotlib.pyplot as plt

%matplotlib inline
%config InlineBackend.figure_format = 'retina'

plt.rcParams.update({'font.size': 12,
                     'axes.titlesize': 18,
                     'axes.labelsize': 16,
                     'axes.labelpad': 14,
                     'lines.linewidth': 1,
                     'lines.markersize': 10,
                     'xtick.labelsize' : 16,
                     'ytick.labelsize' : 16,
                     'xtick.top' : True,
                     'xtick.direction' : 'in',
                     'ytick.right' : True,
                     'ytick.direction' : 'in',})
```

When heat is applied, an ice cube undergoes melting, while water undergoes evaporation. These transformations involve the conversion of a solid into a liquid, which then changes into a vapor. Importantly, all of these changes are reversible. The term “phase” refers to a state of matter that is chemically and physically uniform. A substance can exist in solid, liquid, and gas phases, and some substances, like carbon, can have multiple solid phases, such as graphite and diamond.

A phase transition is the spontaneous conversion of one phase to another, and it occurs at a specific temperature for a given pressure. At atmospheric pressure, ice melts at 0°C, and water boils at 100°C. The transition temperature is determined by the *equality of the chemical potential* of a specific element in the two phases.

A phase diagram is a graphical representation that illustrates the conditions, such as temperature and pressure, at which different phases coexist or are present.

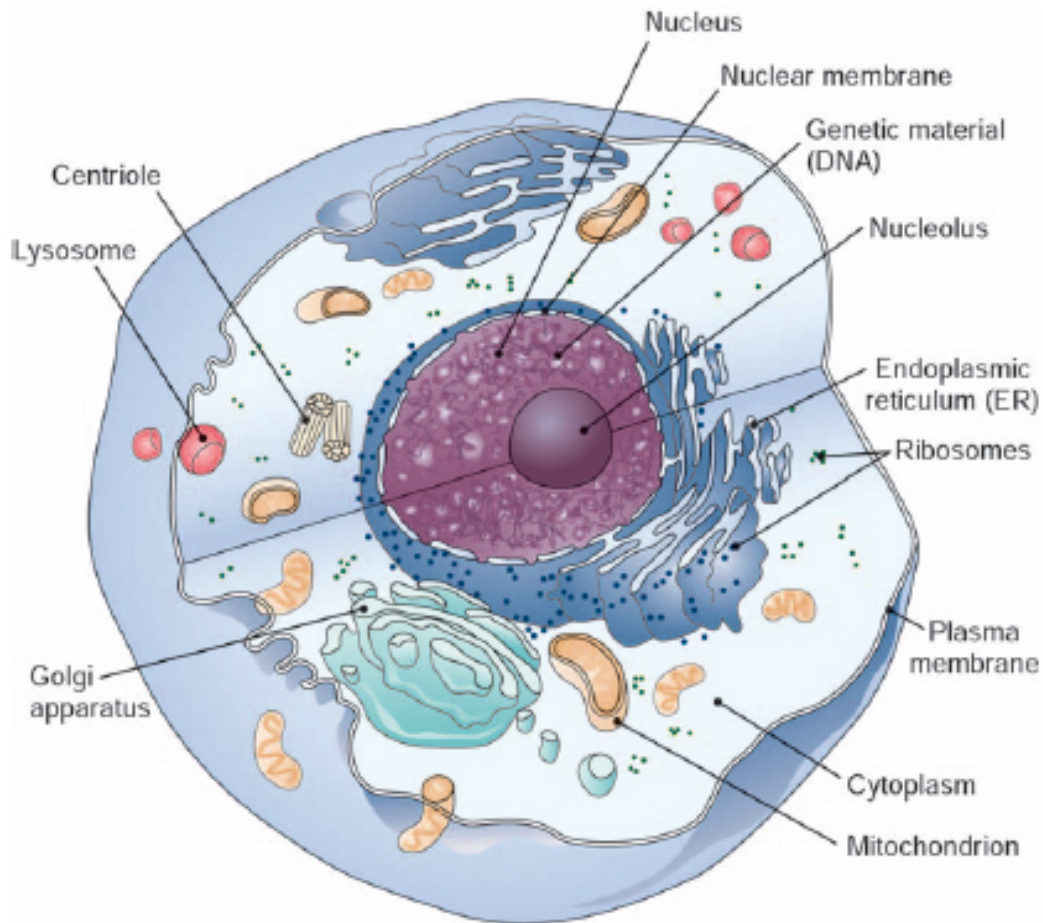


Figure 8.1: cell

We will approach phase transitions no tstarting directly with the solid-liquid phase transition but first exploring the transition of a single macromolecule from the extended conformaiton into globular state. Following that we will have a look at liquid-liquid unmixing as example and later turn into the liquid-solid phase transitions.

8.1 Liquid-Liquid Unmixing

Consider two liquids consisting of molecules A and B, which we will bring together and mix. The mixing should happen at constant volume and temperature. We can therefore use the Helmholtz free energy as the quantity that is minimized.

Initially, the separated components have the free energies F_A and F_B . After the mixing, the free energy that derives from the mixing is $F_{A+B} - (F_A + F_B)$. If the volume fraction of component A is ϕ_A and the one of component B is ϕ_B such that $\phi_A + \phi_B = 1$ (incompressibility of the mixture), then we can calculate the mixing free energy.

First, we calculate the mixing entropy S_{mix} from

$$S = -k_B \sum_i p_i \ln(p_i)$$

which results in

$$S_{\text{mix}} = -k_B(\phi_A \ln(\phi_A) + \phi_B \ln(\phi_B)).$$

In addition to the mixing entropy, we have to calculate the change of the internal energy as well. This internal energy consists of an energy term that comprises the interaction of two molecules of the same type A (ϵ_{AA}), one of two molecules of the same type B (ϵ_{BB}), and one between the molecules A and B (ϵ_{AB}). If we assume that each site in the liquid has a number of neighbors, then the interaction energy of this site is

$$z\phi_A \epsilon_{AA}.$$

A fraction of ϕ_A sites is occupied with molecules A and, thus, the interaction energy reads

$$\frac{z}{2}\phi_A^2 \epsilon_{AA}.$$

Similarly, expressions for the interaction of B molecules and the interaction of A with B can be obtained. To calculate the change in internal energy when mixing the two species, we still have to subtract the internal energy of the two separated components, $z\phi_A \epsilon_{AA}/2$ and $z\phi_B \epsilon_{BB}/2$, such that we obtain

$$U_{\text{mix}} = \frac{z}{2} [(\phi_A^2 - \phi_A)\epsilon_{AA} + (\phi_B^2 - \phi_B)\epsilon_{BB} + 2\phi_A\phi_B\epsilon_{AB}].$$

Using this expression as well as $\phi_A + \phi_B = 1$, we can define an interaction parameter

$$\chi = \frac{z}{2k_B T} (2\epsilon_{AB} - \epsilon_{AA} - \epsilon_{BB})$$

such that

$$\frac{U_{\text{mix}}}{k_B T} = \chi \phi_A \phi_B$$

by utilizing, for example, $(\phi_A^2 - \phi_A)\epsilon_{AA} = \phi_A(\phi_A - 1)\epsilon_{AA} = -\phi_A \phi_B \epsilon_{AA}$.

This finally yields the free energy of mixing

$$\frac{F_{\text{mix}}}{k_B T} = \phi_A \ln(\phi_A) + \phi_B \ln(\phi_B) + \chi \phi_A \phi_B.$$

We can now plot this free energy of mixing as a function of the volume fraction of component A.

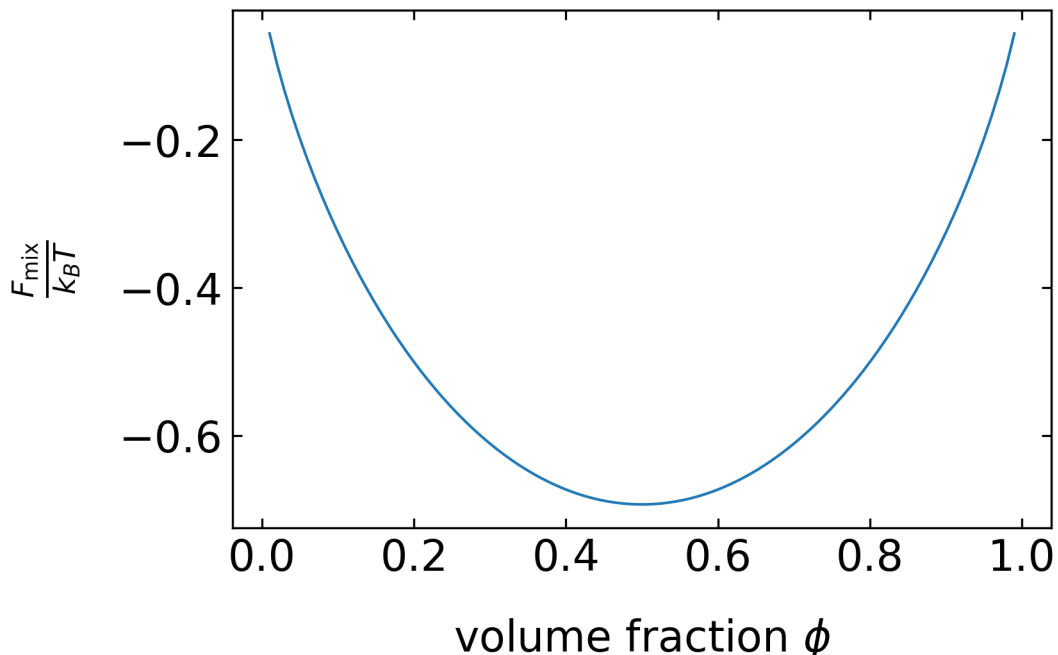


Figure 8.2: mix

```
# define volume fraction variable
phi=np.linspace(0.01,0.99,100)
```

```
# calculate mixing free energy
def mix(x):
    m=phi*np.log(phi)+(1-phi)*np.log(1-phi)+x*phi*(1-phi)
    plt.plot(phi,m)
    plt.ylabel(r"$\frac{F_{\rm mix}}{k_B T}$")
    plt.xlabel(r"volume fraction $\phi$")
    plt.savefig("./img/mix.png", bbox_inches="tight")
    plt.show()
```

Free energy of mixing as a function of the composition of the binary liquid mixture for different interaction parameters.

```
# display interaction slider
#interact(mix, x=widgets.FloatSlider(min=-1, max=5, step=0.1));
```

The free energy function has a minimum at a composition of $\phi = 0.5$ for all χ smaller than 2. In this region of interaction parameters, the two liquids are always miscible at any composition. For χ larger than two, the free energy function reveals two minima, i.e., there are two compositions under which the mixture is stable (one left in phase B and one right in A). The location of these two minima defines what is called the **binodal** or **coexistence curve**, which separates the unstable from the stable region in a phase diagram (Figure 4). As the interaction parameter is proportional to $1/T$, these stable compositions are a function of the temperature.

To understand the stability of a mixture, let us shorten the notation first. In all of the following considerations, we will denote $\phi = \phi_A$. We will start with two mixtures we have prepared, which have a composition ϕ_1 and ϕ_2 . If we take a volume V_1 of the first mixture and a volume V_2 of the second one and combine them to a volume V_0 , then the two mixtures form again a new composition with

$$\phi_0 V_0 = \phi_1 V_1 + \phi_2 V_2.$$

We can divide by V_0 and introduce two new volume fractions α_1, α_2 to yield

$$\phi_0 = \frac{V_1}{V_0} \phi_1 + \frac{V_2}{V_0} \phi_2 = \alpha_1 \phi_1 + \alpha_2 \phi_2.$$

The total free energy of the system of the two separated mixtures at these volume fractions can then be written as

$$F_{\text{sep}} = \alpha_1 F_{\text{mix}}(\phi_1) + \alpha_2 F_{\text{mix}}(\phi_2).$$

We can add this free energy as a function of the volume fraction ϕ_0 to our free energy curve, for example, for an interaction parameter $\chi < 2$. The two initial concentrations lie on the coexistence curve, but the starting composition ϕ_0 is not. Its initial free energy is $F_{\text{sep}}(\phi_0)$ and it is on a line connecting the points with the initial compositions, [Figure 2](#). Since the actual free energy curve of the mixture is always lower than any point of the line denoting the separate free energies, the mixture is **stable**. This is true as long as the free energy curve is convex.

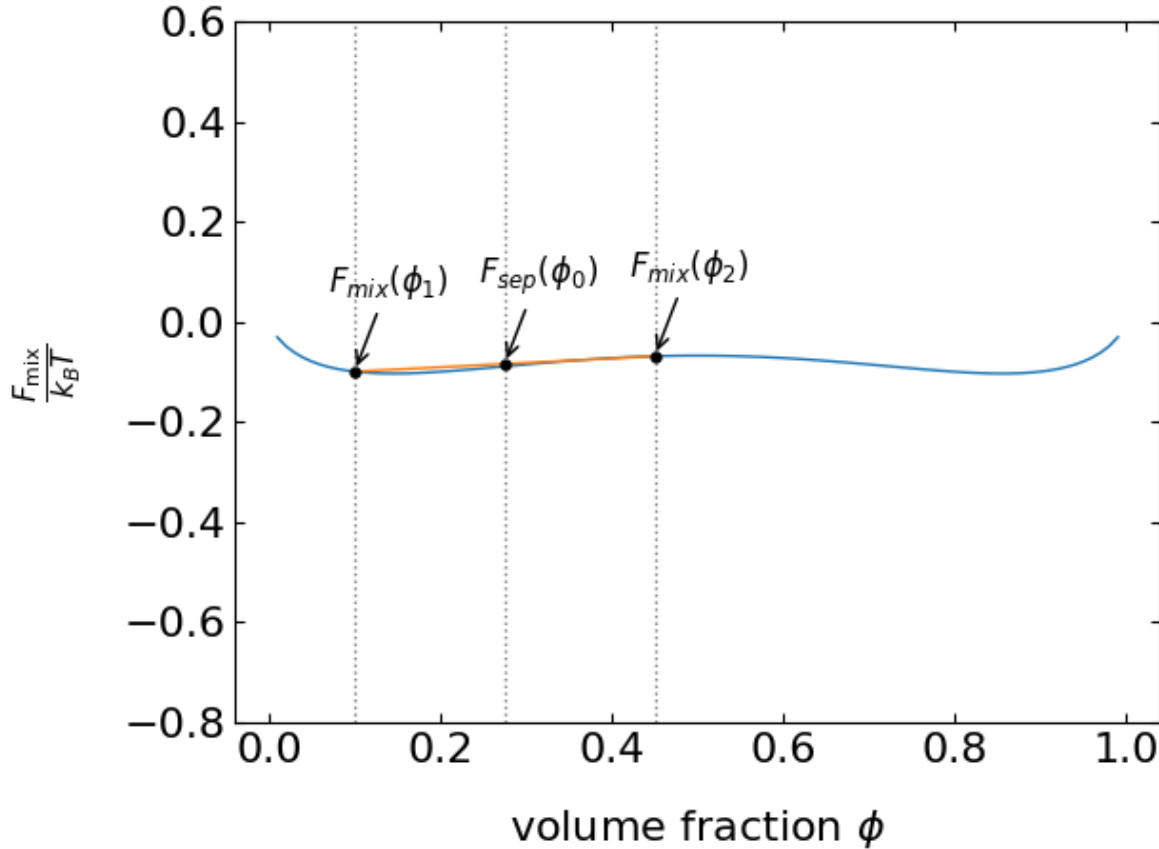


Figure 8.3: mixing free energy example

Let's change the free energy curve to a situation with a maximum at $\phi = 0.5$. If we look at two situations, where one is in the region of the maximum and the second is next to the minimum (???). Close to the maximum, the line with the free energy of the separate components always falls below the free energy curve of the mixture. The composition is therefore **unstable**. Close to the minimum, however, the composition is stable, yet, the mixture is not at the minimum of the free energy curve. Eventually, the system will evolve towards the free energy minimum and thus the mixture is called **metastable**.

```

# calculate mixing free energy
#@interact(x=widgets.FloatSlider(min=0, max=5, step=0.5))
def mix(x):
    m=phi*np.log(phi)+(1-phi)*np.log(1-phi)+x*phi*(1-phi)
    #
    phi_1 = 0
    phi_2 = 0
    F_mix_1 = 0
    F_mix_2 = 0
    #
    if x <= 2:
        phi_1 = 0.1
        phi_2 = 0.8
    #
    if x > 2:
        phi_2 = 0.45
        phi_1 = 0.1
    #
    F_mix_1 = phi_1*np.log(phi_1)+(1-phi_1)*np.log(1-phi_1)+x*phi_1*(1-phi_1)
    F_mix_2 = phi_2*np.log(phi_2)+(1-phi_2)*np.log(1-phi_2)+x*phi_2*(1-phi_2)
    phi_0 = 0.5*phi_1 + 0.5*phi_2
    # F_sep = phi_0*np.log(phi_0)+(1-phi_0)*np.log(1-phi_0)+x*phi_0*(1-phi_0)
    F_sep = 0.5*F_mix_1 + 0.5*F_mix_2
    #
    plt.plot(phi,m)
    plt.plot([phi_1, phi_2], [F_mix_1, F_mix_2])
    plt.axvline(phi_1, color="gray", linestyle="dotted")
    plt.scatter(phi_1, F_mix_1, marker=".", s=50, color="black", zorder=2)
    plt.axvline(phi_2, color="gray", linestyle="dotted")
    plt.scatter(phi_2, F_mix_2, marker=".", s=50, color="black", zorder=2)
    plt.axvline(phi_0, color="gray", linestyle="dotted")
    plt.scatter(phi_0, F_sep, marker=".", s=50, color="black", zorder=2)
    #
    #
    # dynamically annotate the 1st mixture
    xytext_1 = (0, 0)
    if x < 3: xytext_1 = (-10, 30)
    if x >= 3: xytext_1 = (-30, 20)
    plt.annotate(r'$F_{\{mix\}}(\phi_1)$',
                xy=(phi_1, F_mix_1),
                xytext=xytext_1,
                textcoords='offset points',

```

```

#           arrowprops=dict(facecolor='black', arrowstyle='->'))
#
#   # dynamically annotate the separation mixture
#   xytext_sep = (0, 0)
#   if x < 3: xytext_sep = (-10, 30)
#   if x >= 3: xytext_sep = (0, -20)
#   plt.annotate(r'$F_{\rm sep}(\phi_0)$',
#               xy=(phi_0, F_sep),
#               xytext=xytext_sep,
#               textcoords='offset points',
#               arrowprops=dict(facecolor='black', arrowstyle='->'))
#
#   # dynamically annotate the 2nd mixture
#   xytext_2 = (0, 0)
#   if x < 3: xytext_2 = (-10, 30)
#   if x >= 3: xytext_2 = (0, -20)
#   plt.annotate(r'$F_{\rm mix}(\phi_2)$',
#               xy=(phi_2, F_mix_2),
#               xytext=xytext_2,
#               textcoords='offset points',
#               arrowprops=dict(facecolor='black', arrowstyle='->'))
#
#
#   plt.ylabel(r"$\frac{F_{\rm mix}}{k_B T}$")
#   plt.xlabel(r"volume fraction $\phi$")
#   plt.ylim(-0.8, 0.6)
#   plt.tight_layout()
#   plt.savefig("./img/mix_example.png", bbox_inches="tight")
#   plt.show()

```

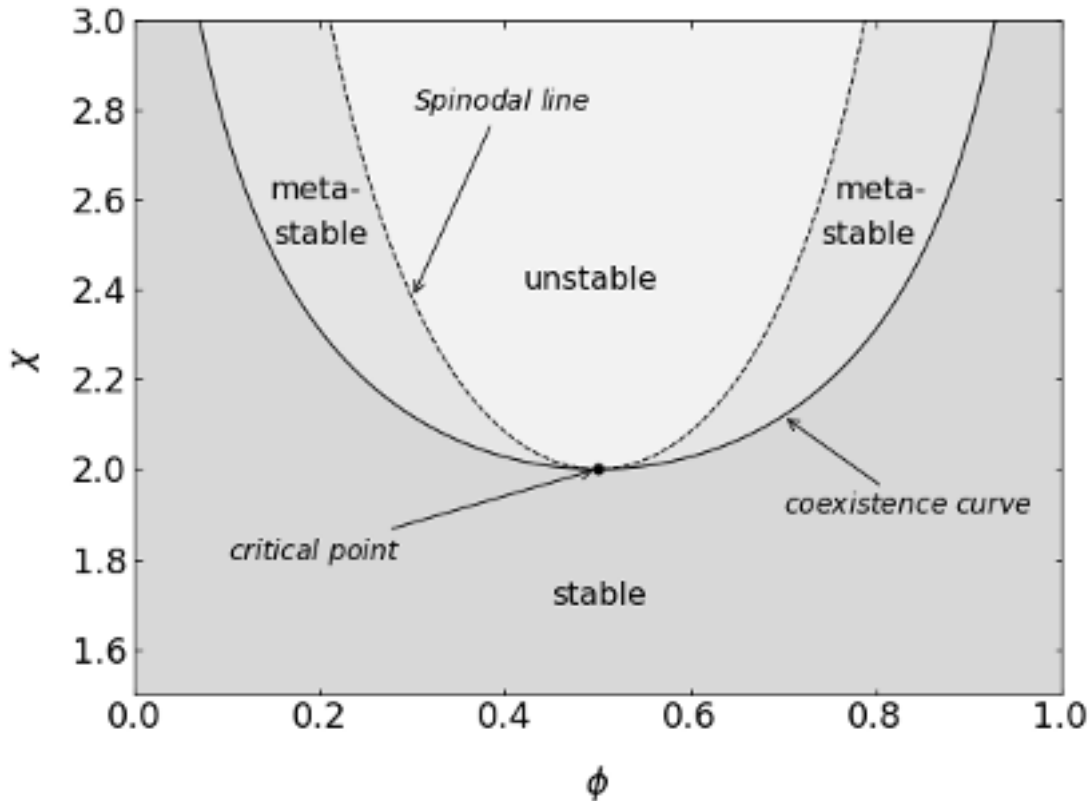


Figure 8.4: image-2.png

Apparently the above analysis has done nothing else than measuring the sign of the curvature of the free energy curve. We can summarize the conditions as

$$\frac{d^2 F_{\text{mix}}}{d\phi^2} > 0 \dots \text{stable}$$

$$\frac{d^2 F_{\text{mix}}}{d\phi^2} < 0 \dots \text{unstable}$$

$$\frac{d^2 F_{\text{mix}}}{d\phi^2} = 0 \dots \text{spinodal line}$$

$$\frac{d^3 F_{\text{mix}}}{d\phi^3} = 0 \dots \text{critical point}$$

The spinodal line therefore separates the metastable from the unstable region. It corresponds to the inflection points of the free energy curve. The critical point, beyond which no phase

separation can be achieved at any concentration ϕ , is defined by setting the third derivative to zero.

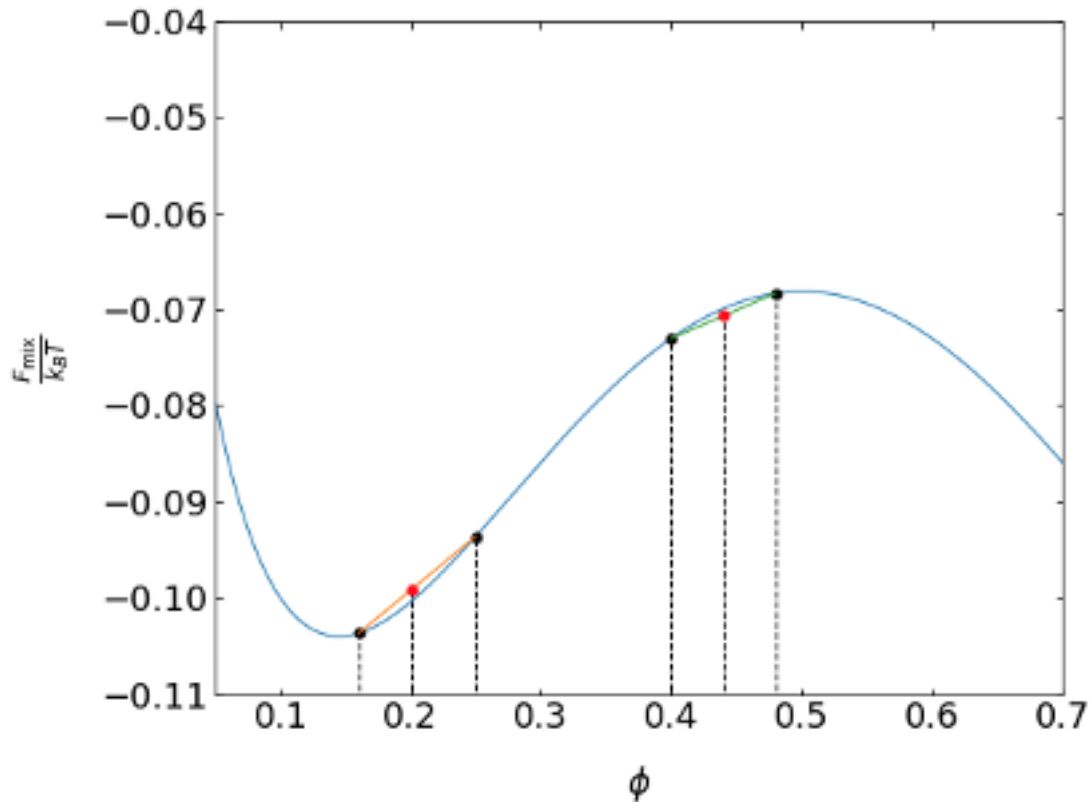


Figure 8.5: image-3.png

Phase diagram of an ideal mixture. The interaction parameter is plotted as a function of the composition. The individual regions as defined by the above equation are indicated.

We can now plot this free energy of mixing as a function of the volume fraction of component A.

Part VII

Lecture 6

9 Kinetics of Liquid–Liquid Unmixing

```
import numpy as np
import matplotlib.pyplot as plt

%config InlineBackend.figure_format = 'retina'
# the lines below set a number of parameters for plotting, such as label font size,
# title font size, which you may find useful
plt.rcParams.update({'font.size': 14,
                     'font.family':'sans-serif',
                     'axes.titlesize': 16,
                     'axes.labelsize': 18,
                     'axes.labelpad': 14,
                     'lines.linewidth': 1,
                     'lines.markersize': 10,
                     'xtick.labelsize' : 18,
                     'ytick.labelsize' : 18,
                     'xtick.top' : True,
                     'xtick.direction' : 'in',
                     'ytick.right' : True,
                     'ytick.direction' : 'in',})
```

If two liquids are brought together at a composition that is either unstable or metastable, they will phase separate. The kinetics of this phase separation can proceed in different ways.

1. **Spinodal Decomposition** – In this case, thermal fluctuations will amplify density fluctuations. The material will diffuse “uphill” to the regions of higher concentration to yield phase separation. The boundaries of the two phases are blurred in this case. Spinodal decomposition is the process of phase separation in the *unstable region*.
2. **Nucleation** – In the case of nucleation, a thermal fluctuation will create a nucleus of a critical size, which further grows in time. The nucleus has a sharp boundary with the other phase. Nucleation is the process of phase separation in the *metastable region*.

We will treat both kinetic regimes separately.

9.3.2 Spinodal decomposition

Based on Fick's law, we know that the diffusion currents occur in the direction against a composition gradient, i.e., $J = -D\nabla\phi$. The result of that diffusion process is an equal composition in the whole sample. For phase separation to happen, material needs to flow from regions of low concentration to regions of higher concentration, so in the direction of the composition gradient. Material transport is therefore not balancing composition gradients. In the section about the chemical potential, we learned that in an open system the chemical potential of all species is balanced. The chemical potential is given by

$$\mu = \left. \frac{dF}{d\phi} \right|_{V,T}.$$

If now the second derivative of the free energy with respect to ϕ is positive, the regions with larger ϕ have larger free energy. Thus regions of lower concentration are favored by the free energy and the diffusion happens to be downhill as given also by Fick's law. If the second derivative of the free energy is, however, negative, then fluctuations in the composition will lower the free energy and, thus, the fluctuations will grow in strength. The fluctuations with different length scales will, however, not grow at the same rate. The spectrum of growth rates can be described by a phenomenological theory known as the Cahn–Hilliard equation, which is applied in many fields. To arrive at that equation, we need to describe the free energy in terms of composition gradients

$$F = A \int \left[f_0(\phi) + \kappa \left(\frac{d\phi}{dx} \right)^2 \right] dx.$$

Here, f_0 is the free energy density, A an area, and x a linear coordinate. To balance the chemical potentials we need to modify Fick's laws

$$J = -D \frac{d\phi}{dx}, \quad \frac{d\phi}{dt} = -\frac{dJ}{dx}, \quad \frac{\partial\phi}{\partial t} = D \frac{\partial^2\phi}{\partial x^2}$$

to an appropriate new law

$$J = -M \frac{d\mu}{dx},$$

where $\mu = \mu_A - \mu_B$ is the difference between the chemical potentials of A and B. This is apparently a linear approximation. According to the definition of the chemical potential, we obtain

$$\mu = \frac{d}{d\phi} \left[f_0(\phi) + \kappa \left(\frac{d\phi}{dx} \right)^2 \right]$$

from which follows

$$\mu = \frac{df_0}{d\phi} + 2\kappa \frac{d^2\phi}{dx^2},$$

where it was applied that

$$\frac{d}{d\phi} \left(\frac{d\phi}{dx} \right)^2 = 2 \frac{d^2\phi}{dx^2}.$$

Inserting this into our modified Fick's law yields

$$J = -Mf_0'' \frac{d\phi}{dx} - 2M\kappa \frac{d^3\phi}{dx^3}$$

with $f_0'' = \frac{d^2f_0}{d\phi^2}$. Finally, inserting the above equation into the continuity equation yields

$$\frac{\partial\phi}{\partial t} = Mf_0'' \frac{\partial^2\phi}{\partial x^2} + 2M\kappa \frac{\partial^4\phi}{\partial x^4}.$$

This is the **Cahn–Hilliard** equation, which extends the diffusion equation for interacting species. The term in front of the second derivative yields an effective diffusion coefficient, i.e., $D_{\text{eff}} = Mf_0''$. While the coefficient M (the Onsager coefficient) is always positive, the second derivative of the free energy density f_0 can be positive or negative. Inside the spinodal line, for example, the curvature of the free energy is negative. Following that, the effective diffusion coefficient is negative, which allows for our uphill diffusion. The Cahn–Hilliard equation can be solved by a Fourier decomposition which yields

$$\phi(x, t) = \phi_0 + A \cos(qx) \exp \left[-D_{\text{eff}} q^2 \left(1 + \frac{2\kappa q^2}{f_0''} \right) t \right].$$

Here q is a wavenumber defining the wavelength of the fluctuations. The exponent can be abbreviated by

$$R(q) = -D_{\text{eff}} q^2 \left(1 + \frac{2\kappa q^2}{f_0''} \right)$$

which is nothing else than an inverse time or a rate coefficient. It provides the relaxation rate for a specific wavenumber. This rate coefficient is positive up to a certain wavenumber q_0 . All fluctuations with wavelengths larger than $\lambda_0 = 2\pi/q_0$ are amplified in time. The fastest-growing fluctuation is obtained at q_{\max} . This wavenumber sets the length scale of the structures, which typically appear during the spinodal decomposition.

Spinodal decomposition

Here is an example of the structure formation by spinodal decomposition taken from a recent paper:

[Prum, R. O., Dufresne, E. R., Quinn, T. & Waters, K. Development of colour-producing -keratin nanostructures in avian feather barbs. J. R. Soc. Interface 6, \(2009\).](#)

The feathers of birds (see image) or even butterflies are in many cases not color because they contain dye molecules whose electronic transitions yield selective absorption.



Figure 9.1: barb

Rather than that, these feathers are equipped with nanostructures at a given lengthscale which coherently scatter light as a Bragg lattice for example, or a photonic crystal. The image below shows two examples of such nanostructures that can selectively scatter light.

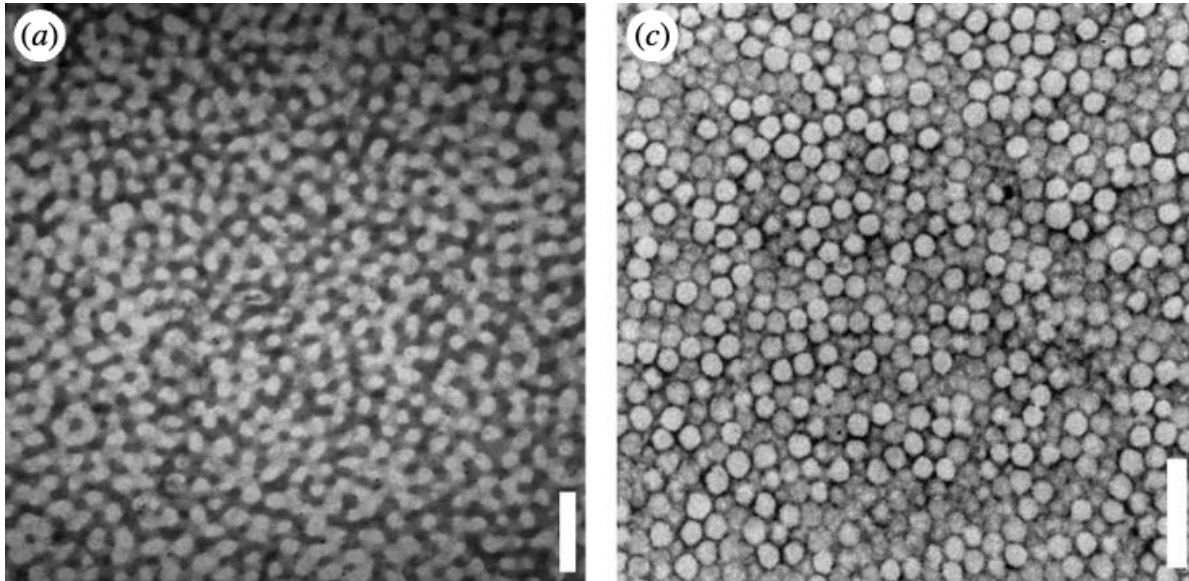


Figure 9.2: barb_structure

These structures are supposed to be formed by spinodal decomposition or nucleation and growth.

9.3.3 Nucleation

Nucleation is the phenomenon of spontaneously generating a phase-separated volume by thermal fluctuations. By doing that, we create an interface between the two phases, which costs energy. We, therefore, have a first simple look at the interfacial energy.

9.3.3.1 Interfacial Tension

If we have a system of two components A and B and those components do not mix but form an interface, then, due to the fact that both sorts of molecules repel each other, we have to spend energy to bring them together. The work done to create an interfacial area is

$$W = F\Delta x = \gamma L\Delta x,$$

where γ denotes the interfacial energy. If work is done, this would require an energy exchange with a reservoir to keep the temperature constant. That, however, also means that the interfacial energy is a free energy per unit area rather than an internal energy. Interfacial energies may contain entropic contributions. In the case of a sharp interface, we can use the interaction parameter χ and the molecular volume v to show

$$\gamma = \frac{1}{2v^{2/3}}(2\epsilon_{AB} - \epsilon_{AA} - \epsilon_{BB}) = \frac{\chi k_B T}{zv^{2/3}}.$$

If we have a liquid mixture now at a certain composition, which is in the metastable region, i.e., $\frac{\partial^2 F}{\partial \phi^2} > 0$, all of the density fluctuations in our system are damped and the spinodal decomposition cannot happen. Therefore, the system has to phase separate by nucleation, i.e., that spontaneously a droplet of a certain size is formed and grows further. As we need energy to create the interface but also gain free energy by forming a volume phase, we need to have a look at the total free energy change when the droplet is formed.

- The volume part is delivering a free energy gain per volume of $\Delta F_v < 0$, which has to be multiplied with the volume of the droplet.
- The creation of an interface requires interfacial energy γ , which is always positive and has to be multiplied with the droplet surface area.

Thus, the total free energy change reads

$$\Delta F(r) = \frac{4}{3}\pi r^3 \Delta F_v + 4\pi r^2 \gamma.$$

Note that the first term is negative as ΔF_v is negative. A typical free energy change with the particle size is shown in the figure below. It has a maximum at the position r^* , which creates a nucleation barrier ΔG^* . Droplets which are spontaneously formed at $r < r^*$ can decrease their free energy by dissolving.

```
def dG(r,dT):
    gamma_sl=38e-3 #(38mJ/m^2)
    Tm=273.15
    dHm=3.34e8 # (J/m^3)
    return(-4*np.pi*r**3*dHm*dT/Tm/3+4*np.pi*r**2*gamma_sl)
```

```
plt.figure(figsize=(8,6))
r=np.linspace(0,1e-8,100)
kbT=3.769e-21
plt.plot(r*1e9,dG(r,10)/kbT,'k-')
plt.xlabel(' radius $r$ [nm] ')
plt.ylabel('free energy change $\Delta G/k_B T$')
```

```
plt.axhline(y=0,ls='--')
plt.tight_layout()
plt.show()
```

ergy change $\Delta G/k_B T$

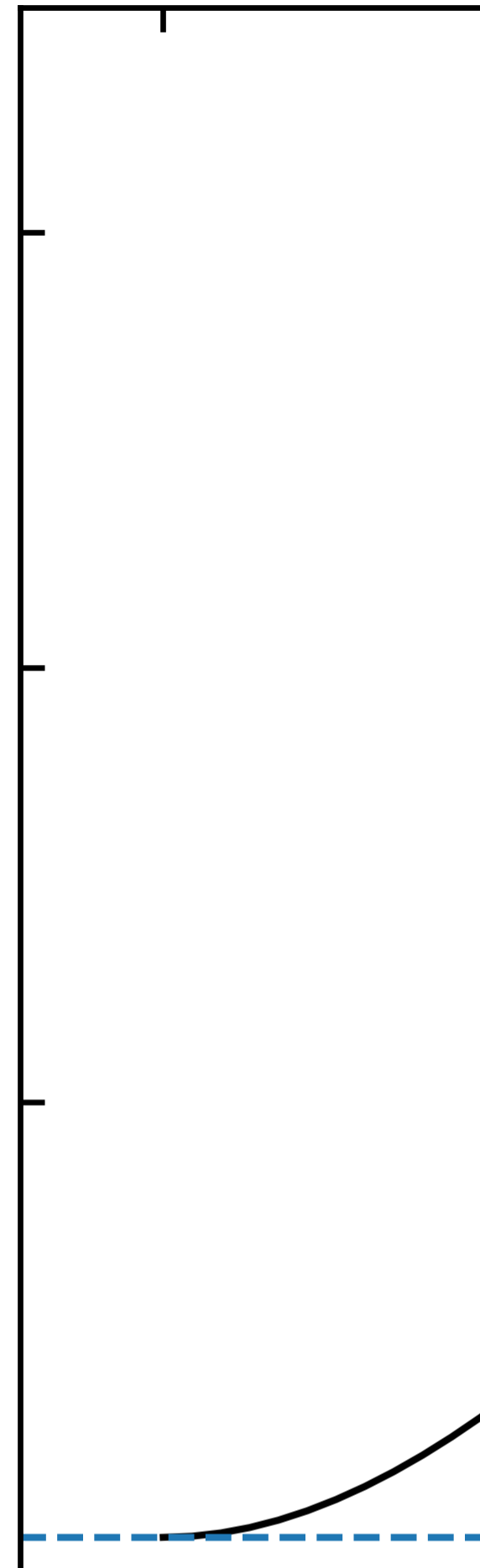
1500

1000

500

80

0



Liquid-Liquid Unmixing - Ouzo Effect

One example of liquid-liquid unmixing by nucleation is the Ouzo or Louche effect. The name denotes the spontaneous formation of a turbid microemulsion when a solution of anethol in ethanol is diluted with water. The figure below shows the phase diagram of this ternary mixture, meaning that it has three components.

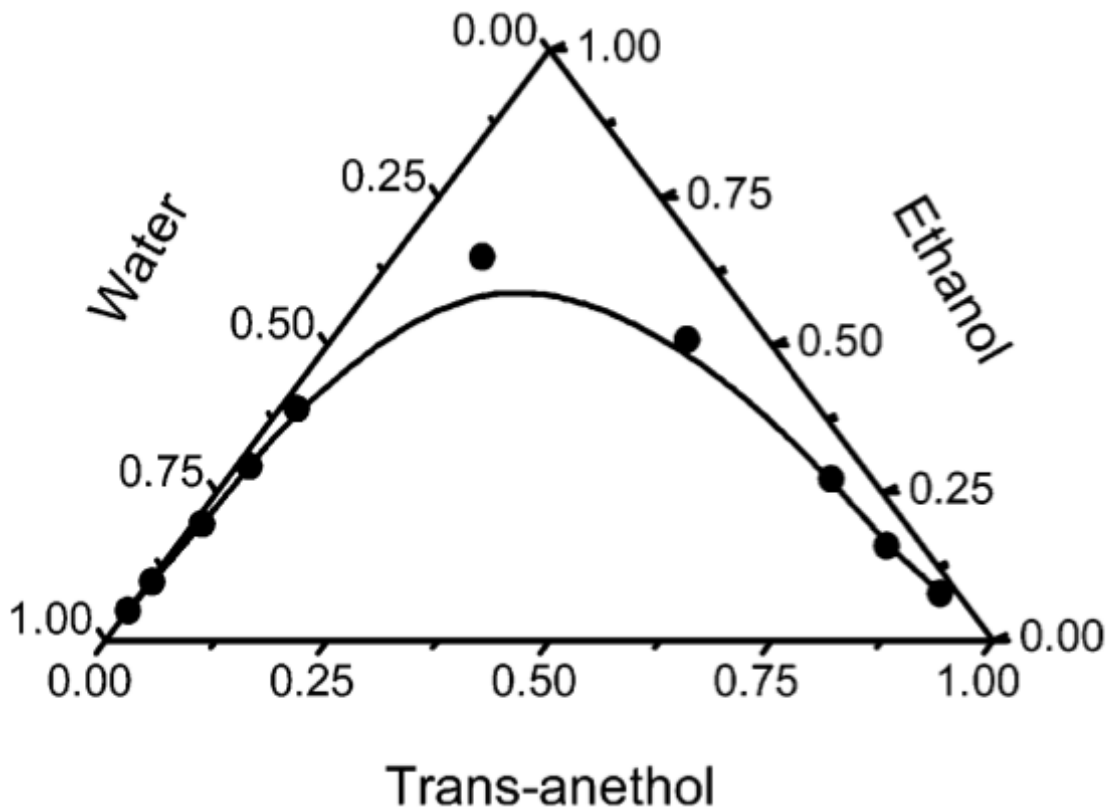


Figure 9.3: ouzo

When the emulsification happens, the solution rapidly moves to the metastable region between the binodal and spinodal lines. It occurs because the alcohol, as it diffuses from the anethol into the water, carries with it some of the anethol molecules that still have a finite solubility in alcohol and alcohol/water mixtures. As the alcohol diffuses further into the water, the associating anethol(oil) molecules become expelled from the water-rich solution and are stranded in the form of fine emulsion droplets. Thus, adding water to a solution of homogeneous oil/ethanol mixtures leads to an abrupt decrease of the solubility of oil in the water-rich continuous phase. This effect causes the strong local concentration fluctuations of solute molecules and homogeneous nucleation can start.

The image below shows the turbidity of the emulsion to appear as the water content is changed.

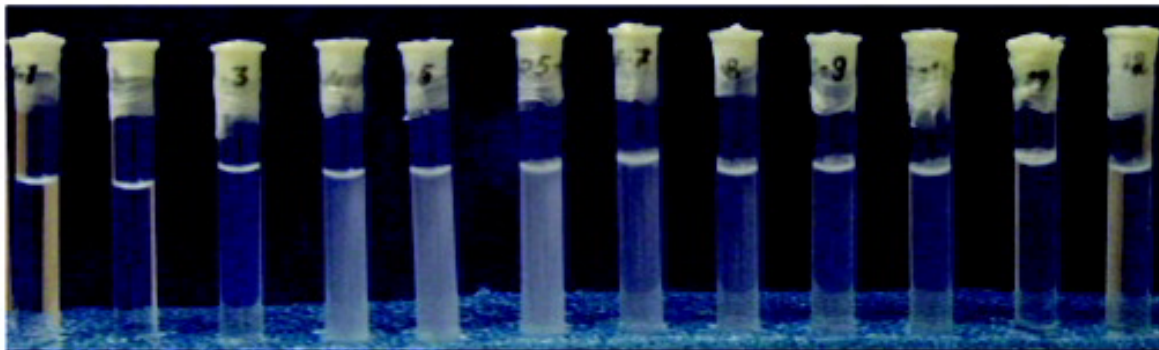


Figure 9.4: ouzo_1

The data has been taken from: Sitnikova, N. L., Sprik, R., Wegdam, G. & Eiser, E. Spontaneously Formed trans-Anethol/Water/Alcohol Emulsions: Mechanism of Formation and Stability. Langmuir 21, 7083–7089 (2005).

Nucleation and Growth

Another example of nucleation and growth is the growth of tiny ssemiconductor nanocrystals from solution. Such quantum dots confine electron hole pairs and have size dependent optical properties. This finding was awarded with the nobel prize in chemistry in 2023.

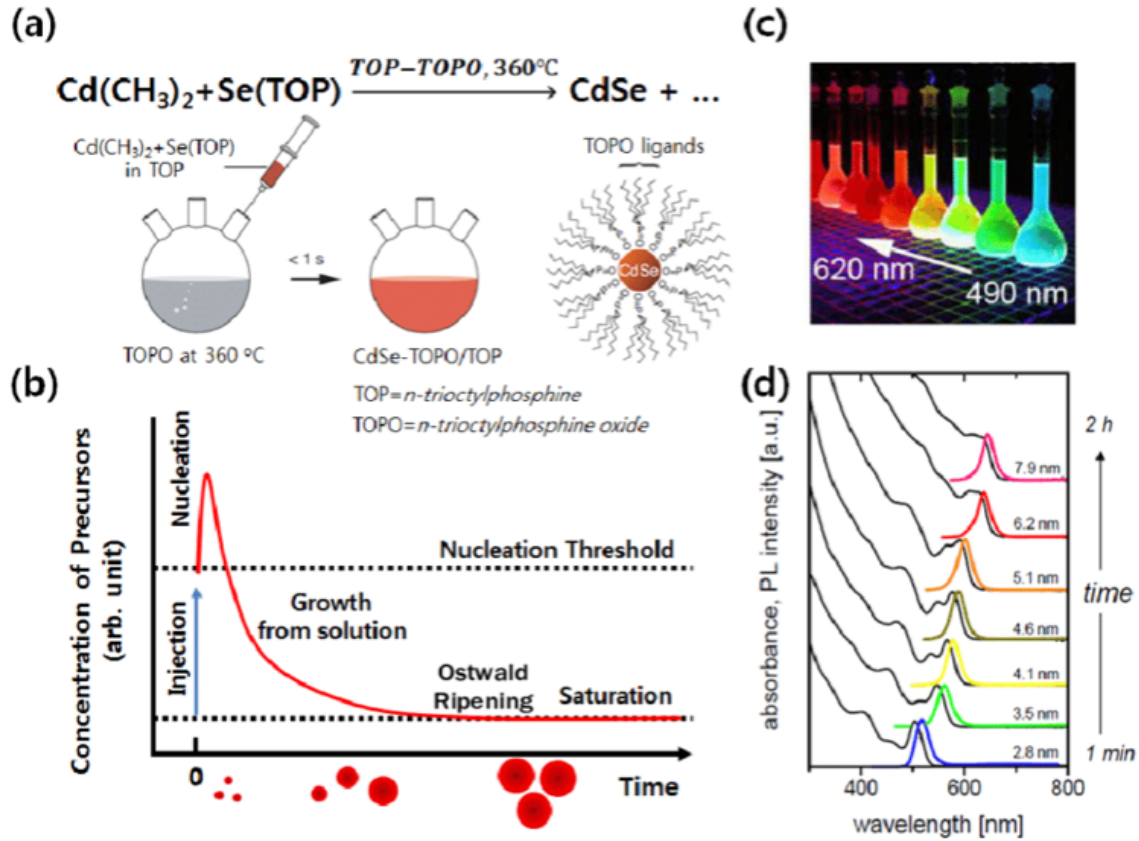


Figure 9.5: nucleation_growth

Part VIII

Lecture 7

10 Solid–Liquid Phase Transitions

```
import numpy as np
import matplotlib.pyplot as plt

%config InlineBackend.figure_format = 'retina'
# the lines below set a number of parameters for plotting, such as label font size,
# title font size, which you may find useful
plt.rcParams.update({'font.size': 14,
                     'font.family':'sans-serif',
                     'axes.titlesize': 16,
                     'axes.labelsize': 18,
                     'axes.labelpad': 14,
                     'lines.linewidth': 1,
                     'lines.markersize': 10,
                     'xtick.labelsize' : 18,
                     'ytick.labelsize' : 18,
                     'xtick.top' : True,
                     'xtick.direction' : 'in',
                     'ytick.right' : True,
                     'ytick.direction' : 'in',})
```

When a liquid is cooled down and reaches the (freezing) melting temperature, the liquid may enter the solid phase. Directly at the melting temperature, the free energy of the solid and the liquid are the same (also the chemical potentials). When forming a crystal, the system needs to spend energy on creating the interface between liquid and solid, which requires a surface free energy to come from somewhere. The transition from the liquid to the solid, however, is not freeing any energy. As a result, the liquid cannot freeze directly at the freezing temperature. To freeze the liquid, undercooling is required. An undercooling by a temperature ΔT would create a free energy difference ΔG between liquid and solid.

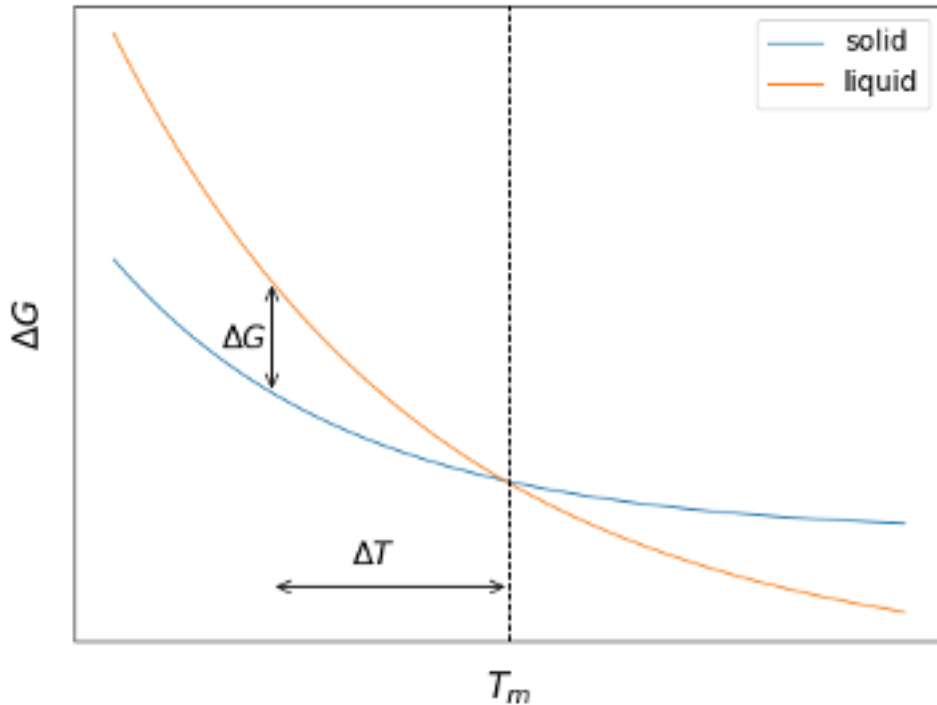


Figure 10.1: image-2.png

Free energy of solid and liquid phase of a material as a function of temperature

10.0.1 Kinetics of the Liquid–Solid Phase Transition

To start the phase transition from a liquid to a solid in the undercooled liquid, a nucleus of a certain size has to appear from thermal fluctuations. This goes along the lines we discussed for the liquid-liquid phase transitions. To create a nucleus of a radius r we need a free energy change

$$\Delta G = \frac{4}{3}\pi r^3 \Delta G_b + 4\pi r^2 \gamma_{sl},$$

where ΔG_b is the free energy change per unit volume when creating the volume phase of the solid material. γ_{sl} denotes the interfacial free energy for the solid/liquid contact. We also know that at a first-order phase transition all energy inserted into the system (the latent heat ΔH_m at the melting temperature T_m) is going into a change in the entropy of the system, i.e.,

$$\Delta S_m = \left(\frac{\partial G_s}{\partial T} \right)_p - \left(\frac{\partial G_l}{\partial T} \right)_p = \frac{\Delta H_m}{T_m}.$$

We can, therefore, extrapolate the free energy change at the undercooled temperature by

$$\Delta G_b = -\frac{\Delta H_m}{T_m} \Delta T$$

which yields

$$\Delta G = -\frac{4}{3}\pi r^3 \frac{\Delta H_m}{T_m} \Delta T + 4\pi r^2 \gamma_{sl}.$$

According to our nucleation theory, this yields a critical radius of the nucleus of

$$r^* = \frac{2\gamma_{sl} T_m}{\Delta H_m \Delta T}.$$

A nucleus of size $r < r^*$ would thus have the tendency to dissolve again, while a nucleus of size $r > r^*$ is ready to grow continuously. The critical radius of the nucleus corresponds to a free energy barrier

$$\Delta G^* = \frac{16\pi}{3} \gamma_{sl}^3 \left(\frac{T_m}{\Delta H_m} \right)^2 \frac{1}{\Delta T^2}.$$

The probability of critical nucleus formation can thus be determined from the Boltzmann factor

$$e^{-\frac{\Delta G^*}{k_B T}}$$

which is a very strong function of temperature. Inserting typical values, e.g., for water/ice, we find the following free energies as a function of the nucleus radius ($\Delta T = 10$ K).

```
def dG(r,dT):
    gamma_sl=38e-3 #(38mJ/m^2)
    Tm=273.15
    dHm=3.34e8 # (J/m^3)
    return(-4*np.pi*r**3*dHm*dT/Tm+3+4*np.pi*r**2*gamma_sl)
```

```
plt.figure(figsize=(8,6))
r=np.linspace(0,1e-8,100)
kbT=3.769e-21
plt.plot(r*1e9,dG(r,10)/kbT, 'k-')
plt.xlabel(' radius $r$ [nm] ')
plt.ylabel('free energy change $\Delta G/k_B T$')
plt.axhline(y=0,ls='--')
plt.tight_layout()
plt.show()
```

ergy change $\Delta G/k_B T$

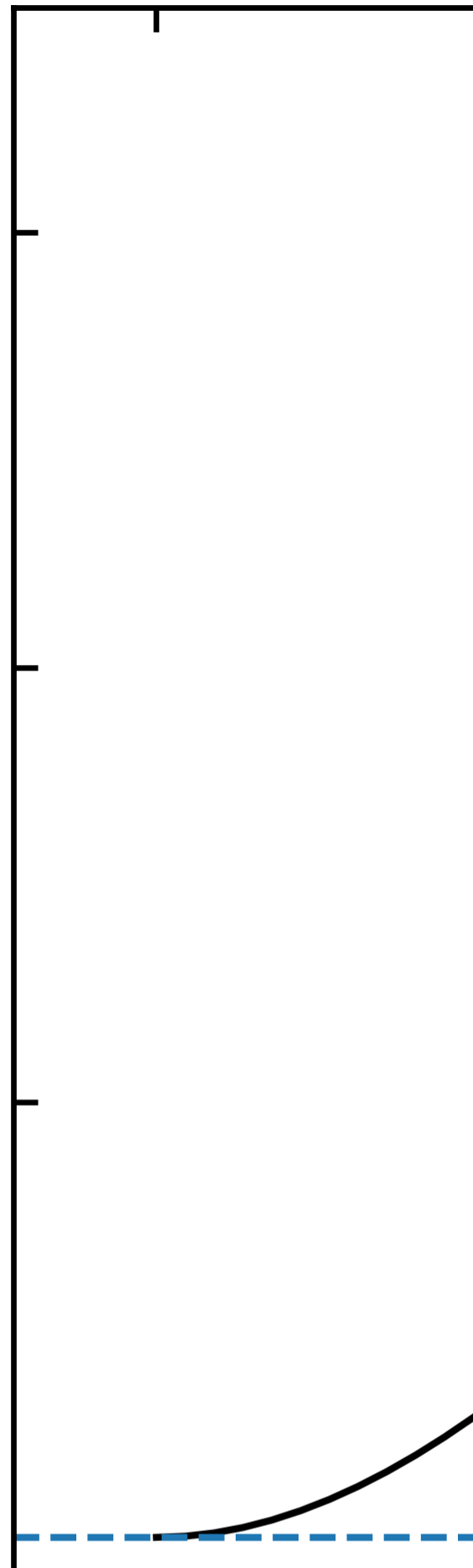
1500

1000

500

89

0



The free energy barrier is therefore about 1500 times bigger than the thermal energy. Homogeneous nucleation from the bulk liquid phase thus essentially never happens. Even at a strong undercooling of about 50 K as shown in the plot below, the free energy barrier is about 65 times bigger than the thermal energy.

```
def dGstar(dT):
    gamma_sl=38e-3 #(38mJ/m^2)
    Tm=273.15
    dHm=3.34e8 # (J/m^3)
    return(16*np.pi*gamma_sl**3*(Tm/dHm)**2/dT**2/3)
```

```
plt.figure(figsize=(8,6))
dt=np.linspace(10,50)
kbT=3.769e-21
plt.plot(dt,dGstar(dt)/kbT)
plt.xlabel(r'$\Delta T$ [K]')
plt.ylabel(r'$\Delta G^*/k_B T$')
plt.tight_layout()
plt.show()
```

$\Delta G^*/k_B T$

1600

1400

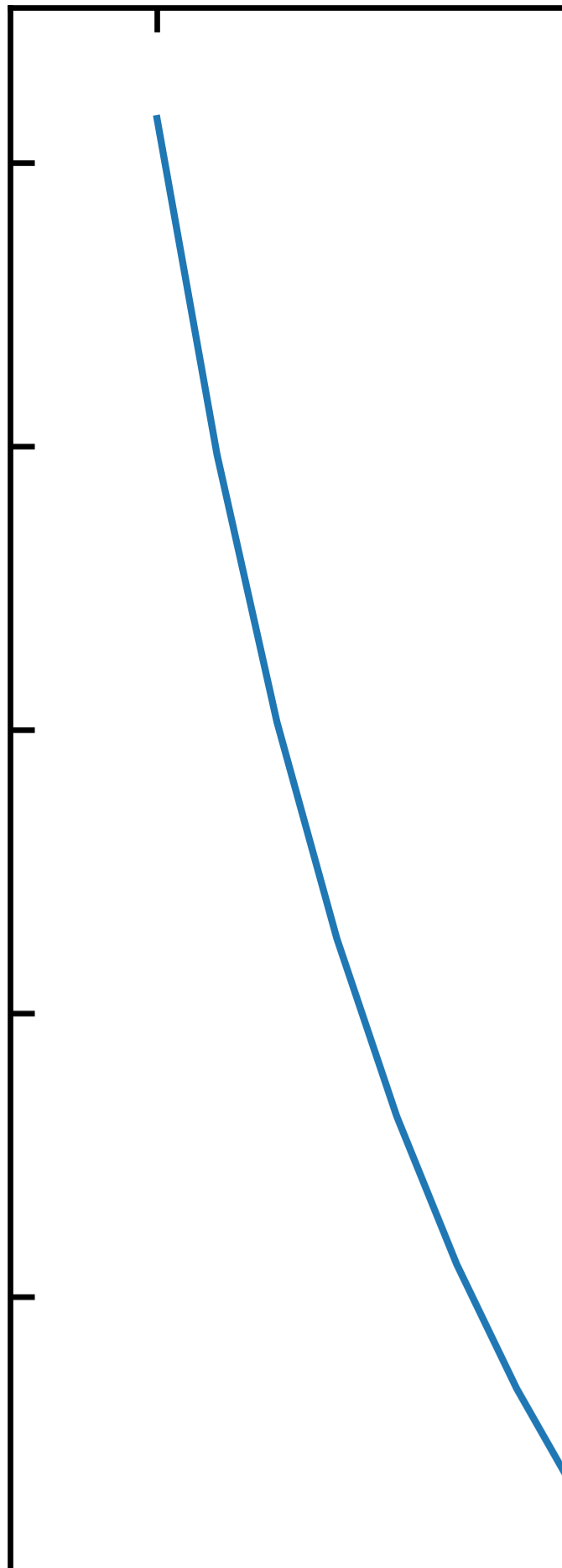
1200

1000

800

600

91



According to that, homogeneous nucleation, i.e., the freezing of a liquid is very unlikely and actually does not happen. More likely are heterogeneous nucleation events, which occur at the boundaries of the container or at impurities.

10.0.2 Heterogeneous Nucleation

To study the process of heterogeneous nucleation, we have a look at a container wall, which acts as a nucleation catalyst. At this container wall, a solid droplet in the form of a spherical cap exists.

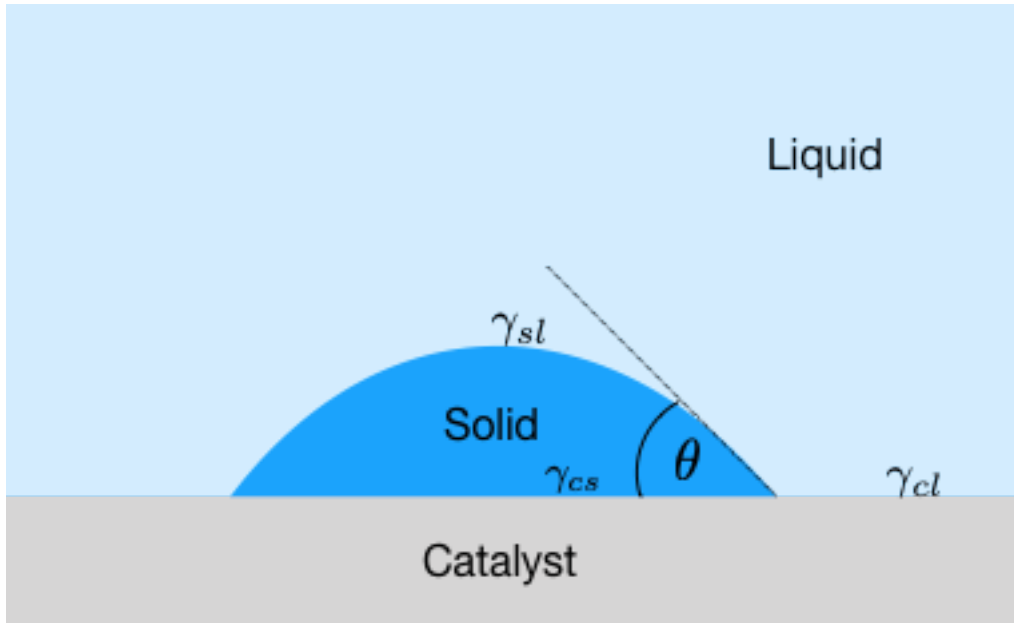


Figure 10.2: image-5.png

The solid material shall have a contact angle of θ with the catalyst surface. In this case, the contact angle obeys Young's law $\gamma_{sl} \cos(\theta) = \gamma_{cl} - \gamma_{cs}$. Further, for the calculation of the volume and interfacial contributions, we need the volume and the surfaces of the spherical cap as well as the surface at the catalyst interface, which all together read:

$$V = \frac{1}{3}\pi r^3(1 - \cos(\theta))^2(2 + \cos(\theta)),$$

$$S_{sl} = 2\pi r^2(1 - \cos(\theta)),$$

$$S_{cs} = \pi r^2 \sin^2(\theta).$$

Following the earlier arguments, we can write down the free energy change upon nucleation of a spherical cap of a radius r at the catalyst surface as:

$$\begin{aligned}\Delta G(r) = & \frac{1}{3}\pi r^3(1 - \cos(\theta))^2(2 + \cos(\theta)) \\ & + \gamma_{\text{sl}}2\pi r^2(1 - \cos(\theta)) \\ & + \gamma_{\text{cs}}\pi r^2 \sin^2(\theta) \\ & - \gamma_{\text{cl}}\pi r^2 \sin^2(\theta).\end{aligned}$$

With the help of Young's equation, we can simplify this to:

$$\Delta G^* = \frac{16\pi}{3}\gamma_{\text{sl}}^3 \left(\frac{T_m}{\Delta H_m} \right)^2 \frac{1}{\Delta T^2} \left(\frac{(1 - \cos(\theta))^2(2 + \cos(\theta))}{4} \right).$$

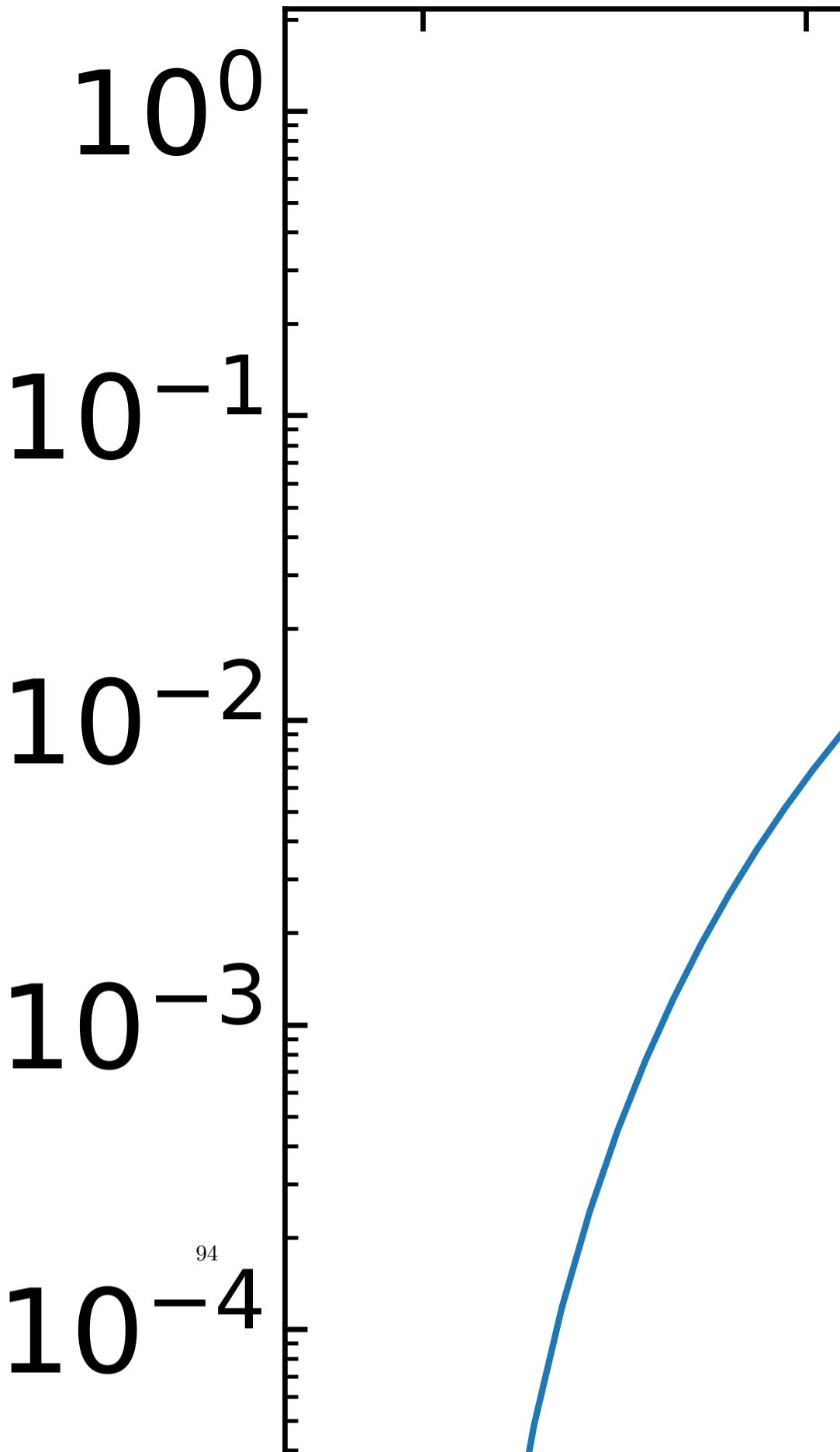
The latter fraction is actually only an additional geometrical factor that depends only on θ , while all factors before just resemble the homogeneous nucleation result. The graph below displays this geometrical factor $f(\theta)$ as a function of the contact angle θ and indicates that the creation of a nucleus with a certain contact angle at a solid wall considerably lowers the nucleation barrier. The nucleation barrier can thus be easily as low as thermal energy, as shown in the graph below for the water/ice system. The nucleus size in that model stays the same, while a contact angle of about 14° yields a nucleation barrier of $1 k_B T$.

```
def f(theta):
    return((1-np.cos(theta))**2*(2+np.cos(theta))/4)
```

```
theta=np.linspace(0,180,100)
```

```
plt.figure(figsize=(8,6))
plt.semilogy(theta,f(theta*np.pi/180))
plt.xlabel(r'contact angle $\theta$ [°]')
plt.ylabel(r'f($\theta$)')
plt.tight_layout()
plt.show()
```

$f(\theta)$

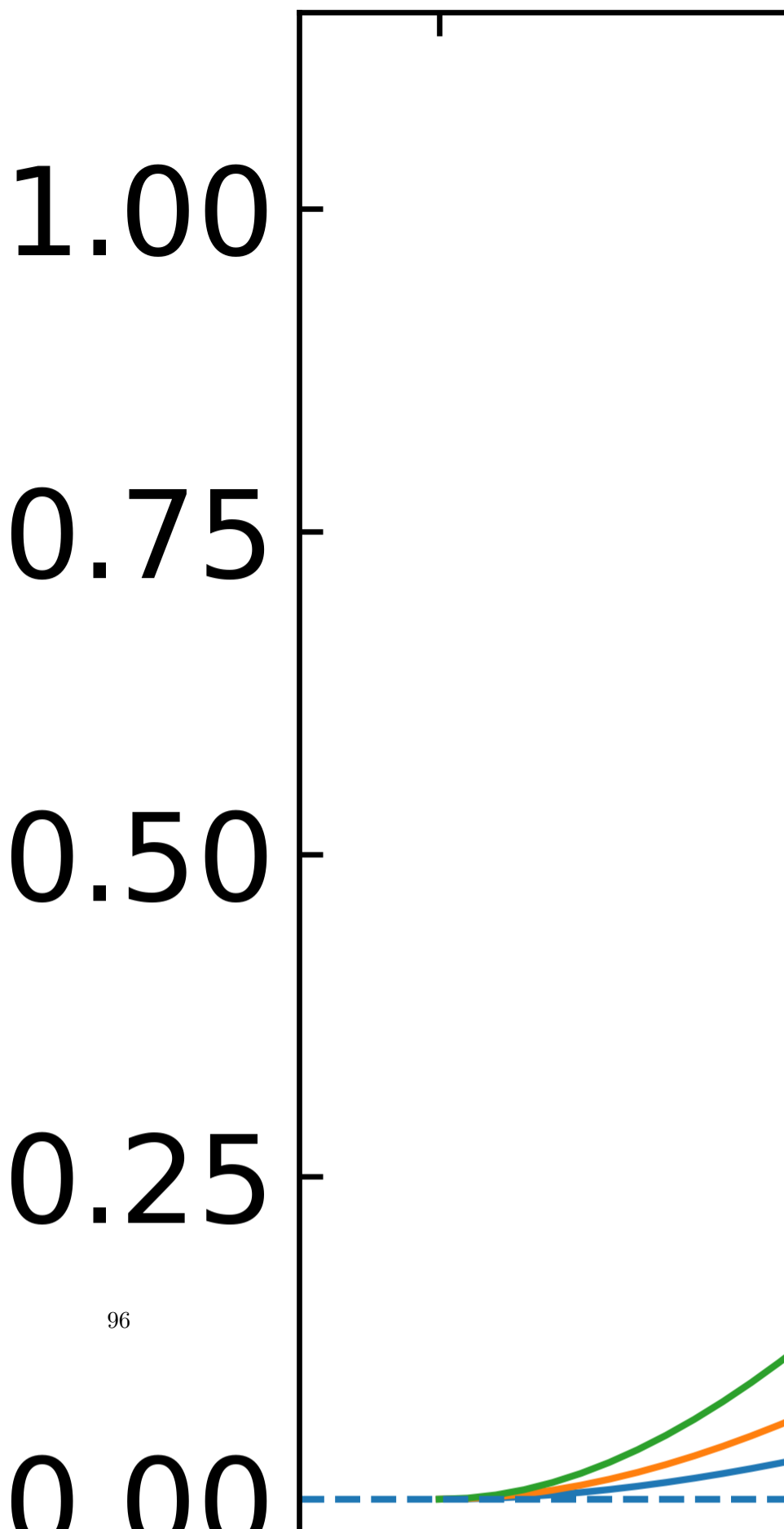


Geometry factor for the heterogeneous nucleation of a droplet with a contact angle at a catalyst wall

```
plt.figure(figsize=(8,6))
r=np.linspace(0,1e-8,100)
kbT=3.769e-21

[plt.plot(r*1e9,dG(r,10)*f(theta*np.pi/180)/kbT,'-',label=str(theta)+"°") for theta in range(0,181,10)]
plt.xlabel(' radius $r$ [nm] ')
plt.ylabel('free energy change $\Delta G/k_B T$')
plt.axhline(y=0,ls='--')
plt.legend()
plt.tight_layout()
plt.show()
```

rgy change $\Delta G/k_B T$



Nucleation barrier as a function of nucleus radius for heterogeneous nucleation at a wall. The curves display the results for the water/ice interface.

10.0.3 Classification of phase transitions

A classification of different phase transitions can be carried out using the scheme of **Ehrenfest**. According to that, a phase transition is categorized based on the order of the derivative of the free energy that shows discontinuity at the transition point.

$$dG = -SdT + VdP + \mu dN$$

$$\left(\frac{\partial G}{\partial T}\right)_P = -S \quad \left(\frac{\partial G}{\partial P}\right)_T = V$$

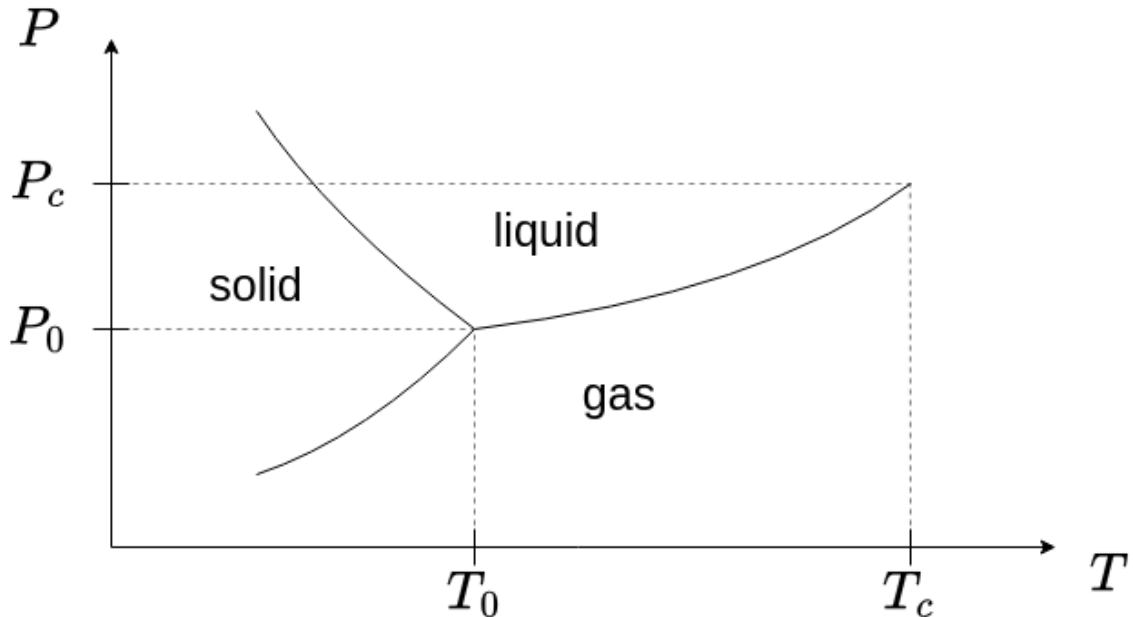


Figure 10.3: classification_fig_01

- phase transitions at the phase boundary
- charge is
 - discontinuous - first order phase transition
 - continuous - second order phase transition

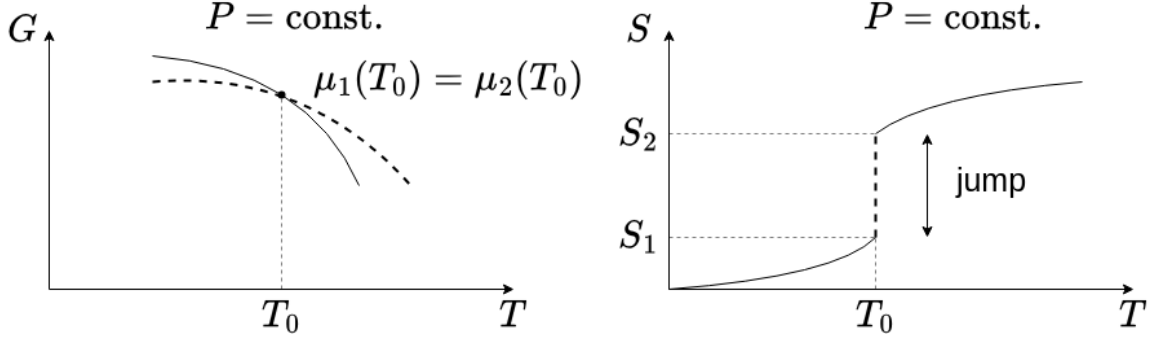


Figure 10.4: classification_fig_02

The Ehrenfest equations with $m = 1, \dots, n - 1$ are

$$\frac{\partial^m G_\alpha}{\partial T^m} \Big|_P = \frac{\partial^m G_\beta}{\partial T^m} \Big|_P \quad \frac{\partial^m G_\alpha}{\partial P^m} \Big|_T = \frac{\partial^m G_\beta}{\partial P^m} \Big|_T$$

and

$$\frac{\partial^m G_\alpha}{\partial T^m} \Big|_P \neq \frac{\partial^m G_\beta}{\partial T^m} \Big|_P \quad \frac{\partial^n G_\alpha}{\partial P^n} \Big|_T = \frac{\partial^n G_\beta}{\partial P^n} \Big|_T.$$

lack at the derivative of G as a fraction of the temperature.

10.0.3.1 1. Order Phase Transitions

$$\frac{\partial G}{\partial T} \Big|_P = -S, \quad \frac{\partial G}{\partial P} \Big|_T = V, \quad \frac{\partial G}{\partial N} \Big|_T = \mu$$

- G has a kink (discontinuous)
- $\simeq S, V$ have a jump
- $\simeq \mu$ has a kink

$$C_P = \left. \frac{dH}{dT} \right|_P = T \left(\frac{\partial S}{\partial T} \right)_P \rightarrow \infty$$

- latent heat \rightarrow melting, evaporation

10.0.3.2 2. Order Phase Transitions

- $G(T, P)$ is continuous
- $S(T, P), V(T, P)$ are continuous
- specific heat

$$C_P = T \left. \frac{\partial S}{\partial T} \right|_P = -T \left(\frac{\partial^2 G}{\partial T^2} \right)_P$$

is discontinuous

- isothermal compressibility

$$\kappa_T = -\frac{1}{V} \left(\frac{\partial V}{\partial P} \right)_T = -\frac{1}{V} \left(\frac{\partial^2 G}{\partial P^2} \right)_T$$

- thermal expansion coefficient

$$\alpha = \frac{1}{V} \left(\frac{\partial V}{\partial T} \right) = \frac{1}{V} \left(\frac{\partial^2 G}{\partial T \partial P} \right)$$

11 Forces and Interactions in Soft Matter

While we have discussed in the previous sections the thermodynamics of systems and the kinetics of phase transitions, we have made as few as possible assumptions on the interactions between the liquid components of a mixture to highlight the importance of entropic and other effects. Now, we would like to have a close look at the possible types of interactions and their order of magnitude in soft matter systems. We may classify the interactions in the following way: - covalent interaction (chemical binding), - electrostatic (Coulomb), - dipolar (vdW), - hydrogen bonding, - dispersion (vdW), - fluctuation, depletion (entropic).

These interactions deliver the forces that hold soft matter together, even though the phases are characterized by *density*, *free energy* and *entropy*, but not by the forces.

```
import numpy as np
import matplotlib.pyplot as plt
from numpy.linalg import norm
from scipy.constants import c,epsilon_0,e,physical_constants

%config InlineBackend.figure_format = 'retina'
# the lines below set a number of parameters for plotting, such as label font size,
# title font size, which you may find useful
plt.rcParams.update({'font.size': 14,
                     'font.family':'sans-serif',
                     'axes.titlesize': 16,
                     'axes.labelsize': 18,
                     'axes.labelpad': 14,
                     'lines.linewidth': 1,
                     'lines.markersize': 10,
                     'xtick.labelsize' : 18,
                     'ytick.labelsize' : 18,
                     'xtick.top' : True,
                     'xtick.direction' : 'in',
                     'ytick.right' : True,
                     'ytick.direction' : 'in',})
```

11.1 Pairwise interaction energy

Before we go into further details, we may have a look at some general behavior again. Let us assume that the interaction energy between two atoms/molecules is given by

$$w(r) = -\frac{C}{r^n} \quad (11.1)$$

with C being an interaction-specific constant, then the force between the two species at a distance r is given by

$$F(r) = -\frac{dw(r)}{dr} = -\frac{nC}{r^{n+1}}. \quad (11.2)$$

For a material, which has a number density ρ and, thus, the total number $\rho 4\pi r^2 dr$ molecules in a shell between $r, r + dr$ around a molecule, we obtain the following total interaction energy per molecule (the standard chemical potential):

$$\mu^0 = \int_{\sigma}^L w(r) \rho 4\pi r^2 dr = \frac{-4\pi C \rho}{(n-3)\sigma^{n-3}} \left[1 - \left(\frac{\sigma}{L} \right)^{n-3} \right]. \quad (11.3)$$

The total interaction energy, and thus also the property of the system will, consequently, depend on the size L of the system, except we assume $n > 3$ and $L \gg \sigma$, where σ is the size of the molecule. This states nothing else, that long range interactions may yield system-dependent properties or bulk properties that do not depend on the volume size only if objects become small. Obviously, Coulomb interactions or dipolar interactions may not satisfy the above assumptions.

11.2 Cohesive energy of a liquid

We can find out some general rule about the cohesive energy of a molecule with its neighbors in a liquid by comparing the molar gas and molar liquid volumes. A typical gas molar volume is $22.400 \text{ cm}^3/\text{mol}$, while this is only $20 \text{ cm}^3/\text{mol}$ for a liquid. If liquid and gas coexist at a certain temperature T , then the chemical potential of gas and liquid must be the same, i.e.:

$$\mu_{\text{gas}}^0 + k_B T \ln(X_{\text{gas}}) = \mu_{\text{liq}}^0 + k_B T \ln(X_{\text{liq}})$$

(with X the dimensionless concentration in the respective phases, e.g., $X_{\text{gas}} = 1/22.400$) or

$$\mu_{\text{gas}}^0 - \mu_{\text{liq}}^0 \approx -\mu_{\text{liq}}^0 = k_{\text{B}}T \ln \left(\frac{X_{\text{liq}}}{X_{\text{gas}}} \right) \approx 7k_{\text{B}}T$$

assuming that there is essentially no cohesive energy in the gas phase. At the vaporization temperature T_{B} , the energy required to release one mole of molecules from its cohesion with its neighboring molecules to the gas phase is thus

$$U_{\text{vap}} = -N_{\text{A}}\mu_{\text{liq}}^0 = 7N_{\text{A}}k_{\text{B}}T_{\text{B}} = 7RT_{\text{B}}.$$

This allows us to estimate the latent heat of vaporization:

$$\Delta H_{\text{vap}} = U_{\text{vap}} + pV \approx 7RT_{\text{B}} + RT_{\text{B}}.$$

According to that, the ratio of latent heat of vaporization to boiling temperature is

$$\frac{\Delta H_{\text{vap}}}{T_{\text{B}}} \approx 8R \approx 80 \frac{\text{J}}{\text{K mol}}$$

per mole, or $9k_{\text{B}}T$ per molecule. If we assume that each molecule has on average 6 neighbors in a liquid, then we obtain a value of $\frac{3}{2}k_{\text{B}}T$ as energy per molecular pair. This approximate rule is called **Trouton's rule** and gives only a very rough estimate of the cohesive energy, as it completely neglects the details of the interactions. However, it demonstrates why thermal energy is important in soft matter.

Trouton's rule

The molar latent heat of vaporization, which is a measure for the cohesive energy of a liquid, is approximately

$$\frac{\Delta H_{\text{vap}}}{k_{\text{B}}T} \approx 8R$$

with R being the gas constant.

11.3 Coulomb forces, charge–charge interactions

The simplest but at the same time also one of the most important types of interaction is the electrostatic interaction, e.g., of simple charges. This type of interaction is important not only due to its relevance in biological systems, but the electrostatic interaction is in principle the only one delivering a long-range repulsive force.

11.3.1 Charge–charge interactions

Charge–charge interactions are mediated by electric fields. Assume that we have a charge Q_1 that creates an electric field

$$E_1 = \frac{Q_1}{4\pi\epsilon_0\epsilon r^2}.$$

We neglect the vectorial character of the electric field to avoid further complications. The electric field creates a force on a second charge Q_2

$$F(r) = Q_2 E_1 = \frac{Q_1 Q_2}{4\pi\epsilon_0\epsilon r^2}.$$

For such a charge assembly at the distance r , an energy is stored, which is the potential energy of assembling these two charges from infinity. The free energy of the two charges thus reads

$$w(r) = \int_{\infty}^r -F(r) \, dr = - \int_{\infty}^r \frac{Q_1 Q_2}{4\pi\epsilon_0\epsilon r^2} \, dr = \frac{Q_1 Q_2}{4\pi\epsilon_0\epsilon r}.$$

If we evaluate this energy, for example, for a sodium and a chlorine ion at a distance of $r = 0.276$ nm, we find a free energy of interaction of $w = -8.4 \cdot 10^{-19}$ J, which corresponds to about $200 k_B T$ at 300 K temperature. This is on the same order of magnitude as covalent interactions. It requires about 3 nN to break this bond. The long-range character of electrostatics becomes clear when evaluating the distance at which this interaction becomes comparable to $k_B T$: $r = 56$ nm. This is only considering a pair of ions. In a NaCl crystal, multiple neighbors contribute to the interaction energy of one sodium ion with its surroundings. One sodium ion has 6 Cl⁻ neighbors at a distance of $r = 0.276$ nm, 12 Na⁺ neighbors at $\sqrt{2}r$, and further 8 Cl⁻ neighbors at $\sqrt{3}r$, and so on. We have to sum up all the interaction energies for the total cohesive energy of the sodium ion in the crystal:

$$\mu^0 = -\frac{e^2}{4\pi\epsilon_0 r} \left[6 - \frac{12}{\sqrt{2}} + \frac{8}{\sqrt{3}} - \frac{6}{2} + \dots \right] = -1.748 \frac{e^2}{4\pi\epsilon_0 r}.$$

The factor in front of the Coulomb term (the one in the square brackets) is termed the **Madelung constant** and is known from solid-state physics. It is characteristic for specific lattice types, such as a simple cubic lattice in this case. Note that the cohesive energy of one sodium ion is therefore about $350 k_B T$ and is thus much larger than the thermal energy, keeping the NaCl crystal stable. Yet, it can be dissolved in water very easily.

11.3.2 Born energy of solvation

The Born energy of solvation calculates the free energy of assembling a charge inside a dielectric medium of dielectric constant ϵ . Let us reconsider the free energy:

$$dU = dQ + dW$$

$$\Rightarrow dU = TdS + dW$$

$$\Leftrightarrow dW = dU - TdS$$

which leads to

$$dF = dU - TdS = dW.$$

Therefore, the free energy change is related to the energy to assemble a charge:

$$\Delta F = \frac{\epsilon\epsilon_0}{2} \int_V E^2 dV = \int dw = \int_0^Q \frac{q dq}{4\pi\epsilon_0\epsilon a} = \frac{1}{2} \frac{Q^2}{4\pi\epsilon_0\epsilon a}.$$

To find the free energy, we integrated the square of the electric field over the volume (this is equivalent to adding tiny charge elements against previously assembled parts of the charge). According to this, the free energy of a charge $Q = ze$ per charge in a medium with dielectric constant ϵ is

$$\mu^0 = \frac{z^2 e^2}{8\pi\epsilon\epsilon_0 a}$$

if the charge has a radius a . Now, if we look at the difference between assembling the charge in vacuum ($\epsilon = 1$) and in a medium with dielectric constant ϵ , we find the following difference in the chemical potential (free energy):

$$\Delta\mu^0 = -\frac{z^2 e^2}{8\pi\epsilon_0 a} \left(\frac{1}{\epsilon} - 1 \right) = -\frac{28z^2}{a} \left(\frac{1}{\epsilon} - 1 \right) k_B T \quad \text{per ion at } T = 300 \text{ K.}$$

This is the **Born free energy of solvation** of a single ion. The molar free energy is obtained by multiplying with Avogadro's number N_A :

$$\Delta G = N_A \Delta \mu^0 = -\frac{69z^2}{a} \left(\frac{1}{\epsilon} - 1 \right) \text{kJ/mol.}$$

Additionally, we have:

$$\Delta \mu^0 \approx \frac{e^2}{4\pi\epsilon_0\epsilon(a_+ + a_-)}.$$

The mole fraction dissolved in water is then found using the Boltzmann factor:

$$X_s = e^{-\frac{\Delta \mu^0}{k_B T}}$$

which is a measure of the solubility of ions. Inserting the formula for the chemical potential yields the proportionality $X_s \propto \exp(-\text{const}/\epsilon)$. This dependency on the dielectric constant of the solvent is observed experimentally, though this is only a trend and some solvents deviate from this behavior.

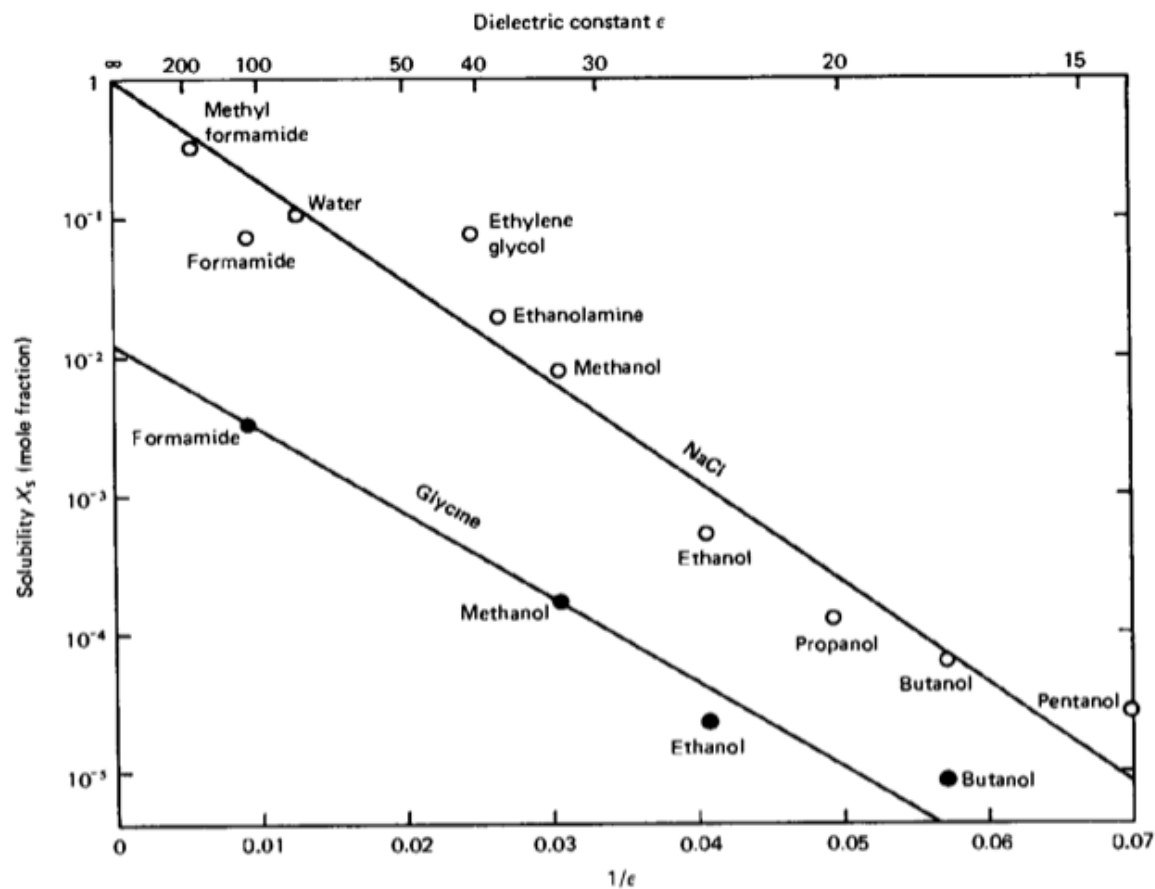


Figure 11.1: Solubility

Compound	Dielectric constant ϵ
Water	78.5
Ethanol	24.3
Acetone	20.7
Hexane	1.9
Polystyrene	2.4
Sodium Chloride	6.0

The reasons for deviations are:

1. The theory assumes continuous changes in interactions, but in reality, there is local ordering.
2. Additional interactions like hydrogen bonds exist.

11.3.3 Interactions involving polar molecules

Many molecules exhibit a dipole or even higher moments due to the uneven distribution of charges over the molecular structure. Some atoms have a stronger tendency to accept charges than others, a property typically measured by electronegativity. This gives an idea of whether atoms donate or accept charge when binding to other atoms. While homo-atomic bonds do not have dipole moments, hetero-atomic bonds often do, as shown in the table below:

Bond	Dipole moment [D]
C–C	0
C–N	0.22
O–H	1.51
F–H	1.94
N=O	2.0

Similarly, molecules have different dipole moments depending on their structure:

Molecule	Dipole moment [D]
Hexane	0
Water	1.85
Ethanol	1.7
Acetone	2.9

The dipole moment of a molecule is measured by the displacement of two charges $\pm q$ from each other:

$$\vec{u} = q\vec{l}.$$

Its direction is from the negative to the positive charge. The dipole creates an electric field given by

$$\vec{E} = \frac{3(\vec{u} \cdot \hat{r})\hat{r} - \vec{u}}{4\pi\epsilon_0\epsilon r^3},$$

where $\hat{r} = \vec{r}/|r|$. The **dipole self-energy**, or the energy required to create the dipole in a solvent, is given by

$$\mu^0 = \frac{1}{4\pi\epsilon_0\epsilon} \left[\frac{q^2}{2a} + \frac{q^2}{2a} - \frac{q^2}{l} \right].$$

For $l = 2a$, this simplifies to

$$\mu^0 = \frac{q^2}{8\pi\epsilon_0\epsilon a} = \frac{u^2}{4\pi\epsilon_0\epsilon l^3}$$

which shows a similar dependence of the chemical potential on the dielectric constant ϵ as in the case of a single charge. As a result, the solubility of polar molecules also depends on the dielectric constant in a manner similar to that of ionic solubility.

The plot below illustrates the electric field of a dipole:

```
plt.figure(figsize=(5, 5))

# generate grid
x=np.linspace(-2, 2, 32)
y=np.linspace(-2, 2, 32)
x, y=np.meshgrid(x, y)

def E(q, a, x, y):
    return q*(x-a[0])/((x-a[0])**2+(y-a[1])**2)**(1.5), \
              q*(y-a[1])/((x-a[0])**2+(y-a[1])**2)**(1.5)

# calculate vector field
Ex1, Ey1=E(-1, [-0.1, 0], x, y)
Ex2, Ey2=E(1, [0.1, 0], x, y)
Ex=Ex1+Ex2
Ey=Ey1+Ey2

E_max=5
E=np.sqrt(Ex**2+Ey**2)

Ex.flat[E.flat[:]>E_max]=np.nan
Ey.flat[E.flat[:]>E_max]=np.nan
# plot vecor field
plt.quiver(x, y, Ex/E, Ey/E, pivot='middle', headwidth=3, headlength=5,scale=40)
plt.xlabel('$x$')
plt.ylabel('$y$')
plt.title('dipole field')
plt.show()
```

γ

2

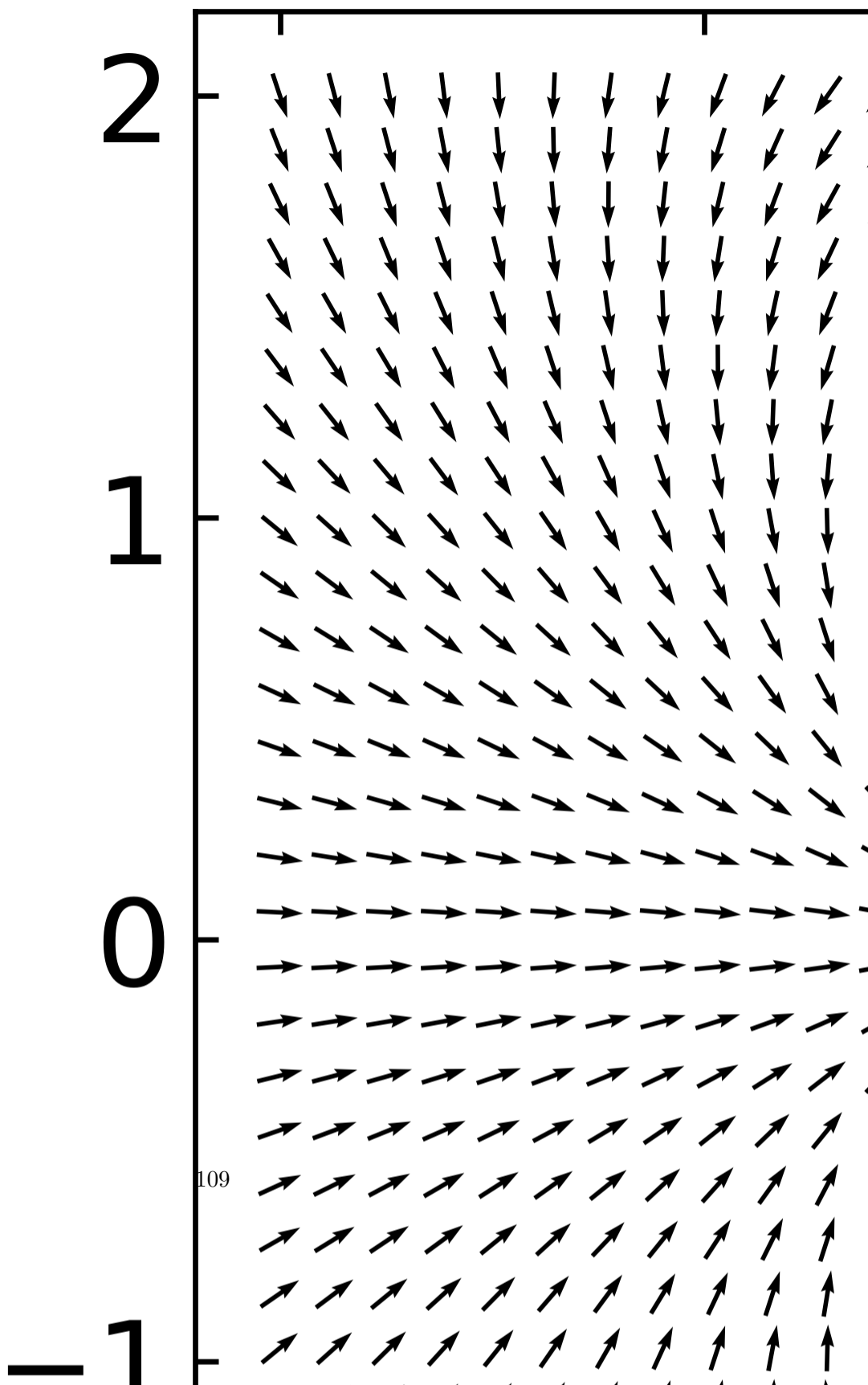
1

0

-1

109

0



11.3.4 Ion-dipole interaction

The interaction energy of a dipole with a charge can be calculated by

$$w(r) = -\frac{qQ}{4\pi\epsilon_0\epsilon} \left[\frac{1}{r - \frac{1}{2}l\cos(\theta)} - \frac{1}{r + \frac{1}{2}l\cos(\theta)} \right] = -\frac{qQ}{4\pi\epsilon_0\epsilon r^2} \cos(\theta) = -uE \cos(\theta),$$

where the last two equations are assuming that the distance between both objects r is much larger than the extent of the dipole l itself. From the last equation, we see that the interaction can be either attractive or repulsive. An angle $\theta = 0^\circ$ results in an attractive interaction, while $\theta = 180^\circ$ yields repulsive interaction. Using a single charge (e.g., an Na^+ ion) and a dipole of $u = 1.85 \text{ D}$ (water molecule) results in an interaction energy of about $39 k_{\text{B}}T$. Ions align and bind polar molecules like water, for example. The alignment is caused by the torque $\tau = \vec{u} \times \vec{E}$. For arbitrary polar molecules this is called **solvation**, while for water the term **hydration** is used. The strength of the hydration can effect the mobility of ions in solution as it makes them effective charges and is of interest, for example, in the study of ion transport through ion channels, as this requires the stripping of the hydration shell.

Example: Sodium Ion Hydration

The plot below shows the ion dipole interaction for a sodium ion and a water molecule as a function of distance.

```
def ion_dipole(u,r,l,theta,epsilon):
    q=u/l
    f=e*q/(4*np.pi*epsilon*epsilon_0)
    return(-f*(1/(r-0.5*l*np.cos(theta))-1/(r+0.5*l*np.cos(theta))))
```



```
D=physical_constants["atomic unit of electric dipole mom."][0]
J2eV=physical_constants["electron volt-joule relationship"][0]
```



```
r=np.linspace(0.1e-9,0.5e-9,200)
l=0.02e-9
```



```
plt.figure(figsize=(6,5))
plt.plot(r*1e9,ion_dipole(1.8*D,r,l,0,1)/J2eV,'k--')
plt.plot(r*1e9,ion_dipole(1.8*D,r,l,np.pi,1)/J2eV,'k--')
plt.plot(r*1e9,ion_dipole(1.8*D,r,l*5,0,1)/J2eV,'k')
plt.plot(r*1e9,ion_dipole(1.8*D,r,l*5,np.pi,1)/J2eV,'k')
plt.ylim(-9.2,9.2)
plt.xlim(0,0.5)
plt.xlabel("distance [nm]")
```

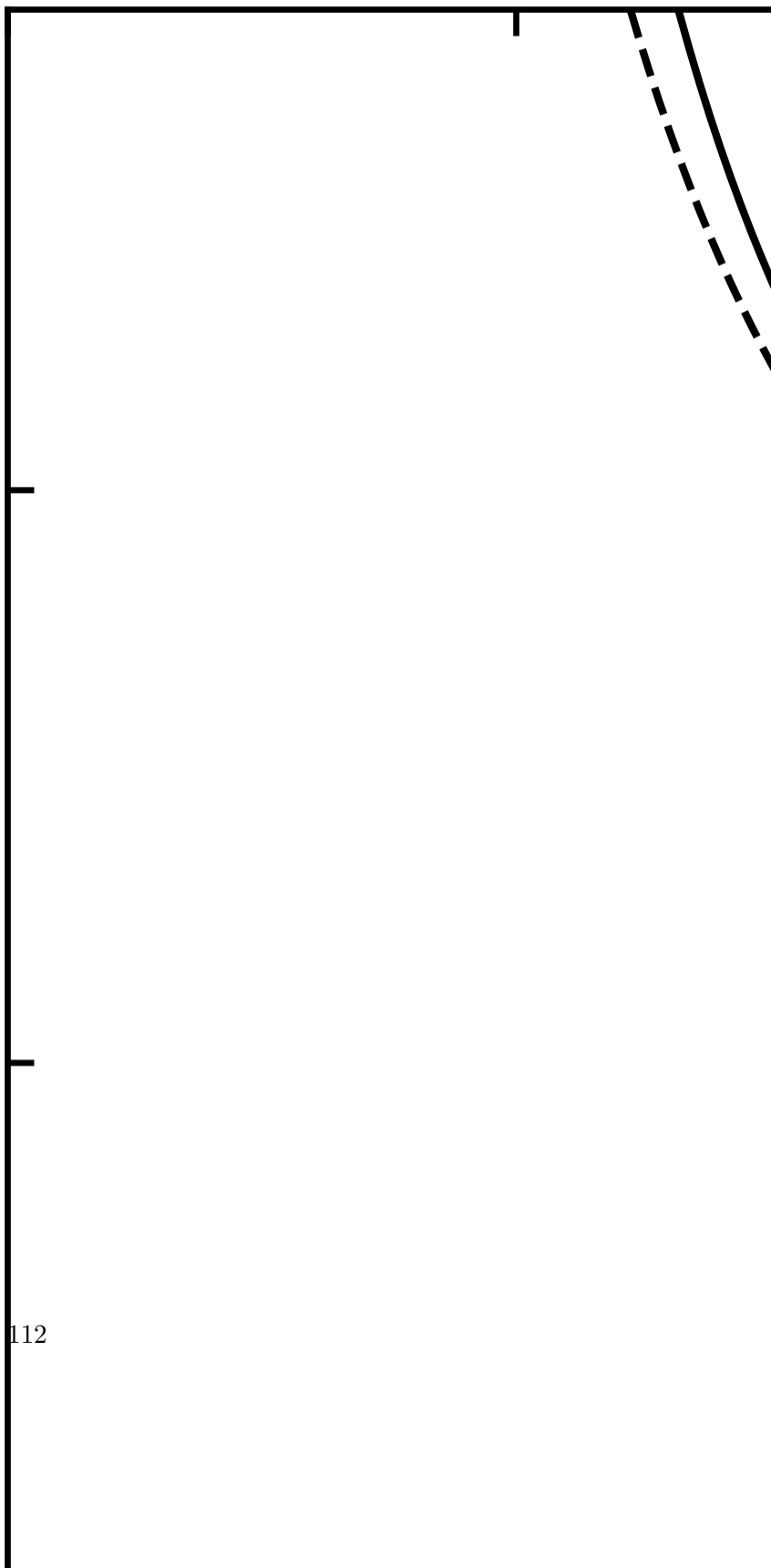
```
plt.ylabel("energy [eV]")
plt.title("dipole charge interaction")
plt.show()
```

energy [eV]

5
0

112

dipo



The table below shows some selected hydration properties of ions. The hydrated radius determines the diffusion of the ion in water. The hydration number is the number of orientationally bound water molecules. Typically, smaller ions have a larger hydration number.

Ion	Bare Ion radius (nm)	Hydrated radius (nm)	Hydration number
Na+	0.095	0.36	4
Mg ²⁺	0.065	0.43	6
Cl-	0.181	0.33	1
OH-	0.176	0.3	3

Part IX

Lecture 8

12 Forces and Interactions in Soft Matter

12.0.4 Interactions involving polar molecules

```
import numpy as np
import matplotlib.pyplot as plt
from numpy.linalg import norm
from scipy.constants import c,epsilon_0,e,physical_constants

%config InlineBackend.figure_format = 'retina'
# the lines below set a number of parameters for plotting, such as label font size,
# title font size, which you may find useful
plt.rcParams.update({'font.size': 14,
                     'font.family':'sans-serif',
                     'axes.titlesize': 16,
                     'axes.labelsize': 18,
                     'axes.labelpad': 14,
                     'lines.linewidth': 1,
                     'lines.markersize': 10,
                     'xtick.labelsize' : 18,
                     'ytick.labelsize' : 18,
                     'xtick.top' : True,
                     'xtick.direction' : 'in',
                     'ytick.right' : True,
                     'ytick.direction' : 'in',})
```

Many molecules exhibit a dipole or even higher moments due to the fact that the charges are not evenly distributed over the molecular structure. Some of the atoms exhibit a stronger tendency to accept charges than others. This is typically measured by electronegativity and provides an idea of whether atoms rather donate or accept a charge when binding to other atoms. While homo-atomic bonds therefore do not have dipole moments, hetero-atomic bonds do (see table).

Bond	Dipole moment [D]
C-C	0
C-N	0.22
O-H	1.51
F-H	1.94
N=O	2.0

Molecule	Dipole moment [D]
hexane	0
water	1.85
ethanol	1.7
acetone	2.9

The dipole moment of a molecule is measured by the displacement of two charges $\pm q$ from each other:

$$\vec{u} = q\vec{l}. \quad (12.1)$$

Its direction is from the negative to the positive side. It creates an electric field that is given by

$$\vec{E} = \frac{3(\vec{u} \cdot \hat{r})\hat{r} - \vec{u}}{4\pi\epsilon_0\epsilon r^3}, \quad (12.2)$$

where $\hat{r} = \vec{r}/|r|$. The dipole self-energy, i.e., the energy to create the dipole in a solvent is given by

$$\mu^0 = \frac{1}{4\pi\epsilon_0\epsilon} \left[\frac{q^2}{2a} + \frac{q^2}{2a} - \frac{q^2}{l} \right]. \quad (12.3)$$

For $l = 2a$ this results in $\mu^0 = q^2/(8\pi\epsilon_0\epsilon a) = u^2/(4\pi\epsilon_0\epsilon l^3)$ and thus yields a similar dependence of the chemical potential on the dielectric function ϵ as in the case of a single charge. The result is a similar dependence of the solubility on the dielectric function.

The plot below shows the electric field of a dipole:

```

plt.figure(figsize=(5, 5))

# generate grid
x=np.linspace(-2, 2, 32)
y=np.linspace(-2, 2, 32)
x, y=np.meshgrid(x, y)

def E(q, a, x, y):
    return q*(x-a[0])/((x-a[0])**2+(y-a[1])**2)**(1.5), \
        q*(y-a[1])/((x-a[0])**2+(y-a[1])**2)**(1.5)

# calculate vector field
Ex1, Ey1=E(-1, [-0.1, 0], x, y)
Ex2, Ey2=E(1, [0.1, 0], x, y)
Ex=Ex1+Ex2
Ey=Ey1+Ey2

E_max=5
E=np.sqrt(Ex**2+Ey**2)

Ex.flat[E.flat[:]>E_max]=np.nan
Ey.flat[E.flat[:]>E_max]=np.nan
# plot vecor field
plt.quiver(x, y, Ex/E, Ey/E, pivot='middle', headwidth=3, headlength=5,scale=40)
plt.xlabel('$x$')
plt.ylabel('$y$')
plt.title('dipole field')
plt.show()

```

γ

2

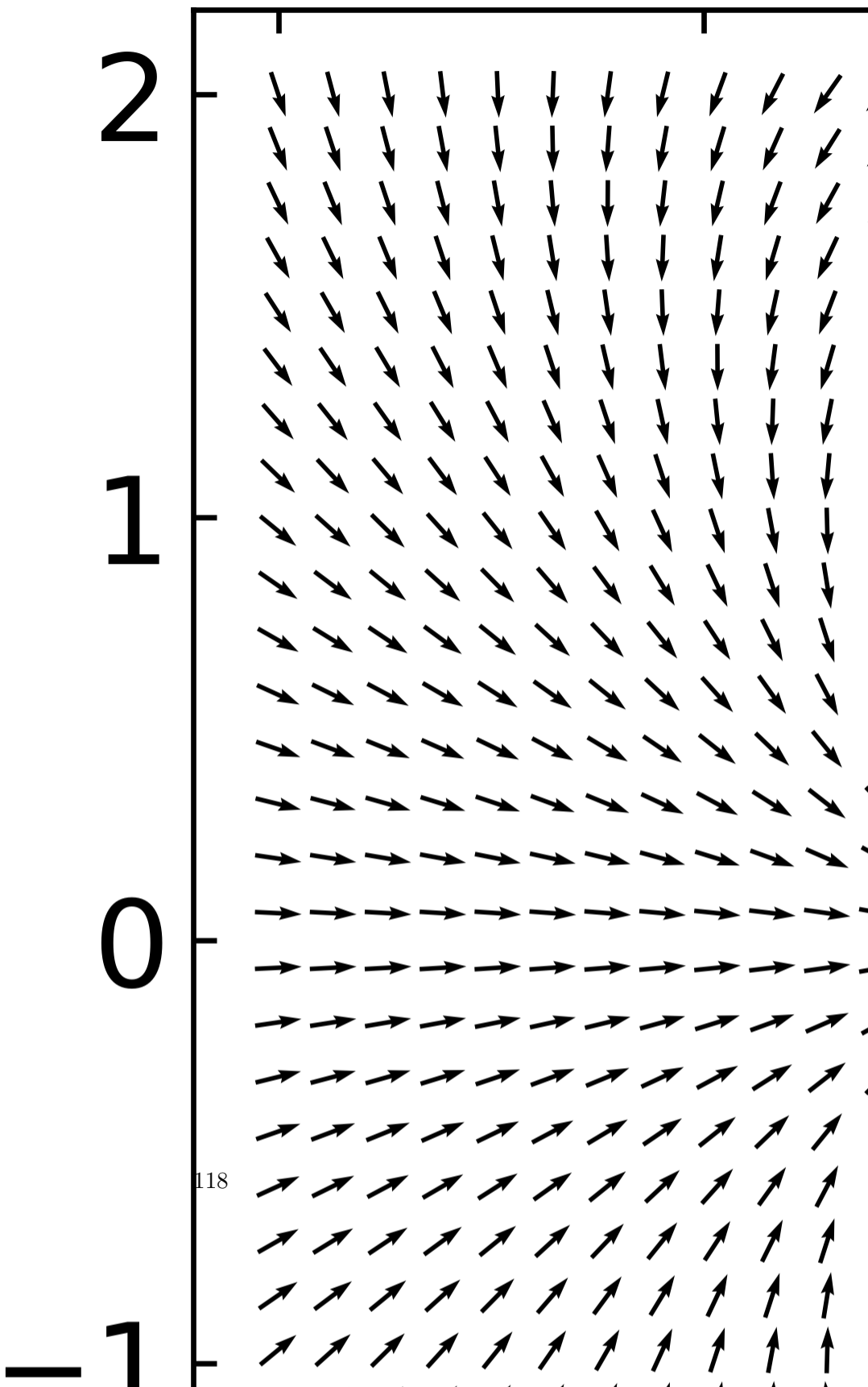
1

0

-1

118

0



12.0.5 Ion–Dipole interaction

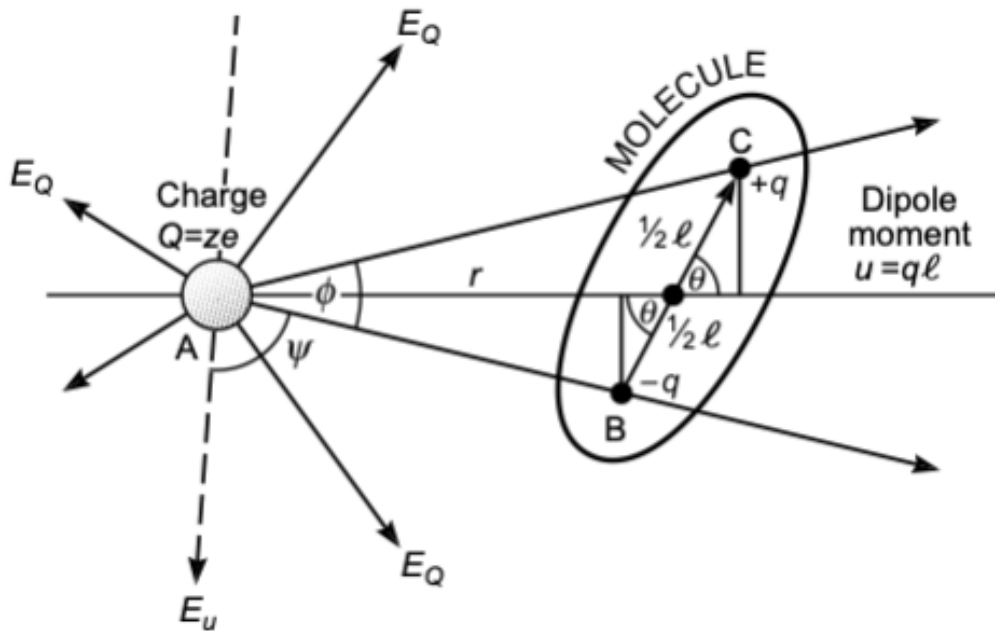


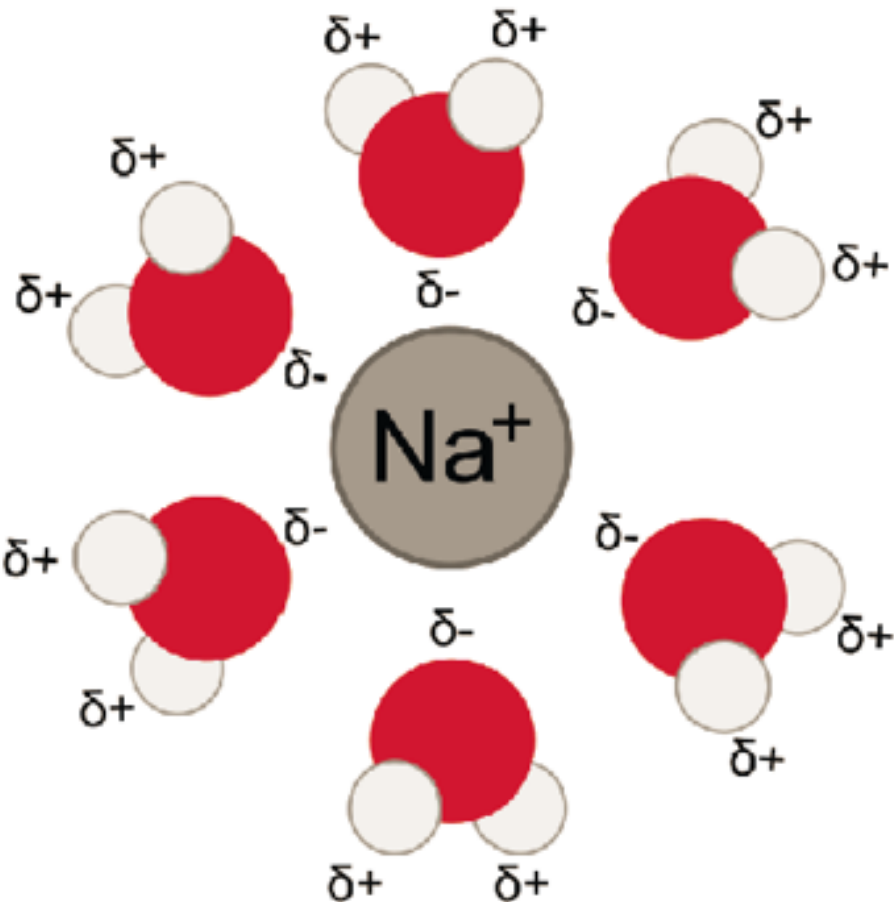
Figure 12.1: Charge Dipole

The interaction energy of a dipole with a charge can be calculated by

$$w(r) = -\frac{qQ}{4\pi\epsilon_0\epsilon} \left[\frac{1}{r - \frac{1}{2}l \cos(\theta)} - \frac{1}{r + \frac{1}{2}l \cos(\theta)} \right] = -\frac{qQ}{4\pi\epsilon_0\epsilon r^2} \cos(\theta) = -uE \cos(\theta) \quad (12.4)$$

where the last two equations are assuming that the distance between both objects r is much larger than the extent of the dipole l itself. From the last equation, we see that the interaction can be either attractive or repulsive. An angle $\theta = 0^\circ$ results in an attractive interaction, while $\theta = 180^\circ$ yields repulsive interaction. Using a single charge (e.g., an Na^+ ion) and a dipole of $u = 1.85 \text{ D}$ (water molecule) results in an interaction energy of about $39 k_B T$. Ions align and bind polar molecules like water, for example. The alignment is caused by the torque $\tau = \vec{u} \times \vec{E}$. For arbitrary polar molecules this is called **solvation**, while for water the term **hydration** is used. The strength of the hydration can effect the mobility of ions in solution as it makes them effective charges and is of interest, for example, in the study of ion transport through ion channels, as this requires the stripping of the hydration shell.

Example: Sodium Ion Hydration



The plot below shows the ion dipole interaction for a sodium ion and a water molecule as a function of distance.

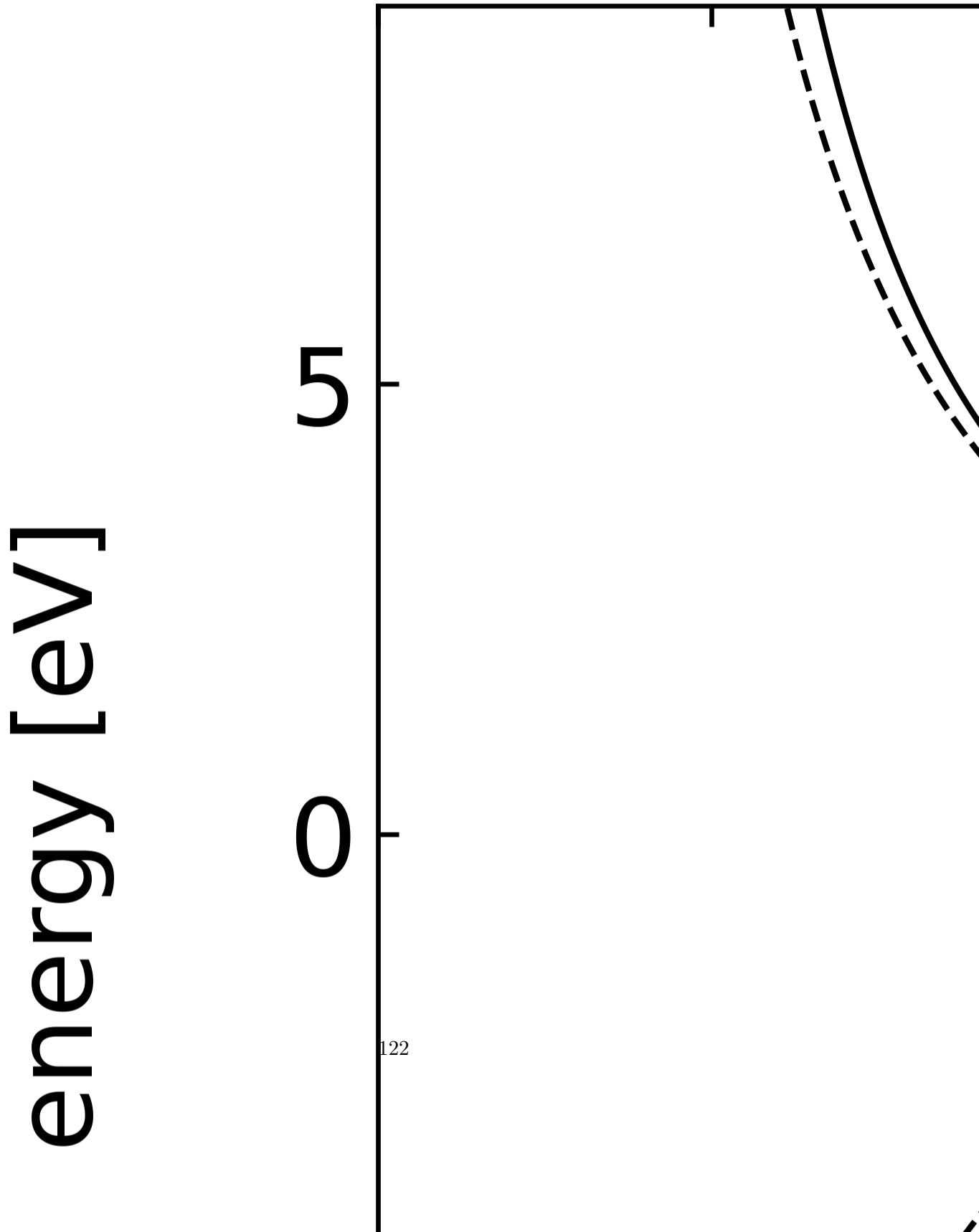
```
def ion_dipole(u,r,l,theta,epsilon):
    q=u/l
    f=e*q/(4*np.pi*epsilon*epsilon_0)
    return(-f*(1/(r-0.5*l*np.cos(theta))-1/(r+0.5*l*np.cos(theta))))
```

```
D=physical_constants["atomic unit of electric dipole mom."][0]
J2eV=physical_constants["electron volt-joule relationship"][0]
```

```
r=np.linspace(0.1e-9,0.5e-9,200)
l=0.02e-9

plt.figure(figsize=(5,5))
plt.plot(r*1e9,ion_dipole(1.8*D,r,l,0,1)/J2eV,'k--')
plt.plot(r*1e9,ion_dipole(1.8*D,r,l,np.pi,1)/J2eV,'k--')
plt.plot(r*1e9,ion_dipole(1.8*D,r,l*5,0,1)/J2eV,'k')
plt.plot(r*1e9,ion_dipole(1.8*D,r,l*5,np.pi,1)/J2eV,'k')
plt.ylim(-9.2,9.2)
plt.xlim(0,0.5)
plt.xlabel("distance [nm]")
plt.ylabel("energy [eV]")
plt.title("dipole charge interaction")
plt.show()
```

dipole c



The table below shows some selected hydration properties of ions. The hydrated radius determines the diffusion of the ion in water. The hydration number is the number of orientationally bound water molecules. Typically, smaller ions have a larger hydration number.

Ion	Bare Ion radius (nm)	Hydrated radius (nm)	Hydration number
Na+	0.095	0.36	4
Mg ²⁺	0.065	0.43	6
Cl ⁻	0.181	0.33	1
OH ⁻	0.176	0.3	3

12.0.6 Dipole-Dipole Interactions

The interaction of two dipole will depend on three angles, the two angles of the dipoles with the connecting axis θ_1, θ_2 and the angle ϕ between the two planes which contain the individual dipoles and the axis. The figure below shows the corresponding geometry.

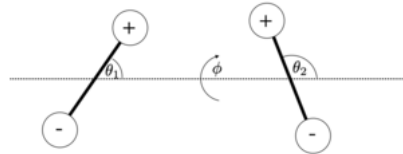


Figure 12.2: Dipole

The energy of the two dipoles at a distance r follows then without a detailed calculation with

$$w(r, \theta_1, \theta_2, \phi) = -\frac{u_1 u_2}{4\pi\epsilon_0 r^3} [2 \cos(\theta_1) \cos(\theta_2) - \sin(\theta_1) \sin(\theta_2) \cos(\phi)]$$

The image below (taken from the book by Israelachvili) shows the dipole-dipole interaction energy for the **parallel** and the **in-line** configuration as indicated. As shown, the in-line configuration with facing opposite charges is more favorable.

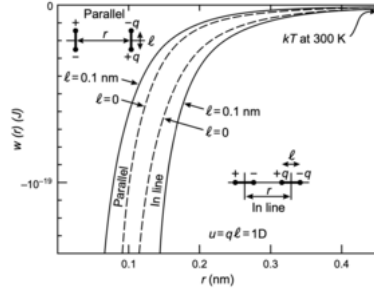


Figure 12.3: Dipole Energy

The energies that are typically found are also larger than the thermal energy at room temperature and therefore lead to ordering effects.

12.0.7 Rotating Dipoles, angle averaged Potential

The equations we derived so far deliver the energy for a specific fixed orientation of dipoles for example. However, molecules with dipoles may rotate and undergo rotational Brownian motion driven by thermal energy. This rotational diffusion can be very fast and the rotational sampling creates an average interaction that may scale differently with the distance. To get an effective distance dependence in the interaction, we have to integrate the Boltzmann factor over the orientational degrees of freedoms, i.e.

$$\exp\left(-\frac{w(r)}{k_B T}\right) = \frac{\int \exp\left(-\frac{w(r, \Omega)}{k_B T} d\Omega\right)}{\int d\Omega} = \left\langle \exp\left(-\frac{w(r, \Omega)}{k_B T}\right) \right\rangle_{\Omega}$$

with

$$d\Omega = \sin(\theta) d\theta d\phi$$

and

$$\int d\Omega = 4\pi$$

$$\exp\left(-\frac{w(r)}{k_B T}\right) = \frac{1}{4\pi} \int_0^{2\pi} d\phi \int_0^{\pi} \exp\left(-\frac{w(r, \phi\theta)}{k_B T}\right) \sin(\theta) d\theta$$

When $w(r, \theta) \ll k_B T$ then we can expand the Boltzmann factor

$$\exp\left(-\frac{w(r)}{k_B T}\right) \approx 1 - \frac{w(r)}{k_B T} + \frac{1}{2} \left(\frac{w(r)}{k_B T}\right)^2 + \dots$$

and therefore obtain

$$w(r) = \langle w(r, \Omega) - \frac{w(r, \Omega)^2}{2k_B T} + \dots \rangle_\Omega$$

which we can readily use to calculate the interaction energy of a charge and a dipole

$$\begin{aligned} w(r) &= \left\langle -\frac{Qu \cos(\theta)}{4\pi\epsilon_0\epsilon r^2} - \left(\frac{Qu}{4\pi\epsilon_0\epsilon r^2}\right)^2 \frac{\cos(\theta)^2}{2k_B T} + \dots \right\rangle \\ &= \frac{Q^2 u^2}{6(4\pi\epsilon_0\epsilon)^2 k_B T r^4} \end{aligned}$$

when $k_B T > \frac{Qu}{4\pi\epsilon_0\epsilon r^2}$. Interestingly, this interaction energy for the freely rotating dipole in the electric field of an ion decays as r^{-4} , while the static interaction decayed as r^{-2} . Also, the interaction of the freely rotating dipole is always attractive as compared to the static dipole charge interaction.

The previous result can also be obtained when using $G = -k_B T \ln(Z)$, where

$$Z = \int \exp\left(-\frac{w(r, \Omega)}{k_B T}\right) d\Omega$$

is the partition function.

12.0.8 Dipole-Dipole interaction with rotating dipoles

We can extend the above calculation now also to two dipoles interacting when freely rotating. The interaction energy was given by

$$w(r, \theta_1, \theta_2, \phi) = -\frac{u_1 u_2}{4\pi\epsilon_0\epsilon r^3} [2 \cos(\theta_1) \cos(\theta_2) - \sin(\theta_1) \sin(\theta_2) \cos(\phi)]$$

and therefore the partition function can be calculated as

$$Z = \int_0^\pi \int_0^\pi \int_0^{2\pi} e^{\beta w(r, \theta_1, \theta_2, \phi)} \sin(\theta_1) \sin(\theta_2) d\phi d\theta_1 d\theta_2$$

The result of this calculation is the **Keesom interaction energy**

$$w(r) = -\frac{u_1^2 u_2^2}{3(4\pi\epsilon_0)^2 k_B T r^6}$$

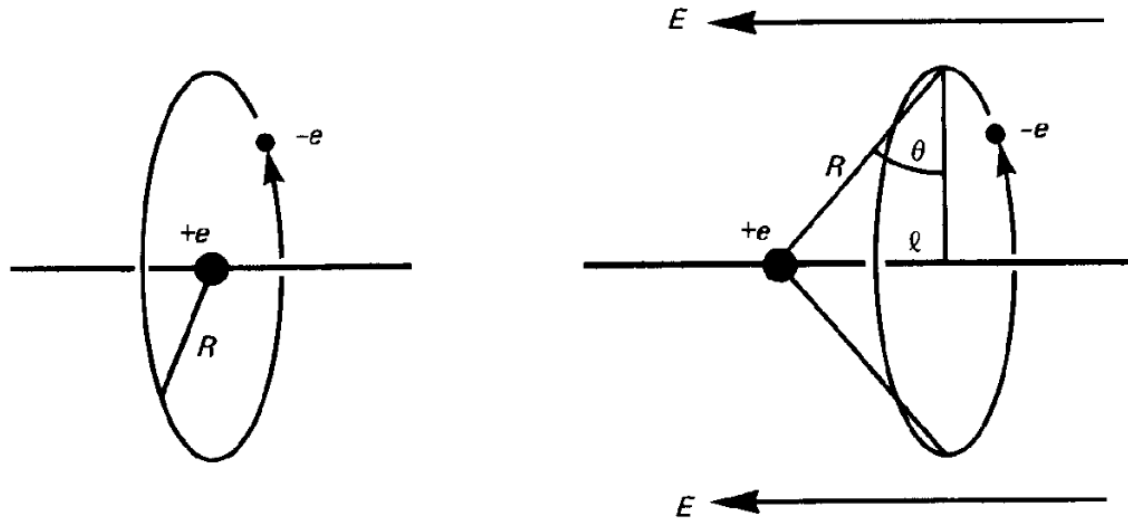
when

$$k_B T > \frac{u_1 u_2}{4\pi\epsilon_0\epsilon r^3}$$

The Keesom interaction tells on one side that permanent dipoles align themselves to be always attractive. It further belongs to a set of 3 different electrostatic interactions, which scale as r^{-6} and which are termed **van der Waals** interactions.

12.0.9 Interactions involving polarizability

All atomic and molecular systems carry the potential to get polarized in an external electric field. This polarization gives rise to a dipole moment u_{ind} , that is in linear response proportional to the external electric field. The dipole itself also creates an electric field. There are different types of polarizability. We will address two of them, i) the electronic polarizability, i.e. shifting the center of mass of positive and negative charges of a molecule or atom, ii) the reorientation of a permanent electric dipole in an external electric field which is an orientational polarization.



We consider a very simple classical model for the electronic polarizability. An electron is orbiting a positive nucleus and is subjected to an electric field according to the above image.

In the stationary state, the forces on the charges exerted by the external electric field and the internal forces balance and give rise to the polarized state with a dipole moment.

The external force on each charge is given by

$$F_{ext} = -eE$$

while the internal force between the two charges is

$$F_{int} = -\frac{e^2}{4\pi\epsilon_0 R^2} \sin(\theta) \approx \frac{e^2 l}{4\pi\epsilon_0 R^3} = -\frac{eu_{ind}}{4\pi\epsilon_0 R^3} = F_{ext}$$

We can transform the latter equation to yield the induced dipole moment

$$u_{ind} = 4\pi\epsilon_0 R^3 E = \alpha_0 E$$

Accordingly, the electronic polarizability of the atom is

$$\alpha_0 = 4\pi\epsilon_0 R^3$$

which just says that the polarizability scales with the volume of the object, which is found in many occasions, including the scattering and absorption cross sections of nanoparticles.

12.0.10 Ion-Induced Dipole Interaction

Ion-induced dipole interactions occur when an ion distorts the electron cloud of a nearby neutral molecule, creating an induced dipole. This interaction can be described through the following key points:

12.0.10.1 Field of the Induced Dipole

The electric field E created by an ion at a distance r induces a dipole moment μ_{ind} in a neutral molecule:

$$\mu_{ind} = \alpha E$$

where α is the polarizability of the molecule, and E is given by:

$$E = \frac{q}{4\pi\epsilon_0 r^2}$$

The resulting induced dipole field E_d is:

$$E_d = -\frac{2\mu_{\text{ind}}}{4\pi\epsilon_0 r^3} = -\frac{2\alpha E}{4\pi\epsilon_0 r^3} = -\frac{2\alpha q}{(4\pi\epsilon_0)^2 r^5}$$

12.0.10.2 Force and Potential Energy

The force F between the ion and the induced dipole is given by:

$$F(r) = -\frac{\partial U}{\partial r} = -2\alpha \left(\frac{q}{4\pi\epsilon_0 r^2}\right)^2 = -\frac{2\alpha q^2}{(4\pi\epsilon_0)^2 r^5}$$

Integrating this force gives the potential energy U :

$$U(r) = \int F dr = -\frac{\alpha q^2}{(4\pi\epsilon_0)^2 r^4}$$

This shows that the interaction energy decreases rapidly with the fourth power of the distance.

12.0.10.3 Polarizability by Polar Molecules

For polar molecules, an electric field E induces a dipole moment that can be averaged over all orientations, leading to an additional orientational polarization. The total induced dipole moment μ_{ind} for a polar molecule with permanent dipole moment μ_0 is:

$$\mu_{\text{ind}} = \mu_0 \cos(\theta) + \alpha E \cos^2(\theta)$$

Averaging over all orientations gives the mean induced dipole moment:

$$\langle \mu_{\text{ind}} \rangle = \frac{\mu_0^2 E}{3k_B T}$$

Therefore, the overall polarizability α_{total} is a combination of the intrinsic polarizability α_0 and the orientational contribution:

$$\alpha_{\text{total}} = \alpha_0 + \frac{\mu_0^2}{3k_B T}$$

For example, for an ion-induced dipole interaction at 300 K with $\mu_0 = 4 \times 10^{-30} \text{ Cm}$ and α_0 :

$$\alpha_{\text{total}} = 4\pi\epsilon_0 \times 8 \times 10^{-30} \text{ m}^3 + \frac{\mu_0^2}{3k_B T}$$

These principles explain how ion-induced dipole interactions influence the behavior of molecules in various environments, including solutions and biological systems.

12.0.11 Polarizability of polar molecules

12.0.12 Dipole Induced Dipole

Part X

Lecture 9

13 Electric Double Layer

```
import matplotlib.pyplot as plt
import numpy as np
from scipy.constants import *
from scipy.optimize import fsolve
from ipywidgets import interact, interactive, fixed, interact_manual
import ipywidgets as widgets
import json

%matplotlib inline
%config InlineBackend.figure_format = 'retina'

with open('style.json', 'r') as fp:
    style = json.load(fp)

plt.rcParams.update(style)
```

13.1 Charges surfaces in solution, no salt

We are going to consider first a situation, in which there is a solid surface (for example glass) in contact with a solution, which is presumably water. In this case, surface chemical groups on the solid may dissociate due to the high dielectric constant of water such that the residual surface is charged and some ions are dissolved in the solution. We will assume that there is no extra salt which is dissolved in water.

The questions that arise now are

- How are the dissolved ions distributed in space?
- How does the ion distribution depend on the surface charge?
- How is the electrostatic potential inside the liquid?

As the ions populate the regions according to their potential energy in the electric field of the surface charges, we have to combine the Poisson equation with the Boltzmann equation to have a complete description. This combination will deliver us a mean field approach.

13.2 Poisson-Boltzmann equation

If we name the electrostatic potential ψ and number density of ions of a valancy z ρ , we can on one side write down the Boltzmann equation

$$\rho = \rho_0 \exp\left(-\frac{ze\psi}{k_B T}\right) \quad (\text{Boltzmann equation})$$

and the Poisson equation as

$$ze\rho = -\epsilon_0 \epsilon \frac{d^2\psi}{dx^2} \quad (\text{Poisson equation})$$

As both contain the charge density ρ we can combine them to yield

$$\frac{d^2\psi}{dx^2} = -\frac{ze\rho}{\epsilon_0 \epsilon} = -\frac{ze\rho_0}{\epsilon_0 \epsilon} \exp\left(-\frac{ze\psi}{k_B T}\right) \quad (\text{Poisson-Boltzmann equation})$$

the Poisson-Boltzmann equation, which is a non-linear differential equation in the potential ψ and therefore difficult to solve.

In the following we would like to determine the surface values for the potential ψ_s , the electric field E_s and the density ρ_s , which are called contact values. We will do that for a system of two solid surfaces each with a surface charge density σ according to the configuration shown below.

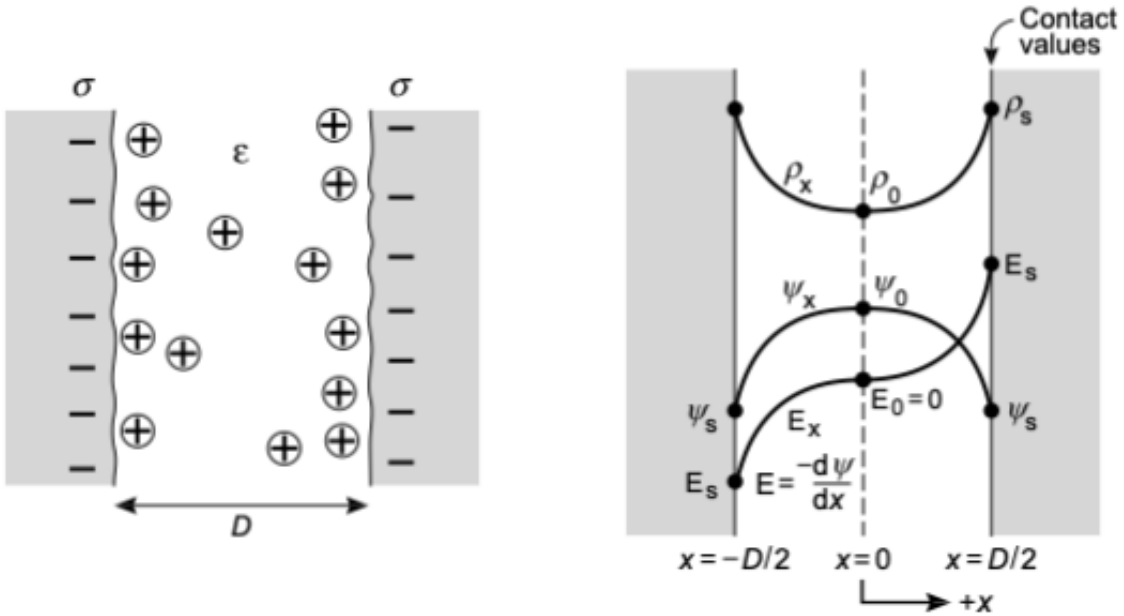


Figure 13.1: Config

This system is symmetric with respect to the mid-plane at $x = 0$ and thus the potential is $\psi_0 = \psi(x = 0) = 0$ and the charge number density is $\rho_o = \rho(x = 0)$. Also, due to symmetry we have $\frac{d\psi}{dx}|_{x=0} = 0$. It follows from this symmetry that

$$\sigma = - \int_0^{D/2} zeq dx = \epsilon_0 \epsilon \int_0^{D/2} \left(\frac{d^2 \psi}{dx^2} \right)^2 dx = -\epsilon_0 \epsilon \left(\frac{d\psi}{dx} \right) |_{D/2} = -\epsilon_0 \epsilon \left(\frac{d\psi}{dx} \right) |_S = -\epsilon_0 \epsilon E_s \quad (13.1)$$

To obtain the charge number density, we use the derivative of the Boltzmann equation with respect to the position

$$\frac{d\rho}{dx} = -\frac{ze\rho_0}{k_B T} \exp\left(-\frac{ze\psi}{k_B T}\right) \frac{d\psi}{dx} \quad (13.2)$$

The term on the right side can be replaced to yield

$$\frac{d\rho}{dx} = -\frac{ze\rho_0}{k_B T} \exp\left(-\frac{ze\psi}{k_B T}\right) \frac{d\psi}{dx} = \frac{\epsilon_0 \epsilon}{k_B T} \left(\frac{d\psi}{dx} \right) \left(\frac{d^2 \psi}{dx^2} \right) = \frac{\epsilon_0 \epsilon}{k_B T} \frac{d}{dx} \left(\frac{d\psi}{dx} \right)^2 \quad (13.3)$$

thus we can integrate both sides

$$\rho_x - \rho_0 = \int_0^x d\rho = \frac{\epsilon_0 \epsilon}{2k_B T} \left(\frac{d\psi}{dx} \right)_x^2 \quad (13.4)$$

or

$$\rho_x = \rho_0 + \frac{\epsilon_0 \epsilon}{2k_B T} \left(\frac{d\psi}{dx} \right)_x^2 \quad (13.5)$$

The term $\frac{d\psi}{dx}$, which appears as a square in the last formula is just the electric field evaluated at the position x . With the contact value of the electric field E_s obtained above, we can immediately write the contact value of the charge number density as

$$\rho_s = \rho_0 + \frac{\sigma^2}{2\epsilon_0 \epsilon k_B T} \quad (13.6)$$

Thus even in the case, when the two surfaces are separated by an infinite distance $\rho_0 \rightarrow 0$, the surface charge number density never falls below $\frac{\sigma^2}{2\epsilon_0 \epsilon k_B T}$.

To obtain the charge number density, the potential and the electric field we must solve the Poisson Boltzmann equation. The solution in the case of no additional electrolyte is given by

$$\psi = \frac{k_B T}{ze} \ln(\cos^2(Kx)) \quad (13.7)$$

or

$$\exp\left(-\frac{ze\psi}{k_B T}\right) = \frac{1}{\cos^2(Kx)} \quad (13.8)$$

where the constant K is given by

$$K^2 = \frac{(ze)^2 \rho_0}{2\epsilon_0 \epsilon k_B T} \quad (13.9)$$

To find the value of the constant K , we can take the derivative of the potential to obtain the electric field

$$E_x = -\frac{d\psi}{dx} = \frac{2k_B T K}{ze} \tan(Kx) \quad (13.10)$$

which is given at the surface to be

$$E_s = -\frac{d\psi}{dx}\Big|_s = \frac{2k_B T K}{ze} \tan\left(K \frac{D}{2}\right) = -\frac{\sigma}{\epsilon_0 \epsilon} \quad (13.11)$$

If the surface charge density σ is fixed and the thickness of the liquid layer D is known, the latter equation can be graphically solved to obtain the value of K . The counter ion density in the solution is then given by

$$\rho(x) = \rho_0 \exp\left(\frac{-ze\psi}{k_B T}\right) = \frac{\rho_0}{\cos^2(Kx)} \quad (13.12)$$

13.2.1 Example

Two surfaces with a charge density of $\sigma = 0.2 \text{ C} \cdot \text{m}^{-2}$ are at a distance of $D = 2 \text{ nm}$ in water at $T = 293 \text{ K}$. We calculate the counter ion surface charge, the charge density, the electric field and the potential inside the water film between the two layers. We therefore first calculate a value of

$$KTK = \frac{ze\sigma}{2k_B T \epsilon_0 \epsilon} \quad (13.13)$$

which shall be equal to $K \tan(KD/2)$.

```
sigma=0.2 # C/m^2
epsilon=80 # water
D=2e-9 # m
T=293 # K

KTK=e*sigma/(2*k*T*epsilon_0*epsilon)
```

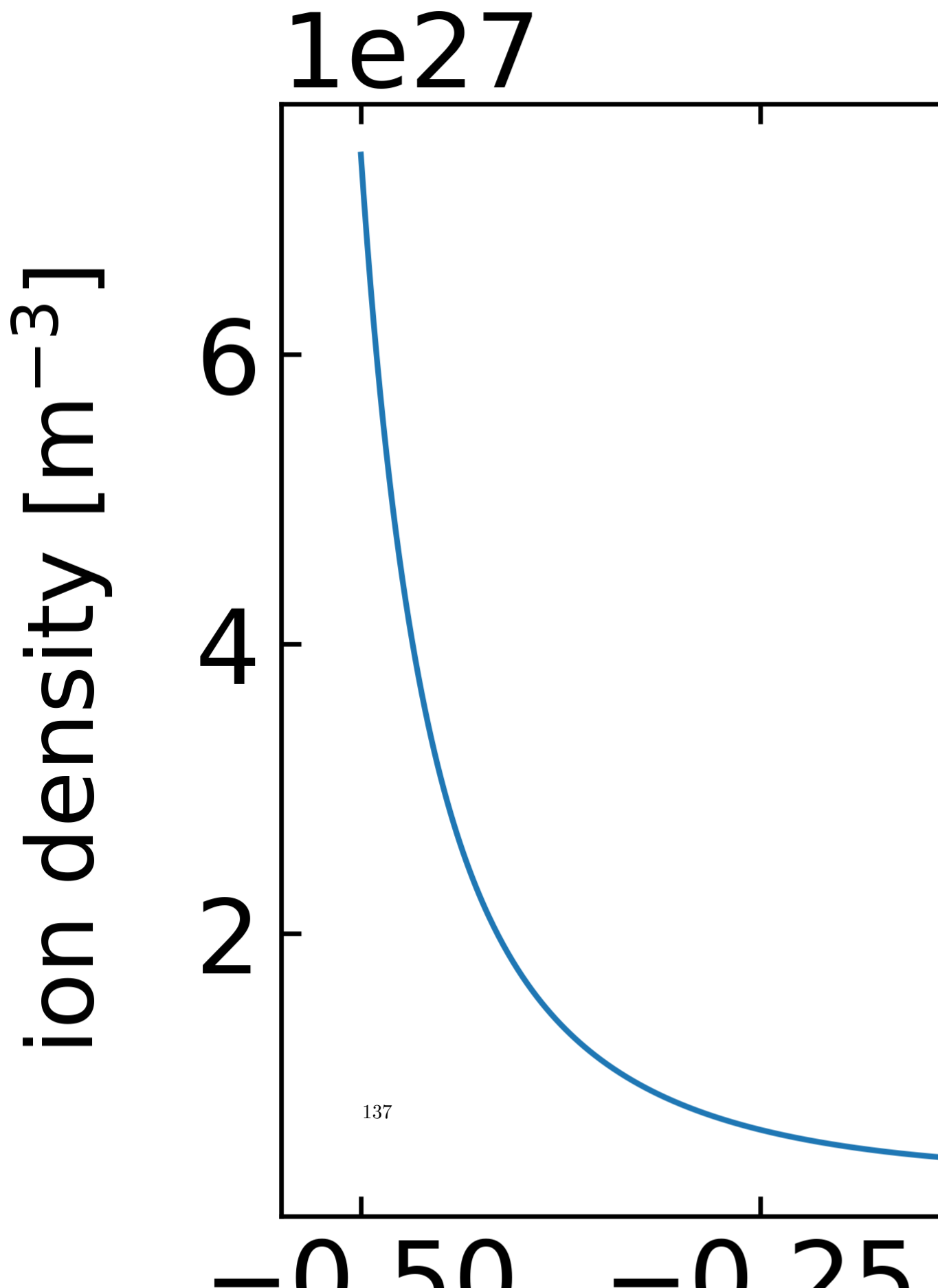
With the help of the previous definitions, we may search for the solution which gives the value of K .

```
# numerically solve for K
func = lambda K : KTK - K*np.tan(K*D/2)
K_initial_guess = 0.8*np.pi/D
K = fsolve(func, K_initial_guess)
```

13.2.1.1 Plot of the charge density

```
# ion density in the mid plane
rho0=K**2*2*epsilon_0*epsilon*k*T/e**2

# ion density in the gap
x=np.linspace(-D/2,D/2,1000)
plt.plot(x/D,rho0/(np.cos(K*x)**2))
plt.xlabel(r'x/D',fontsize=16)
plt.ylabel(r'ion density [m$^{-3}$]',fontsize=16)
plt.show()
```



13.2.1.2 Plot of the electric potential

```
# potential in the gap
x=np.linspace(-D/2,D/2,1000)
plt.plot(x/D,k*T*np.log(np.cos(K*x)**2)/e)
plt.xlabel(r'x/D',fontsize=16)
plt.ylabel(r'electric potential [V]',fontsize=16)
plt.show()
```

electric potential [V]



139

13.2.1.3 Plot of the electric field

```
# field in the gap
x=np.linspace(-D/2,D/2,1000)
plt.plot(x/D,2*k*T*K*np.tan(K*x)/e)
plt.xlabel(r'x/D',fontsize=16)
plt.ylabel(r'electric field [V/m]',fontsize=16)
plt.show()
```

electric field [V/m]

1e8

2

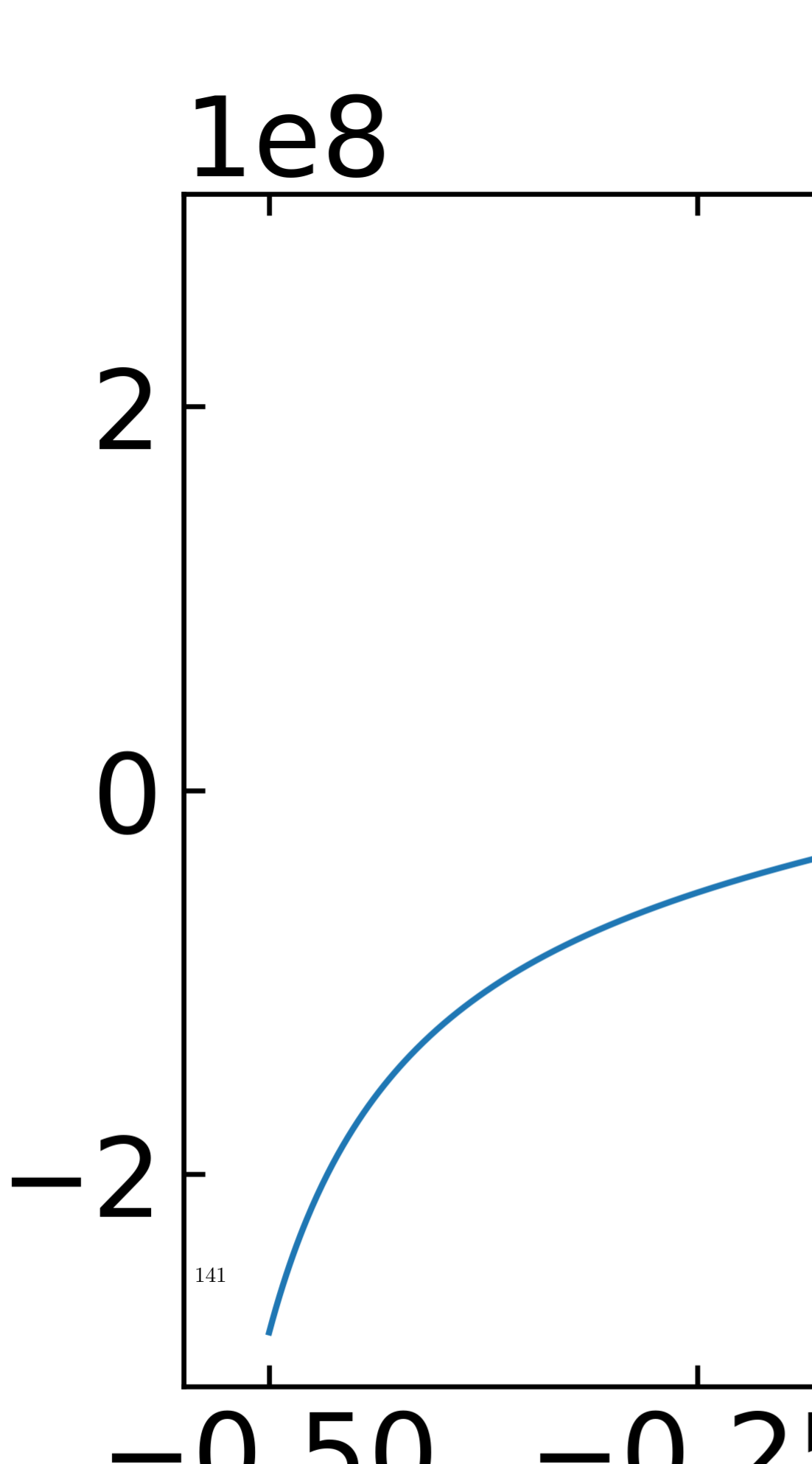
0

-2

141

-0.50

-0.25



Part XI

Lecture 10

14 van der Waals Interactions

So far we have considered electrostatic forces between charged and dipolar molecules. We have also introduced interactions which rely on the polarizability of molecules, either just the electronic polarizability or also an orientational polarization of dipolar molecules.

A part of these interactions showed a specific distance dependence, which was r^{-6} . In particular, we identified the **Keesom interaction**, i.e. the interaction of two freely rotating dipoles as well as the **Debye interaction**, i.e. the interaction of an induced dipole with a permanent dipole as two parts of the so-called van der Waals interaction.

Yet there also interaction between non-charged and non-polar molecules and this interaction is also belonging to this class and is specifically called **dispersion interaction** or **London interaction**.

As compared to other interactions, van der Waals interactions are typically

- long range
- attractive and orienting
- not additive

```
import numpy as np
import matplotlib.pyplot as plt
from numpy.linalg import norm
from scipy.constants import c,epsilon_0,e,physical_constants
import json

%config InlineBackend.figure_format = 'retina'

with open('style.json', 'r') as fp:
    style = json.load(fp)

plt.rcParams.update(style)
```

14.1 Dispersion Interaction

The dispersion part in particular, will require a quantum electrodynamic approach, which is beyond the scope of this lecture. We will consider a much simpler approach at the beginning and later study the more general approach by McLachlan.

Consider first two atoms which have

- no time averaged dipole
- no residual charge

Despite this fact, the atoms may have an instantaneous dipole, which is causing and induced dipole in the other atom. Similarly, the second atom may cause a corresponding dipole in the first atom as well. This will effectively lead to an attractive interaction, which carries the spirit of the dispersion interaction. We can put that into a simple and very crude model based on the most basic semi-classical description of an atom.

This atom may consist of an electron and proton, which are separated by a distance a_0 , which corresponds to the Bohr radius. In this atom, the Coulomb interaction is given by

$$E_{\text{pot}} = \frac{e^2}{4\pi\epsilon_0 a_0}$$

This potential energy corresponds for an hydrogen atom to the ionization potential $I = 13.6$ eV. To ionize the atom, we can use electromagnetic radiation of the frequency $\nu = 3.3 \times 10^{15}$ s⁻¹. Thus, in principle a photon of energy $h\nu = 2.2 \times 10^{-18}$ J would be sufficient to ionize the atom.

Accordingly, we have

$$h\nu = \frac{e^2}{4\pi\epsilon_0 a_0}$$

or we can write, that the Bohr radius of the electron orbit is given by

$$a_0 = \frac{e^2}{4\pi\epsilon_0 h\nu}$$

In this simple classical picture the atom has an instantaneous dipole which corresponds to $u = a_0 e$. This dipole creates a dipole field, that induces a dipole in the second atom. Using our previous findings for the dipole - induced dipole interaction yields

$$w(r) = -\frac{u^2 \alpha_0}{(4\pi\epsilon_0)^2 r^6} = -\frac{(a_0 e)^2 \alpha_0}{(4\pi\epsilon_0)^2 r^6} \quad (14.1)$$

where α_0 is the electronic polarizability $\alpha_0 = 4\pi\epsilon_0 a_0^3$. The latter gives

$$a_0^2 = \frac{\alpha_0}{4\pi\epsilon_0 a_0}$$

from which we finally find the interaction energy

$$w(r) = -\frac{a_0^2 e^2 \alpha_0}{(4\pi\epsilon_0)^2 r^6} = -\frac{\alpha_0^2}{(4\pi\epsilon_0)^2} \frac{e^2}{4\pi\epsilon_0 a_0} \frac{1}{r^6}$$

or

$$w(r) = -\frac{\alpha_0^2 h\nu}{(4\pi\epsilon_0)^2 r^6}$$

This simple semi-classical description corresponds to the result London (up to a factor of 3/4) obtained with a quantum-mechanical perturbation theory, which is

$$w(r) = -\frac{C_{\text{disp}}}{r^6} = -\frac{3}{4} \frac{\alpha_0^2 h\nu}{(4\pi\epsilon_0)^2 r^6} = -\frac{3}{4} \frac{\alpha_0^2 I}{(4\pi\epsilon_0)^2 r^6}$$

So far, we assumed that both molecules have the same polarizability and thus are of the same type. If this is not the case, the interaction energy is given by

$$w(r) = -\frac{3}{2} \frac{\alpha_{01}, \alpha_{02}}{(4\pi\epsilon_0)^2 r^6} \frac{I_1 I_2}{I_1 + I_2}$$

Example: Estimating the Boiling Point of Noble Gases

We can use this formula for the dispersion energy to estimate the boiling point of noble gases.

$$w(r) + E_{\text{kin}} = -\frac{3\alpha_0^2}{4(4\pi\epsilon_0)^2 \sigma^6} h\nu_I + \frac{3}{2} k_B T_m = 0$$

For Neon and Argon for example, we have the following parameters:

- Ne: $\sigma = 3.08 \text{ Angstroem}$, $h\nu_I = 21.6 \text{ eV}$, $\frac{\alpha_0}{4\pi\epsilon_0} = 0.39 \times 10^{-30} \text{ m}^{-3}$, from which we obtain a boiling temperature of $T_b = 22 \text{ K}$, which nicely corresponds to the experimental value of $T_b = 27 \text{ K}$

- Ar: $\sigma = 3.76$ Angstroem, $h\nu_I = 15.8$ eV, $\frac{\alpha_0}{4\pi\epsilon_0} = 1.63 \times 10^{-30}$ m⁻³, from which we obtain a boiling temperature of $T_b = 85$ K, which nicely corresponds to the experimental value of $T_b = 87$ K

Table 6.1 Strength of Dispersion Interaction between Quasi-Spherical Nonpolar Molecules of Increasing Size^d

Interacting Molecules	Molecular Diameter σ (nm) (From Figure 7.1)	Polarizability $\alpha_0/4\pi\epsilon_0$ (10^{-30} m ³)	Ionization Potential $I = h\nu_I$ (eV) ^b	London Constant		Molar Cohesive Energy, U (kJ mol ⁻¹)	Boiling Point, T_B (K)		
				$C_{\text{disp}} =$ $3\alpha_0^2 h\nu_I / 4(4\pi\epsilon_0)^2$ (10^{-79} J m ⁶)					
				Theoretical Eq. (6.3)	Measured from Gas Law Eq. (6.14) ^a				
Ne–Ne	0.308	0.39	21.6	3.9	3.8	2.0	2.1	22	
Ar–Ar	0.376	1.63	15.8	50	45	7.7	7.7	85	
CH ₄ –CH ₄	0.400	2.60	12.6	102 ^c	101 ^c	10.9	9.8	121	
Xe–Xe	0.432	4.01	12.1	233	225	15.6	14.9	173	
CCl ₄ –CCl ₄	0.550	10.5	11.5	1520	2960	23.9	32.6	265	
						$\frac{3\alpha_0^2 h\nu_I}{4(4\pi\epsilon_0)^2 \sigma^6 (1.5k)}$		350	

^aVan der Waals constants *a* and *b* taken from the *Handbook of Chemistry and Physics*, CRC Press, 56th ed.

^b1 eV = 1.602×10^{-19} J.

^cAs an example of the reliability of the approximate equations for C_{disp} , Eqs. (6.3) and (6.14), ab initio calculation for two CH₄ molecules (Fowler et al., 1989; Szczesniak et al., 1990) give $\sim 114 \times 10^{-79}$ J m⁶, which is about 10% higher than the theoretical value given here. The most reliable experimental value, based on a number of different types of measurements (Thomas and Meath, 1977), is $C_{\text{disp}} = 124 \times 10^{-79}$ J m⁶, which is about 20% higher than the value given here.

^dSee Pacheco and Ekardt (1992) for simple expressions and computed values for C_{disp} for metal atoms and small metal clusters.

Figure 14.1: Dispersion Interaction

While the theory above provides us only with some idea about the dispersion interaction, we can now summarize all three contributions to the van der Waals interaction

$$w_{\text{vdW}}(r) = - \underbrace{\frac{u_1^2 u_2^2}{3k_B T (4\pi\epsilon_0)^2 r^6}}_{\text{Keesom}} - \underbrace{\frac{u_1^2 \alpha_{02} + u_2^2 \alpha_{01}}{(4\pi\epsilon_0)^2 r^6}}_{\text{Debye}} - \underbrace{\frac{3h\nu_1 \nu_2 \alpha_{01} \alpha_{02}}{(4\pi\epsilon_0)^2 2(\nu_1 + \nu_2) r^6}}_{\text{London}}$$

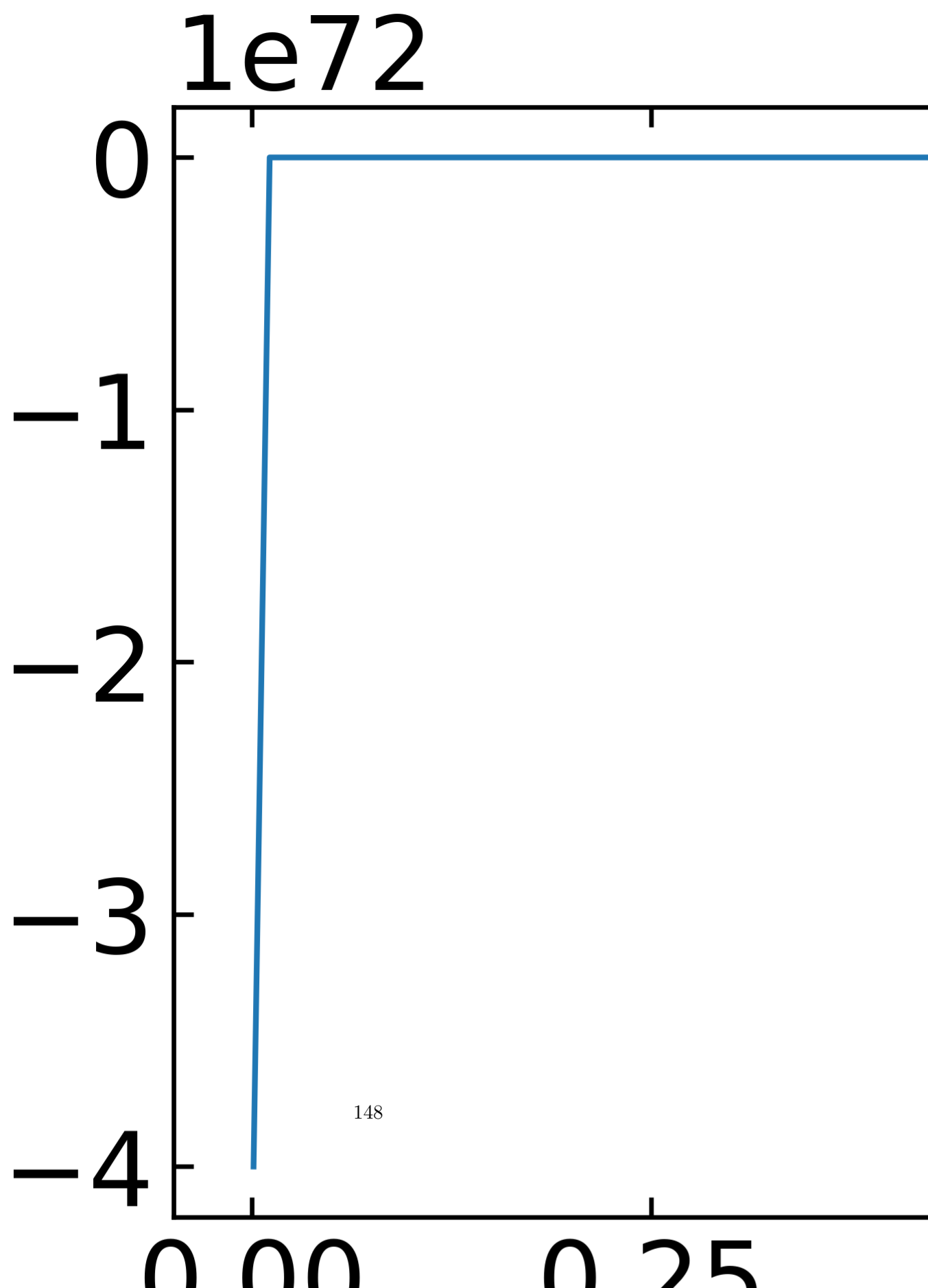
or simply

$$w_{\text{vdW}}(r) = - \frac{C_{\text{vdW}}}{r^6} = - \frac{C_{\text{Debye}} + C_{\text{Keesom}} + C_{\text{disp}}}{r^6}$$

```
def vdW(r,C_debye, C_keesom, C_disp):
    return -(C_debye + C_keesom + C_disp)/r**6
```

```
vdW_args={
    "Interacting Molecules": ["Ne–Ne", "CH4–CH4", "HCl–HCl", "HBr–HBr", "HI–HI"],
    "C_ind": [0, 0, 6, 4, 2],
    "C_orient": [0, 0, 11, 3, 0.2],
    "C_disp": [4, 102, 106, 182, 370]
}
```

```
r=np.linspace(1e-12, 1e-9, 100)
plt.plot(r, vdW(r, vdW_args["C_ind"] [0], vdW_args["C_orient"] [0], vdW_args["C_disp"] [0]))
plt.show()
```



The individual contributions have different strength, but it is not difficult to see that the dispersion interaction is typically the biggest one as shown in the table below. The reason for that is the ionization potential and we will address this issue later in the section of the McLachlan theory.

Similar Molecules Interacting Molecules	Van der Waals Energy Coefficients C (10^{-79} J m^6)							From Gas Law Eq. (6.14)	Dispersion Energy Contribution to Total (Theoretical) (%)
	Electronic Polarizability $\frac{\alpha_0}{4\pi\epsilon_0} (10^{-30}\text{m}^3)$	Permanent Dipole Moment u (D) ^a	Ionization Potential $I = h\nu_l$ (eV) ^b	C_{ind} $\frac{2u^2\alpha_0}{(4\pi\epsilon_0)^2}$	C_{orient} $\frac{u^4}{3kT(4\pi\epsilon_0)^2}$	C_{disp} $\frac{3\alpha_0^2h\nu_l}{4(4\pi\epsilon_0)^2}$	Theoretical Eq. (6.17)		
Ne–Ne	0.39	0	21.6	0	0	4	4	4	100
CH ₄ –CH ₄	2.60	0	12.6	0	0	102	102	101	100
HCl–HCl	2.63	1.08	12.7	6	11	106	123	157	86
HBr–HBr	3.61	0.78	11.6	4	3	182	189	207	96
HI–HI	5.44	0.38	10.4	2	0.2	370	372	350	99
CH ₃ Cl–CH ₃ Cl	4.56	1.87	11.3	32	101	282	415	509	68
NH ₃ –NH ₃	2.26	1.47	10.2	10	38	63	111	162	57
H ₂ O–H ₂ O	1.48	1.85	12.6	10	96	33	139	175	24

Figure 14.2: Comparison vdW

Part XII

Lecture 11

15 van der Waals Interactions

15.1 McLachlan Theory

The first complete microscopic theory for the vdW interaction involving 2 atoms in a medium, was proposed by McLachlan, which is expressed as

$$w_{\text{vdW}}(r) = -\frac{6k_B T}{(4\pi\epsilon_0)^2 r^6} \sum'_{n=0}^{\infty} \frac{\alpha_1(iv_n)\alpha_2(iv_n)}{\epsilon_3^2(iv_n)} \quad (15.1)$$

The \sum' notation denotes that the first term in the summation is multiplied by 1/2. The frequencies are sampled, only at discrete values that $hv_n = 2\pi k_B T n$ (known as the Matsubara frequencies). The typical $\alpha(iv) - v$ plots of polar and non-polar molecules using the Lorentz model can be seen in the Figure below.

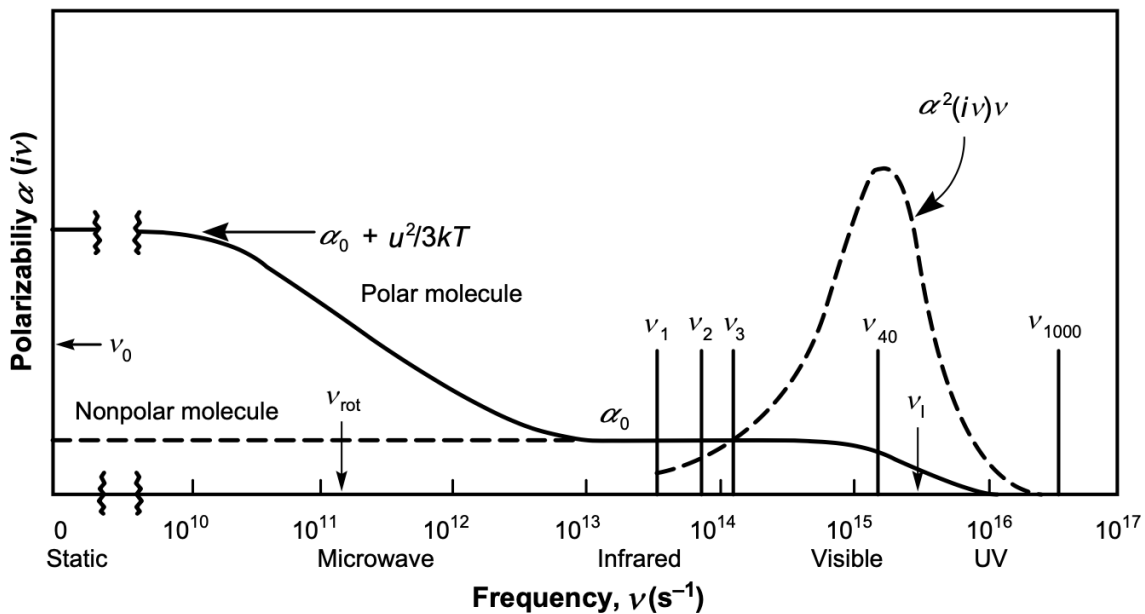


Figure 15.1: Polarizability

15.1.1 Frequency Dependent Polarizability

The electronic polarizability of a single atom can classically be approximated by a damped harmonic oscillator, i.e.

$$m_e \ddot{x} + \Gamma m_e \dot{x} + m_e \omega_0^2 x = -e E(\omega) \quad (15.2)$$

Here ω_0 is the resonance frequency, m_e the electron mass, Γ the damping constant and E the external electric field. Solving this differential equation and using $\omega = 2\pi\nu$ yields the frequency dependent electronic polarizability

$$\alpha(\nu) = \frac{\alpha_0}{1 - i\Gamma \frac{\nu}{\nu_0^2} - \left(\frac{\nu}{\nu_0}\right)^2} \quad (15.3)$$

```
import numpy as np
import matplotlib.pyplot as plt

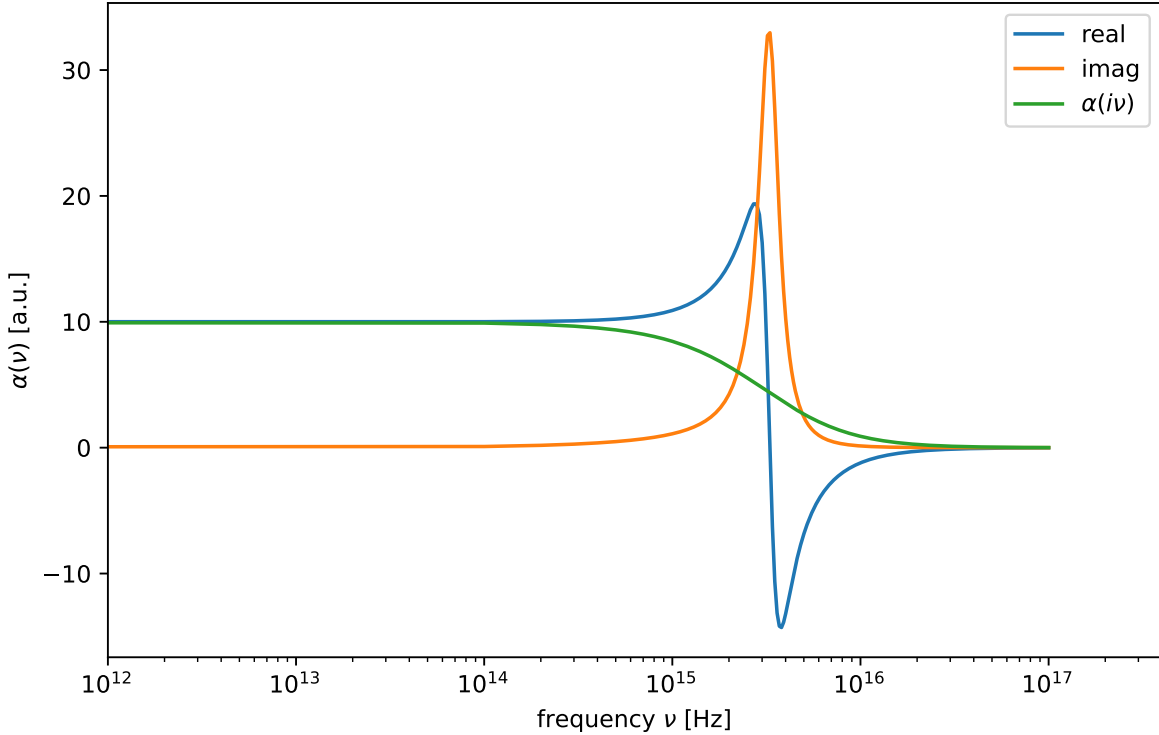
def alpha(nu,nu_0,gamma):
    return(10/(1-1j*gamma*nu/nu_0**2-(nu/nu_0)**2))

nu=np.linspace(1e5,1e17,1000)

plt.figure(figsize=(8,5))

nu_0=3.3e15

plt.semilogx(nu,alpha(nu,nu_0,1e15).real,label="real")
plt.semilogx(nu,alpha(nu,nu_0,1e15).imag,label="imag")
plt.semilogx(nu,alpha(1j*nu,nu_0,1e15).real,label=r"$\alpha(i\nu)$")
plt.xlabel(r"frequency $\nu$ [Hz]")
plt.ylabel(r"$\alpha(\nu)$ [a.u.]")
plt.xlim(1e12)
plt.legend()
plt.show()
```



15.1.1.1 Zero Frequency Contribution

At zero frequency, we know that the polarizability reduces to the form of

$$\alpha = \alpha_0 + \frac{u^2}{3k_B T}$$

which results in the first term of the sum

$$\begin{aligned} w_{\text{vdW}}(\nu = 0, r) &= -\frac{1}{2} \frac{6k_B T (\alpha_{01} + u_1^2 / (3k_B T)) (\alpha_{02} + u_2^2 / (3k_B T))}{(4\pi\epsilon_0\epsilon_3^2)^2 r^6} \\ &= -\underbrace{\frac{u_1^2 u_2^2}{3k_B T (4\pi\epsilon_0\epsilon_3)^2 r^6}}_{\text{Keesom}} - \underbrace{\frac{u_1^2 \alpha_{02} + u_2^2 \alpha_{01}}{(4\pi\epsilon_0\epsilon_3)^2 r^6}}_{\text{Debye}} - \underbrace{\frac{3k_B T \alpha_{01} \alpha_{02}}{(4\pi\epsilon_0\epsilon_3)^2 r^6}}_{\text{London(n=0)}} \end{aligned}$$

We immediately see the recovery of the Keesom and Debye energies, as well as the $\alpha_{01}\alpha_{02}$ term from mathematical derivation. In fact, the last part is the zero-frequency part of the dispersion energy. Comparing the magnitudes of $k_B T$ and $h\nu$, we can see that the zero-frequency contribution to the dispersion energy is negligible.

15.1.2 Optical Frequency Contribution

The lowest legal frequency $hv_1 = 2\pi k_B T \approx 0.16\text{eV}$. The permanent dipoles cannot respond to such high frequency, therefore the dipole polarizability has no effect on the dispersion energy at optical frequencies. The electronic polarizability govern the dispersion energy at such frequencies. We first consider $\epsilon_3 = 1$, that the 2 molecules are in vacuum.

The summation in the original equation can be estimated using continuous integral at optical frequencies, if temperature is very low. Since $h d\nu = 2\pi k_B T dn$, we can rewrite the integral from $n = 1$ to

$$w_{\text{vdw}}(\nu > 0) = \frac{h}{2\pi} \frac{6}{(4\pi\epsilon_0)^2 r^6} \int_{\nu_1}^{\infty} \alpha_1(iv)\alpha_2(iv)dv \quad (15.4)$$

Using the approximate form of the polarizability

$$\alpha(iv) = \frac{\alpha_0}{[1 + (v/v_I)^2]}$$

and $\epsilon_3 = 1$ we end up at

$$w(\nu > 0, r) = -\frac{3\alpha_{01}\alpha_{02}}{2(4\pi\epsilon_0)^2 r^6} \frac{hv_{I1}v_{I2}}{v_{I1} + v_{I2}} \quad (15.5)$$

which is finally the London form of dispersion energy. Now we know why this interaction is called “dispersion”. The largest contribution to the energy comes from the range where v is close to v_I . Since v_I is usually in UV range, such interaction is dominated by the polarizabilities from Vis to UV frequencies. As the polarizability and permittivity are closely related to the dispersion of light, it is not hard to understand why it is originally coined as “dispersion interaction”.

16 van der Waals Interaction

16.1 Interaction Between Macroscopic Bodies

The equations that we derived before are essentially valid between small objects at distances larger than their size. If objects become macroscopic, we have to consider the interaction of all components of a body with all components of the second body. To calculate those interactions, we will assume that all interactions are additive, while we know that this is not completely true for van der Waals forces.

We will generalize also our law of interaction of the individual units to

$$w(r) = -\frac{C}{r^n}$$

where C is the interaction constant. C comprises all additional constants in the interaction law. In the McLachlan case the constant C would be given as

$$w_{\text{vdW}}(r) = -\underbrace{\frac{6k_{\text{B}}T}{(4\pi\epsilon_0)^2} \sum_{n=0}^{\infty} \frac{\alpha_1(iv_n)\alpha_2(iv_n)}{\epsilon_3^2(iv_n)} \frac{1}{r^6}}_C \quad (16.1)$$

We start by evaluating the interaction of

- a) a single molecule with a wall

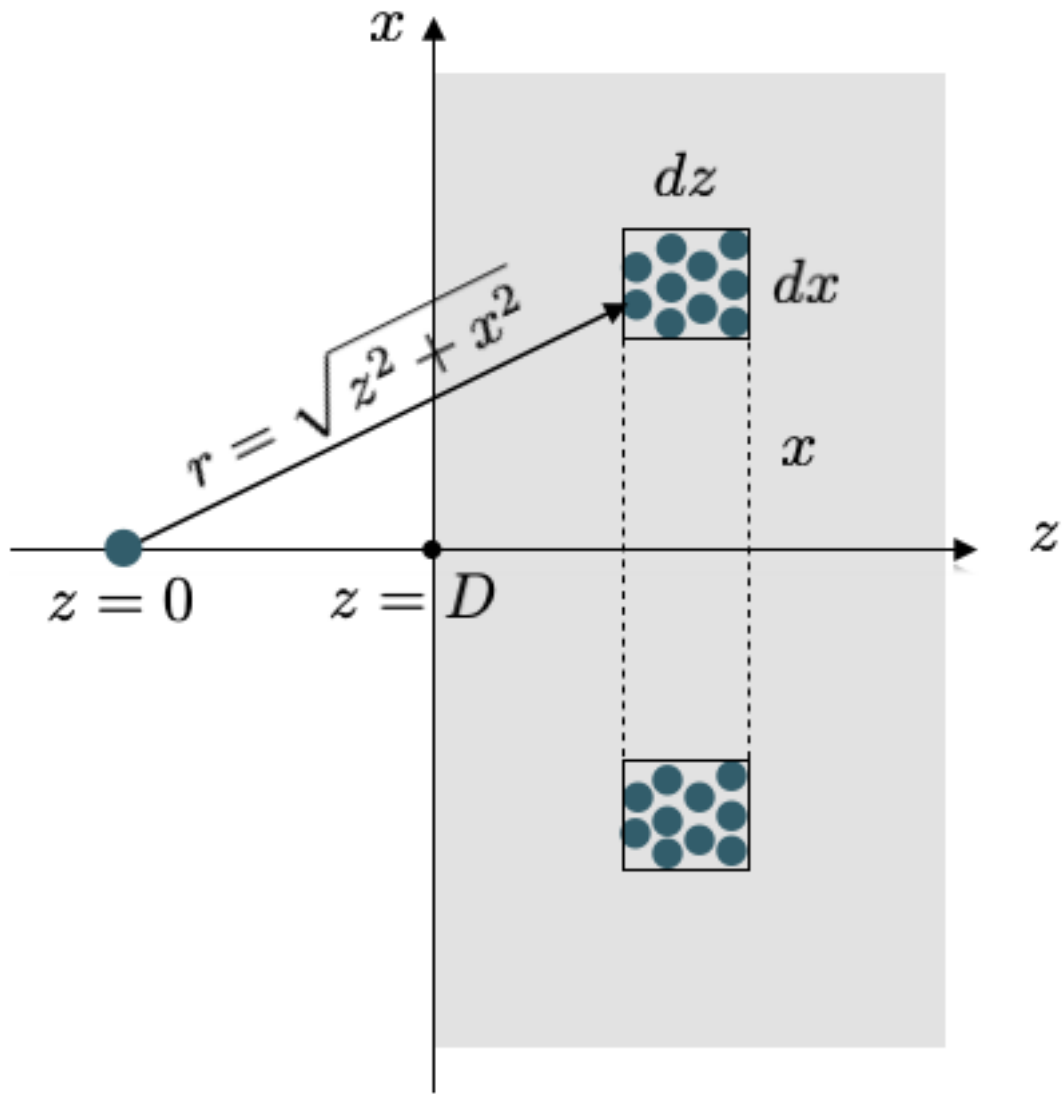


Figure 16.1: molecule_wall

According to the image above we see that the single molecule interacts with all molecules in a tiny volume element at a distance $r = \sqrt{x^2 + y^2}$ in the same way. This cylindrical volume is given by

$$2\pi x dx dz$$

and contains, based on the number density ρ of molecules in the wall and amount of $2\pi x dx dz \rho$

molecules. We then only have to sum up all contributions of shells with different x and different z which readily yields

$$w(D) = -2\pi C\rho \int_z D^\infty dz \int_{x=0}^\infty \frac{xdx}{(z^2 + x^2)(n/2)} = -\frac{2\pi C\rho}{n-2} \int_D^\infty \frac{dz}{z^{n-2}} \quad (16.2)$$

$$= -\frac{2\pi C\rho}{(n-2)(n-3)D^{n-3}} \forall n > 3 \quad (16.3)$$

Thus, if we would use the van der Waals interaction with $n = 6$ we obtain

$$w(D) = -\frac{\pi C\rho}{6D^3} \quad (16.4)$$

which decays much weaker than the original power law of the van der Waals interaction law. This is a very general results, that the interactions law, which were obtained for point-like objects turn now into distance dependences that are more complex due to the extended shape of macroscopic bodies.

b) Interaction of a sphere with a wall

If we now turn now to a sphere in front of a wall, we have to add up all contributions of molecules in the sphere, which are at a certain distance D . Each of these molecules contributes according to a), so we have to add interactions of slices of the sphere, which are at a distance $D + z$.

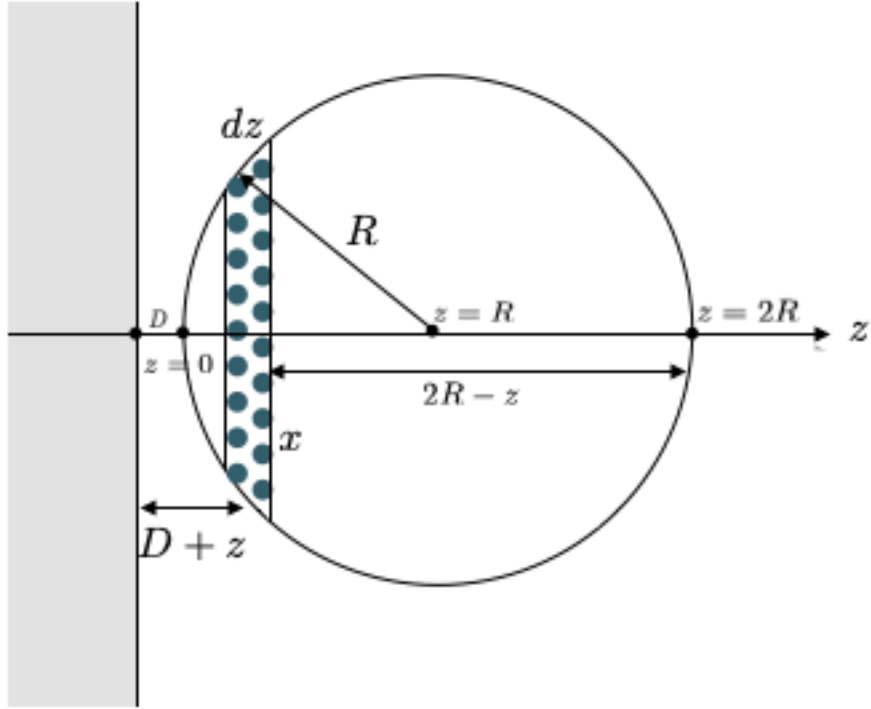


Figure 16.2: Sphere Wall

According to the figure, the radius of the slices is given by

$$x^2 = (2R - z)z$$

which gives a volume of the slice, which is $\pi x^2 dz = \pi(2R - z)z dz$ that finally gives the number of molecules $\rho\pi(2R - z)dz$ with ρ being the number density of wall and sphere. Summing now up over all slices at a distance z results in

$$w(D) = -\frac{2\pi^2 C \rho^2}{(n-2)(n-3)} \int_0^{2R} \frac{(2R - z)z dz}{(D + z)^{n-3}} \quad (16.5)$$

This results can be considered in different limits.

For $D \ll R$ we have mainly contributions from $z \approx D$, which yield then

$$w(D) = -\frac{4\pi^2 C \rho^2 R}{(n-2)(n-3)(n-4)(n-5)D^{n-5}} \quad (16.6)$$

which would give for van der Waals interactions

$$w(D) = -\frac{\pi^2 C \rho^2 R}{6D} \quad (16.7)$$

which reveals a much weaker distance dependence than the original formula for the van der Waals interaction. This is again a general result for the interaction for the interaction of bodies at small distances.

If the separation of sphere and wall is much larger than the sphere itself $D \gg R$, we can approximate the above integral with

$$w(D) = -\frac{2\pi C \rho (4\pi R^3 \rho / 3)}{(n-2)(n-3) D^{n-3}} \quad (16.8)$$

16.2 Hamaker Constant

Independent of the distance law that is resulting from the shape of the solid bodies that are interacting, there are some parameters, which persist in all of the equations and are related to the materials.

This factor is

$$A = \pi^2 C \rho_1 \rho_2$$

and is called the **Hamaker Constant**. It comprises the interaction constant C and the number density ρ , which is the same for the cases studied above where ρ^2 appears. If the number densities of the interacting bodies are different we have to consider ρ_1 and ρ_2 , of course.

Due to the fact that the Hamaker constant is related to the interaction constant C , which contains the according to the McLachlan theory the sum over the polarizabilities of the microscopic units it is strong where the polarizabilities and density are large as for example in diamond or metals. Yet we have to establish a description that is related to the continuum quantities dielectric function or refractive index, which is the Lifshitz theory following in the next lecture.

Table 13.2 Nonretarded Hamaker Constants for Two Identical Media Interacting in a Vacuum (Inert Air) at Room Temperature

Medium	Dielectric Constant ϵ	Refractive Index n	Absorption Frequency ν_e (10^{15} s^{-1})	Hamaker Constant A (10^{-20} J)		
				Eq. (13.16) $\epsilon_3 = 1$	Exact solutions ^a	Experiment ^b
Liquid He	1.057	1.028	5.9	0.057		
Water	80	1.333	3.0	3.7	3.7–5.5	
<i>n</i> -Pentane (C_5H_{12})	1.84	1.349	3.0	3.8	3.75	
<i>n</i> -Octane	1.95	1.387	3.0	4.5	4.5	
<i>n</i> -Dodecane	2.01	1.411	3.0	5.0	5.0	
<i>n</i> -Hexadecane	2.05	1.423	2.9	5.1	5.2	
Hydrocarbon (crystal)	2.25	1.50	3.0	7.1		10
Diamond	5.66	2.375	2.6	28.9	29.6	
Cyclohexane (C_6H_{12})	2.03	1.426	2.9	5.2		
Benzene (C_6H_6)	2.28	1.501	2.1	5.0		
Carbon tetrachloride (CCl_4)	2.24	1.460	2.7	5.5		
Acetone ($CH_3)_2CO$	21	1.359	2.9	4.1		
Ethanol (C_2H_5OH)	26	1.361	3.0	4.2		
Polystyrene	2.55	1.557	2.3	6.5	6.6–7.9	
Polyvinyl chloride	3.2	1.527	2.9	7.5	7.8	
PTFE (Teflon)	2.1	1.359	2.9	3.8	3.8	
Silica (SiO_2)	3.8	1.448	3.2	6.3	6.5	5–6
Mica	5.4–7.0	1.60	3.0	10	7–10	13.5
CaF_2	7.4	1.427	3.8	7.0	7.0	
Silicon (Si)	11.6	3.44	0.80	18	19–21	
Silicon nitride (Si_3N_4)	8	1.98	2.45	17	17	
Silicon carbide (SiC)	10.2	2.65	1.8	25	25	
α -Alumina, sapphire (Al_2O_3)	10.1–11.6	1.75	3.2	15	15	
Zirconia (n -ZrO ₂)	18	2.15	2.1	18	20	
Zinc sulfide (ZnS)	8.5	2.26	1.6	16	15–17	
Metals (Au, Ag, Cu)	∞	—	3–5	25–40 Eq. (13.19)	20–50	

Figure 16.3: molecule_wall

We can now use the Hamaker constant to simplify the expressions of the interactions of bodies:

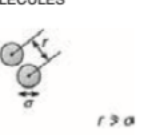
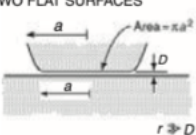
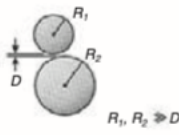
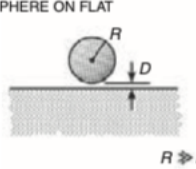
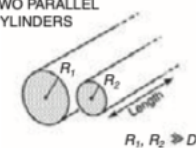
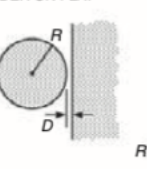
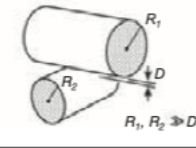
Geometry of bodies with surfaces D apart ($D \ll R$)		Van der Waals Interaction*	
		Energy, W	Force, $F = -dW/dD$
Two atoms or small molecules	TWO ATOMS or SMALL MOLECULES 	$-C/r^6$	$-6C/r^7$
Two flat surfaces (per unit area)	TWO FLAT SURFACES 	$W_{\text{flat}} = -A/12\pi D^2$	$-A/6\pi D^3$
Two spheres or macromolecules of radii R_1 and R_2	TWO SPHERES 	$\frac{-A}{6D} \left(\frac{R_1 R_2}{R_1 + R_2} \right)$	$\frac{-A}{6D^2} \left(\frac{R_1 R_2}{R_1 + R_2} \right)$ Also $F = 2\pi \left(\frac{R_1 R_2}{R_1 + R_2} \right) W_{\text{flat}}$
Sphere or macromolecule of radius R near a flat surface	SPHERE ON FLAT 	$-AR/6D$	$-AR/6D^2$ Also $F = 2\pi R W_{\text{flat}}$
Two parallel cylinders or rods of radii R_1 and R_2 (per unit length)	TWO PARALLEL CYLINDERS 	$\frac{-A}{12\sqrt{2}D^{3/2}} \left(\frac{R_1 R_2}{R_1 + R_2} \right)^{1/2}$	$\frac{-A}{8\sqrt{2}D^{5/2}} \left(\frac{R_1 R_2}{R_1 + R_2} \right)^{1/2}$
Cylinder of radius R near a flat surface (per unit length)	CYLINDER ON FLAT 	$\frac{-A\sqrt{R}}{12\sqrt{2}D^{3/2}}$	$\frac{-A\sqrt{R}}{8\sqrt{2}D^{5/2}}$
Two cylinders or filaments of radii R_1 and R_2 crossed at 90°	CROSSED CYLINDERS 	$\frac{-A\sqrt{R_1 R_2}}{6D}$	$\frac{-A\sqrt{R_1 R_2}}{6D^2}$ Also $F = 2\pi\sqrt{R_1 R_2} W_{\text{flat}}$

Figure 16.4: molecule_wall

To understand the meaning of the Hamaker constant a bit better we can have a look at the following example. We take a body made out of certain units that have a size D_0 and form a lattice. If we split an infinite body of made out of these units into two half spaces, we create two interfaces at a distance D .

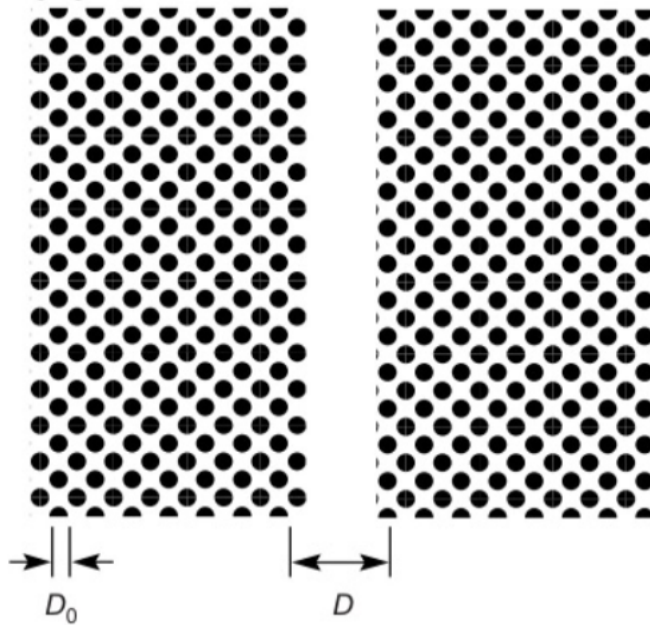


Figure 16.5: molecule_wall

The difference in interaction energy per unit area according to the above table is then given by

$$w(D) = -\frac{A}{12\pi} \left(\frac{1}{D_0^2} - \frac{1}{D^2} \right)$$

If we take the limit of $D \rightarrow \infty$, we obtain

$$\frac{A}{12\pi D_0^2} = 2\gamma$$

The energy per unit surface area is a surface energy and actually the energy to create two surfaces. It therefore corresponds to the interfacial energy of the material γ multiplied by two. So the Hamaker constant is related to the interfacial energies.

While the above equations are derived for two objects of the same material with the same Hamaker constant, there is also a rule for the interaction of two different materials. If we

have two bodies of material L and material S interacting with each other, then the Hamaker constants can be combined by

$$A_{SL} = \sqrt{A_S A_L}$$

Part XIII

Lecture 12

17 van der Waals Interaction

17.1 Lifshitz Theory

This needs to be written

The semiclassical theory we have developed in the last lecture is still based on microscopic quantities, which are the polarizabilities. We would like to base that description rather on continuum quantities to simplify the descriptions. This is done in the Lifshitz theory. It is using continuum quantities like the dielectric function ϵ_i or the refractive index n_i to describe the interactions of macroscopic bodies.

Normal calculation

$$w_{q\alpha} = -\frac{q^2 \alpha_1}{(4\pi\epsilon_0\epsilon_3)^2 r^4}$$

$$w_{q1} = \int_{\delta}^{\infty} dx \int_0^{\infty} w_{q\alpha} (r = \sqrt{(x^2 + y^2)}) \rho_1(2\pi y) dy$$

$$w_{q1} = -\frac{\pi q^2 \rho_1 \alpha_1}{(4\pi\epsilon_0\epsilon_3)^2 \delta}$$

Image charge calculation

$$\phi(x, y) = \frac{1}{(4\pi\epsilon_0)\epsilon_l} \left[\frac{q}{\sqrt{(\delta+x)^2 + y^2}} + \frac{q'}{\sqrt{(\delta-x)^2 + y^2}} \right], x < 0$$

$$\phi(x, y) = \frac{1}{(4\pi\epsilon_0)\epsilon_r} \frac{q''}{\sqrt{(\delta+x)^2 + y^2}}, x > 0$$

$$D_x^l = D_x^r$$

$$\left. \frac{\partial \phi}{\partial x} \varepsilon_l \right|_{x=0-} = \left. \frac{\partial \phi}{\partial x} \varepsilon_r \right|_{x=0+}$$

$$\frac{(q - q') \delta}{\sqrt{(\delta^2 + y^2)^3}} = \frac{(q'') \delta}{\sqrt{(\delta^2 + y^2)^3}}$$

$$E_y^l = E_y^r$$

$$\left. \frac{\partial \phi}{\partial y} \right|_{x=0-} = \left. \frac{\partial \phi}{\partial y} \right|_{x=0+}$$

$$\frac{(q + q') y}{\varepsilon_l \sqrt{(\delta^2 + y^2)^3}} = \frac{q'' y}{\varepsilon_r \sqrt{(\delta^2 + y^2)^3}}$$

$$q' = -\frac{\varepsilon_r - \varepsilon_l}{\varepsilon_r + \varepsilon_l} q$$

$$q'' = \frac{2\varepsilon_r}{\varepsilon_r + \varepsilon_l} q$$

$$w_{q1} = w_{qq'} = \frac{qq'}{(4\pi\varepsilon_0)\varepsilon_3(2\delta)} = -\frac{q^2}{(4\pi\varepsilon_0)\varepsilon_3(2\delta)} \frac{\varepsilon_1 - \varepsilon_3}{\varepsilon_1 + \varepsilon_3}$$

$$\rho_1\alpha_1 = 2\varepsilon_0\varepsilon_3 \frac{\varepsilon_1 - \varepsilon_3}{\varepsilon_1 + \varepsilon_3}$$

$$A = \frac{3kT}{2} \sum_{n=0}^{\infty} \left[\frac{\varepsilon_1(i\nu_n) - \varepsilon_3(i\nu_n)}{\varepsilon_1(i\nu_n) + \varepsilon_3(i\nu_n)} \right] \left[\frac{\varepsilon_2(i\nu_n) - \varepsilon_3(i\nu_n)}{\varepsilon_2(i\nu_n) + \varepsilon_3(i\nu_n)} \right]$$

Using this polarizability, we can write down the van der Waals interaction energy by McLachlan as

Zero Frequency

$$w(r) = -\frac{3k_B T a_1^3 a_2^3}{r^6} \left(\frac{\epsilon_1(0) - \epsilon_3(0)}{\epsilon_1(0) + \epsilon_3(0)} \right) \left(\frac{\epsilon_2(0) - \epsilon_3(0)}{\epsilon_2(0) + \epsilon_3(0)} \right) \quad (17.1)$$

and at

Optical Frequencies

$$w(r) = -\frac{3ha_1^3a_2^3}{\pi r^6} \int_{\nu_1}^{\infty} \left(\frac{\epsilon_1(i\nu) - \epsilon_3(i\nu)}{\epsilon_1(i\nu) + \epsilon_3(i\nu)} \right) \left(\frac{\epsilon_2(i\nu) - \epsilon_3(i\nu)}{\epsilon_2(i\nu) + \epsilon_3(i\nu)} \right) d\nu \quad (17.2)$$

To calculate the interaction energy we therefore need to know the dielectric function over the whole frequency range, which is often not easily accessible. Yet, if there is a strong absorption of the material at ν_e then the dielectric function can be written as

$$\epsilon(\nu) = 1 + \frac{n^2 - 1}{1 - \left(\frac{\nu}{\nu_e}\right)^2}$$

which can be inserted and integrated in the above equations as a replacement.

van der Waals interactions

Overall the van der Waals interactions have the following general properties

- since $h\nu_e \gg k_B T$ the dispersion interaction is much bigger than the rest of the interaction. For $\epsilon = n^2 \approx 2$, and $\nu_e = 3 \times 10^{15} \text{ s}^{-1}$ we find $h\nu_e/2\sqrt{3}k_B T \approx 140$
- the van der Waals interaction is greatly reduced in a solvent as compared to vacuum. For $n_1 = n_2 = 1.5$ and $n_3 = 1.4$ we obtain a factor of 32 as compared to $n_3 = 1$
- the van der Waals force between like molecules is always attractive. The dispersion part can be repulsive, however, if n_3 is between n_1 and n_2
- the van der Waals interaction is not additive
- the dispersion interaction shows retardation effects, at distances larger than 100 nm, it decays with r^{-7}

Part XIV

Lecture 13

18 Depletion Forces

Depletion forces are entropic forces which arise from osmotic pressure differences. These osmotic pressure differences are the result of regions in space which are excluded from the access of certain components of a solution. In the simplest case, the a component of s solution is excluded due to steric interactions, i.e. the component does not fit into the region due to its size.

```
import numpy as np
import matplotlib.pyplot as plt
from numpy.linalg import norm
from scipy.constants import c,epsilon_0,e,physical_constants
import json

%config InlineBackend.figure_format = 'retina'

with open('style.json', 'r') as fp:
    style = json.load(fp)

plt.rcParams.update(style)
```

18.1 Depletion force between two plates

Consider the picture below, where colloids are contained in a suspension together with two plates. Then there is a region, which is inaccessible by the centers of the colloids of radius $\sigma/2$ that is indicated by the dashed lines. If these regions between the plates overlap, not colloid can enter this region and the number density of the colloids is different inside as compared to the outside. This creates an osmotic pressure difference.

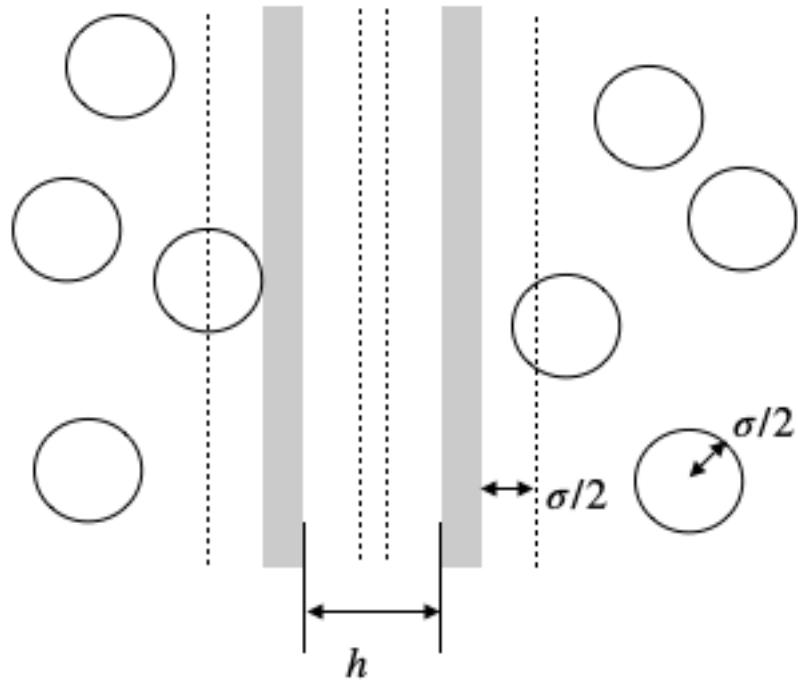


Figure 18.1: depletion_plates

The osmotic pressure difference can be calculated with the help of the van't Hoff equation for the osmotic pressure $\Pi = nk_B T$, where n is the number density. In the case the distance of the two plates is larger than the diameter of the two plates, $h > \sigma$, we have $\Pi_i = \Pi_o = nk_B T$ so the difference $P = \Pi_i - \Pi_o = 0$, so there is not pressure difference. In the case when there is no colloid between the plates we have $\Pi_i = 0$ and $\Pi_o = nk_B T$ such that

$$P = \Pi_i - \Pi_o = -nk_B T$$

Thus there is an effective pressure that is compressing the two plates. As the force per area that is required is the pressure and thus

$$P = -\frac{dw}{dh}$$

we can calculate the energy per area that is needed to separate the two plates to a distance h . This is then found to be linear in the distance h

$$w(h) = -nk_B T(\sigma - h)$$

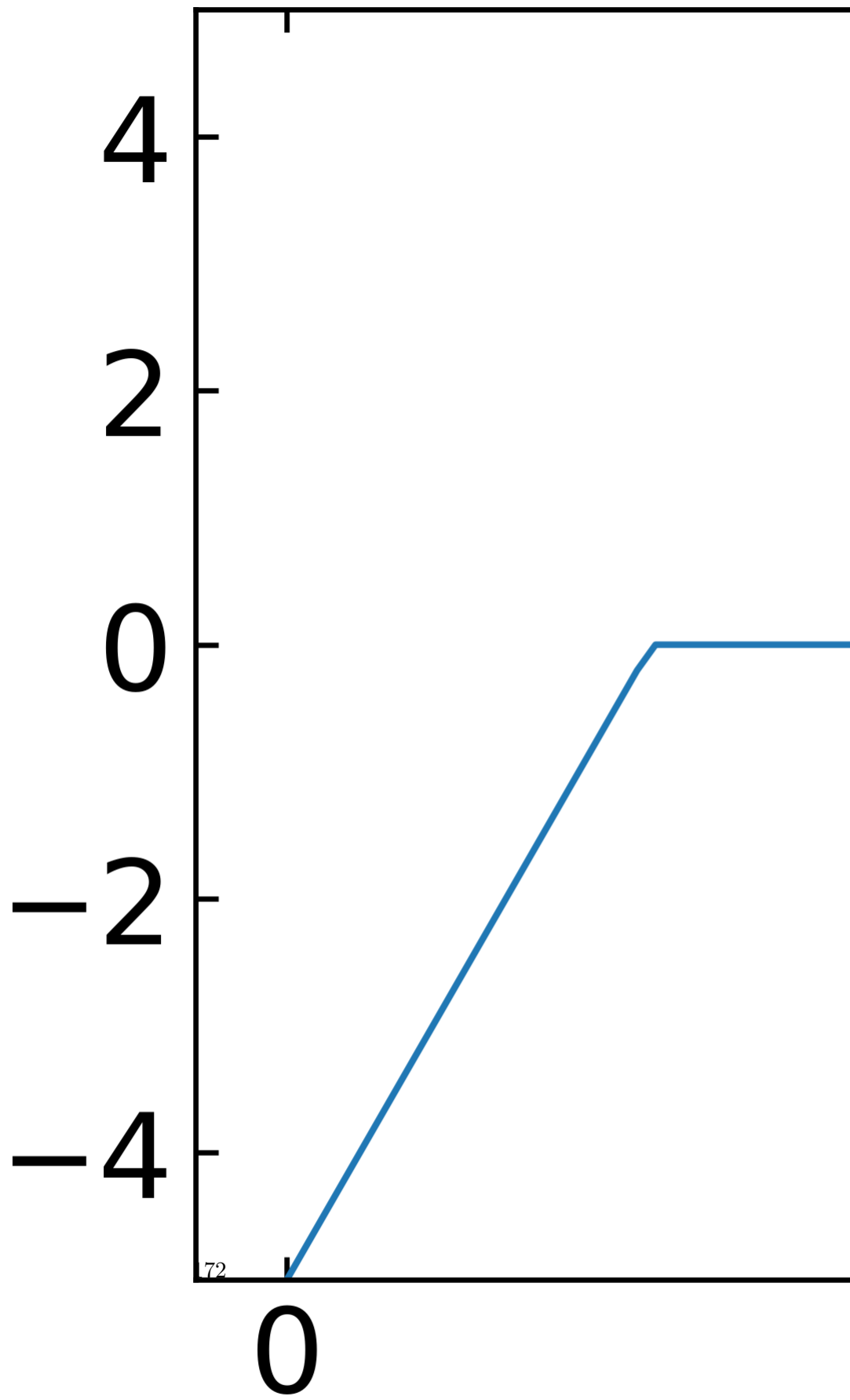
for all $h < \sigma$, while it is zero for $h > \sigma$.

```
def depletion(h,sigma,n):
    return(np.where(h<sigma, -n*(sigma-h),0))
```

```
sigma=1
h=np.linspace(0,5,100)
```

```
plt.plot(h,depletion(h,sigma,5))
plt.xlabel(r"distance h $[\mu m]$")
plt.ylabel("energy per area $[k_B T]$")
plt.ylim(-5,5)
plt.show()
```

energy per area [$k_B T$]



18.2 Depletion force between two spheres

To describe the depletion interaction between two spheres (radius R) in a solution of smaller spheres (radius $\sigma/2$), we may use the same approach of assuming an isotropic osmotic pressure of the smaller spheres. The smaller spheres can actually not approach a spherical shell of thickness $\sigma/2$ around the larger spheres or a total volume of $4\pi(R + \sigma/2)^3/3$. The pressure on the large spheres has no consequences except in the case where the two spheres approach closer than $r \leq 2(R + \sigma/2) = 2R_d$. In this case the two excluded volumes around each sphere overlap to a lens-like volume. Due to this overall, the forces which create the pressure on the spherical surface up to an angle θ_0 are unbalanced from the other side of the surface (see image) and result in an attractive interaction. The surface element between θ and $\theta d\theta$ is then given by

$$2\pi R_d^2 \sin(\theta) d\theta$$

but only the force components along the connecting line contribute.

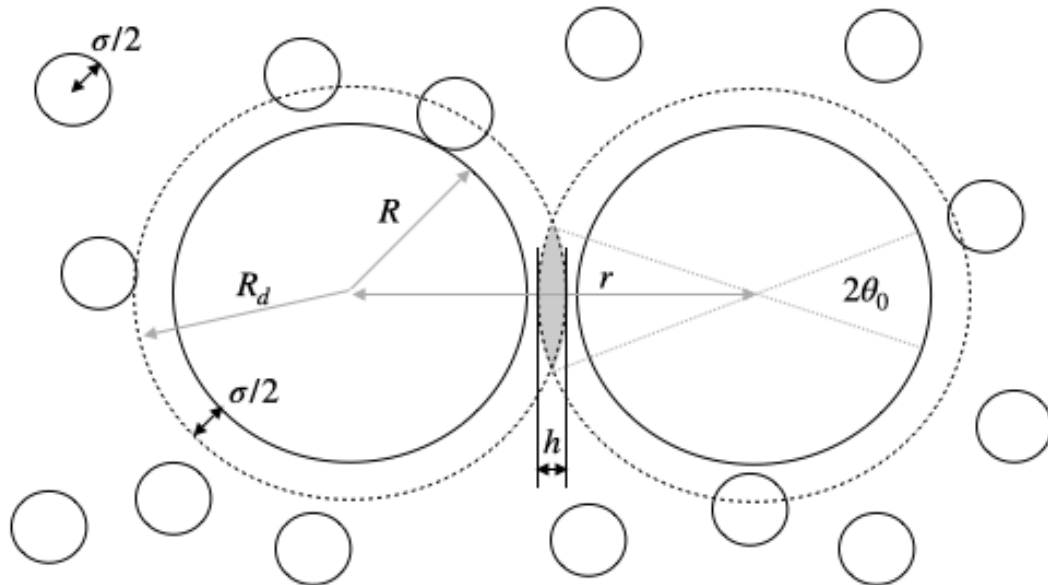


Figure 18.2: depletion_spheres

The total force is then calculated from the osmotic pressure times the surface area of the spherical cap by just taking into account the force components along the connecting line (an additional factor $\cos(\theta)$). This the read

$$F(r) = -2nk_B T \pi (R + \sigma/2)^2 \int_0^{\theta_0} \sin(\theta) \cos(\theta) d\theta$$

resulting in

$$F(r) = -nk_B T \pi (R_d)^2 \left[1 + \left(\frac{r}{2R_d} \right)^2 \right]$$

which is valid if the distance between the centers of the large spheres is $r < 2(R + \sigma/2)$. For $r \geq 2(R + \sigma/2)$ there is no depletion of the smaller spheres from the region between the larger spheres and the force is zero, i.e., $F(r) = 0$.

Calculating again the interaction free energy $w(r)$, we have to integrate the force between r and $2R_d$, which is given by

$$w(r) = \int_r^{2R_d} F(r) dr = -nk_B T V_{ov}(r)$$

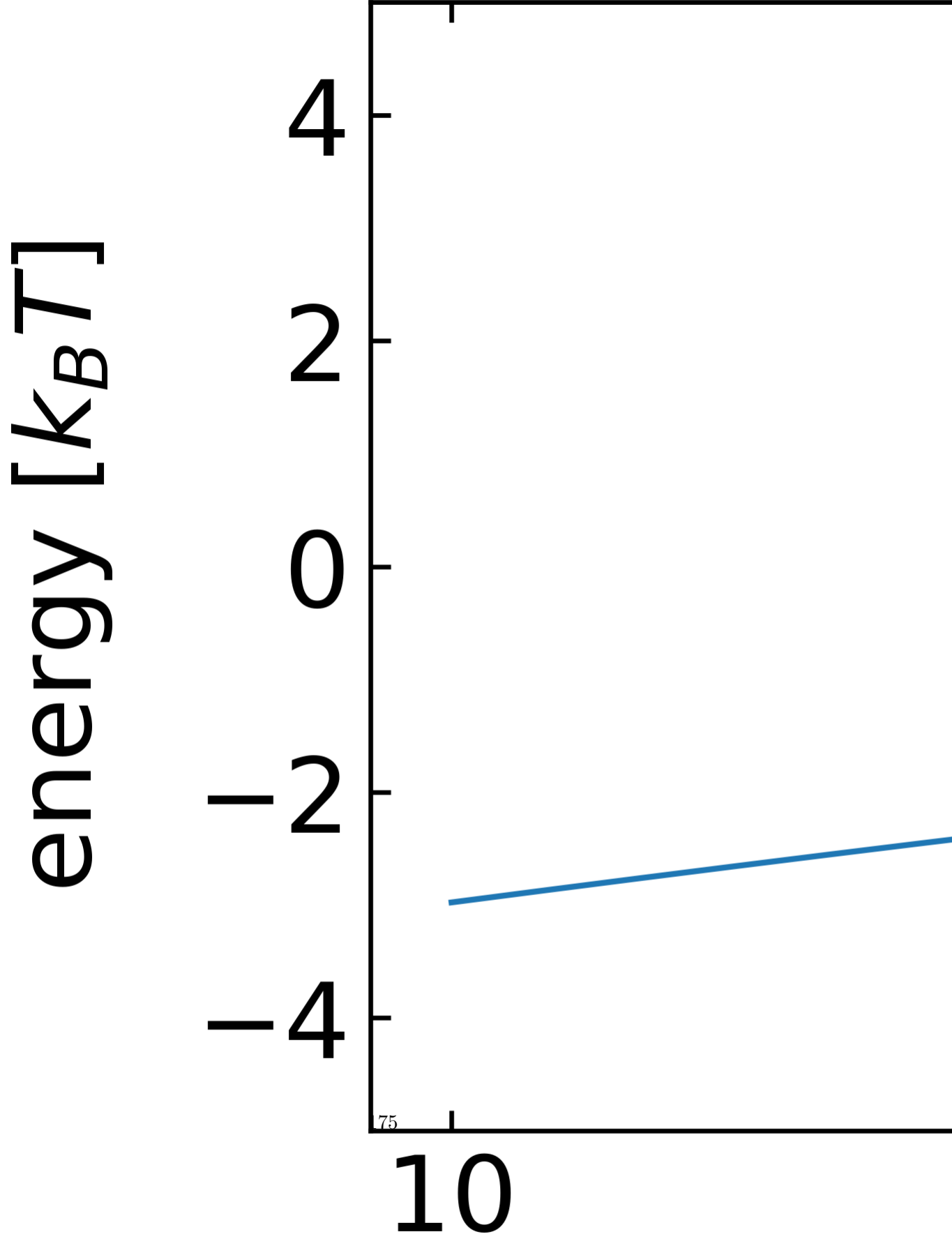
where

$$V_{ov} = \frac{4\pi}{3} R_d^3 \left[1 - \frac{3}{4} \frac{r}{R_d} + \frac{1}{16} \left(\frac{r}{R_d} \right)^3 \right]$$

```
def depletion_sphere(r,R,sigma,n):
    Rd=2*R+sigma
    Vov=4*np.pi*Rd**3/3*(1-3*r/4/Rd+(r/Rd)**3/16)
    return(np.where(r>=2*R,np.where(r<2*R+sigma, -n*Vov, 0),0))
```

```
sigma=2
R=5
n=1e-3
r=np.linspace(2*R,15,500)
```

```
plt.plot(r,depletion_sphere(r,R,sigma,n))
plt.xlabel(r"distance r $[\mu m]$")
plt.ylabel("energy $[k_B T]$")
plt.ylim(-5,5)
plt.show()
```



18.3 General description

A more general description of the depletion interaction may be obtained based on our introduction into statistical physics at the beginning of the course. There we stated that the probability of finding a system in a set of energy E is

$$p(E) = \frac{e^{-\beta E}}{Z},$$

where $\beta = 1/k_B T$ and the partition function Z is

$$Z = \sum_i e^{-\beta E_i}$$

for a system with a discrete number of states numbered by the index. For a single particle with a continuous number of energies the energy may look like

$$E = \frac{p^2}{2m} + U(q),$$

where q is some general coordinate. The classical partition function for a system of N particles is then

$$Z = \frac{1}{N! h^{3N}} \int d^3 p^N \int d^3 q^N \exp \left(-\beta \left[\sum_i \frac{p_i^2}{2m} + U(q^N) \right] \right),$$

where we use the notation p^N and q^N to denote the whole set of variables. The prefactor is appropriate for indistinguishable particles and the phase space normalization factor h (Planck's constant) for every pair of p and q . Since there is no issue of the non-commutation of positions and momenta we can perform the momentum integrals exactly, yielding

$$Z = \frac{1}{N!} \frac{1}{\Lambda^{3N}} \int d^3 q^N \exp(-\beta U(q^N)),$$

where the thermal de Broglie wavelength Λ is

$$\Lambda = \frac{h}{\sqrt{2\pi m k_B T}}.$$

In the case of two interacting large spheres in a solution of small spheres with all spheres being hard spheres, the integration over the exponential function yields

$$Z = \frac{V_A^N}{N! \Lambda^{3N}}$$

with V_A being the volume available to the small spheres, i.e., $\$V_A=V-V_{{\{E\}}}\hat{{\{}}}\$$ for $r < D + d$ and $V_A = V - V_E$ for $r > D + d$ with $V_E = \pi(D + d)^3/3$ and $V'_E = V_E - (2\pi l^2)/3[3(D+d)/2-l]$ and $l = (D+d)/2-r/2$. The calculation then yields the free energy

$$G = -k_B T \ln(Z) = -k_B T \ln \left(\frac{V_A^N}{N! \Lambda^{3N}} \right).$$

Using Stirling's formula again this can be turned into

$$G = G_{\text{ideal}} - N k_B \ln \left(\frac{V_A}{V} \right).$$

The ideal contribution to the free energy is constant with the separation of the large sphere, so it does not contribute to the depletion force. It reads

$$G_{\text{ideal}} = -N k_B T \left(1 - \ln \left(\frac{N \Lambda^3}{V} \right) \right).$$

The distance-dependent part still contains the logarithm which we can approximate by

$$\ln \left(\frac{V_A}{V} \right) \approx -\frac{V_E}{V} + \frac{\pi}{6V} (D + d - r)^2 (D + d + r/2)$$

for the case of the overlapping excluded volumes. This gives then finally a force

$$F = -\frac{N}{4V} k_B T \pi (D + d - r) (D + d + r)$$

for $r < d + D$. For all other distances of the two centers of the spheres, the depletion force is zero.

Part XV

Lecture 14

19 Depletion Forces

Depletion forces are entropic forces which arise from osmotic pressure differences. These osmotic pressure differences are the result of regions in space which are excluded from the access of certain components of a solution. In the simplest case, the a component of s solution is excluded due to steric interactions, i.e. the component does not fit into the region due to its size.

```
import numpy as np
import matplotlib.pyplot as plt
from numpy.linalg import norm
from scipy.constants import c,epsilon_0,e,physical_constants
import json

%config InlineBackend.figure_format = 'retina'

with open('style.json', 'r') as fp:
    style = json.load(fp)

plt.rcParams.update(style)
```

19.1 Depletion force between two plates

Consider the picture below, where colloids are contained in a suspension together with two plates. Then there is a region, which is inaccessible by the centers of the colloids of radius $\sigma/2$ that is indicated by the dashed lines. If these regions between the plates overlap, not colloid can enter this region and the number density of the colloids is different inside as compared to the outside. This creates an osmotic pressure difference.

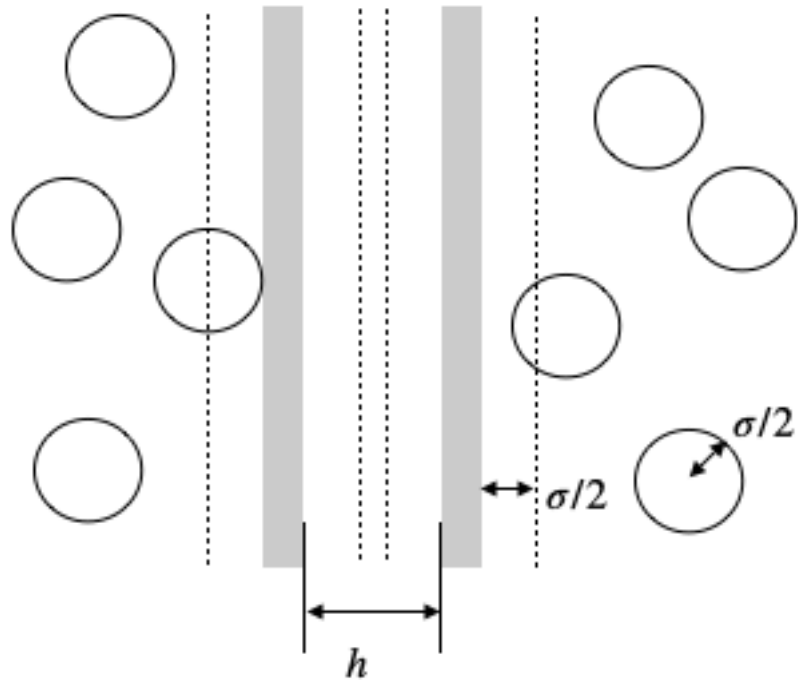


Figure 19.1: depletion_plates

The osmotic pressure difference can be calculated with the help of the van't Hoff equation for the osmotic pressure $\Pi = nk_B T$, where n is the number density. In the case the distance of the two plates is larger than the diameter of the two plates, $h > \sigma$, we have $\Pi_i = \Pi_o = nk_B T$ so the difference $P = \Pi_i - \Pi_o = 0$, so there is not pressure difference. In the case when there is no colloid between the plates we have $\Pi_i = 0$ and $\Pi_o = nk_B T$ such that

$$P = \Pi_i - \Pi_o = -nk_B T \quad (19.1)$$

Thus there is an effective pressure that is compressing the two plates. As the force per area that is required is the pressure and thus

$$P = -\frac{dw}{dh} \quad (19.2)$$

we can calculate the energy per area that is needed to separate the two plates to a distance h . This is then found to be linear in the distance h

$$w(h) = -nk_B T(\sigma - h) \quad (19.3)$$

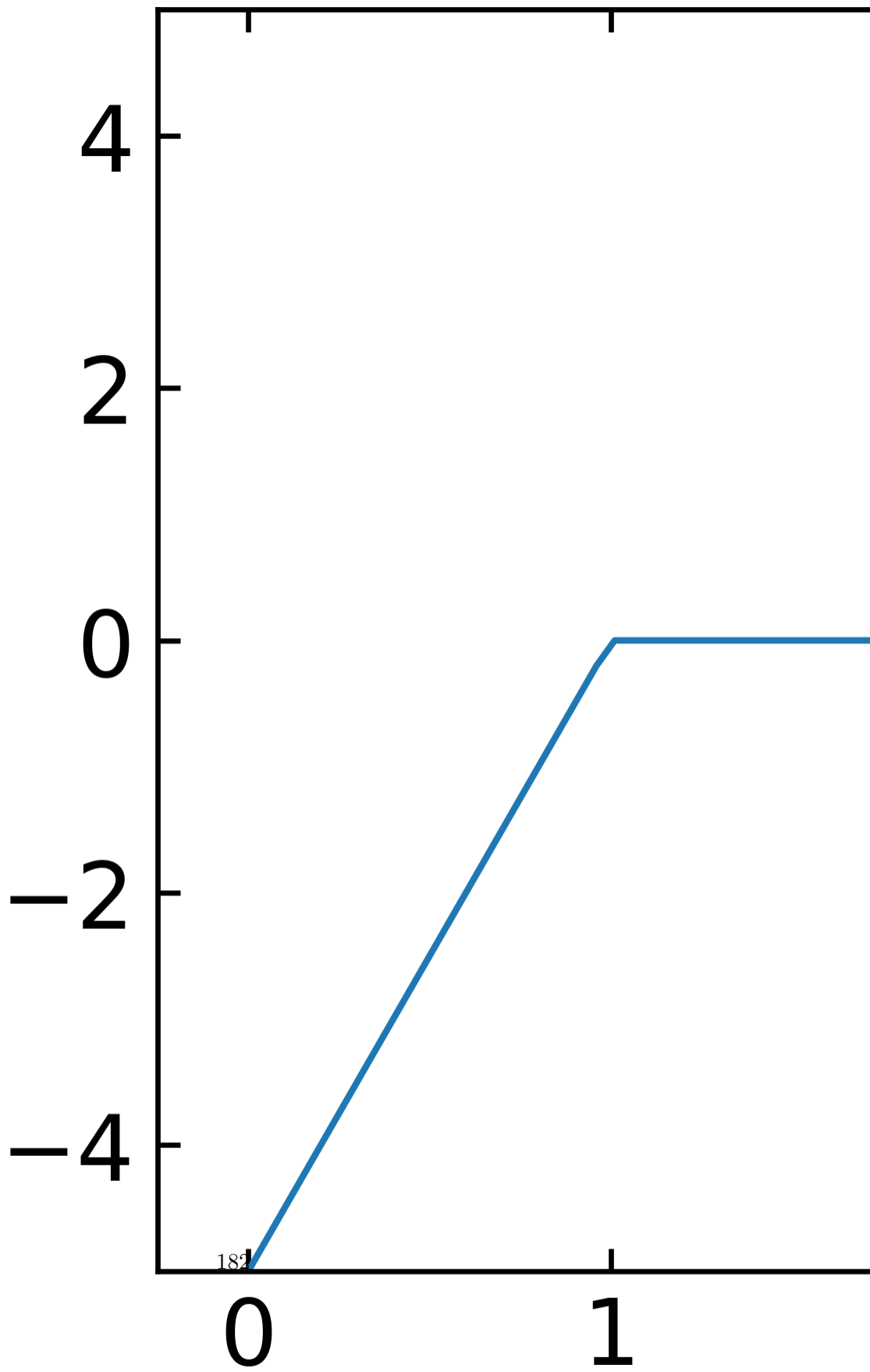
for all $h < \sigma$, while it is zero for $h > \sigma$.

```
def depletion(h,sigma,n):
    return(np.where(h<sigma, -n*(sigma-h),0))
```

```
sigma=1
h=np.linspace(0,5,100)
```

```
plt.plot(h,depletion(h,sigma,5))
plt.xlabel(r"distance h $[\mu m]$")
plt.ylabel("energy per area $[k_B T]$")
plt.ylim(-5,5)
plt.show()
```

energy per area [$\kappa_B T$]



19.2 Depletion force between two spheres

To describe the depletion interaction between two spheres (radius R) in a solution of smaller spheres (radius $\sigma/2$), we may use the same approach of assuming an isotropic osmotic pressure of the smaller spheres. The smaller spheres can actually not approach a spherical shell of thickness $\sigma/2$ around the larger spheres or a total volume of $4\pi(R + \sigma/2)^3/3$. The pressure on the large spheres has no consequences except in the case where the two spheres approach closer than $r \leq 2(R + \sigma/2) = 2R_d$. In this case the two excluded volumes around each sphere overlap to a lens-like volume. Due to this overall, the forces which create the pressure on the spherical surface up to an angle θ_0 are unbalanced from the other side of the surface (see image) and result in an attractive interaction. The surface element between θ and $\theta d\theta$ is then given by

$$2\pi R_d^2 \sin(\theta) d\theta \quad (19.4)$$

but only the force components along the connecting line contribute.

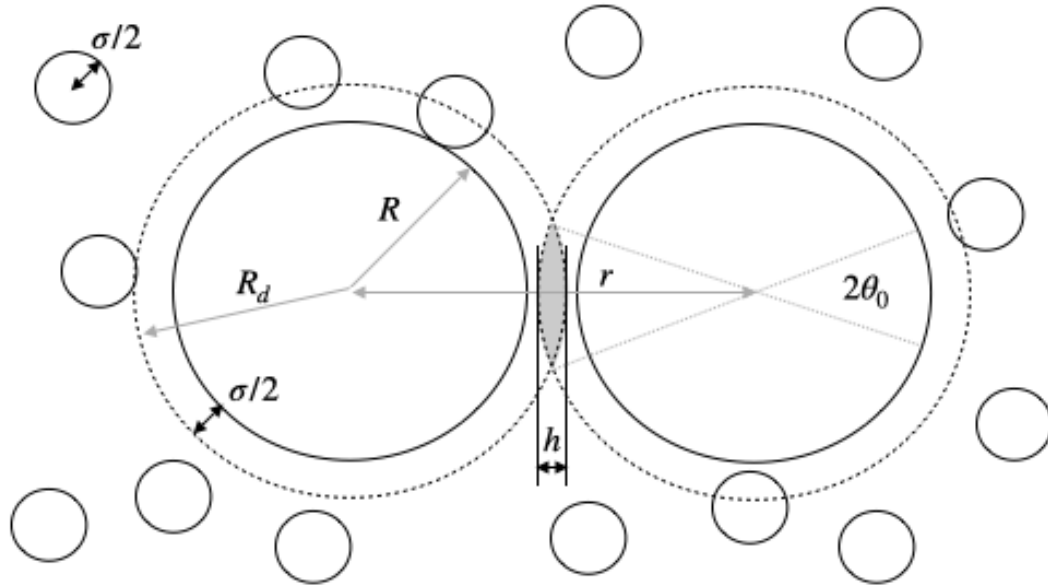


Figure 19.2: depletion_spheres

The total force is then calculated from the osmotic pressure times the surface area of the spherical cap by just taking into account the force components along the connecting line (an additional factor $\cos(\theta)$). This the read

$$F(r) = -2nk_B T \pi (R + \sigma/2)^2 \int_0^{\theta_0} \sin(\theta) \cos(\theta) d\theta \quad (19.5)$$

resulting in

$$F(r) = -nk_B T \pi (R_d)^2 \left[1 + \left(\frac{r}{2R_d} \right)^2 \right] \quad (19.6)$$

which is valid if the distance between the centers of the large spheres is $r < 2(R + \sigma/2)$. For $r \geq 2(R + \sigma/2)$ there is no depletion of the smaller spheres from the region between the larger spheres and the force is zero, i.e., $F(r) = 0$.

Calculating again the interaction free energy $w(r)$, we have to integrate the force between r and $2R_d$, which is given by

$$w(r) = \int_r^{2R_d} F(r) dr = -nk_B T V_{ov}(r)$$

where

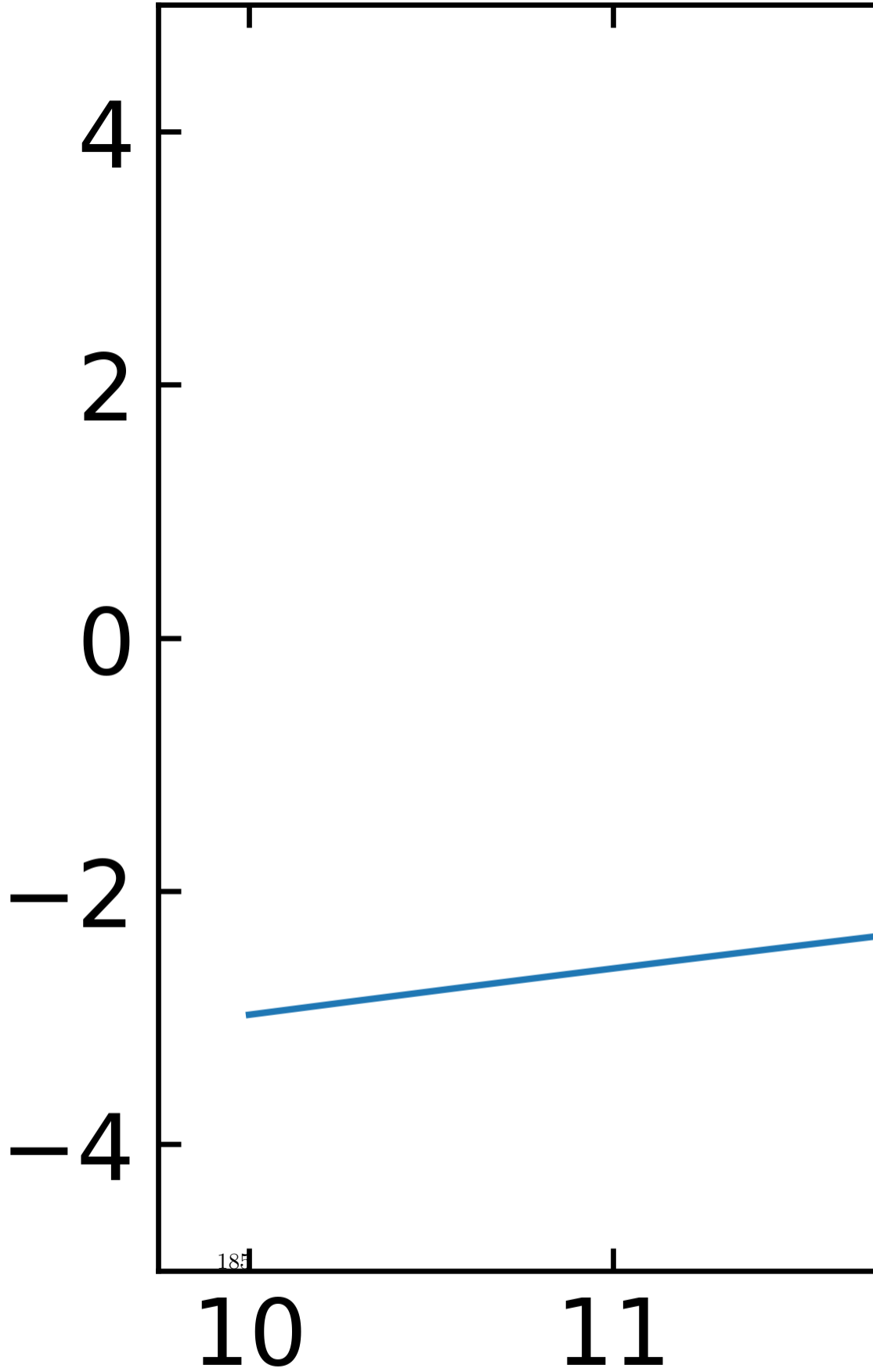
$$V_{ov} = \frac{4\pi}{3} R_d^3 \left[1 - \frac{3}{4} \frac{r}{R_d} + \frac{1}{16} \left(\frac{r}{R_d} \right)^3 \right]$$

```
def depletion_sphere(r,R,sigma,n):
    Rd=2*R+sigma
    Vov=4*np.pi*Rd**3/3*(1-3*r/4/Rd+(r/Rd)**3/16)
    return(np.where(r>=2*R,np.where(r<2*R+sigma, -n*Vov, 0),0))
```

```
sigma=2
R=5
n=1e-3
r=np.linspace(2*R,15,500)
```

```
plt.plot(r,depletion_sphere(r,R,sigma,n))
plt.xlabel(r"distance r $[\mu m]$")
plt.ylabel("energy $[k_B T]$")
plt.ylim(-5,5)
plt.show()
```

energy [$\kappa_B T$]



19.3 General description

A more general description of the depletion interaction may be obtained based on our introduction into statistical physics at the beginning of the course. There we stated that the probability of finding a system in a set of energy E is

$$p(E) = \frac{e^{-\beta E}}{Z}, \quad (19.7)$$

where $\beta = 1/k_B T$ and the partition function Z is

$$Z = \sum_i e^{-\beta E_i} \quad (19.8)$$

for a system with a discrete number of states numbered by the index. For a single particle with a continuous number of energies the energy may look like

$$E = \frac{p^2}{2m} + U(q), \quad (19.9)$$

where q is some general coordinate. The classical partition function for a system of N particles is then

$$Z = \frac{1}{N! h^{3N}} \int d^3 p^N \int d^3 q^N \exp \left(-\beta \left[\sum_i \frac{p_i^2}{2m} + U(q^N) \right] \right), \quad (19.10)$$

where we use the notation p^N and q^N to denote the whole set of variables. The prefactor is appropriate for indistinguishable particles and the phase space normalization factor h (Planck's constant) for every pair of p and q . Since there is no issue of the non-commutation of positions and momenta we can perform the momentum integrals exactly, yielding

$$Z = \frac{1}{N!} \frac{1}{\Lambda^{3N}} \int d^3 q^N \exp(-\beta U(q^N)), \quad (19.11)$$

where the thermal de Broglie wavelength Λ is

$$\Lambda = \frac{h}{\sqrt{2\pi m k_B T}}. \quad (19.12)$$

In the case of two interacting large spheres in a solution of small spheres with all spheres being hard spheres, the integration over the exponential function yields

$$Z = \frac{V_A^N}{N! \Lambda^{3N}} \quad (19.13)$$

with V_A being the volume available to the small spheres, i.e., $\$V_A=V-V_{{\{E\}}}\hat{{\{}}}'\$$ for $r < D + d$ and $V_A = V - V_E$ for $r > D + d$ with $V_E = \pi(D + d)^3/3$ and $V'_E = V_E - (2\pi l^2)/3[3(D+d)/2-l]$ and $l = (D+d)/2-r/2$. The calculation then yields the free energy

$$G = -k_B T \ln(Z) = -k_B T \ln \left(\frac{V_A^N}{N! \Lambda^{3N}} \right). \quad (19.14)$$

Using Stirling's formula again this can be turned into

$$G = G_{\text{ideal}} - N k_B \ln \left(\frac{V_A}{V} \right). \quad (19.15)$$

The ideal contribution to the free energy is constant with the separation of the large sphere, so it does not contribute to the depletion force. It reads

$$G_{\text{ideal}} = -N k_B T \left(1 - \ln \left(\frac{N \Lambda^3}{V} \right) \right). \quad (19.16)$$

The distance-dependent part still contains the logarithm which we can approximate by

$$\ln \left(\frac{V_A}{V} \right) \approx -\frac{V_E}{V} + \frac{\pi}{6V} (D + d - r)^2 (D + d + r/2) \quad (19.17)$$

for the case of the overlapping excluded volumes. This gives then finally a force

$$F = -\frac{N}{4V} k_B T \pi (D + d - r) (D + d + r) \quad (19.18)$$

for $r < d + D$. For all other distances of the two centers of the spheres, the depletion force is zero.

20 Flows and Transport in Liquids

```
import numpy as np
import matplotlib.pyplot as plt
import scipy.special as sp
import json
from ipywidgets import interact

%config InlineBackend.figure_format = 'retina'

with open('style.json', 'r') as fp:
    style = json.load(fp)

plt.rcParams.update(style)
```

20.1 Translational Diffusion

For describing the transport and the dynamics of objects we need to write down some basic relations that will later govern our analysis. One is of course the continuity equation essentially stating that in the absence of sources or sinks, material flowing into a system has to move out of it as well. The flow is characterized by a current density \mathbf{j} . The flow through a surface is then governed by the normal components of the flow with respect to the surface having a normal \mathbf{n} .

The total flow through a surface is then

$$\int_S \mathbf{j} \cdot \mathbf{n} dS$$

If f is now some quantity (a density, probability density or other) that can be transported through a surface or exist inside a volume surrounded by an area, the total amount inside the volume is given by

$$\int_V f \cdot dV$$

The change of the total content inside the volume with time is then

$$\frac{d}{dt} \int_V f \cdot dV = \int_V \frac{df}{dt} \cdot dV$$

This then yields the continuity equation

$$\frac{df}{dt} + \nabla \mathbf{j} = 0 \quad (\text{Continuity Equation})$$

If we specifically consider the number density n and insert this as f

$$\frac{dn}{dt} + \nabla(n\mathbf{v}) = 0 \quad (\text{Continuity Equation for } n)$$

The continuity equation states that the amount of the quantity (such as mass, charge, or energy) within a defined system can only change if there is a flow of that quantity into or out of the system. More generally, the continuity equation may have a source term on the right side instead of the 0 when there is a production or destruction of the quantity in the volume.

As the next step, we would like to obtain an equation, which tells us about the flow of the density of objects, due to their Brownian motion. We consider a vertical wall of area A , which separates two regions. There are $N(x)$ on the left and $N(x + \Delta x)$ on the right of area A .

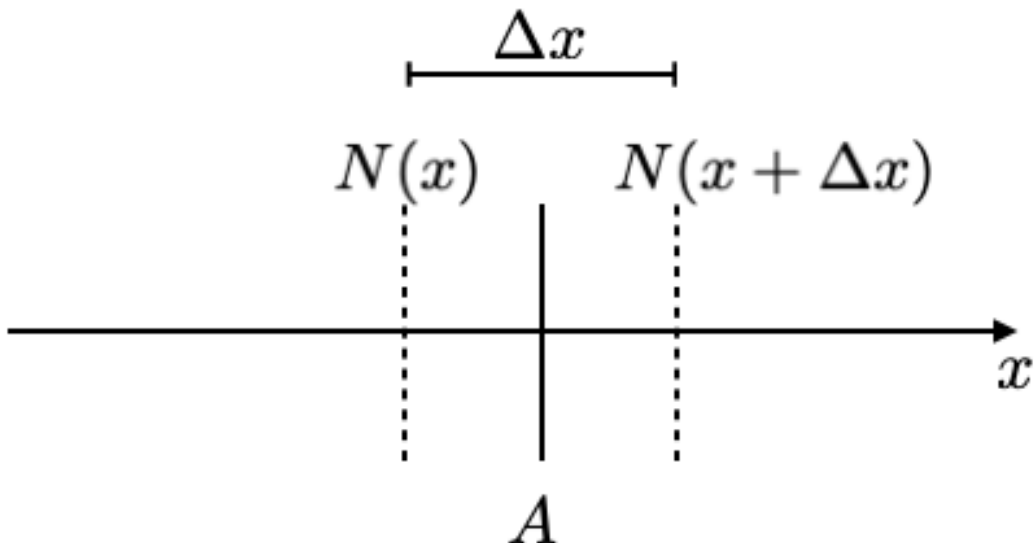


Figure 20.1: Diffusion

We can calculate the number of particles that goes through the area from the difference of the number of particles on the left and on the right side and divided by the area where the particles go through and the time τ they need to go through that this is the current density j

$$j = -\frac{1}{2} \frac{N(x + \Delta x) - N(x)}{A\tau}$$

The fact, the one half makes sure that we consider only 50% of the particles on the left side going through the area while the other 50% go further to the left.

We can also rewrite the number of particles in terms of the density n

$$n(x) \equiv \frac{N(x)}{A\Delta x}$$

where Δx and A span a volume from which the particles travel through the area A . With the help of the density, we can replace the number of particles in the equation before and obtain an equation, which only contains the density of the particles.

$$j = -\frac{1}{2} \frac{n(x + \Delta x)A\Delta x - n(x)A\Delta x}{A\tau}$$

$$j = -\frac{1}{2} \frac{\Delta x^2}{\tau} \frac{n(x + \Delta x) - n(x)}{\Delta x}$$

You can see that the area A drops out of the equation and we can sub summarise the term with Δx^2 and τ into a new coefficient, which is the diffusion coefficient D . We just arrived at the DA fusion law, which is fixed first law, which tells us that the current density is proportional to the diffusion coefficient times the negative gradient of the density.

$$j = -D \frac{dn}{dx}$$

with

$$D = \frac{\Delta x^2}{2\tau}$$

In 3 dimensions this yields

$$\mathbf{j} = -D \nabla n \quad (1. \text{ Ficks Law})$$

which we can also combine with the continuity equation to give

$$\frac{dn}{dt} = D\nabla^2 n \quad (2. \text{ Ficks Law})$$

which describes the time evolution of the density n . This type of diffusion equation is found for many transport problems. We just have to exchange the density n by other densities:

flux	transport property	gradient
particles	diffusivity	particle density
charge	conductivity	potential
liquid	permeability	pressure
momentum	viscosity	momentum density
energy	heat conductivity	temperature

20.1.1 Diffusion in External Potential - Smoluchowski Equation

And some of the cases we may need to describe the diffusion in the presence of an external force field like we did already for the sedimentation problems we studied at the beginning of the course. The force is given by a potential gradient.

$$F = -\frac{dU}{dx}$$

If the force, for example, acts on a colloid in a liquid, a steady speed of the colloid will appear after a while, when the force is balanced by the frictional force in the liquid, which amounts to $F_s = -6\pi\eta Rv$, where R is the radius of the colloid, η is the viscosity of the liquid. The steady speed of the colloid in the liquid under a force F is therefore given as

$$v = -\frac{1}{\xi} \frac{dU}{dx}$$

where $\xi = 6\pi\eta R$ is the friction coefficient for a sphere. Therefore we have an additional current density due to the external force, which is given by $j = nv$ and therefore the total current density is given by

$$j = -D \frac{dn}{dx} - \frac{n}{\xi} \frac{dU}{dx}$$

As we will see later, the diffusion coefficient can be als written as $D = k_B T / \xi$, which results in

$$j = -\frac{1}{\xi} \left(k_B T \frac{dn}{dx} + n \frac{dU}{dx} \right)$$

using

$$\frac{d}{dx} \ln(n(x)) = \frac{1}{n(x)} \frac{dn}{dx}$$

we find

$$j = -\frac{1}{\xi} n \frac{d}{dx} \left(\underbrace{k_B T \ln(x) + U}_{\text{chemical potential}} \right) = -\frac{1}{\xi} n \frac{d\mu}{dx}$$

where we recognize the term in the bracket as chemical potential. In general, an inhomogeneous chemical potential drives currents in a system. This is the general version of Fick's first law, while Ficks second law results in

$$\frac{dn}{dt} = -\frac{dj}{dx} = \frac{1}{\xi} \frac{d}{dx} \left(k_B T \frac{dn}{dx} + n \frac{dU}{dx} \right)$$

or

$$\frac{dn}{dt} = \nabla \left(D \nabla n + n \frac{\mathbf{F}}{\xi} \right) \quad (\text{Smoluchowski equation})$$

This may be even further generalized and leads to the Fokker-Planck-Equation, which we leave out here in the discussion.

The time dependet diffusion equation

$$\frac{\partial}{\partial t} n(\vec{r}, t | \vec{r}_0, t_0) = D \nabla^2 n(\vec{r}, t | \vec{r}_0, t_0)$$

can be solved for given boundary and initial conditions. For the following

$$n(\vec{r}, t \rightarrow t_0 | \vec{r}_0, t_0) = \delta(\vec{r} - \vec{r}_0) \quad (\text{initial condition})$$

$$n(|\vec{r}| \rightarrow \infty, t | \vec{r}_0, t_0) = 0 \quad (\text{boundary condition})$$

we obtain the Greens function

$$n(\vec{r}, t | \vec{r}_0, t_0) = \frac{1}{(4\pi D(t - t_0))^{3/2}} e^{-\frac{(\vec{r} - \vec{r}_0)^2}{4D(t - t_0)}} \quad (\text{Greens function})$$

for the diffusion equation and the corresponding boundary conditions. The Greens function is the impulse response. With the help of it, new solutions for any initial condition can be constructed. Lets assume we have an initial condition given by

$$n(\vec{r}, t \rightarrow 0) = f(\vec{v}_0)$$

then the time dependent solution is a superposition of the Greens function solutions

$$n(\vec{r}, t) = \int n(\vec{r}, t | \vec{r}_0, t_0) f(\vec{r}_0) d\vec{r}_0$$

Let us quickly consider the solution in 1 dimension and derive some simple properties of it. The first is the mean position of the density. The mean position is calculated by

$$\langle x \rangle = \int_{-\infty}^{+\infty} x \frac{\Delta}{\sqrt{4\pi D(t - t_0)}} \cdot e^{\frac{-(x-x_0)^2}{4D(t-t_0)}} dx$$

and the result states

$$\langle x \rangle = x_0$$

that it is constant, i.e. the initial position is stationary even though the particles spread in space. This is of course expected as there is no drift in the system to one or the other direction. As the particles still spread in space, the change is in the second moment of the distribution, which is the variance calculated by

$$\langle (x - x_0)^2 \rangle = \int_{-\infty}^{+\infty} (x - x_0)^2 n(x, t) dx = 2Dt$$

The result of this corresponds to the mean squared displacement of a single particle. The variance of the distribution grows linearly in time and the coefficient characterizing the spread of the particles is the diffusion coefficient D . The law obtained here, can be generalized to $d = 3$ dimensions by

$$\langle (\mathbf{r} - \mathbf{r}_0)^2 \rangle = 2dDt = 6Dt$$

A mean distance travelled is therefore related to the square root of time. This diffusion processes are rapid at short distances but very slow for large distance as can be seen from the table below.

Object	Distance diffused		
	1nm	10nm	1m
K ⁺	0.13 ns	2.1 s	2.5×10^9 s (700 years)
Proton	5 nm	10 s (1 min)	5×10^9 s (5 days)
Oxygen	1 m	10^4 s (4 days)	5×10^9 s (10 years) (10 million years)

Note: K⁺:Radius = 0.1 nm, T = 20°C, D = 200μm²/s.
Proton: Radius = 5 nm, viscosity = 0.013 mPa·s⁻¹, T = 27°C, D = 10μm²/s.

Figure 20.2: Table Diffusion

20.1.2 Application: Fluorescence Recovery after Photobleaching

One application of our Greens function approach that is frequently used in studying biological materials is Fluorescence Recovery after Photobleaching or short **FRAP**.

Initial condition:

$$n(x, t_0) = \Theta(-a - x) + \Theta(x - a)$$

Boundary Condition

$$\lim_{|x| \rightarrow \infty} n(x, t) = 0$$

Greens Function

$$n(x, t | x_0, t_0) = \frac{1}{\sqrt{4\pi D(t - t_0)}} e^{-\frac{(x-x_0)^2}{4D(t-t_0)}}$$

Therefore the total solution

$$n(x, t) = \int_{-\infty}^{+\infty} dx_0 n(x, t | x_0, t_0) \cdot [\Theta(-a - x) + \Theta(x - a)] \quad (20.1)$$

$$= \int_{-\infty}^{-a} dx_0 \frac{1}{\sqrt{4\pi D(t - t_0)}} e^{-\frac{(x-x_0)^2}{4D(t-t_0)}} \quad (20.2)$$

$$= \int_a^{\infty} dx_0 \frac{1}{\sqrt{4\pi D(t - t_0)}} e^{-\frac{(x-x_0)^2}{4D(t-t_0)}} \quad (20.3)$$

The solution of the integration is

$$n(x, t) = 1 - \frac{1}{2} \left(\operatorname{erf} \left[\frac{x+a}{2\sqrt{D(t-t_0)}} \right] - \operatorname{erf} \left[\frac{x-a}{2\sqrt{D(t-t_0)}} \right] \right)$$

with erf being the error function

$$\operatorname{erf}(x) = \frac{1}{\sqrt{\pi}} \int_{-x}^x e^{-t^2} dt = \frac{2}{\sqrt{\pi}} \int_0^x e^{-t^2} dt$$

```
## Example of a FRAP density profile
def heaviside(x):
    return np.where(x >= 0, 1, 0)

def n_step(x, a):
    return heaviside(-a - x) + heaviside(x - a)

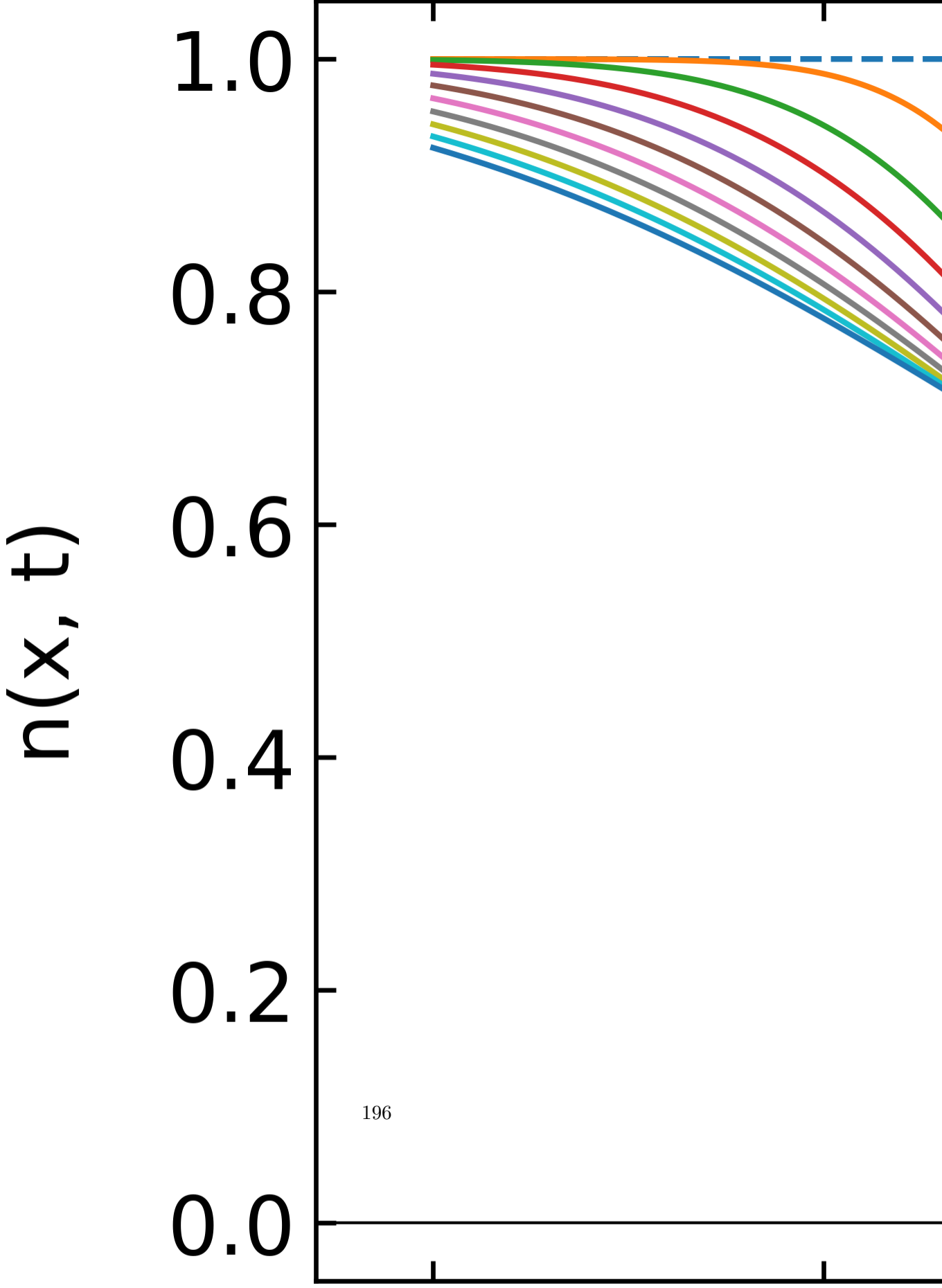
def n_solution(x, a, D, t, t0):
    term1 = sp.erf((x + a) / (2 * np.sqrt(D * (t - t0))))
    term2 = sp.erf((x - a) / (2 * np.sqrt(D * (t - t0))))
    return 1 - 0.5 * (term1 - term2)

# Parameters
a = 1 # size of the bleached region
D = 0.1 # diffusion coefficient
t0 = 0 # initial time
times = np.arange(1, 11) # times from 1 to 10 seconds
x = np.linspace(-3, 3, 400) # range of x values

plt.figure(figsize=(8, 4))
plt.plot(x, n_step(x, a), label='n(x, t0)', linestyle='--')

for t in times:
    plt.plot(x, n_solution(x, a, D, t, t0), label=f'n(x, t={t}s)')

plt.xlabel('x')
plt.ylabel('n(x, t)')
plt.axhline(0, color='black', linewidth=0.5)
plt.axvline(0, color='black', linewidth=0.5)
plt.show()
```



We can also characterize the amount of density in the bleached region as a function of time. This gives a single time trace, which we can analyze to obtain the diffusion coefficient

$$N(t, t_0) = \int_{-a}^{+a} n(x, t) dx$$

The integration of the previously obtained density then results in

$$N(t, t_0) = \frac{\sqrt{D(t - t_0)}}{a\sqrt{\pi}} \left(1 - \exp \left[-\frac{a^2}{D(t - t_0)} \right] \right) + 1 - \operatorname{erf} \left[\frac{a}{\sqrt{D(t - t_0)}} \right]$$

which is plotted below.

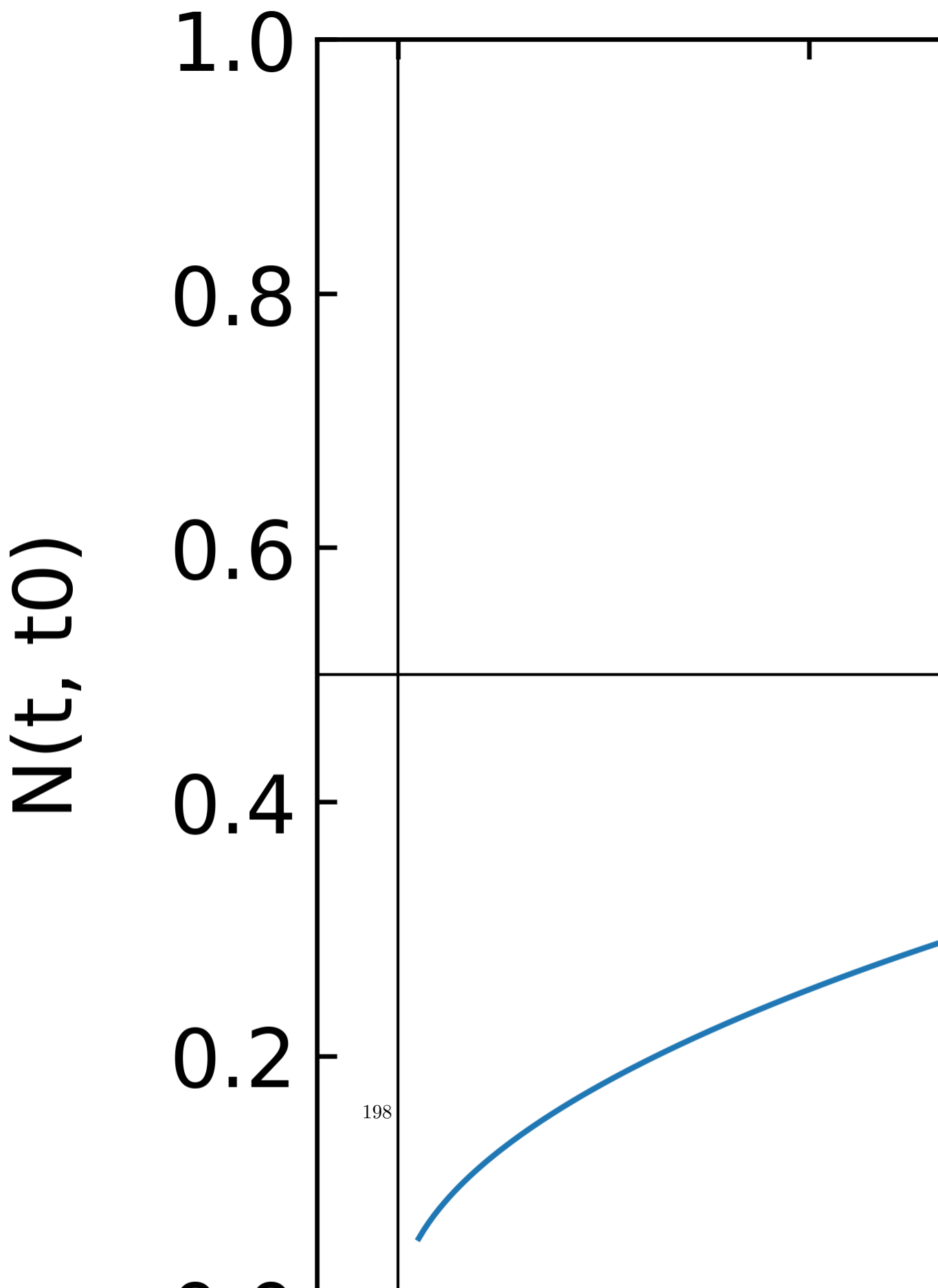
```
def N(t, t0, D, a):
    term1 = (np.sqrt(D * (t - t0)) / (a * np.sqrt(np.pi))) * (1-np.exp(-a**2 / (D * (t - t0))
    term2 = 1 - sp.erf(a / np.sqrt(D * (t - t0)))
    return (term1 + term2)

# Interactive plotting function
def plot_function(D):
    a = 1 # constant a
    t0 = 0 # initial time t0
    t = np.linspace(0.1, 10, 400) # time range from 0.1 to 10

    plt.figure(figsize=(7, 4))
    plt.plot(t, N(t, t0, D, a), label=f'Diffusion Coefficient: D={D}')
    plt.xlabel('t - t0')
    plt.ylabel('N(t, t0)')
    plt.axhline(0.5, color='black', linewidth=0.5)
    plt.axvline(0, color='black', linewidth=0.5)
    plt.ylim(0,1)
    plt.legend()
    plt.show()

# Create the widget
#interact(plot_function, D=(0.01, 1.0, 0.01));

plot_function(0.1)
```



20.2 Rotational Diffusion

If we constrain all the points that are diffusing to a sphere of radius 1, i.e. $|\vec{r}_0| = |\vec{r}| = 1$, then we have in a spherical coordinate system no radial motion just angular motion along the remaining two angular coordinates ϕ and θ .

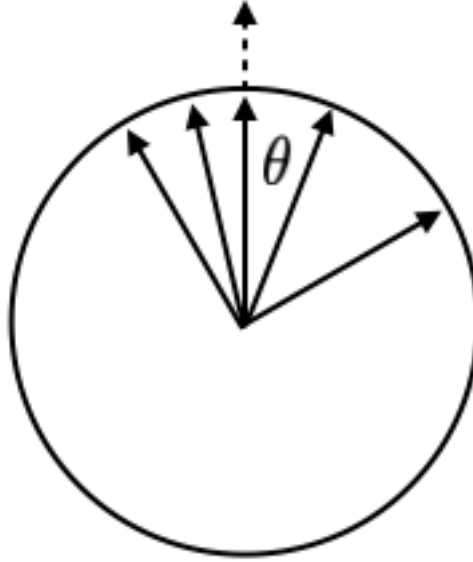


Figure 20.3: Rotational Diffusion

The dynamics of the vector from the center of the unit sphere to the surface is therefore a orientational diffusion, which obeys the following diffusion equation

$$\frac{\partial n(\Omega, t | \Omega_0, t_0)}{\partial t} = D_{\text{rot}} \left[\frac{1}{\sin \theta} \frac{\partial}{\partial \theta} \left(\sin \theta \frac{\partial}{\partial \theta} \right) + \frac{1}{\sin^2 \theta} \frac{\partial^2}{\partial \varphi^2} \right] n(\Omega, t, \Omega_0, t_0) \quad (20.4)$$

The differential operator has, without any surprise, spherical harmonics as eigenfunctions, i.e.

$$Y_l^m = N e^{im\phi} P_l^m(\cos \theta)$$

where N is a normalization factor and P_l^m are the associated Legendre polynomials. The time dependent solution of the density n at the surface of the sphere can therefore be expressed as a

sum over all surface harmonics with time dependent amplitudes $A_{lm}(t, \Omega_0, t_0)$, which depend on the initial distribution at t_0 .

$$n(\Omega, t | \Omega_0, t_0) = \sum_{l=0}^{\infty} \sum_{m=-l}^{+l} A_{lm}(t, \Omega_0, t_0) Y_l^m(\Omega)$$

To obtain a solution for the amplitudes, we insert the series into the diffusion equation to yield

$$\sum_{l=0}^{\infty} \sum_{m=-l}^{+l} \frac{\partial A_{lm}}{\partial t} Y_l^m = -\frac{1}{\tau_R} \sum_{l=0}^{\infty} \sum_{m=-l}^{+l} l(l+1) A_{lm} Y_l^m$$

where $D_{\text{rot}} = 1/\tau_R$ is the rotational diffusion coefficient. Due to the orthogonality of the surface harmonics, this finally yields

$$\frac{\partial A_{lm}}{\partial t} = -\frac{l(l+1)}{\tau_R} A_{lm}$$

for each value of the integer number l and m . This is solved by an exponential function

$$A_{lm}(t | \Omega_0, t_0) = e^{-l(l+1)\frac{(t-t_0)}{\tau_R}} a_{lm}(\Omega_0)$$

where the coefficients a_{lm} are determined by the initial conditions.

The final solution is therefore

$$n(\Omega, t | \Omega_0, t_0) = \sum_{l=0}^{\infty} \sum_{m=-l}^{+l} e^{-l(l+1)\frac{(t-t_0)}{\tau_R}} a_{lm}(\Omega_0) Y_l^m \quad (\text{rotational diffusion})$$

A more specific solution can be obtained by assuming that there is a delta function for the density n as the initial condition, i.e.

$$n(\Omega, t_0 | \Omega_0, t_0) = \delta(\Omega - \Omega_0)$$

The delta function can be expressed in spherical coordinates as

$$\delta(\Omega - \Omega_0) = \sum_{l=0}^{\infty} \sum_{m=-l}^{+l} Y_{lm}^*(\Omega_0) Y_{ln}(\Omega)$$

an yields

$$a_{lm}(\Omega_0) = Y_{lm}(\Omega_0)$$

and this finally

$$n(\Omega, t | \Omega_0, t_0) = \sum_{l=0}^{\infty} \sum_{m=-l}^k e^{-l(l+1)\frac{(t-t_0)}{\tau_R}} Y_{lm}^*(\Omega_0) Y_{lm}(\Omega)$$

Analyzing this equation we see that the amplitudes decay exponentially with a time constant $\tau_R/(l(l+1))$. The largest time constant, i.e. the time constant that prevails at long times is $\tau_R/2$, while the dynamic behavior at short times can be multi-exponential.

20.2.1 NMR Spectroscopy/Dielectric Relaxation

The results have some immediate consequences for the analysis of experimental data coming from dielectric spectroscopy or nuclear magnetic resonance (NMR). Both techniques are very common for studying soft matter, as they address either molecular electric dipoles or nuclear magnetic dipoles, which respond to a perturbation by an external field through various processes, among them an orientational diffusion.

For dielectric spectroscopy one measures a dielectric polarization, i.e. a projection of dipoles onto an axis given by an electric field. Similarly NMR uses the projection of magnetic dipoles (nuclear spins) to the magnetic field direction to create a magnetization. If the dipole makes an angle θ with the corresponding field, then the projection of the dipole is $\mu \cos(\theta)$, which is responsible for the polarization/magnetization. What is probed by NMR or dielectric spectroscopy is therefore the relaxation of that cosine term.

In the sum of spherical surface harmonics, this is actually the term with $l = 1$, which is accompanied with the first Legendre polynomial:

$$P_1^0 = P_0 \cos(\theta) \quad l = 1$$

So both techniques would probe the first Legendre polynomial, but

$$\langle P_1^0 \rangle = \frac{1}{4\pi} \int d\Omega P_0 \cos(\theta) \rightarrow 0$$

This is because the dynamics of the dipoles is uncorrelated and doing Brownian motion. Yet, you can have a look at the dynamics if you calculate the autocorrelation function

$$\begin{aligned}
\langle P_1^0(t)P_1^{0,*}(t_0) \rangle &= P_0^2 \int d\Omega \int d\Omega_0 \cos(\theta) \cos(\theta_0) n(\Omega, t|\Omega_0, t_0) n_0(\Omega_0) \\
&= \frac{4\pi}{3} P_0^2 \sum_{m=1}^l e^{-l(l+1)\frac{t-t_0}{\tau_R}} |C_{10lm}|^2
\end{aligned} \tag{20.5}$$

where the C_{10lm} are again defined by the initial conditions. So if these are delta functions, one quickly finds that

$$\langle P_3(t)P_3^*(t_0) \rangle = \frac{4\pi}{3} P_0^2 e^{-2(t-t_0)/\tau_R}$$

So the correlation function decay with a time constant that is half the rotational diffusion time due to the projection of the dipole to a certain direction. Here are some more details on measurements based on NMR, even though focused on [magnetic resonance imaging](#).

Part XVI

Lecture 16

21 Brownian Motion

Brownian motion is a hallmark of soft matter as it reveals besides the discrete nature of matter also the presence of thermal fluctuations. The overall dynamics of the motion of a colloid or molecule inside a liquid is, however rather complex. We will first do some estimates of colloidal/molecular dynamics

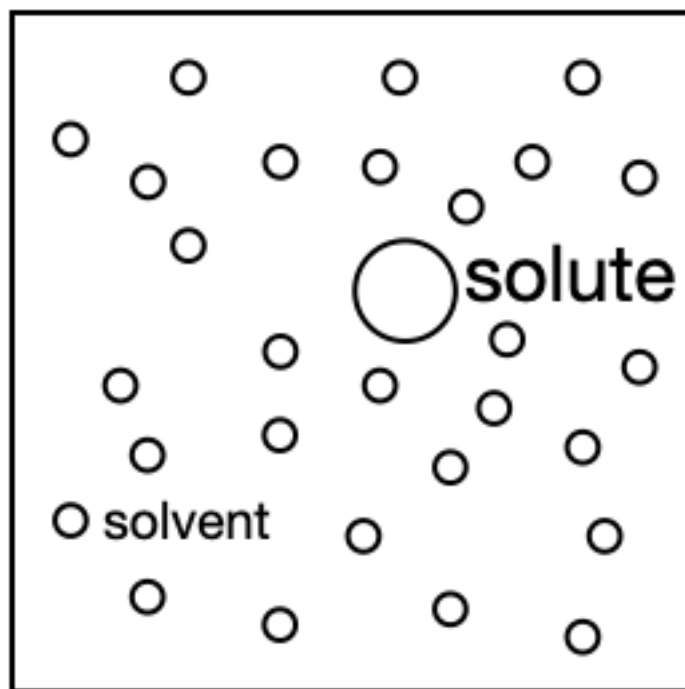


Figure 21.1: Colloidal Setup

We will for the following assume a colloid (solute) in a solvent (water) with the following properties:

sphere radius	$R = 100 \text{ nm}$
sphere mass density	$\rho = 1 \text{ g/cm}^3$
temperature	$T = 298 \text{ K}$
water viscosity	$\eta = 1 \text{ cP}$

The dynamics of the colloid will span all times and the shortest relevant timescale is the one determining the collisions between the molecules of the solvent.

1. Molecular Collision Time
2. Momentum Relaxation Time
3. Brownian Motion

21.1 Langevin Theory

```
import numpy as np
import matplotlib.pyplot as plt
from numpy.linalg import norm
from scipy.constants import c, epsilon_0, e, physical_constants
import json

%config InlineBackend.figure_format = 'retina'

with open('style.json', 'r') as fp:
    style = json.load(fp)

plt.rcParams.update(style)
```

21.1.1 Langevin Equation

Langevin theory provides now an equation of motion for objects which are subject to fluctuating forces. In the most general way, Newton's equation of motion is written as

$$m \frac{d\vec{v}}{dt} = \vec{F}(t)$$

and contains on the right side the sum of all forces \vec{F} acting on a particle. This total force can be separated into

- a viscous drag force, e.g. $6\pi\eta R\vec{v}$ for a spherical particle

- a force coming from an external potential U
- random fluctuating force $\vec{\zeta}$ due to the collisions with the solvent

With the force arising from an external potential we find the Langevin equation

$$m \frac{d\vec{v}}{dt} = -6\pi\eta R\vec{v} - \nabla U + \vec{\zeta}(t) \quad (\text{Langevin Equation})$$

The time dependence of the fluctuating force is not known in detail. Thus we can only refer to the statistical properties (e.g. its moments) when solving the Langevin equation. Therefore also no analytical solution for the position can be written down, only average properties over an ensemble or over time (given ergodicity).

The first moment (the mean) of the fluctuating force gives

$$\langle \vec{\zeta}(t) \rangle = 0$$

i.e. there is no net force acting on average on the particle considered. Yet the mean velocity of the particle is not zero, $\langle \vec{v} \rangle \neq 0$. Considering the mean velocity at short times, for example, yields

$$m \frac{d\langle \vec{v} \rangle}{dt} = -6\pi\eta R \langle \vec{v} \rangle$$

giving

$$\langle \vec{v} \rangle = \vec{v}(0) \exp\left(-\frac{t}{\tau_{mr}}\right)$$

with τ_{mr} being the momentum relaxation time we discussed already earlier. We can further continue to derive the mean squared position by taking the scalar product of the Langevin equation with \vec{r} and neglecting the potential. Taking the ensemble average yields

$$m \frac{d}{dt} \langle \vec{r} \cdot \vec{v} \rangle = -6\pi\eta R \langle \vec{r} \cdot \vec{v} \rangle + m \langle v^2 \rangle$$

since

$$\vec{r} \cdot \frac{d\vec{v}}{dt} = \frac{d}{dt}(\vec{r} \cdot \vec{v}) - v^2$$

and $\langle \vec{r} \cdot \vec{\zeta} \rangle = 0$. Using our previous result for the mean squared velocity, i.e. $\langle v^2 \rangle = 3k_B T$ we obtain after integrating over time

$$\langle \vec{r} \cdot \vec{v} \rangle = C \exp\left(-\frac{t}{\tau_{mr}}\right) + \frac{k_B T}{2\pi\eta R}$$

Using the initial condition $\vec{r}(t = 0) = 0$ this gives

$$\langle \vec{r} \cdot \vec{v} \rangle = \frac{k_B T}{2\pi\eta R} \left(1 - \exp\left(-\frac{t}{\tau_{mr}}\right) \right)$$

A second integration over time of $\langle \vec{r} \cdot \vec{v} \rangle$ can be carried out using

$$\langle \vec{r} \cdot \vec{v} \rangle = \frac{1}{2} \frac{d}{dt} \langle r^2 \rangle$$

and we finally obtain the mean squared displacement

$$\langle r^2 \rangle = \frac{k_B T}{\pi\eta R} \left[t - \tau_{mr} \left(1 - \exp\left(-\frac{t}{\tau_{mr}}\right) \right) \right]$$

This is the mean squared displacement for an Ornstein Uhlenbeck process, a process, which has a persistence for a certain time and then is randomized. It described the transition from the ballistic to diffusive regime for a Brownian particle except that it misses the hydrodynamic memory in the intermediate regime.

```
t=np.logspace(-15,0,1000)
k_B=1.381e-23 #J/K
T=300 #K
eta=1e-3 #mPa s
R=200e-9 #m
gamma=6*np.pi*eta*R
k=1e-9 #N/m

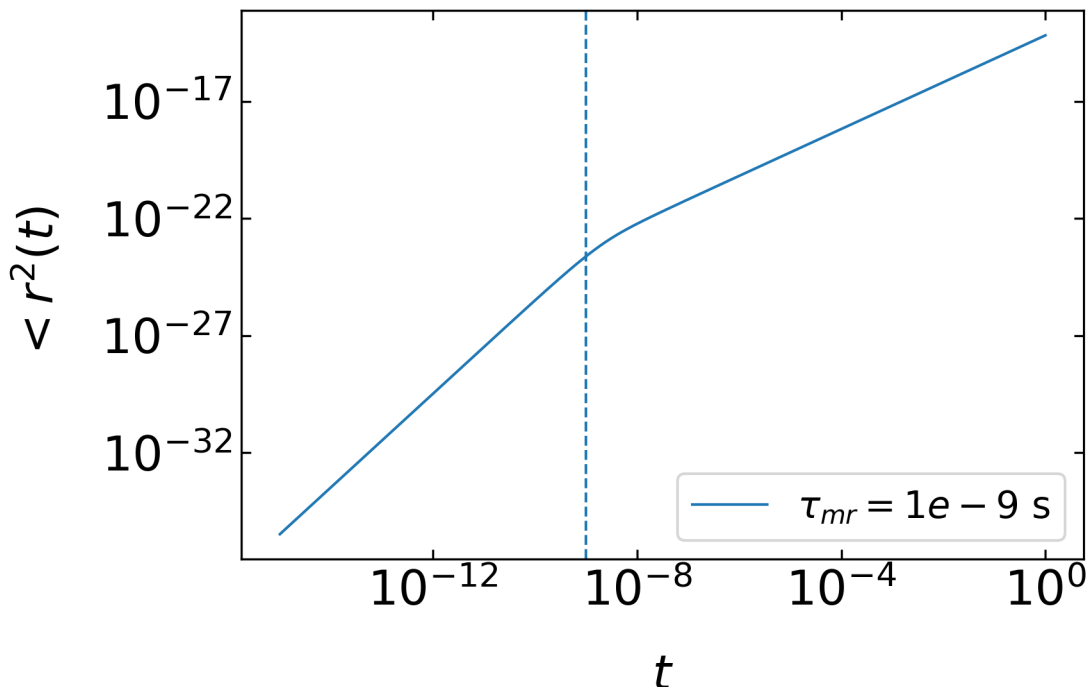
def MSD(t,taumr):
    return(k_B*T/(np.pi*R)*(t-taumr*(1-np.exp(-t/taumr))))
```

```
fig=plt.figure(figsize=(6,4))
plt.ion()
plt.loglog(t,MSD(t,1e-9),label=r"\tau_{mr}=1e-9$ s")
plt.axvline(x=1e-9,linestyle="--")
plt.xlabel(r"$t$")
plt.ylabel(r"$\langle r^2(t) \rangle$")
plt.legend()
```

```

plt.tight_layout()
plt.savefig("img/test1.png")
plt.close(fig)

```



We can look at different limits of the process with respect to the momentum relaxation time, ie.

1) long time limits: $t \gg \tau_{mr}$

In this regime, the exponential function has already decayed to zero and we obtain

$$\langle r^2 \rangle = 6Dt$$

with

$$D = \frac{k_B T}{6\pi\eta R}$$

1) short times: $t \approx \tau_{mr}$

For short times, we can expand the exponential function up to second order

$$\exp\left(-\frac{t}{\tau_{mr}}\right) \approx 1 - \frac{t}{\tau_{mr}} + \frac{t^2}{2\tau_{mr}^2}$$

to obtain for

$$t - \tau_{mr} \left(1 - \exp\left(-\frac{t}{\tau_{mr}}\right) \right) \approx \frac{t^2}{2\tau_{mr}}$$

and for the mean squared displacement

$$\langle r^2 \rangle \propto t^2$$

which is the result we expect for ballistic motion. Between both regimes, the MSD could be complicated as the short time motion starts a hydrodynamic flux in the environment which is influencing the particle motion again. These hydrodynamic memory effects cause the so called long time tails in the mean squared displacement. The Langevin equation in one dimension then reads like

$$M' \ddot{x}(t) = -6\pi\eta R \dot{x}(t) - 6R^2 \sqrt{\pi\rho_f\eta} \int_0^t (t-t')^{-1/2} \ddot{x}(t') dt' - \nabla U + \zeta(t) \quad (21.1)$$

and contains the effective mass of the colloidal M' , the fluid density ρ_f and the external potential U . The full MSD for a colloidal particle is displayed in the figure below as measured for example in an optical tweezer in the Molecular Nanophotonics group. Note that the MSD axis goes down to 10^{-21} m, which corresponds to 30 picometer displacement, which is far below the size of a hydrogen atom.

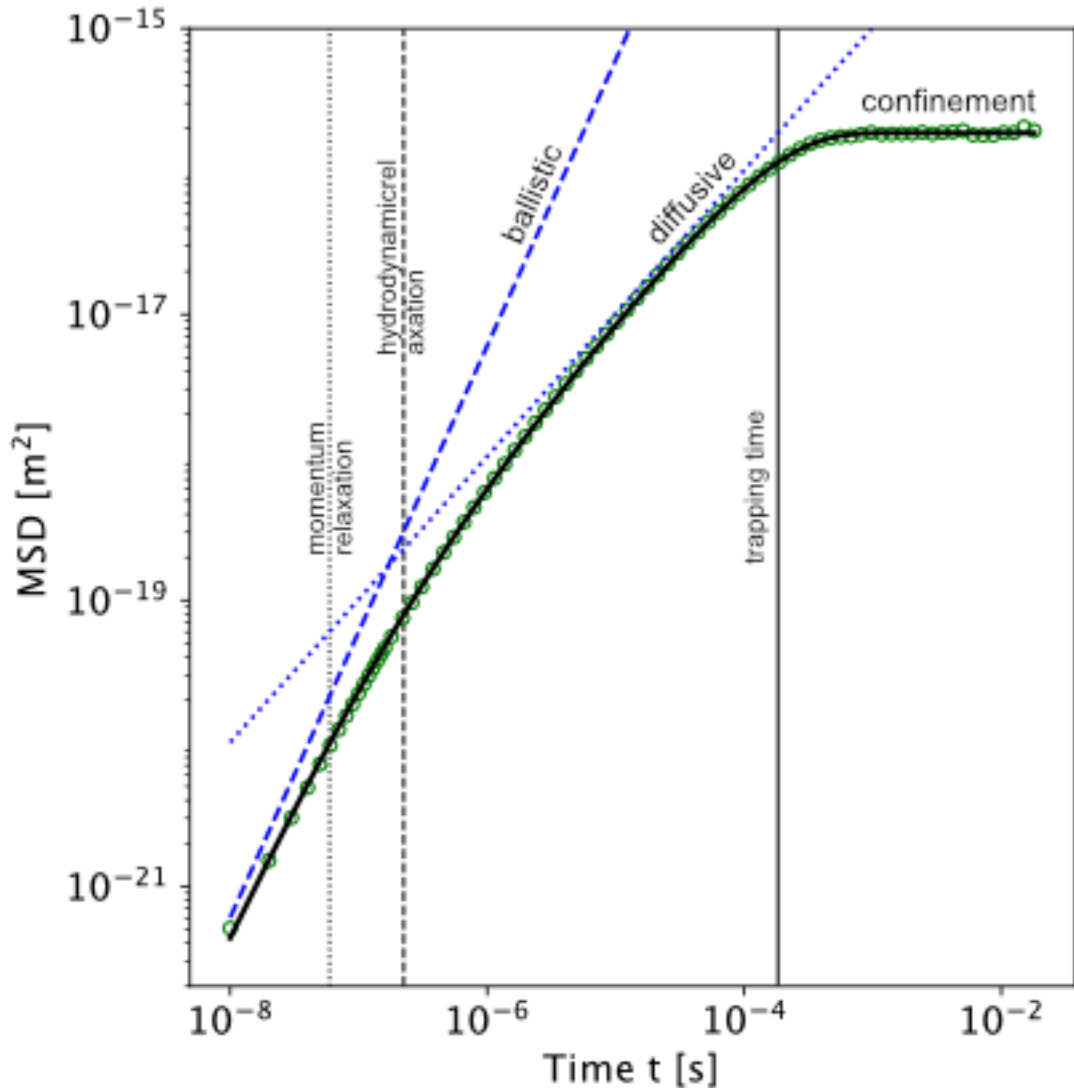


Figure 21.2: MSD

While we so far only know that $\langle \vec{\zeta}(t) \rangle = 0$, we also know that there must be a certain magnitude of the random force that is connected to the temperature of the sample. The short time autocorrelation of the noise should be of the type

$$\langle \vec{\zeta}(t_1) \cdot \vec{\zeta}(t_2) \rangle = A\delta(t_1 - t_2)$$

stating the the forces are truly random and only correlated, when the times coincide. We would like to determine the prefactor A now. We can write down the Langevin equation with

$$\frac{d}{dt} \vec{v}(t) = -\frac{1}{\tau_{mr}} \vec{v}(t) + \frac{1}{m} \vec{\zeta}(t)$$

and multiply by $\exp(t/\tau_{mr})$, which results in

$$\exp\left(\frac{t}{\tau_{mr}}\right) \frac{d}{dt} \vec{v}(t) + \frac{1}{\tau_{mr}} \exp\left(\frac{t}{\tau_{mr}}\right) \vec{v}(t) = \frac{d}{dt} \left(\exp\left(\frac{t}{\tau_{mr}}\right) \vec{v}(t) \right) = \exp\left(\frac{t}{\tau_{mr}}\right) \frac{1}{m} \vec{\zeta}(t)$$

Integrating both sides of the two right parts over time results in

$$\vec{v}(t) = \vec{v}(0) \exp\left(-\frac{t}{\tau_{mr}}\right) + \exp\left(-\frac{t}{\tau_{mr}}\right) \frac{1}{m} \int_0^t \exp\left(\frac{t'}{\tau_{mr}}\right) \vec{\zeta}(t') dt'$$

which is the time evolution of the velocity. To obtain $\langle \vec{\zeta}(t_1) \cdot \vec{\zeta}(t_2) \rangle$, we need to calculate the product of the velocity at two times and take the ensemble average. The calculation is essentially a writing exercise which at the end yields three different terms.

The first term contains

$$\langle v_0^2 \rangle \exp\left(-\frac{2t}{\tau_{mr}}\right) \rightarrow 0$$

which decays to zero for long times. The second term contains two mixed terms of the type

$$\frac{v_0}{m} \exp\left(-\frac{t}{\tau_{mr}}\right) \int \dots \rightarrow 0$$

which also decay to zero for long times. The last term contains

$$\frac{1}{m^2} \int_{-\infty}^t dt' \int_{-\infty}^t dt'' \exp\left(-\frac{t-t'}{\tau_{mr}}\right) \exp\left(-\frac{t-t''}{\tau_{mr}}\right) \langle \vec{\zeta}(t') \cdot \vec{\zeta}(t'') \rangle$$

which is the only nonzero term. Inserting our initial assumption $\langle \vec{\zeta}(t_1) \cdot \vec{\zeta}(t_2) \rangle = A\delta(t_1 - t_2)$ results in the mean squared velocity

$$\langle v^2 \rangle = \frac{A}{2m} \int_{-\infty}^t dt' \exp\left(-\frac{2(t-t')}{\tau_{mr}}\right) = \frac{A\tau_{mr}}{2m^2}$$

Since the velocity also has to comply with equipartition, i.e.

$$\langle v^2 \rangle = \frac{k_B T}{m} = \frac{A\tau_{mr}}{2m^2}$$

we find

$$A = 2\gamma k_B T$$

with $\gamma = 6\pi\eta R$ or

$$\langle \vec{\zeta}(t_1) \cdot \vec{\zeta}(t_2) \rangle = 2\gamma k_B T \delta(t_1 - t_2)$$

which is a very fundamental result. It states that the fluctuating force $\vec{\zeta}(t)$ are related to the viscous forces expressed by the friction coefficient γ . This makes sense, since the friction forces must dissipate energy into heat. The motion would thus come to a rest if heat and dynamics would be decoupled. The law we obtained is thus stating the dissipated energy goes back again into kinetic energy. This is the statement of the fluctuation dissipation theorem,

21.2 Fluctuation Dissipation Theorem

The fluctuation dissipation theorem (FDT) generalizes the previous finding into

$$\chi''(\omega) = \frac{\omega}{2k_B T} \langle |x_\omega|^2 \rangle \quad (\text{Fluctuation dissipation relation})$$

which is now converted into frequency space. On the left side is the imaginary part of a response function or susceptibility χ , which is connected to the dissipation. The right side contains the power spectral density of the fluctuation of a variable x_ω at the frequency ω . So the amplitude of a fluctuation at a certain frequency is connected to the dissipation in equilibrium.

21.2.1 Damped Driven Harmonic Oscillator

We would like to have a look at the FDT using a 1d damped driven oscillator given by the following equation

$$m\ddot{x} + \gamma\dot{x} + kx = F(t)$$

with k being the spring constant of the harmonic potential and γ the friction coefficient. Solving this differential equation yields for the amplitude of the oscillation at a certain driving frequency of $F(t)$

$$x_\omega = \frac{1}{k - m\omega^2 - i\gamma\omega} F_\omega$$

which is clearly a linear response relation as amplitude and force dependent linearly on each other. The amplitude of the force is actually the amplitude of the fluctuating force, we obtained for the Langevin equation before, e.g. $F_\omega = A = \sqrt{2\gamma k_B T}$. As this is white noise, the amplitude at different frequencies is the same. The term converting the force into an amplitude is the response function

$$\chi(\omega) = \frac{1}{k - m\omega^2 - i\gamma\omega} \quad (\text{response function})$$

which can be split into real and imaginary part, i.e. $\chi = \chi'(\omega) + i\chi''(\omega)$. A quick calculation shows that

$$\chi''(\omega) = \frac{\omega\gamma}{(k - m\omega^2)^2 + (\omega\gamma)^2}$$

In the overdamped regime (i.e. $m = 0$) we therefore find for the imaginary part

$$\chi''(\omega) = \frac{\omega\gamma}{k^2 + (\omega\gamma)^2}$$

If we further switch off the harmonic potential we just have

$$\chi''(\omega) = \frac{\omega\gamma}{\omega^2\gamma^2}$$

which is the response function for Brownian motion. From this we find

$$\frac{\chi''(\omega)}{\omega} = \frac{1}{\omega^2\gamma} \langle |x_\omega|^2 \rangle = \frac{1}{\gamma\omega^2}$$

or

$$\langle |x_\omega|^2 \rangle = \frac{2k_B T}{\gamma\omega^2}$$

for the amplitude and

$$\langle |v_\omega|^2 \rangle = \frac{2k_B T}{\gamma}$$

for the velocity amplitude. This is the frequency spectrum of the positional and speed fluctuations of a Brownian particle. This is exactly what is found in an optical tweezer for a Brownian particle at high frequencies. At lower frequencies the particle bounces from the harmonic potential and the motion of the colloid is restricted.

$$\frac{\chi''(\omega)}{\omega} = \frac{\gamma}{k^2 + (\omega\gamma)^2} = \frac{1}{2k_B T} \langle |x_\omega|^2 \rangle$$

From this follows the power spectral density of the positional fluctuations in an optical tweezers

$$\langle |x_\omega|^2 \rangle = \frac{2k_B T \gamma}{k^2} \frac{1}{1 + (\omega/\omega_0)^2}$$

Here $\omega_0 = k/\gamma$ is a particular frequency at which the $1/\omega^2$ dependence of the power spectrum turns into a plateau at small frequencies. The last equation is heavily used to calibrate optical tweezers, as it can be used to measure the force constant k .

```
omega=np.logspace(-3,3,1000)
k_B=1.381e-23 #J/K
T=300 #K
eta=1e-3 #mPa s
R=200e-9 #m
gamma=6*np.pi*eta*R
k=1e-9 #N/m

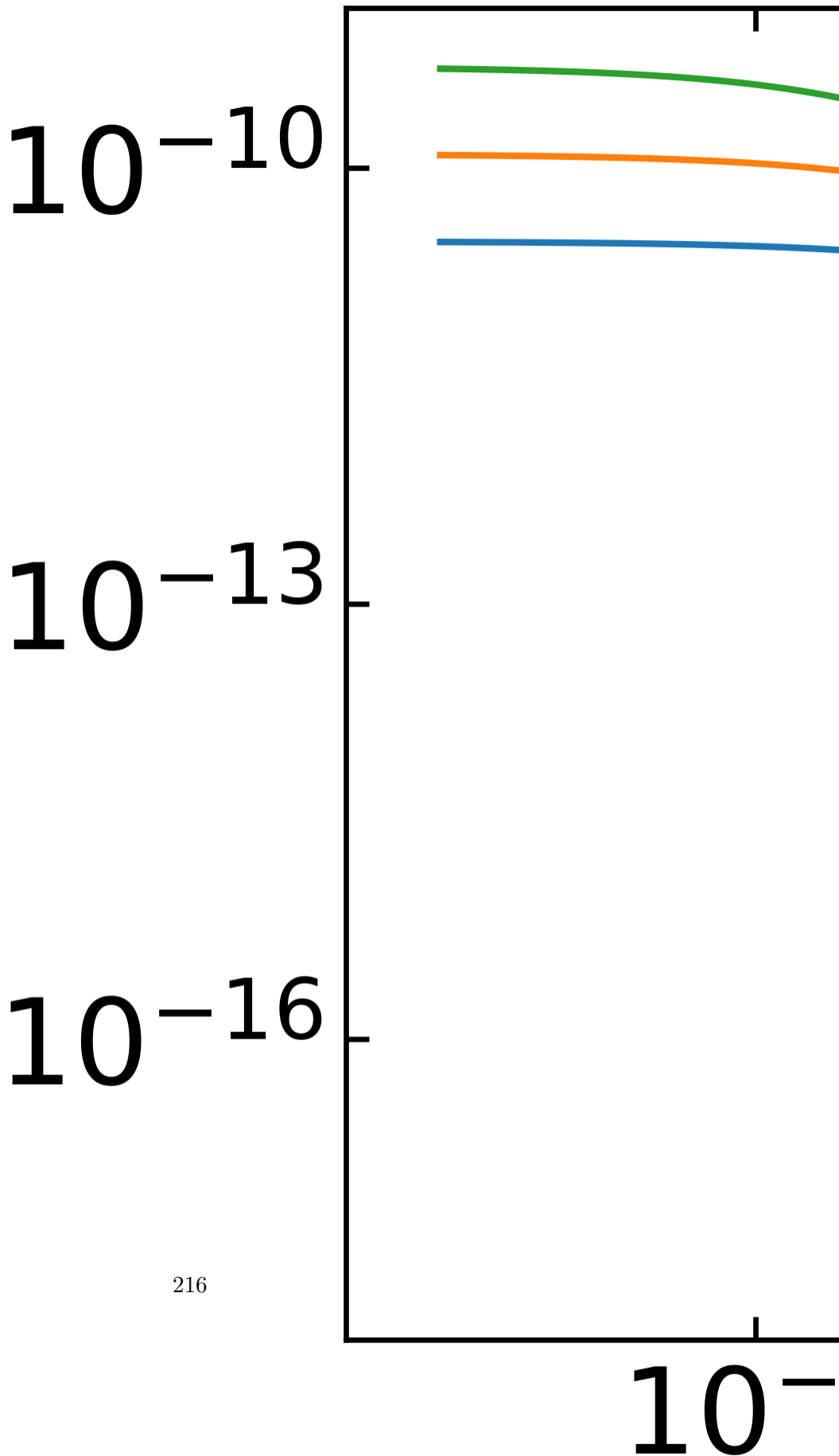
def PSD(omega,k):
    return(2*k_B*T*gamma/(k**2*(1+omega*gamma/k)**2))
```

```
fig=plt.figure(figsize=(6,4))

plt.loglog(omega,PSD(omega,k),label=r"$k=1\text{ N}$")
plt.loglog(omega,PSD(omega,k/2),label=r"$k=0.5\text{ N}$")
plt.loglog(omega,PSD(omega,k/4),label=r"$k=0.25\text{ N}$")
plt.axvline(x=k/gamma,linestyle="--",color="k")
plt.axvline(x=k/gamma/2,linestyle="--",color="k")
plt.axvline(x=k/gamma/4,linestyle="--",color="k")
plt.xlabel(r"\omega")
```

```
plt.ylabel(r"$|x_{\omega}|^2$")
plt.legend()
plt.tight_layout()
#plt.savefig("img/test.png")
plt.show()
```

$$\propto |\chi_\omega|^2$$



Part XVII

Lecture 17

22 Hydrodynamics

Hydrodynamics provides the fundamental equations to describe the motion of a fluid. Note that a fluid can thereby be a gas or a liquid. Gases and liquids may have completely different flow properties as in liquids the mean free path of a molecule is much smaller than the size of the liquid container. This is something, that is not always true for gases.

In fluid dynamics, we are interested in the motion of a volume element of a fluid, which moves with a velocity \vec{u} . As the whole fluid moves, each volume element may have a different flow velocity, which results in a flow field $\vec{u}(\vec{r}, t)$. Each component of the flow field depends now on each coordinate, i.e.

$$\vec{u} = \begin{Bmatrix} u(x, y, z, t) \\ v(x, y, z, t) \\ w(x, y, z, t) \end{Bmatrix}$$

In case of a stationary flow, the components do not explicitly depend on time, which means

$$\frac{\partial \vec{u}}{\partial t} = 0$$

Streamline

A streamline is a curve where each point on the curve has the same direction as \vec{u} without requiring the \vec{u} is constant along the streamline. This means that there are no perpendicular velocity components along a streamline, i.e. $d\vec{r} \times \vec{u} = 0$.

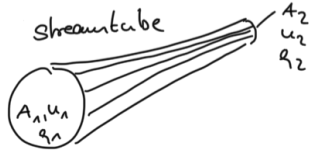


Figure 22.1: Streamtube

When we now follow the motion of a fluid element in space and time we notice that a change in the velocity $d\vec{u}$ can be achieved by

$$d\vec{u} = \frac{\partial \vec{u}}{\partial t} \Big|_{\vec{r}} dt + \frac{\partial \vec{u}}{\partial x} \Big|_{\vec{r}} dx + \frac{\partial \vec{u}}{\partial y} \Big|_{\vec{r}} dy + \frac{\partial \vec{u}}{\partial z} \Big|_{\vec{r}} dz$$

which when dividing by dt results in

$$\frac{d\vec{u}}{dt} = \frac{\partial \vec{u}}{\partial t} + \frac{\partial \vec{u}}{\partial x} \frac{dx}{dt} + \frac{\partial \vec{u}}{\partial y} \frac{dy}{dt} + \frac{\partial \vec{u}}{\partial z} \frac{dz}{dt} \quad (22.1)$$

$$= \frac{\partial \vec{u}}{\partial t} + (\vec{u} \cdot \nabla) \vec{u} \quad (22.2)$$

This is the total derivative, which is called the *substantial derivative*:

$$\frac{D}{Dt} = \frac{\partial}{\partial t} + \vec{u} \nabla$$

and states, that a change in the velocity can be caused by a temporal change but also by a convective motion (different places have different velocities). The term $\vec{u} \nabla$ is therefore called the *convective derivative*.

22.1 Navier Stokes Equation

We obtain a force density from the above equations if we multiply the above derived velocity change with the mass density ρ of the fluid. This force density is the result of all possible

forces that are present in the system. We thus have to consider possible forces on a volume element.

- a) We would like to simplify our considerations by assuming an incompressibility of the liquid, i.e.

$$\nabla \cdot \vec{u} = 0 \quad (\text{incompressibility})$$

- b) One of the causes of a flow could be a pressure acting on the surface of a volume element

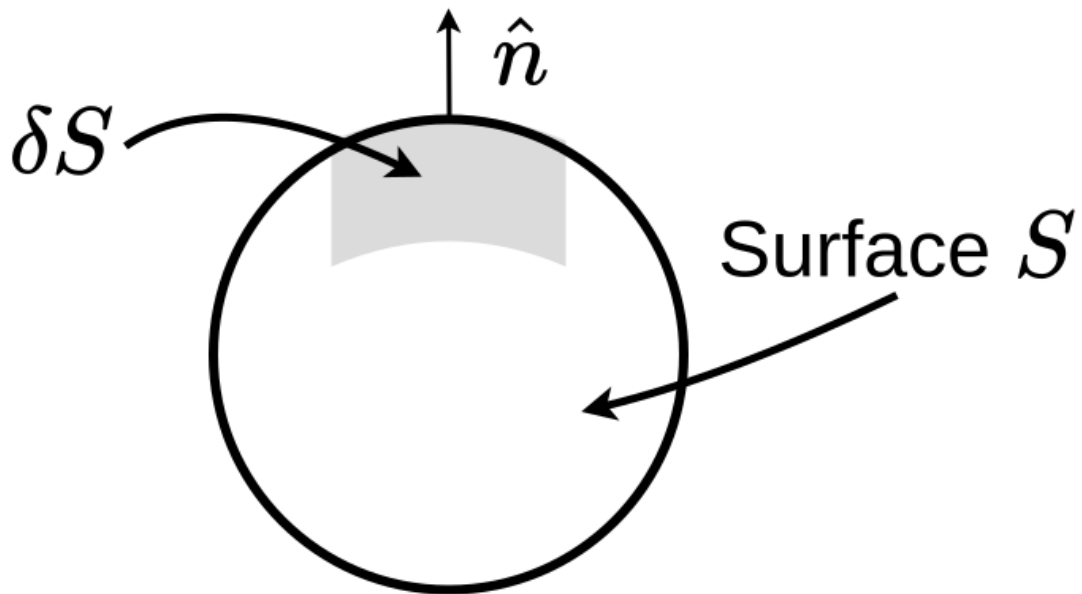


Figure 22.2: Surface with volume element

If the pressure p acts on the surface we have for a surface element δS with a normal vector \hat{n} a force $-\hat{n}p\delta S$ on the surface element. If we integrate the force over the whole surface we can write

$$-\oint p\hat{n}\delta S = - \int \nabla p dV$$

stating the the integral of the pressure over the whole surface should amount for the volume integral (over the volume enclosed by the surface) of the gradient pressure. Thus the net force cause by a pressure gradient is $-\nabla p dV$ and the pressure gradient is just the force density.

$$-\nabla p \quad (\text{pressure force density})$$

c) Additionally, flow may be caused by external forces, like gravity (or others)

The force density by an external force, like gravity is just given by

$$\rho \vec{g} \quad (\text{external force density})$$

The sum of these components of the force density make up the **Euler equation**

$$\rho \frac{D\vec{u}}{Dt} = \rho \left[\frac{\partial \vec{u}}{\partial t} + (\vec{u} \nabla) \vec{u} \right] = -\nabla p + \rho \vec{g} \quad (\text{Euler equation})$$

The Euler equation describes the flow of ideal fluids due to pressure gradients or external forces. It is, however, only valid for ideal fluids with no internal friction. Thus, it essentially describes the flow of dilute gases or superfluids like superfluid Helium.

To go beyond that limitation, we have to introduce friction into the equations. Since this is a good occasion, we will introduce the stress tensor at the same time, which is expressing all possible force on a volume element of a fluid.

d) Introduce internal friction

Let's consider the following system with two fluid sheets, which only have a constant velocity component along the x-direction, i.e. $\vec{u} = \{u(y), 0, 0\}$ and $\partial u(y)/\partial x = 0$.

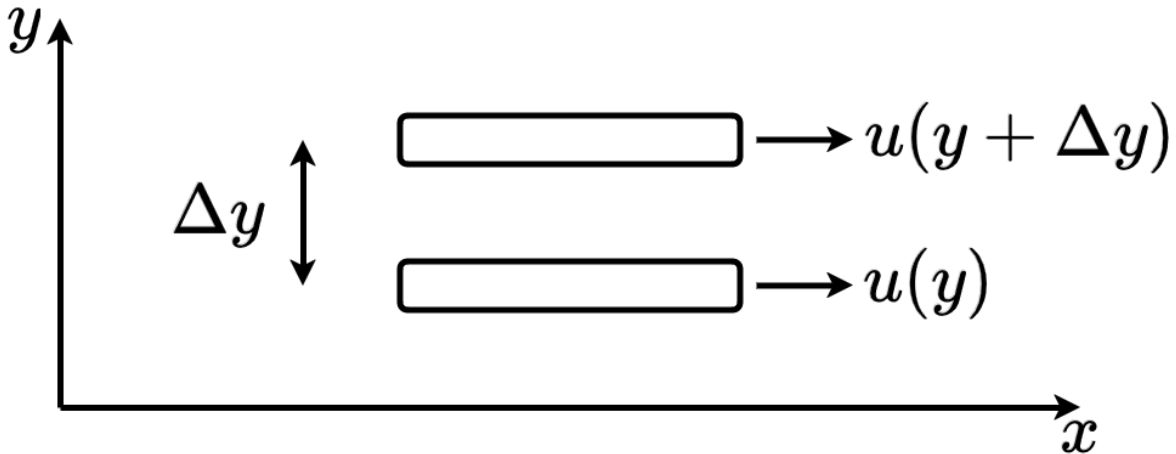


Figure 22.3: viscosity_new

The sheet at y moves along the x-direction with a speed $u(y)$. The sheet at $y + \Delta y$, which is Δy away from the other sheet moves with a speed $u(y + \Delta y)$. Consider now the momentum $\vec{p} = \{mu(y), 0, 0\}$ of the fluid sheet (don't confuse with the pressure p). The total momentum change $d\vec{p}$ can be written as a substantial derivative

$$d\vec{p} = \frac{\partial \vec{p}}{\partial t} dt + \underbrace{\frac{\partial \vec{p}}{\partial x} dx}_{=0} + \underbrace{\frac{\partial \vec{p}}{\partial y} dy}_{=0} + \underbrace{\frac{\partial \vec{p}}{\partial z} dz}_{=0} \quad (22.3)$$

from which we obtain

$$\frac{d\vec{p}}{dt} = \frac{\partial \vec{p}}{\partial t} + \frac{\partial \vec{p}}{\partial y} \frac{dy}{dt} = \frac{\partial mu(y)}{\partial y} \frac{dy}{dt} \quad (22.4)$$

which is a force. This is the force that is responsible for the change in the fluid velocity along the y direction, which is parallel to the x-direction.

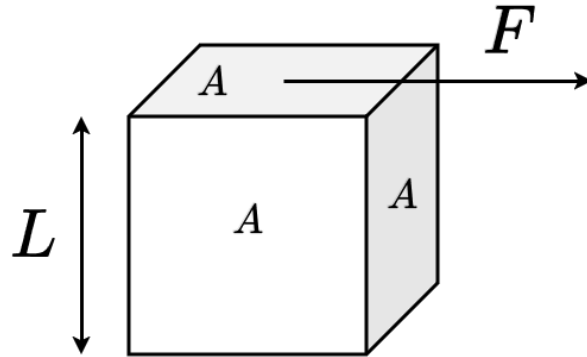


Figure 22.4: Stress

Such a force tangential to an area in the direction of motion is called a shear stress τ , i.e.

$$\tau = \frac{F}{A} = \frac{1}{A} \frac{d\vec{p}}{dt} = \underbrace{\frac{dy}{dt} \frac{\partial mu(y)}{\partial y}}_{\frac{d\vec{p}}{dt}} \frac{1}{A} \quad (22.5)$$

With $m = \rho V$ and $v = AL$ this turns into

$$\tau = L \underbrace{\frac{dy}{dt}}_{\frac{m^2}{s}} \frac{\partial \rho u(y)}{\partial y} \quad (22.6)$$

where $\rho u(y)$ indicates a momentum density. This equation is actually a diffusion equation. On the left side we have a momentum current density (τ) and on the right side a momentum density gradient, which is multiplied by a prefactor with a unit of the diffusion coefficient. This prefactor, the momentum diffusion coefficient, is the kinematic viscosity

$$\nu = \frac{\eta}{\rho} \quad (\text{kinematic viscosity})$$

and thus

$$\tau_{yx} = \frac{\eta}{\rho} \frac{\partial \rho u(y)}{\partial y} = \eta \frac{\partial u(y)}{\partial y} \quad (22.7)$$

where I have sneaked in the **dynamic viscosity** η and the index yx , as this is one element of the stress tensor for a momentum transport along the y-axis when stresses are applied along the x-axis.

22.1.1 Viscous Stress Tensor

A similar treatment can be done for other velocity and force components can be done as well to construct the so-called viscous stress tensor, which contains all the viscous stress components. They are

$$\tau_{xy} = \tau_{yx} = \eta \left(\frac{\partial u}{\partial y} + \frac{\partial v}{\partial x} \right) \quad (22.8)$$

$$\tau_{xz} = \tau_{zx} = \eta \left(\frac{\partial u}{\partial z} + \frac{\partial w}{\partial x} \right) \quad (22.9)$$

$$\tau_{yz} = \tau_{zy} = \eta \left(\frac{\partial v}{\partial z} + \frac{\partial w}{\partial y} \right) \quad (22.10)$$

for the off-diagonal elements and

$$\tau_{xx} = 2\eta \frac{\partial u}{\partial x} \quad (22.11)$$

$$\tau_{yy} = 2\eta \frac{\partial v}{\partial y} \quad (22.12)$$

$$\tau_{zz} = 2\eta \frac{\partial w}{\partial z} \quad (22.13)$$

for the diagonal elements. Together they create the viscous stress tensor

$$\boldsymbol{\tau} = \begin{bmatrix} \tau_{xx} & \tau_{xy} & \tau_{xz} \\ \tau_{yx} & \tau_{yy} & \tau_{yz} \\ \tau_{zx} & \tau_{zy} & \tau_{zz} \end{bmatrix} \quad (22.14)$$

which is, as you see from the equations a symmetric tensor.

So far we have only considered the situation where $\eta/\rho = \text{const.}$, without saying it. This situation actually corresponds to what we call **Newtonian Liquids**. The transport coefficient for the momentum is constant in this case.

More generally, the transport coefficient may depend on the *shear rate* $\frac{\partial u}{\partial y}, \dots$. Thus we write more generally

$$\tau_{yx} = k \left(\frac{\partial u}{\partial y} \right)^n \quad (22.15)$$

where k is the so-called *consistency index* and n is the *flow behavior index*. The above equation can be transformed into

$$\tau_{yx} = \underbrace{k \left(\frac{\partial u}{\partial y} \right)^{n-1}}_{\text{apparent viscosity}} \frac{\partial u}{\partial y}$$

which takes the known form of the momentum diffusion equation with a shear rate dependent prefactor, which is the momentum diffusion coefficient or the *apparent viscosity*.

Depending on the shear rate dependence of the apparent viscosity, we can now classify liquids into

- Newtonian liquids
- Non-Newtonian liquids
 - shear thinning (ketchup)
 - shear thickening (corn starch)

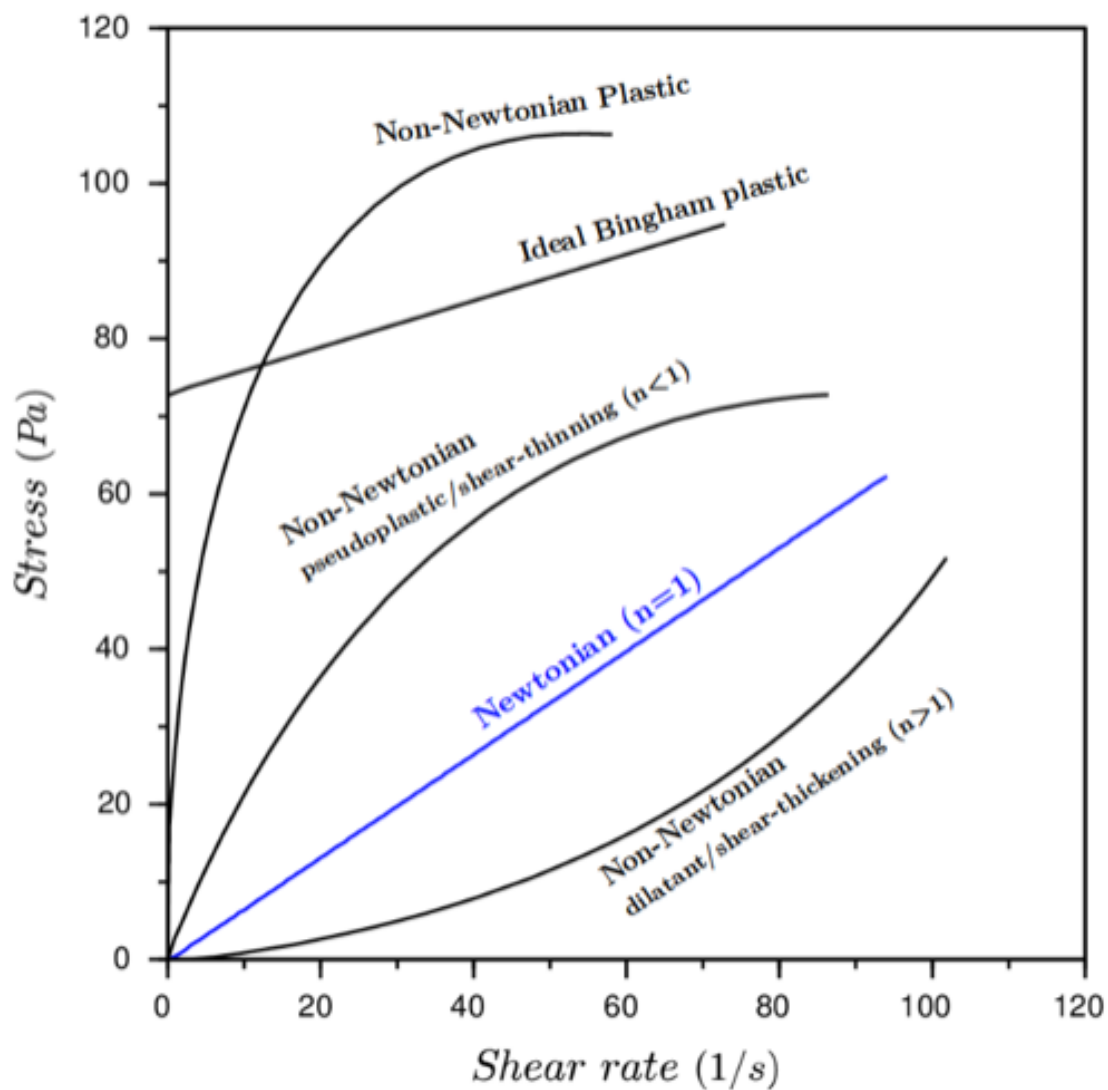


Figure 22.5: Classification

Stress vector

$$\vec{S} = \hat{n}\tau = [T_{xx}, T_{xy}, T_{xz}]$$

total force

$$\vec{F} = \oint \vec{S} dS = \oint \hat{n}\tau dS = \int \nabla\tau dV$$

$$\nabla \tau = \left[\frac{\partial \tau_{xx}}{\partial x} + \frac{\partial \tau_{yx}}{\partial y} + \frac{\partial \tau_{zx}}{\partial z}, \dots \right]$$

where $\nabla \tau$ is the viscous force density, which we can add to the Euler equation to introduce friction

$$\rho \frac{D\vec{u}}{Dt} = \rho \left[\frac{\partial \vec{u}}{\partial t} + (\vec{u} \nabla) \vec{u} \right] = -\nabla p + \rho \vec{g} + \nabla \tau \quad (22.16)$$

22.1.2 Mechanical Stress Tensor

Together with the pressure, we can define the mechanical stress tensor

$$T = -pI + \tau$$

where

$$I = \begin{bmatrix} 1 & 0 & 0 \\ 0 & 1 & 0 \\ 0 & 0 & 1 \end{bmatrix} \quad (22.17)$$

is the identity matrix. As we need a force density for the Navier Stokes equation, we can take as before the divergence of the mechanical stress tensor which yields

$$\nabla T = \left(-\frac{\partial p}{\partial x} + \frac{\partial \tau_{xx}}{\partial x} + \frac{\partial \tau_{yx}}{\partial y} + \frac{\partial \tau_{zx}}{\partial z} \right) \hat{e}_x + \quad (22.18)$$

$$= (\dots) \hat{e}_y + \quad (22.19)$$

$$= (\dots) \hat{e}_z \quad (22.20)$$

Just looking for the moment at the x-component only and inserting the viscous stress tensor elements results in

$$-\frac{\partial p}{\partial x} + 2\eta \underline{\frac{\partial^2 u}{\partial x^2}} + \eta \left(\underline{\frac{\partial^2 u}{\partial y^2}} + \underline{\frac{\partial^2 v}{\partial x \partial y}} \right) + \eta \left(\underline{\frac{\partial^2 u}{\partial z^2}} + \underline{\frac{\partial^2 w}{\partial x \partial z}} \right)$$

The underlined components can actually be understood as

$$\frac{\partial}{\partial x} (\nabla \cdot \vec{u})$$

which is actually *zero* due to the fact that we assume an incompressible fluid ($\nabla \cdot \vec{u} = 0$).

$$\rho \frac{Du}{Dt} = -p_x + \eta(u_{xx} + u_{yy} + u_{zz}) + f_{B,x} \quad (22.21)$$

$$\rho \frac{Dv}{Dt} = -p_y + \eta(v_{xx} + v_{yy} + v_{zz}) + f_{B,y} \quad (22.22)$$

$$\rho \frac{Dw}{Dt} = -p_z + \eta(w_{xx} + w_{yy} + w_{zz}) + f_{B,z} \quad (22.23)$$

which corresponds to the components of the Navier-Stokes equation

$$\rho \frac{D\vec{u}}{Dt} = -\nabla p + \underbrace{\vec{f}_B}_{\text{e.g. } \rho \vec{g}} + \eta \Delta \vec{u} \quad (\text{Navier-Stokes-Equation})$$

under the incompressibility condition

$$\nabla \cdot \vec{u} = 0 \quad (\text{incompressibility condition})$$

Part XVIII

Lecture 18

23 Reynolds Number

```
import numpy as np
import matplotlib.pyplot as plt
from numpy.linalg import norm
from scipy.constants import c, epsilon_0, e, physical_constants
from IPython.display import YouTubeVideo
import json

%config InlineBackend.figure_format = 'retina'

with open('style.json', 'r') as fp:
    style = json.load(fp)

plt.rcParams.update(style)
```

Hydrodynamics is full of dimensionless number, mainly also due to its relevance for engineering. For example, you may want to compare the flow around the same object at large and small scales. Ideally, you could just build a model of a small airplane and study the flow field around the small airplane in a lab, as it is naturally less expensive than studying it on a large one.

A number which is useful with this respect is the **Reynold number**, which tells of how to scale the flow velocity when scaling the object.

To obtain the Reynold number and its meaning, we introduce a Navier Stokes equation with dimensionless quatities. These use characteristic dimensions of the system to rescale. We use

$$\begin{aligned}x &= x'L \\ \vec{u} &= \vec{u}'U \\ t &= t'\frac{L}{U}\end{aligned}$$

for the rescaling, where L is the characteristic size of the object, U a characteristic velocity and L/U the characteristic time for a fluid volume element to pass the object of size L . Using these quantities, the differential operators turn into

$$\begin{aligned}\nabla &= \frac{\nabla'}{L} \\ \frac{\partial}{\partial t} &= \frac{\partial}{\partial t'} \frac{U}{L} \\ p &= p' U^2 / \rho\end{aligned}$$

Using these relations in the Navier Stokes equation

$$\rho \left[\frac{\partial}{\partial t} + (\vec{u} \nabla) \right] \vec{u} = -\nabla p + \eta \Delta \vec{u}$$

yields

$$\rho \left[\frac{\partial}{\partial t'} \frac{U}{L} + U \left(\vec{u}' \frac{\nabla'}{L} \right) \right] \vec{u}' U = -\frac{\nabla'}{L} p' U^2 \rho + \eta \frac{1}{L^2} \Delta' \vec{u}'$$

Dividing the previous equation by $\rho U^2 / L$ gives us the dimensionless Navier-Stokes equation

$$\left[\frac{\partial}{\partial t'} + \vec{u}' \nabla \right] \vec{u}' = -\nabla p' + \frac{1}{\text{Re}} \Delta \vec{u}'$$

where

$$\text{Re} = \frac{\rho}{\eta} U L \quad (\text{Reynolds number})$$

is the Reynolds number. This number now tells us, that if we scale the size of the object by a factor of 2, we have to increase the velocity by a factor of two to get the same flow field as for the larger object. This is probably not what we would have simply anticipated by our intuition.

The Reynolds number has also a very important meaning for the classification of flows. It may help you to make a distinction between the realm of turbulent and laminar flow. When we start just start from the stationary Navier Stokes equation

$$\rho [(\vec{u} \nabla)] \vec{u} = -\nabla p + \eta \Delta \vec{u}$$

we can also make a dimension analysis with the help of the individual quantities. In this way we find

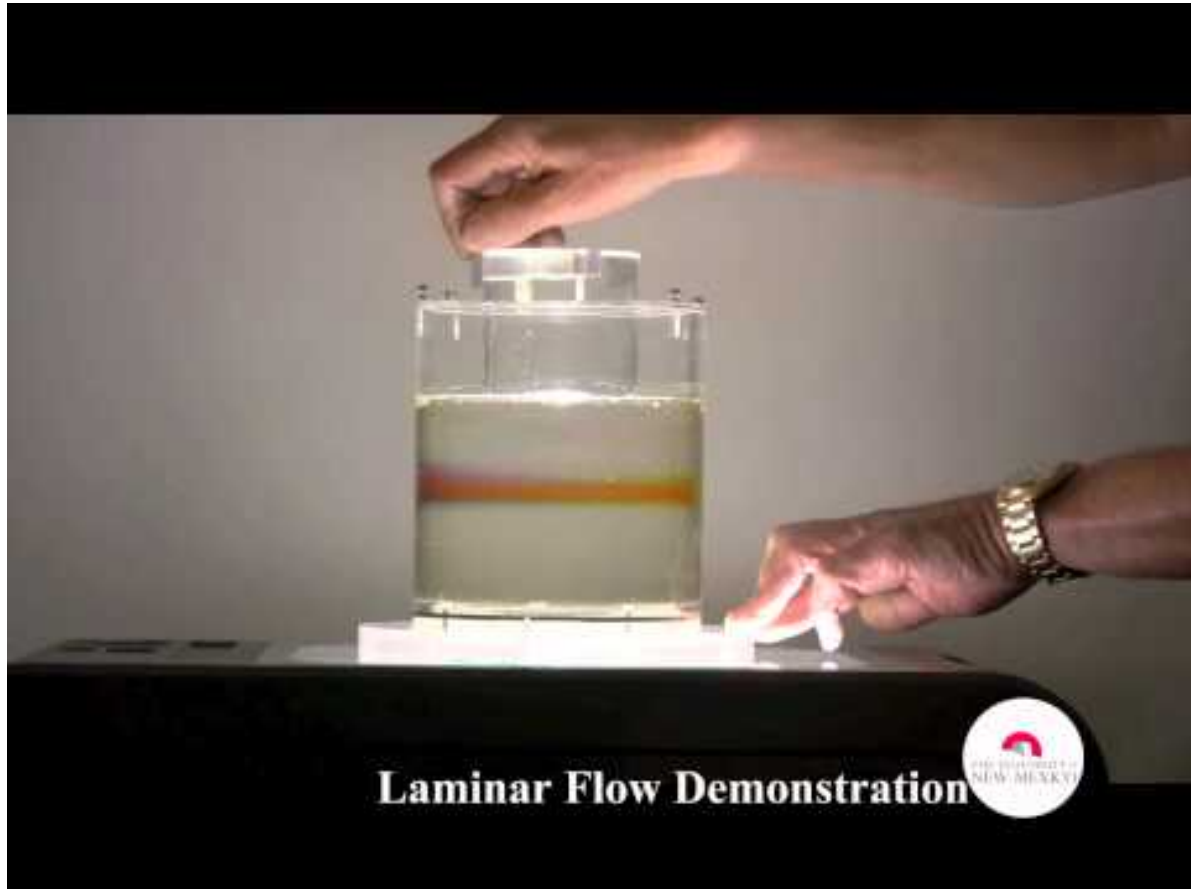
$$\underbrace{\rho \frac{U^2}{L}}_{\text{inertia}} = -\nabla p + \underbrace{\eta \frac{U}{L^2}}_{\text{viscous}}$$

where the left side corresponds to the inertial and the right side to the viscous force densities. If we compare the inertial to the viscous force densities, we obtain

$$\frac{\rho \frac{U^2}{L}}{\eta \frac{U}{L^2}} = \rho \frac{UL}{\eta} = \text{Re}$$

which is just the Reynolds number. Thus large Reynolds numbers ($\text{Re} > 1$) state that inertia are important as compared to viscous forces and the flow may be turbulent. Otherwise, for $\text{Re} < 1$, viscous forces dominate the flow and the flowfield will always be laminar.

```
YouTubeVideo('_dbnH-BBSNo', width=800, height=600)
```



23.1 Stokes Equation

In the realm of very small Reynolds number we may even neglect the inertial terms in the Navier Stokes equation and obtain just the Stokes equation

$$0 = -\nabla p + \eta \Delta \vec{u} + \vec{f} \quad (\text{Stokes Equation})$$

with the incompressibility condition

$$\nabla \cdot \vec{u} = 0 \quad (23.1)$$

23.2 Solutions of the Stokes Equation

The Stokes equation is easier to solve than the Navier-Stokes equation as it has no time dependence. This also means that it is time symmetric and the reversal of the motion of an object typically also creates a reversed flow field. This is very important for example for micro-organisms that would like to swim in water. Due to their small dimension they live at low Reynolds numbers and every symmetric motion they take is just yielding a wiggling back and forth but no net motion. They therefore have to come up with some time-asymmetric motion to swim. This is summarized in a theorem that has been put forward by Edward Purcell. We will talk about this later.

We would first like to obtain two general solutions for the flow field from the Stokes equation and thereby consider two solid surfaces which confine a water film of height h according to the drawing below.

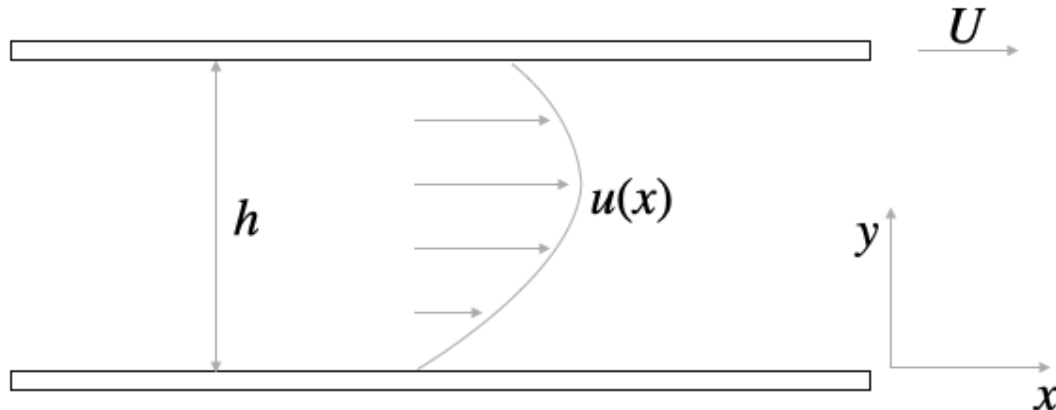


Figure 23.1: Flow Field

We chose the coordinate system in the way that the horizontal axis is the x -axis and the vertical one the y -axis. In two dimensions the Stokes equation is now the following

$$\eta \frac{d^2 u}{dy^2} = \frac{dp}{dx} \quad (23.2)$$

without any external forces. We can readily integrate the both sides two times

$$\int \frac{d^2 u}{dy^2} = \frac{1}{\eta} \int \frac{dp}{dx} \quad (23.3)$$

which results in

$$\int \frac{du}{dy} = \int \left[\frac{1}{\eta} \frac{dp}{dx} y + C_1 \right] dy \quad (23.4)$$

and finally gives

$$u(y) = \frac{1}{2\eta} \frac{dp}{dx} y^2 + C_1 y + C_2 \quad (23.5)$$

where C_1 and C_2 are integration constants, which we have to determine from the boundary conditions.

We assume the following no-slip boundary conditions

$$u(y = 0) = 0 \quad (23.6)$$

and

$$u(y = h) = U \quad (23.7)$$

With the help of these we obtain

$$u(y) = \frac{1}{2\eta} \frac{dp}{dx} y(y - h) + \frac{Uy}{h} \quad (23.8)$$

for the flow profile of the liquid film.

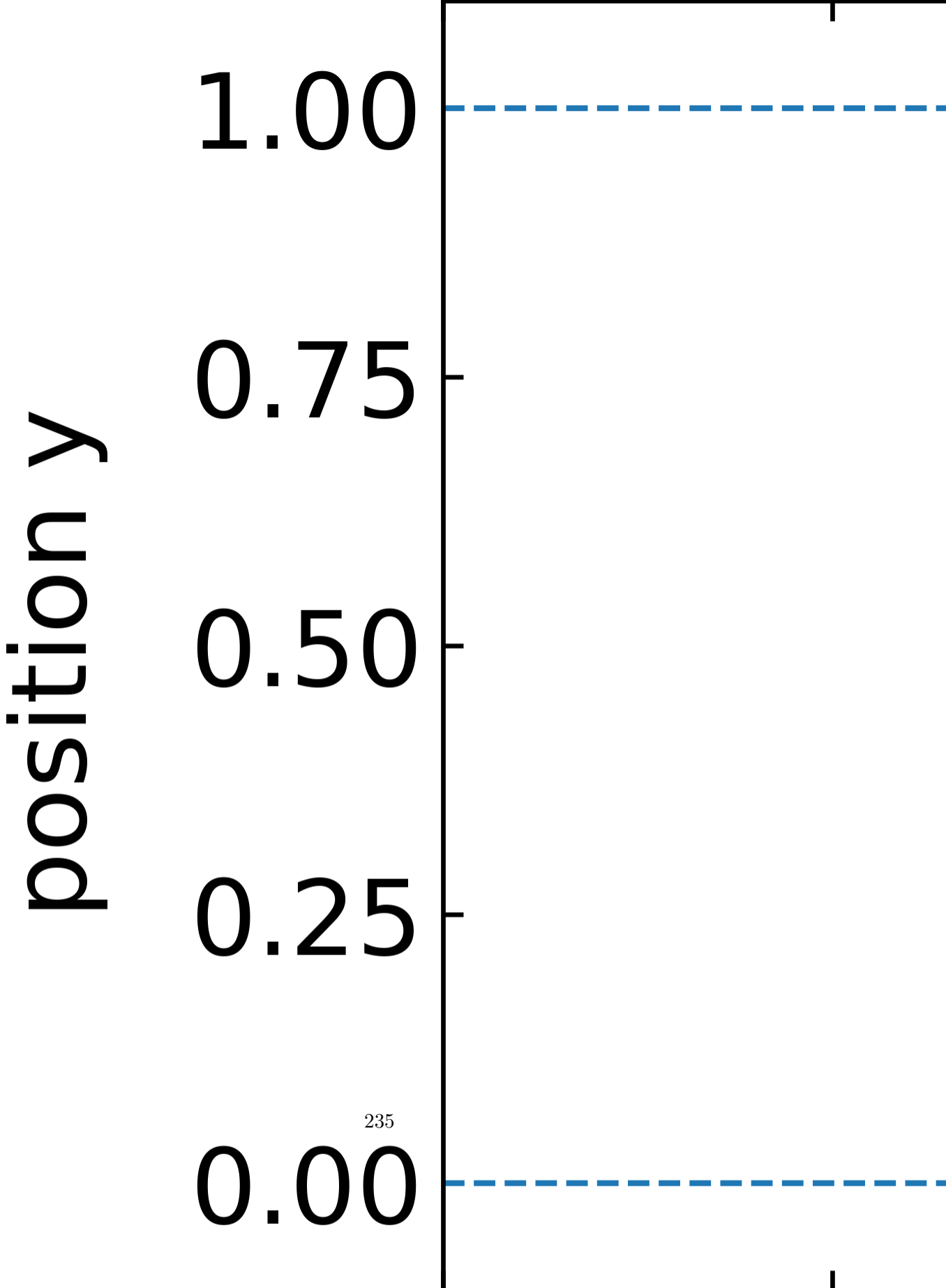
We can now recognize two different solutions in the flow field.

23.2.1 Couette Flow - Shear Driven Flow

To obtain a flow field purely driven by shear, we assume that $\frac{dp}{dx} = 0$, which is leaving a flow velocity which linearly increases with the position y

$$u(y) = U \frac{y}{h} \quad (23.9)$$

```
plt.figure(figsize=(6,4))
plt.axhline(y=0,linestyle="--")
plt.axhline(y=1,linestyle="--")
[plt.arrow(0.5,y,y*0.31-0.03,0,head_width=0.02) for y in np.arange(0.1,1.1,0.1)]
y=np.arange(0,1.1,0.1)
plt.plot(y*0.31/1+0.5,y)
plt.ylim(-0.1,1.1)
plt.xlim(0,1)
plt.xlabel("position x ")
plt.ylabel("position y ")
plt.show()
```



23.2.2 Poiseuille Flow - Pressure Driven Flow

If we assume that both boundaries are at rest in the laboratory frame and the pressure gradient along the x-axis is constant, we find a parabolic flow field, which is typical for pressure driven flows.

$$u(y) = \frac{1}{2\eta} \frac{dp}{dx} y(y - h) \quad (23.10)$$

```
plt.figure(figsize=(6,4))
plt.axhline(y=0,linestyle="--")
plt.axhline(y=1,linestyle="--")
[plt.arrow(0.5,y,-y*(y-1)-0.03,0,head_width=0.02) for y in np.arange(0.1,1.,0.1)]
y=np.arange(0,1.1,0.1)
plt.plot(-y*(y-1)+0.5,y)
plt.ylim(-0.1,1.1)
plt.xlim(0,1)
plt.xlabel("position x ")
plt.ylabel("position y ")
plt.show()
```

position y

1.00

0.75

0.50

0.25

0.00

237

24 Boundary Hydrodynamics

```
import numpy as np
import matplotlib.pyplot as plt
from numpy.linalg import norm
from scipy.constants import c,epsilon_0,e,physical_constants
import json

%config InlineBackend.figure_format = 'retina'

with open('style.json', 'r') as fp:
    style = json.load(fp)

plt.rcParams.update(style)
```

As another important example of hydrodynamical flow fields we would like to have a look at hydrodynamic flows that arise from interfacial forces. In most of the cases, these interfacial forces are often caused by osmotic pressure differences and are termed osmotic flows. The osmotic pressure difference may thereby arise from various properties, e.g. temperature gradients, electrostatic potential gradients, concentration gradients.

To analyze this type of boundary flow, we first look at the geometry below.

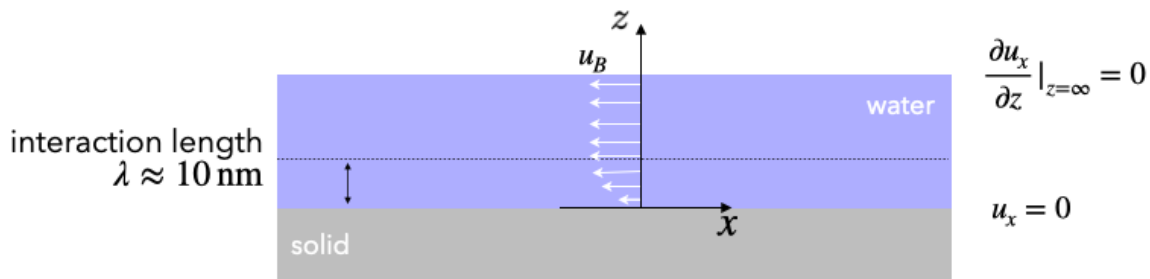


Figure 24.1: Boundary Flow

The boundary flows are the results of the fact that the interaction between liquid molecules is altered by the presence of the substrate depicted below (some symmetry breaking). This altered interaction is present at a length scale of nanometers (!) only. Think for example about the influence of van der Waals forces or the electric double layer. Beyond this interfacial region of a few nanometers the influence of the solid surface has decayed and the liquid exhibits bulk-like properties. It is this tiny interfacial region which we will consider in the description below.

According to the above picture, we can use the Stokes equation

$$\eta \Delta \vec{u} = -\nabla p - \vec{f} \quad (24.1)$$

and split it according to the x (tangential) and z (normal) components.

```
<div style="display: inline-block; width: 50%">
    <h4>normal to surface</h4>
     $\frac{\partial^2 \vec{u}}{\partial z^2} = 0$ 
    <p>
         $0 = \frac{\partial p}{\partial z} - f_z$ 
</div>
<div style="display: inline-block;">
    <h4>tangential to surface</h4>
     $\eta \frac{\partial^2 \vec{u}}{\partial z^2} = \frac{\partial p}{\partial x} - f_x$ 
</div>
```

We assume that close to the boundary there will be no flow component normal to the surface, which simplifies the normal components of the Stokes equation into a balance of pressure gradient (presumably osmotic pressure) and normal force density.

For the tangential component we have a tangential pressure gradient (osmotic) and a tangential force density which determine the flow.

We can now integrate the equation for the tangential component by parts with two boundary conditions, i.e. $u(z = 0) = 0$ and $u(z \gg \lambda) = u_B = \text{const.}$ and find

$$u_B = \frac{1}{\eta} \int_0^\infty z \left(f_x - \frac{dp}{dx} \right) dz \quad (24.2)$$

for the value of the boundary velocity u_B , which is established roughly at a distance λ from the interface. Note that this upper boundary condition says that there is no solid boundary (with no-slip boundary condition) at infinity. We can introduce the boundary condition at large distance later. The question is now what in detail the term in the brackets of the previous equation is.

24.1 Thermo-osmosis

We want to evaluate the boundary flow for the case when the surface is charged and in contact with an electrolyte solution. In this case, we can refer to the Debye-Hückel theory, which we earlier developed. In addition, this double layer is subject to a temperature gradient tangential to the surface, which will be the source of the osmotic pressure gradient along the surface.

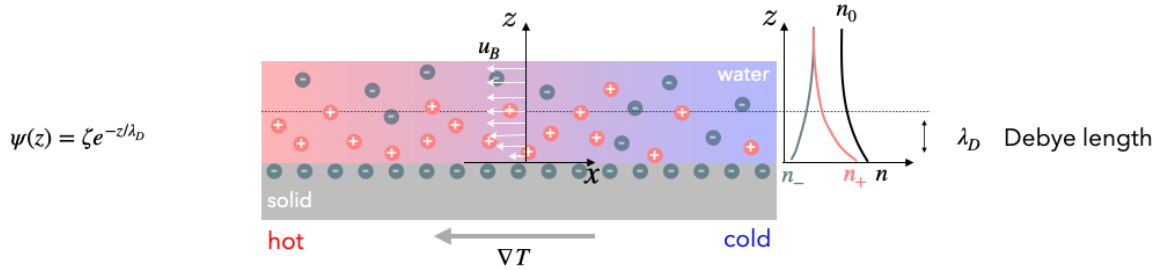


Figure 24.2: DoubleLayer

For this situation we have all equations at hand. We have first of all

- excess charge density: $\rho = e(n_+ - n_-)$
- total ion density: $n = n_+ + n_-$
- the ion density distribution: $n_{\pm} = n_0(\exp(-\frac{e\psi}{k_B T}) - 1)$
- n_0 the bulk ion density
- ψ the electrostatic potential

The force density in the system is given by

$$f = -\rho \nabla \psi + \dots$$

where the dots denote other terms (electrostriction, change of dielectric constant ...), which exist, but which we neglect.

Further, we can write the pressure as the osmotic pressure of the ion density

$$p = nk_B T = (n_+ + n_-)k_B T = \left(n_0(\exp(-\frac{e\psi}{k_B T}) - 1) + n_0(\exp(\frac{e\psi}{k_B T}) - 1) \right) k_B T$$

The task is now to calculate the term $f_x - \frac{\partial p}{\partial x}$ using derivatives of the above written pressure. Note that we have to take the derivative of the temperature with respect to the position but assume the temperature in the Boltzmann factors constant.

The result of this a bit more lengthy calculation is that

$$f_x - \frac{\partial p}{\partial x} = -nk_B T \frac{1}{T} \frac{\partial T}{\partial x} - \rho\psi \frac{1}{T} \frac{\partial T}{\partial x}$$

or in 3-dimensions

$$\mathbf{f} - \nabla p = -(\varrho\psi + nk_B T) \frac{\nabla T}{T}$$

The term in front of the fraction is an electrostatic interaction energy related term and a term corresponding to the ideal gas pressure. Both terms together clearly make up an enthalpy (energy + pressure x volume). In this case, they correspond to an excess enthalpy density as there is no contribution if there is no electrostatic surface charge involved.

We can therefore also write the boundary velocity u_B as

$$u_B = -\frac{1}{\eta} \int_0^\infty z h(z) dz \frac{\nabla T_{||}}{T} \quad (24.3)$$

where $h(z)$ is the excess enthalpy density of the interaction of the liquid with the solid as compared to the liquid alone. As the interaction between liquid and solid is often attractive (van der Waals alone already is attractive), the excess enthalpy density is negative and the difference of force density and pressure density results in forces along the temperature gradient, e.g. from the cold region to the hot region. If the excess enthalpy is positive, the flow is driven from hot to cold regions. Note that this flow is established in a thin liquid layer of thickness λ , which is only a few nanometers thin. Within these few nanometers the flow velocity rises from 0 to a few $10 \mu\text{m/s}$.

The plot below calculates the integral over the product of z and the excess enthalpy for the electric double layer, assuming that some of the constants are 1 and the temperature gradient just gives a minus sign (assuming hot is on the left and cold is on the right).

```
## electrostatic potential
def psi(z, lam_D):
    return(np.exp(-z/lam_D))

## n+
def npl(z, lam_D, n):
    return(n*(np.exp(-psi(z, lam_D))-1))

## n-
def nmi(z, lam_D, n):
    return(n*(np.exp(psi(z, lam_D))-1))
```

```

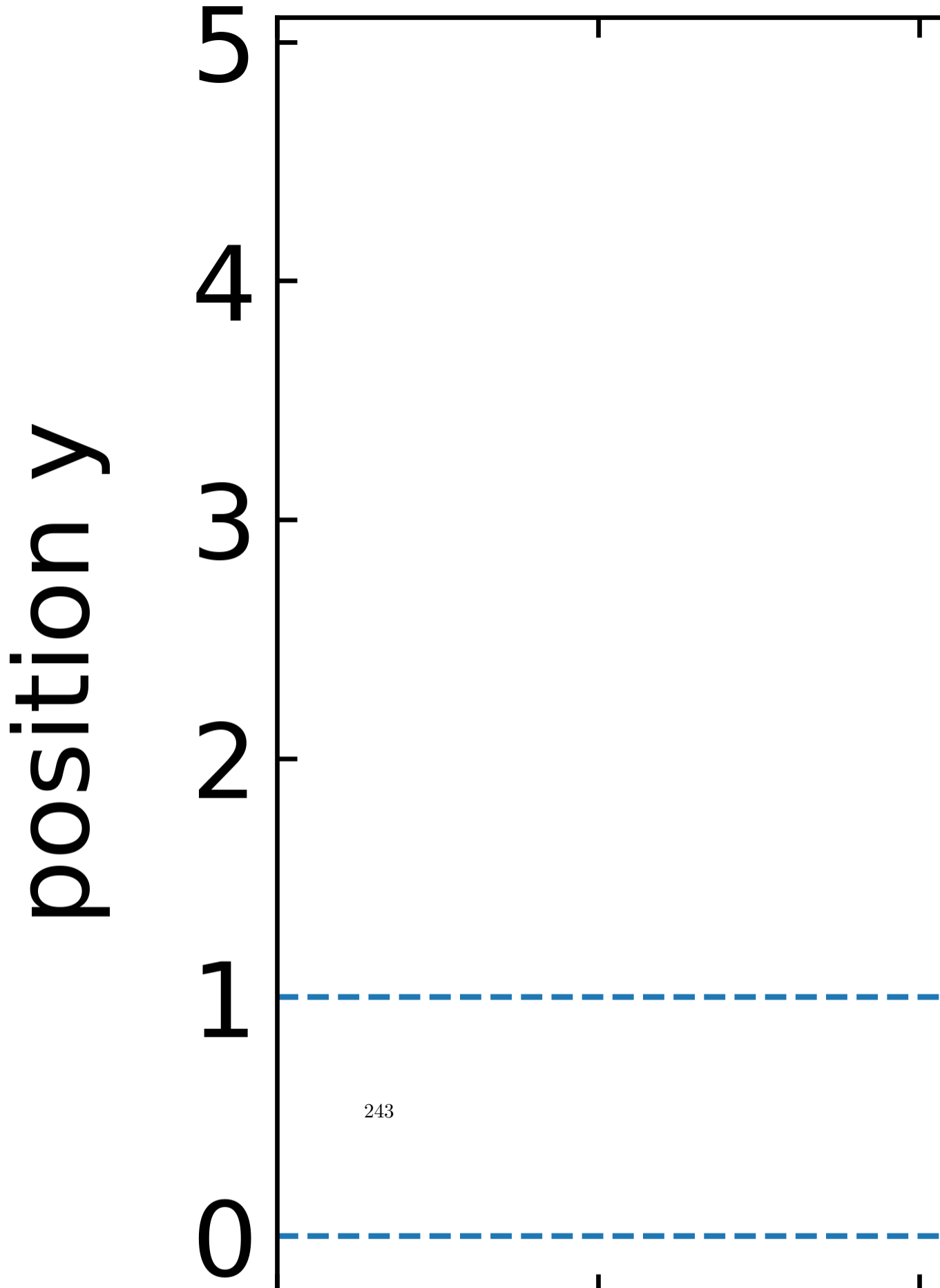
## total n
def nt(z, lam_D, n):
    return(2*n*(np.cosh(psi(z, lam_D))-1))

## excess enthalpy

def h(z, lam_D, n):
    return((npl(z, lam_D, 1)-nmi(z, lam_D, 1))*psi(z, lam_D)+nt(z, lam_D, 1))

plt.figure(figsize=(6,4))
plt.axhline(y=0, linestyle="--")
plt.axhline(y=1, linestyle="--")
z=np.linspace(0.1,5,1000)
inth=-np.cumsum(z*(h(z, 1, 1))*(z[1]-z[0])) ## numerically integrate the excess enthalpy *z
[plt.arrow(0,z[l],-inth[l]*5,0,head_width=0.2,head_length=0.1) for l in range(0,len(z),50)]
plt.xlim(-4,2)
plt.xlabel("position x ")
plt.ylabel("position y ")
plt.show()

```



The flow profile we have calculated saturates at the boundary velocity u_B as we have assumed this as the boundary condition at infinite distance. If there is a second surface at some distance, even though at finite distance but still large as compared to the interaction range, the velocity magnitude has to decay to zero towards this surface. Instead of assuming the complicated flow profile as depicted below, we can in cases where all other distances are large as compared to the interaction range λ_D assume that the velocity directly at the interface is u_B . The hydrodynamic boundary condition is thus altered from a **no-slip boundary condition** to a **slip boundary condition** with the slip velocity u_B .

Part XIX

Lecture 19

25 Electro-osmosis

26 Polymers

```
import numpy as np
import matplotlib.pyplot as plt
from numpy.linalg import norm
from scipy.constants import c,epsilon_0,e,physical_constants
import json

%config InlineBackend.figure_format = 'retina'

with open('style.json', 'r') as fp:
    style = json.load(fp)

plt.rcParams.update(style)
```

26.1 Freely Jointed Chain

One of the simplest models of a polymer chain is a 3D random walk with constant step length, the freely jointed chain (FJC). The step length corresponds to a distance b , which is called the *Kuhn* length. The Kuhn length is typically larger than the bond length between the monomers of the polymer as neighboring bond may still have correlations. Neighboring Kuhn segments are in the model of the FJC completely independent. The image below shows an example random walk

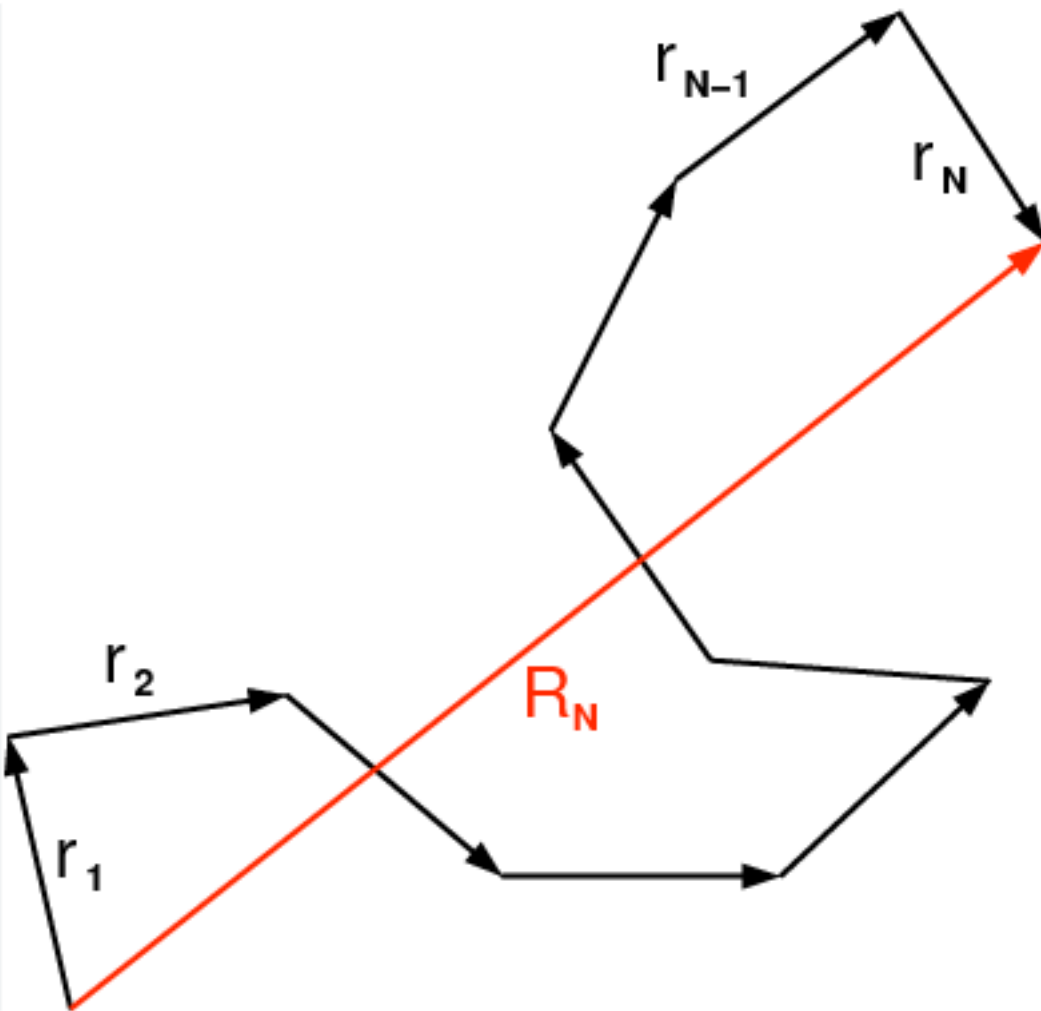


Figure 26.1: Freely Jointed Chain

26.1.1 Mean-squared end-to-end distance of a FJC

Let us calculate some properties of the freely jointed chain. One is the sum of all bonding vectors \vec{r}_i . This will give us the end-to-end distance, vector of the polymer chain.

$$\vec{R}_N = \sum_{i=1}^N \vec{r}_i$$

Of course, this is only a single realisation of a polymer conformation. In general, the polymer can accommodate many different conformations with different end-to-end vectors \vec{R}_N .

Therefore, ensemble average of the end to end vector has to be zero.

$$\langle \vec{R}_N \rangle = 0.$$

The next higher moment of the end to vector distance is the mean squared end to end distance. The mean squared end to end distance is calculated by

$$\begin{aligned} \langle R^2 \rangle \equiv \langle \vec{R}_N^2 \rangle &= \langle \vec{R}_N \cdot \vec{R}_N \rangle = \left\langle \left(\sum_{i=1}^N \vec{r}_i \right) \cdot \left(\sum_{j=1}^N \vec{r}_j \right) \right\rangle \\ &= \sum_{i=1}^N \sum_{j=1}^N \langle \vec{r}_i \cdot \vec{r}_j \rangle. \end{aligned}$$

The dot product in the last double sum can now be replaced by

$$\vec{r}_i \cdot \vec{r}_j = b^2 \cos \theta_{ij}$$

such that we obtain

$$\langle R^2 \rangle = \sum_{i=1}^N \sum_{j=1}^N \langle \vec{r}_i \cdot \vec{r}_j \rangle = b^2 \sum_{i=1}^N \sum_{j=1}^N \langle \cos \theta_{ij} \rangle$$

As all bond angles θ_{ij} are allowed equally, the ensemble average over the cosine is just zero and we obtain

$$\langle R^2 \rangle = n \cdot b^2 = L \cdot b$$

which is not too surprising. This is the random walk with a step length of b but not with time steps but N segments. While the contour length of the polymer would be $N^2 b^2$ the mean squared end to end distance is shorter and just Nb^2 .

26.1.2 Distribution of the end-to-end distances

The calculation before just addressed the mean squared end to end distance. Again, since this is a random walk, which has many realisations, there must be also a distribution function for the end to end distance. This will tell us by how much the end to end distance fluctuates, and what is the probability to find a certain end to end distance. If we look just at the first segment, we have an end to end vector \vec{R}_1 magnitude squared, and we can calculate the length of this vector from its components.

$$\langle |\vec{R}_1|^2 \rangle = \langle x_1^2 + y_1^2 + z_1^2 \rangle = b^2 = \langle x_1^2 \rangle + \langle y_1^2 \rangle + \langle z_1^2 \rangle$$

As the vector can rotate isotropically, the mean squared value of each of the components is just one third of the square length of the Kuhn segment b , i.e.

$$\langle x_1^2 \rangle = \langle y_1^2 \rangle = \langle z_1^2 \rangle = b^2/3$$

That means now, a chain of N segments results in the mean squared components which are

$$\langle x_N^2 \rangle = \langle y_N^2 \rangle = \langle z_N^2 \rangle = N \cdot b^2/3$$

This is the variance of how far a random walk travels in x-direction after N step. The distribution function for the random walk as we know is a Gaussian:

$$p(x, N) = \frac{1}{\sqrt{2\pi(Nb^2/3)}} e^{-x^2/(2Nb^2/3)}$$

As all 3 dimensions of the random walk are equivalent, i.e.

$$\langle R_N^2 \rangle = \langle x_N^2 \rangle + \langle y_N^2 \rangle + \langle z_N^2 \rangle = 3 \cdot N \cdot b^2/3 = N \cdot b^2$$

the probability density of finding a certain end to end vector is the product of the three 1d probability densities

$$\begin{aligned} p(\vec{R}, N) &= p(x, N) \cdot p(y, N) \cdot p(z, N) \\ &= \sqrt{\frac{3}{2\pi Nb^2}} e^{-3x^2/(2Nb^2)} \sqrt{\frac{3}{2\pi Na^2}} e^{-3y^2/(2Nb^2)} \sqrt{\frac{3}{2\pi Na^2}} e^{-3z^2/(2Nb^2)} \end{aligned}$$

and thus

$$p(\vec{R}, N) = \left(\frac{3}{2\pi Nb^2} \right)^{\frac{3}{2}} e^{-3R^2/(2Nb^2)}$$

The corresponding radial distribution function then reads

$$p(R, N) dR = \left(\frac{3}{2\pi Nb^2} \right)^{\frac{3}{2}} e^{-3R^2/(2Nb^2)} 4\pi R^2 dR$$

Such an end to end distribution could be measured if both ends of the polymer can be tagged for example with a dye molecule. The distance of the two dye molecules can then be measured, for example, with the help of fluorescence resonance energy transfer (FRET) if some additional requirements are fulfilled. This can be done for a single polymer molecule and the above ensemble averages could then also be replaced by a time average since the polymer fluctuates due to thermal energy.

26.1.3 Radius of gyration

Not in all cases the end to end distance can be measured or even two ends exist (circular polymers). Then, it is more interesting to characterize the spatial extent of the polymer chain by the radius of gyration R_g , whose square is defined like this

$$R_g^2 \equiv \frac{1}{N} \sum_{i=1}^N (\vec{R}_i - \vec{R}_{cm})^2$$

$$\vec{R}_{cm} \equiv \frac{1}{N} \sum_{j=1}^N \vec{R}_j.$$

$$\langle R_g^2 \rangle = \frac{1}{N^2} \sum_{i=1}^N \sum_{j=i}^N \langle (\vec{R}_i - \vec{R}_j)^2 \rangle$$

$$\begin{aligned} \sum_{i=1}^N &\rightarrow \int_0^N du \\ \langle R_g^2 \rangle &= \frac{1}{N^2} \int_0^N \int_u^N \langle (\vec{R}(u) - \vec{R}(v))^2 \rangle dv du. \end{aligned}$$

$$\langle (\vec{R}(u) - \vec{R}(v))^2 \rangle = (v - u)b^2$$

$$\langle R_g^2 \rangle = \frac{b^2}{N^2} \int_0^N \int_u^N (v - u) dv du = \frac{b^2}{N^2} \int_0^N \int_0^{N-u} v' dv v' du$$

$$\langle R_g^2 \rangle = \frac{b^2 N}{6} = \frac{\langle R^2 \rangle}{6}$$

Ideal chains	Linear	Ring	f -arm star	H-polymer
$\langle R_g^2 \rangle$	$Nb^2/6$	$Nb^2/12$	$[(N/f)b^2/6](3-2/f)$	$(Nb^2/6)89/625$

$$R_g^2 \equiv \frac{1}{N} \sum_{i=1}^N \left(\vec{R}_i - \vec{R}_{\text{cm}} \right)^2$$

$$\vec{R}_{\text{cm}} \equiv \frac{1}{N} \sum_{j=1}^N \vec{R}_j.$$

$$\langle R_g^2 \rangle = \frac{1}{N^2} \sum_{i=1}^N \sum_{j=i}^N \left\langle \left(\vec{R}_i - \vec{R}_j \right)^2 \right\rangle$$

$$\sum_{i=1}^N \rightarrow \int_0^N du \\ \langle R_g^2 \rangle = \frac{1}{N^2} \int_0^N \int_u^N \left\langle (\vec{R}(u) - \vec{R}(v))^2 \right\rangle dv du.$$

$$\left\langle (\vec{R}(u) - \vec{R}(v))^2 \right\rangle = (v - u)b^2$$

$$\langle R_g^2 \rangle = \frac{b^2}{N^2} \int_0^N \int_u^N (v - u) dv du = \frac{b^2}{N^2} \int_0^N \int_0^{N-u} v' dv v' du$$

$$\langle R_g^2 \rangle = \frac{b^2 N}{6} = \frac{\langle R^2 \rangle}{6}$$

Ideal chains	Linear	Ring	f -arm star	H-polymer
$\langle R_g^2 \rangle$	$Nb^2/6$	$Nb^2/12$	$[(N/f)b^2/6](3-2/f)$	$(Nb^2/6)89/625$

26.2 Force-extension behavior of a FJC

$$E_{pot,1} = -\vec{f} \cdot \vec{r}_1 = -f \cdot r_{1,z} = -f \cdot b \cos \theta$$

$$Z_1 = \int_0^\pi \int_0^{2\pi} e^{-ft \cos \theta / k_B T} \sin \theta \cdot d\varphi d\theta$$

$$Z_1 = 2\pi \int_{-1}^1 e^{fb y / k_B T} dy = 2\pi \frac{k_B T}{fb} e^{fay / k_B T} \Big|_{-1}^1 = 2\pi \frac{k_B T}{fb} (e^{fb / k_B T} - e^{-fb / k_B T}) = 4\pi \frac{k_B T}{fa} \sinh \left(\frac{fb}{k_B T} \right)$$

$$Z^* = \sum_i e^{-\beta(E_i - f_{1,z})}$$

$$\langle r_{1,z} \rangle = \frac{1}{\beta} \frac{\partial}{\partial f} \ln(Z^*)$$

$$\langle r_{1,z} \rangle = k_B T \frac{\partial}{\partial f} \ln Z_1 = k_B T \frac{1}{Z_1} \frac{\partial Z_1}{\partial f} = k_B T \left(-\frac{1}{f} + \frac{b}{k_B T} \frac{e^{fb / k_B T} + e^{-fb / k_B T}}{e^{fb / k_B T} - e^{-fb / k_B T}} \right)$$

$$\langle r_{1,z} \rangle = b \left(\coth \left(\frac{fb}{k_B T} \right) - \frac{k_B T}{fb} \right) = L \left(\frac{fa}{k_B T} \right)$$

$$\langle r_{N,z} \rangle = Nb \left(\coth \left(\frac{fb}{k_B T} \right) - \frac{k_B T}{fb} \right)$$

$$\frac{e^x + e^{-x}}{e^x - e^{-x}} - \frac{1}{x} \approx \frac{2 + 2x^2}{2x + 2x^3/6} - \frac{1}{x} = \frac{1 + x^2 - 1 - x^2/6}{x + x^3/6} \approx \frac{x}{3}$$

$$f = \frac{3k_B T}{Nb^2} \langle r_{N,z} \rangle$$

Thus, for low forces, i.e. small extensions compared to the contour length the system behaves as a Hookean spring that is purely entropic in nature, called entropic spring. The entropic nature causes also a temperature dependence of the entropic spring constant, such that temperature affects the elasticity of elastomers, such as rubber, in an unusual way. Since elastomers consist of networks of flexible polymer chains that are in a partially stretched state, heating causes an elastomer to contract!

Part XX

Lecture 20

27 Ideal Polymer Models

```
import numpy as np
import matplotlib.pyplot as plt
from numpy.linalg import norm
from scipy.constants import c,epsilon_0,e,physical_constants
import json

#%config InlineBackend.figure_format = 'retina'
#
#with open('style.json', 'r') as fp:
#    style = json.load(fp)
#
#plt.rcParams.update(style)
```

27.1 Freely Rotating Chain

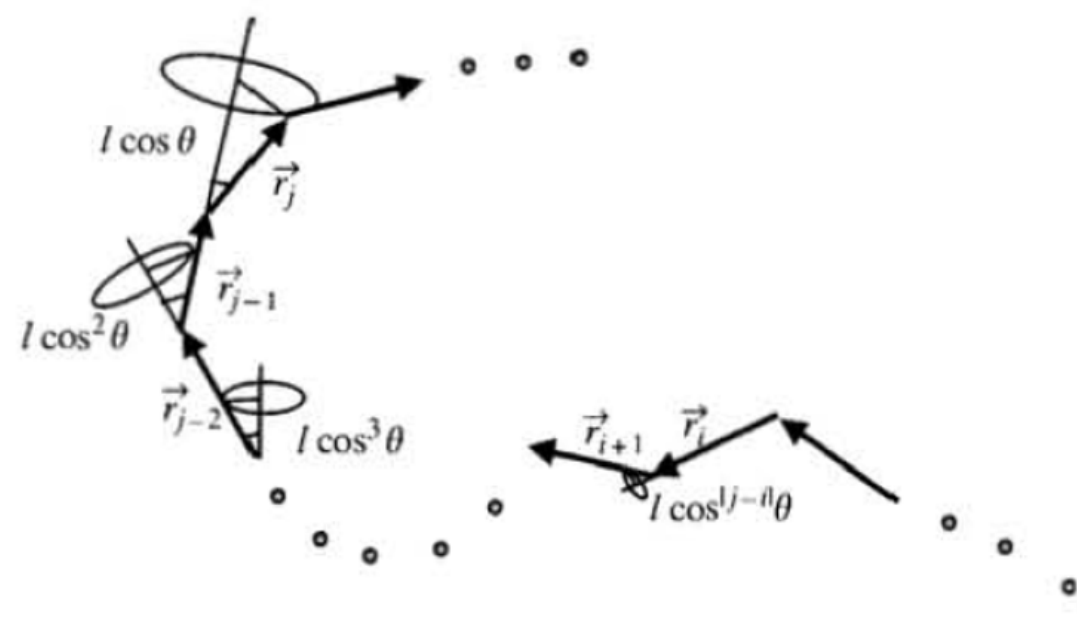


Figure 27.1: FRC

$$\langle \vec{r}_i \cdot \vec{r}_j \rangle = l^2(\cos \theta)^{|j-i|}$$

$$\langle R^2 \rangle = \sum_{i=1}^n \sum_{j=1}^n \langle \vec{r}_i \cdot \vec{r}_j \rangle$$

$$\langle R^2 \rangle = nl^2 + 2nl^2 \frac{\cos \theta}{1 - \cos \theta} = nl^2 \frac{1 + \cos \theta}{1 - \cos \theta}$$

$$C_\infty = \frac{1 + \cos \theta}{1 - \cos \theta} \cong 2$$

27.2 Gaussian Chain

We have previously seen that in the limit of $N \rightarrow \infty$ all ideal chains become identical and follow the normal distribution as long as each step of the random walk for the chain conformation satisfies that it is uncorrelated with the previous step. A generalization of this concept is the

Gaussian chain, which no longer considers the exact Kuhn segment length, but divides a long chain into equal flexible segments of arbitrary length:

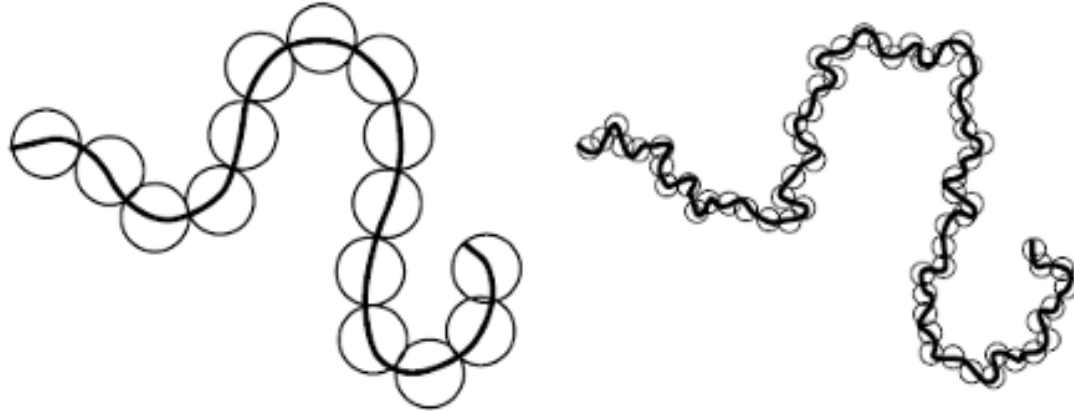


Figure 27.2: SSC

In this case, the “segment length” b is not a real length, but the ends of a segment have a square end-to-end distance of b . The end-to-end distance of a segment is also no longer fixed/rigid. Instead, the end-to-end vector of each segment is determined by the Gaussian probability distribution for an ideal chain:

$$p(\vec{r}_i; N) = \left(\frac{3}{2\pi b^2} \right)^{\frac{3}{2}} e^{-3|\vec{r}_i|^2/(2b^2)}$$

with a variance of b^2 . The probability distribution for the end-to-end vector of the whole chain containing N Gaussian chain segments is according to the central limit theorem again Gaussian distributed and has N times the single segment variance:

$$\langle R_N^2 \rangle = N \cdot b^2$$

Let us now consider that each segment is composed of n smaller Gaussian chain segments with root-mean-squared end-to-end distance of b_0 . In this case the mean squared end-to-end distance of the large Gaussian segments is given as:

$$b^2 = nb_0^2$$

The mean-squared end-to-end distance of the whole chain is then given as:

$$\langle R_N^2 \rangle = \underbrace{N \cdot n}_{n_0} \cdot b_0^2$$

with n_0 being the total number of small Gaussian chain segments in the whole chain, i.e. which is the expected result when using small segments for the whole chain. This shows that ideal chains are self-similar (one also calls this the fractal nature), i.e. the length range of the compartmentalization does not matter and provides the same result for small and large compartments. Using this approach the contour length of the whole chain remains however undefined.

One can represent the Gaussian chain also as a bead-spring model, where each spring has the spring constant k of an entropic spring:

$$\vec{f}_i = \underbrace{\frac{3k_B T}{b^2}}_k \langle \vec{r}_i \rangle$$

The total free energy of the chain is then given by the elastic (entropic) spring energy as well as its configurational entropy.

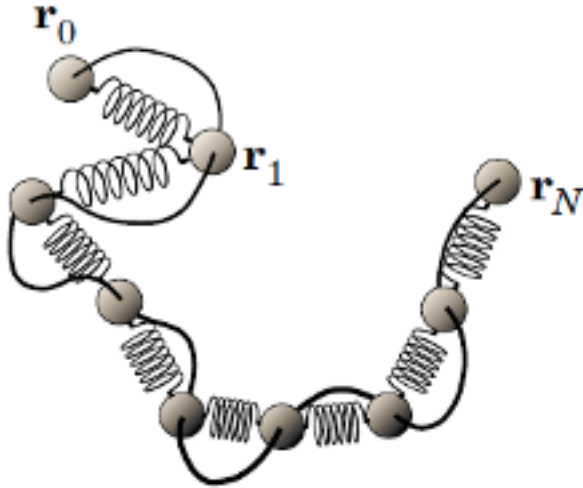


Figure 27.3: GC

The Gaussian chain model can be applied as long as each Gaussian segment can be approximated by the Gaussian statistics.

27.3 Wormlike Chain

Many polymers, especially biological filaments, are often freely articulated and there are no single discrete bond angles leading to the chain conformations. Such polymers are called semiflexible polymers or wormlike chains because they appear stiff on short length scales but flexible on long length scales due to the L³ dependence of the deflection of a cantilevered beam under load:

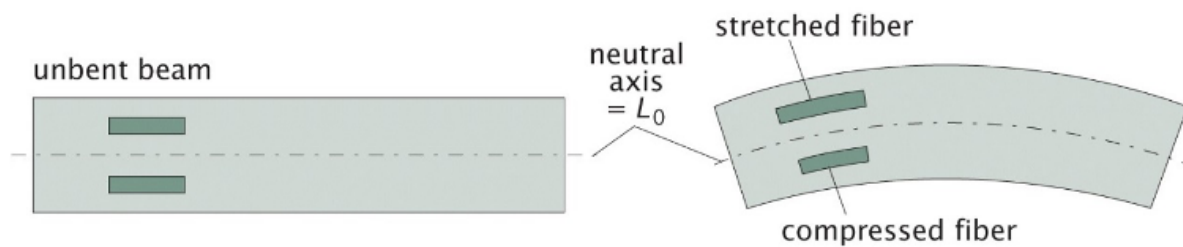


Figure 10.3 Physical Biology of the Cell, 2ed. (© Garland Science 2013)

Figure 27.4: wlc

$$\varepsilon(z) = \frac{L(z) - L(0)}{L(0)} = \frac{(R + z)\theta - R\theta}{R\theta} = \frac{z}{R}$$

$$\kappa(s) = \frac{1}{R(s)} = \left| \frac{d\theta}{ds} \right|$$

$$W(\varepsilon) = \frac{1}{2}E\varepsilon^2$$

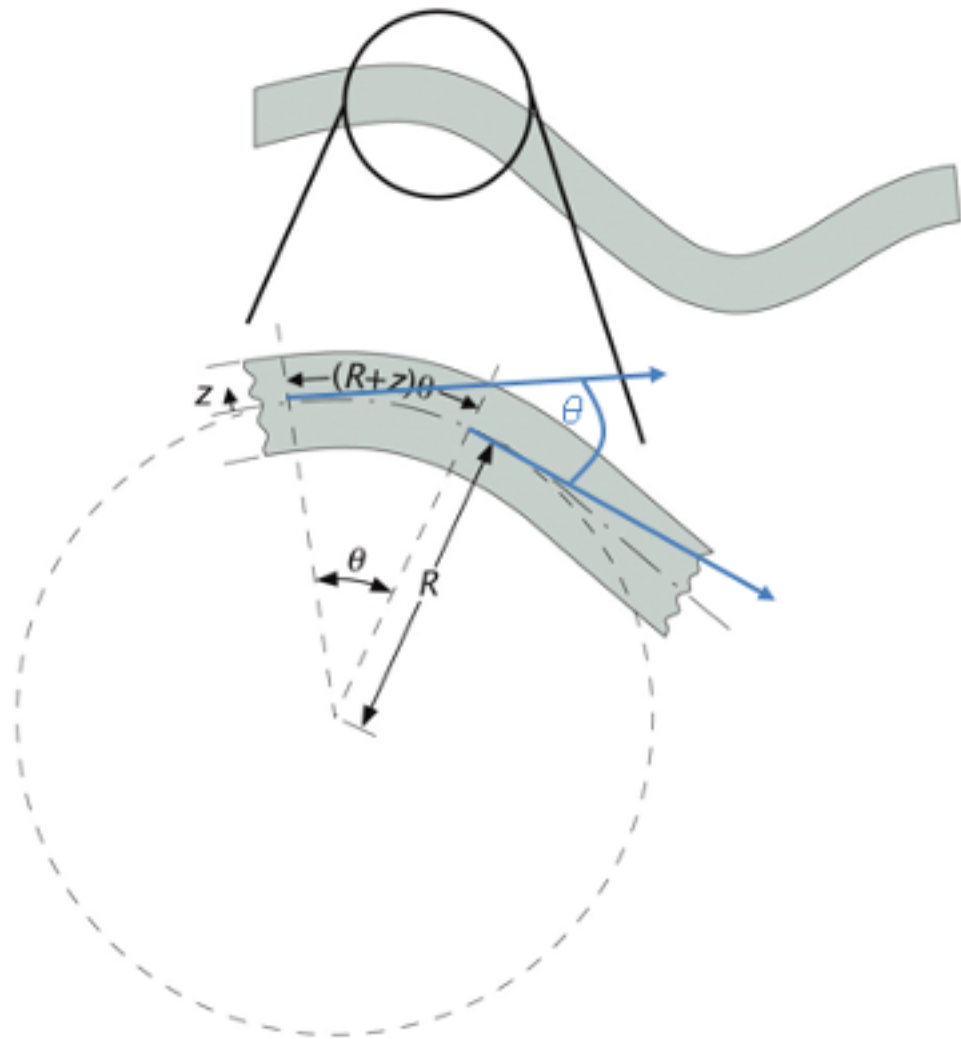


Figure 27.5: Curve

$$dE_{\text{bend}} = ds \int_{\delta\Omega} dA \cdot W(\varepsilon) = ds \int_{\delta\Omega} dA \frac{E}{2} \varepsilon(z)^2 = ds \int_{\delta\Omega} dA \frac{E}{2R(s)^2} z^2$$

$$dE_{\text{bend}} = ds \frac{EI}{2R(s)^2}$$

$$I = \int_{\delta\Omega} dA \cdot z^2$$

Shape	Second moment I
Solid cylinder (radius r)	$\frac{\pi}{4} r^4$
Hollow cylinder (outer radius r_2 , inner radius r_1)	$\frac{\pi}{4} (r_2^4 - r_1^4)$
Ring-like filament of n -cylinders each with radius r (e.g. microtubule)	$\left(\frac{2}{\pi^2} n^3 + n\right) \frac{\pi}{4} r^4$

Persistence Length

Now let us consider thermal fluctuations of a short semi-flexible beam segment of length Δs in 2D(within a plane). Its mean bending energy is given by the equipartition theorem as, since the fluctuations have only one degree of freedom:

$$\langle \Delta E_{\text{bend}} \rangle = \left\langle \Delta s \frac{EI}{2} \left(\frac{\Delta\theta}{\Delta s} \right)^2 \right\rangle = \frac{EI}{2} \frac{\langle \Delta\theta^2 \rangle}{\Delta s} = \frac{1}{2} k_B T$$

i.e. the mean-squared angular displacement is given as:

$$\langle \Delta\theta^2 \rangle = \frac{k_B T}{EI} \cdot \Delta s = \frac{\Delta s}{p} \quad \text{if } \Delta\theta^2 \ll 1$$

It is proportional to the beam length, i.e. longer beams appear more flexible. The fraction in the central equation defines an inverse length based on kT and the beam material and shape parameters. We call the ratio:

$$p = \frac{EI}{k_B T}$$

persistence length p , that provides the a measure of the flexural rigidity per length of the beam balanced by the thermal fluctuations.

Let us describe the deflection of the tangent angles over larger length scales. i.e. Δs may be larger than p . Instead of the mean angular displacement we take the tangent-tangent correlation function as descriptor:

$$g(s) = \langle \vec{t}(s) \cdot \vec{t}(0) \rangle = \langle \cos \theta(s) \rangle$$

$$\Delta \langle \cos \theta(s) \rangle = \frac{d \langle \cos \theta(s) \rangle}{ds} \Delta s = \langle \cos \underbrace{\theta(s + \Delta s) - \theta(s)}_{\Delta \theta} \rangle - \langle \cos \theta(s) \rangle$$

$$\Delta \langle \cos \theta(s) \rangle = \underbrace{\langle \cos \theta \cos \Delta\theta - \sin \theta \sin \Delta\theta \rangle}_{\langle \cos \theta \rangle \langle \cos \Delta\theta \rangle - \underbrace{\langle \sin \theta \rangle \sin \Delta\theta \rangle_0} - \langle \cos \theta(s) \rangle = \langle \cos \theta(s) \rangle (\langle \cos \Delta\theta \rangle - 1)$$

$$\Delta\theta \langle \cos \Delta\theta \rangle \approx 1 - \langle \Delta\theta^2 \rangle / 2$$

$$\frac{d \langle \cos \theta(s) \rangle}{ds} \Delta s = \langle \cos \theta(s) \rangle \frac{\langle \Delta\theta^2 \rangle}{2} = \langle \cos \theta(s) \rangle \frac{\Delta s}{2p}$$

$$\int_1^{\langle \cos \theta(s) \rangle} \frac{d \langle \cos \theta(s) \rangle}{\langle \cos \theta(s) \rangle} = \int_0^s \frac{ds}{2p}$$

$$\langle \cos \theta(s) \rangle = e^{-s/2p}$$

In 3D we have an additional degree of freedom for the angular fluctuations, such that the mean-squared angular deflection for a short segment is twice as large. In 3D the tangent correlation function thus becomes:

$$\langle \vec{t}(s) \cdot \vec{t}(0) \rangle = e^{-sk_B T I(EI)} = e^{-s/p}$$

i.e. the persistence length provides the distance scale at which the correlation between the tangent angles decays. The persistence length thus defines the length over which a polymer is still remaining rigid.

Mean-square end-to-end distance of a long semiflexible chain (worm-like-chain)

$$\mathbf{R} = \int_0^L d\mathbf{s} \mathbf{t}(s)$$

$$\langle \mathbf{R}^2 \rangle = \left\langle \int_0^L d\mathbf{s} \mathbf{t}(s) \cdot \int_0^L d\mathbf{u} \mathbf{t}(u) \right\rangle$$

$$\begin{aligned}
\langle \vec{R}^2 \rangle &= \left\langle \int_0^L ds \int_0^L du \vec{t}(s) \cdot \vec{t}(u) \right\rangle \\
&= \int_0^L ds \int_0^L du \cdot e^{-|u-s|/p} \\
&= 2 \int_0^L ds \int_s^L du \cdot e^{-(u-s)/p} \\
&= 2 \int_0^L ds \int_0^{L-s} dx \cdot e^{-x/p} \\
&= 2p \int_0^L ds (1 - e^{-(L-s)/p})
\end{aligned}$$

$$\langle \vec{R}^2 \rangle = 2pL \left[1 - \frac{p}{L} (1 - e^{-L/p}) \right]$$

$$\langle R_G^2 \rangle = \frac{1}{6} \langle \vec{R}^2 \rangle = \frac{1}{6} Lb$$

$$\langle R_G^2 \rangle = \frac{1}{3} Lp$$

Organism	genome length in bp	R_G in μm	compartment size in μm
λ -phage	50,000	0.5	0.1 (capsid)
<i>E. coli</i>	$6 \cdot 10^6$	6.8	1
H.sapiens	$6 \cdot 10^9$	200	few μm (nucleus)

Force-extension relation of a worm-like chain!

$$F = \frac{k_B T}{p} \left[\frac{1}{4(1-z/L_0)^2} + \frac{z}{L} - \frac{1}{4} \right]$$

Adding elastic stretching to entropic force-extension behavior

$$\frac{z_{\text{total}}}{L_0} = \frac{z_{\text{entr}}}{L_0} + \frac{z_{\text{elastic}}}{L_0} = \frac{z_{\text{entr}}}{L_0} + \frac{F}{S}$$

$$\langle z_{\text{total}} \rangle = L_0 \left[\coth \left(\frac{aF}{k_B T} \right) - \frac{k_B T}{aF} + \frac{F}{S} \right]$$

$$F=\frac{k_BT}{p}\left[\frac{1}{4\left(1-z/L_0+F/S\right)^2}+\frac{z}{L}-\frac{F}{S}-\frac{1}{4}\right]$$

Part XXI

Lecture 22

28 Real Polymers

[File as PDF](#)

```
import numpy as np
import matplotlib.pyplot as plt
from numpy.linalg import norm
from scipy.constants import c,epsilon_0,e,k,physical_constants
import json

%config InlineBackend.figure_format = 'retina'

with open('style.json', 'r') as fp:
    style = json.load(fp)

plt.rcParams.update(style)
```

We want to look at properties of real polymers in the following, which means that we have to incorporate interactions between monomers, which are of finite size and also have interactions with the solvent. We will do that in a mean field model introducing the so-called Mayer f-function.

28.1 Mayer f-function and excluded volume

Consider for that purpose the interaction by two monomers in a solvent with an effective potential $U(r)$. This potential typically has some large repulsive component at very short distances, some attractive components (negative) at intermediate length scales and a zero value at very large length scales.

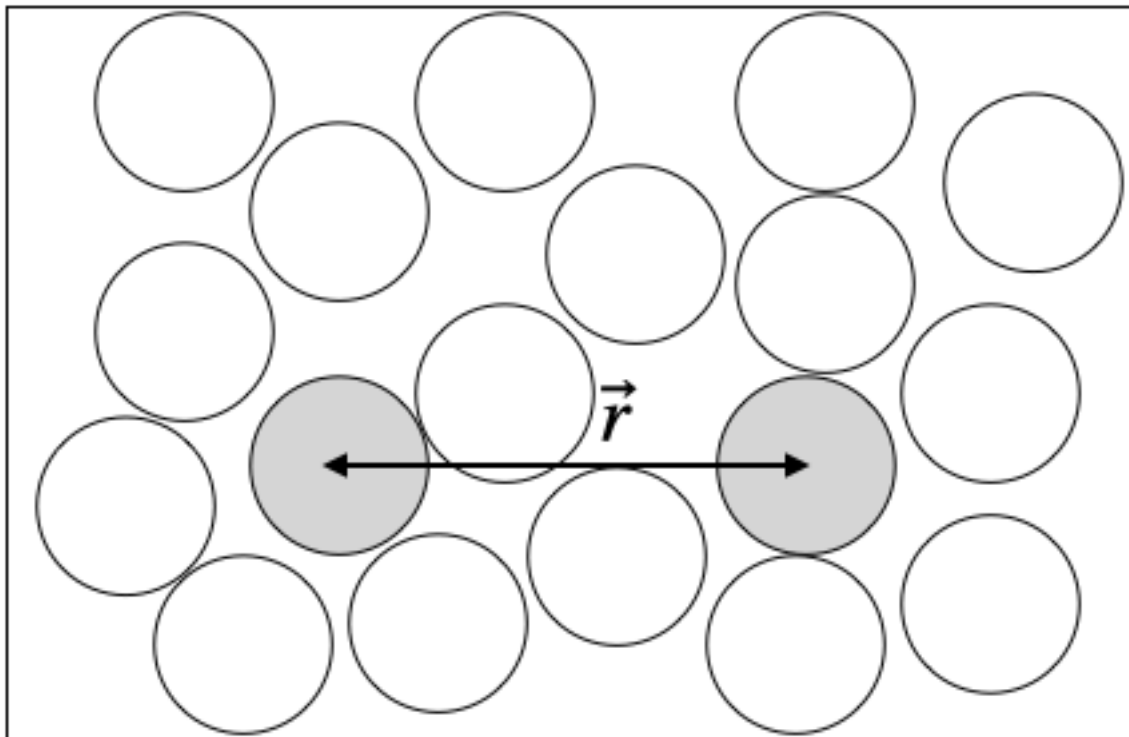


Figure 28.1: Interaction

28.1.1 Interaction potential

The plots below show some example interaction potentials. The left graph displays the Lennard-Jones potential, the right one the hard sphere potential, which is also called an athermal potential, as there is no temperature in it due to the missing minimum.

Note again, that this potential includes all effects of the solvent as well.

```
def LJ(eps,sig,r):
    return(4*eps*((sig/r)**12-(sig/r)**6))

r=np.linspace(0.1,10,100)

fig=plt.figure(figsize=(10,5))
plt.ion()
plt.subplot(121)
plt.plot(r,LJ(1,3,r),'k--')
```

```

plt.ylim(-3,3)
plt.axhline(y=0)
plt.xlabel("distance r")
plt.ylabel(r"$U(r)$")
plt.subplot(122)
plt.plot([2,2],[0,3],'k--')
plt.axhline(y=0)
plt.plot([1,10],[0,0],'k--')
plt.ylim(-3,3)
plt.xlim(0)
plt.xlabel("distance r")
plt.ylabel(r"$U(r)$")
plt.tight_layout()
plt.savefig("img/tmp1.png")
plt.close(fig)

```

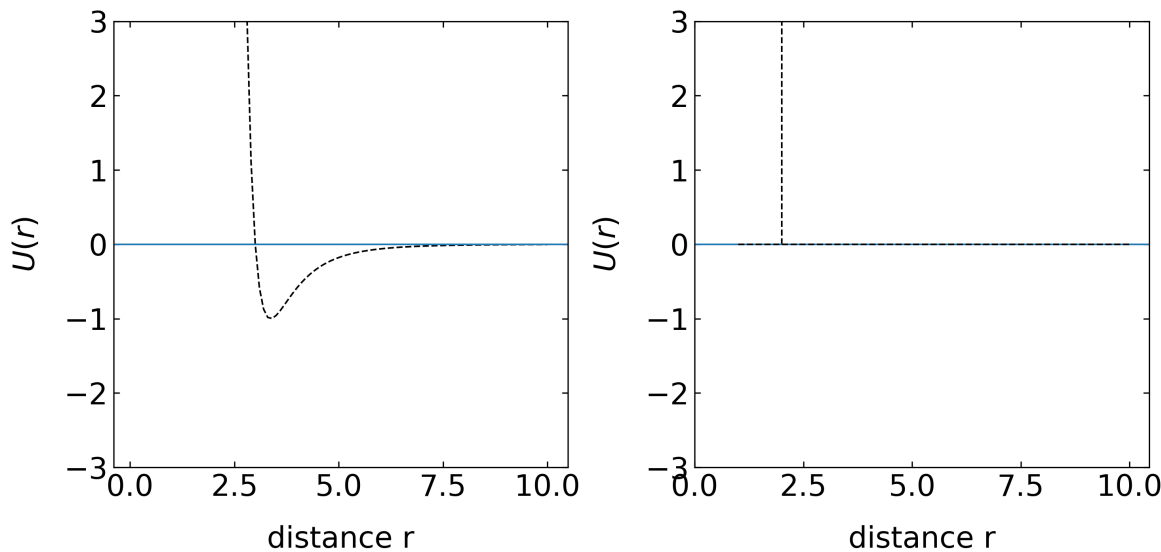


Figure 28.2: tmp1

28.1.2 Probability distribution

The probability distribution for finding the monomers at a certain distance r is then given by the Boltzman factor

$$p(r) = \exp\left(-\frac{U(r)}{k_B T}\right) \quad (28.1)$$

For the two potentials shown above, the probability therefore is zero wherever the potential is infinitely large. Whenever the potential is zero we find a probability density value of 1 while it is larger than 1 in the regions, where the potential is attractive.

```
fig=plt.figure(figsize=(10,5))
plt.ion()
plt.subplot(121)
plt.plot(r,np.exp(-LJ(1,3,r)), 'k--')
plt.ylim(-3,3)
plt.axhline(y=0)
plt.xlabel("distance r")
plt.ylabel(r"$p(r)$")
plt.subplot(122)
plt.plot(r,np.heaviside(r-2,1), 'k--')
plt.axhline(y=0)
plt.plot([1,10],[0,0], 'k--')
plt.ylim(-3,3)
plt.xlim(0,10)
plt.xlabel("distance r")
plt.ylabel(r"$p(r)$")
plt.tight_layout()
plt.savefig("img/tmp2.png")
plt.close(fig)
```

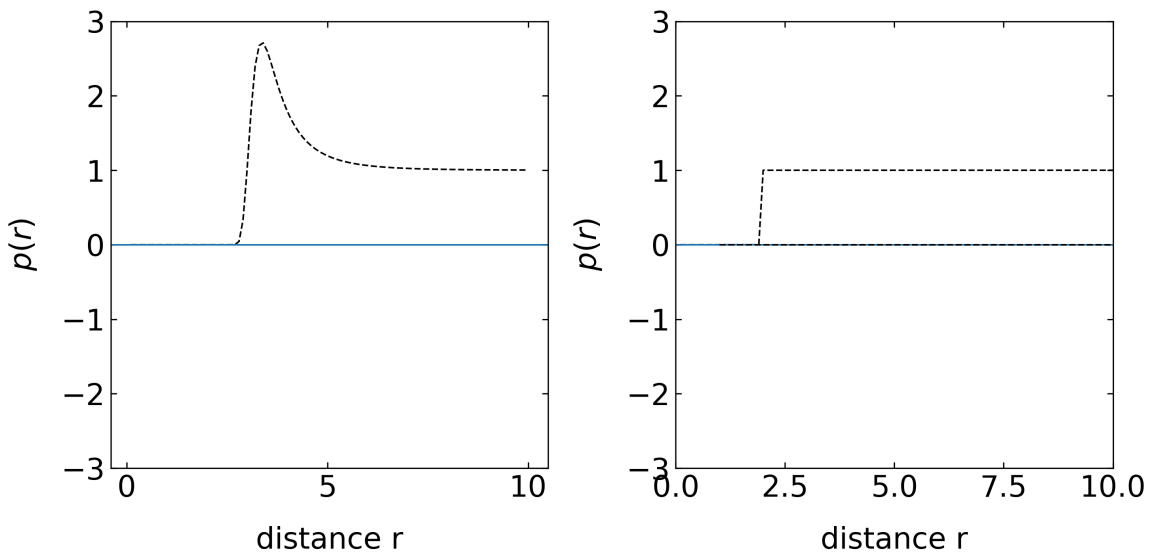


Figure 28.3: tmp2

28.1.3 Mayer f-function

The Mayer f-function measures now the deviation of the probability from the regions where the potential is zero or the probability density gives 1. It is defined by

$$f(r) = \exp\left(-\frac{U(r)}{k_B T}\right) - 1 \quad (\text{Mayer f-function})$$

```
fig=plt.figure(figsize=(10,5))
plt.subplot(121)
plt.plot(r,np.exp(-LJ(1,3,r))-1,'k--')
plt.ylim(-3,3)
plt.axhline(y=0)
plt.xlabel("distance r")
plt.ylabel(r"$f(r)$")
plt.subplot(122)
plt.plot(r,np.heaviside(r-2,1)-1,'k--')
plt.ylim(-3,3)
plt.xlim(0,10)
plt.xlabel("distance r")
plt.ylabel(r"$f(r)$")
```

```

plt.tight_layout()
plt.savefig("img/tmp3.png")
plt.close(fig)

```

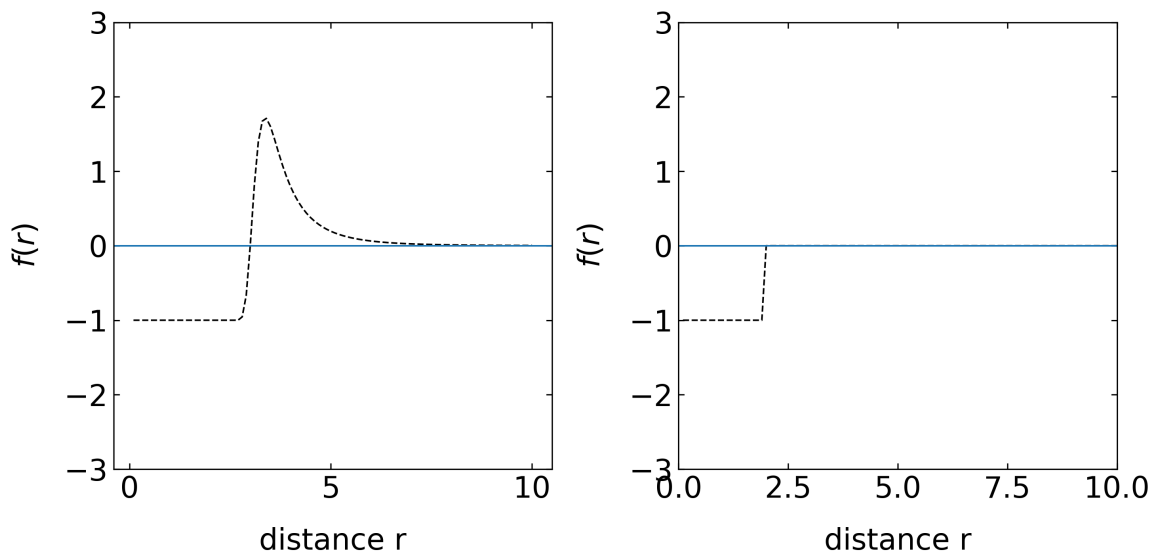


Figure 28.4: tmp3

This definition makes sense if we consider the right example of a hard sphere interaction. The free volume can then be calculated by

$$v = - \int f(r) d^3r = \int \left[1 - \exp \left(-\frac{U(r)}{k_B T} \right) \right] d^3r \quad (28.2)$$

which is giving in the case of the hard sphere interaction just $4\pi R^3/3$, where R is the contact separation distance of the two spheres. Thus the volume integral over the Mayer f -function is directly giving the excluded volume for the pairwise interaction. Note that the excluded volume can also be negative. This happens, when the attractive interaction is very strong. It can also be zero, when both positive and negative areas under the Mayer f -function are of the same size.

28.1.4 Polymer chain as a real gas

Our further calculations will now base the excluded volume influence on the conformation of a polymer chain under the assumption that all monomers (or actually Kuhn segments) are

independet and don't correlate in their position. They will thus behave like a real gas and show effect which we know from the **van der Waals gas**, such as co-volume and cohesive pressure. The two effects are actually corrections to the equation of state of the **ideal gas**, which can be written as

$$Z \equiv \frac{pV_m}{RT} = 1 \quad (\text{compressibility factor})$$

where p is the pressure, V_m the molar volume and R is the gas constant, i.e. $R = k_B N_A$. For a real gas, the corrections have to scale with the density of the objects $\rho = 1/V_m$ and we can write the compressibility factor as a Taylor series expansion

$$Z = \frac{pV_m}{RT} = 1 + B(T)\rho + C(T)\rho^2 + D(T)\rho^3 + \dots \quad (\text{virial expansion})$$

which is the viral expansion of the compressibility factor for a real gas. The coefficients $B(T), C(T), D(T)$ are called the viral expansion coefficient.

Let's have a look at the first one in the case of a van der Waals gas, which is $B(T)$. The presure of a van der Waals gas reads

$$p = \frac{RT}{(V_m - b)} - \frac{a}{V_m^2} \quad (28.3)$$

where b denotes the co-volume (the volume taken by the molecules themselves) and a amounts for the cohesive pressure of the gas molecules. If we set $a = 0$ we can write the compressibility factor

$$Z = \frac{PV_m}{RT} = \frac{1}{1 - \frac{b}{V_m}} \quad (28.4)$$

For $b/V_m < 1$, we can do a Taylor expansion which yields

$$Z = 1 + b\frac{1}{V_m} + b^2\frac{1}{V_m^2} + \dots = 1 + b\rho + b^2\rho^2 + \dots \quad (28.5)$$

Comparing with the virial expansion above yields the fact that the virial expansion coefficient

$$B(T) = b$$

where b was the molar co-volume in the van der Waals equation, e.g. the excluded volume. Correspondingly, the virial expansion coefficient is given by the integral over the Mayer f-function, i.e. in spherical coordinates

$$B(T) = - \int f(r) d^3r = -4\pi \int_0^\infty \left(e^{-\frac{U(r)}{k_B T}} - 1 \right) r^2 d^3r$$

Using this relation, we have a way to introduce the monomer-monomer and monomer-solvent interaction that is hidden in the May f-function into the equation of state of a real gas of polymer segments. We will come back to this solution.

28.2 Non-spherical segments and Free energy of interaction of a real chain

While we have assumed so far (without emphasizing it too much) that the interaction of the monomers is radially symmetric (monomers are spheres), typical monomers are rather rod-like. Thus we should get an idea about how the free volume changes when we go from a sphere to the rod. The procedure below considers the free energy of the interaction and replaces a rod by a set of spheres. We can get an idea about the free energy of a chain by coming back to our osmotic pressure formula

$$\Pi = nk_B T \quad (28.6)$$

where n is the number density of molecules. The unit of pressure is N/m^2 or J/m^3 , which is an energy density. The formula above tells us that adding a single molecule comes at some cost, which is $k_B T$. Yet, this is an ideal gas consideration. If we want to add a contribution of the excluded volume, we can refer to the overlap fraction

$$\Phi^* = b^3 \frac{N}{R^3}$$

where b was the Kuhn length and R the root mean squared end-to-end distance. The number of monomer-monomer contacts was $N\Phi^*$, which finally gives N^2/R^6 contacts per volume. The free energy of interaction per volume is therefore

$$\frac{F_{\text{int}}}{V} = k_B T (vc_m^2 + wc_m^3 + ...) = k_B T (v \frac{N^2}{R^6} + w \frac{N^3}{R^9} + ...) \quad (28.7)$$

where $c_m = N/R^3$ is the monomer concentration. The first term in the above equation results from the monomer-monomer contacts as we introduced. The second term is accordingly the result of the contact between three monomers and so on. Therefore, this is also a virial expansion and the first virial expansion coefficient v is the excluded volume of the bimolecular monomer contact.

This consideration helps us to understand the role of non-spherical rodlike monomers or segments. If we have a rodlike segment of length b and radius d , then the rod can be replaced by spherical monomers of radius d . The number of spherical monomers per segment is then b/d . Thus if a chain has N rodlike segments, then it can be replaced by $n = Nb/d$ spherical monomers.

In case of hard-sphere interactions the overall contribution of the excluded volume to the free energy shall be independent of the fact if the rods are replaced by spheres so the term

$$vN^2/R^6$$

shall give the same results, and therefore

$$v_s n^2 = v_c N^2$$

or

$$w_s n^3 = w_c N^3$$

With the spherical volume $v_s = d^3$ and $w_s = d^6$ we find

$$v_c = v_s \left(\frac{n}{N} \right)^2 = v_s \left(\frac{b}{d} \right)^2 = b^2 d$$

Thus the excluded volume for the interaction of two rods is larger than the actual rod volume itself, which is

$$v_0 = bd^2$$

which is the result of random orientations. If the aspect ratio, i.e. the ratio of the two volumes v_c/v_0 is large, this excess excluded volume is the driving force for a nematic (alignment) ordering of the rodlike segments as originally described by Onsager for liquid crystalline systems.

28.3 Solvent Classification

- **Athermal Solvents** Here, v is independent of temperature. The system only features hard core repulsion and $v \approx b^2d$. Monomer-monomer contact is energetically indistinguishable from monomer-solvent contact, for example.
- **Good solvents** Excluded volume is reduced due to monomer-monomer attraction. The effect of this attraction is greater at lower temperatures, causing a reduction in the excluded volume. $0 < v < b^2d$
- **Theta solvent** The (positive) contribution to excluded volume from hard core repulsion is exactly balanced by that (negative) due to attractions and so $v = 0$. The chains thus have nearly ideal conformations. This occurs at a temperature called the theta temperature, Θ , which is analogous to the Boyle temperature in thermodynamics.
- **Poor solvents** Excluded volume is negative due to large attractive interactions between the monomers, which prefer monomer-monomer contact strongly over monomer-solvent contact. Chain dimensions are reduced relative to ideal. $-b^2d < v < 0$.
- **Non-solvents** Here, $v \approx -b^2d$ and the polymer collapses into a very compact structure that excludes all solvent.

28.4 Flory theory (in a good solvent)

Flory treated the question of equilibrium conformation of real chains using a mean field approach. The equilibrium size is set by a balance between excluded volume which tends to expand the chain size, and a restoring force due to loss of conformational entropy due to swelling. The energetic contribution due to excluded volume is given by the number of excluded volume interactions within a coil and the cost of each exclusion, $k_B T$. The number of excluded volume interactions is just the probability of finding a monomer within the excluded volume of another. If we assume a mean density of monomers in the coil, N/R^3 , then the number of excluded volume interactions per monomer is vN/R^3 and for N monomers in the coil, the energetic contribution is

$$F_{\text{int}} \approx k_B T v \frac{N^2}{R^3}$$

The entropic energy due to expansion of the coil is, as we have calculated before, given as

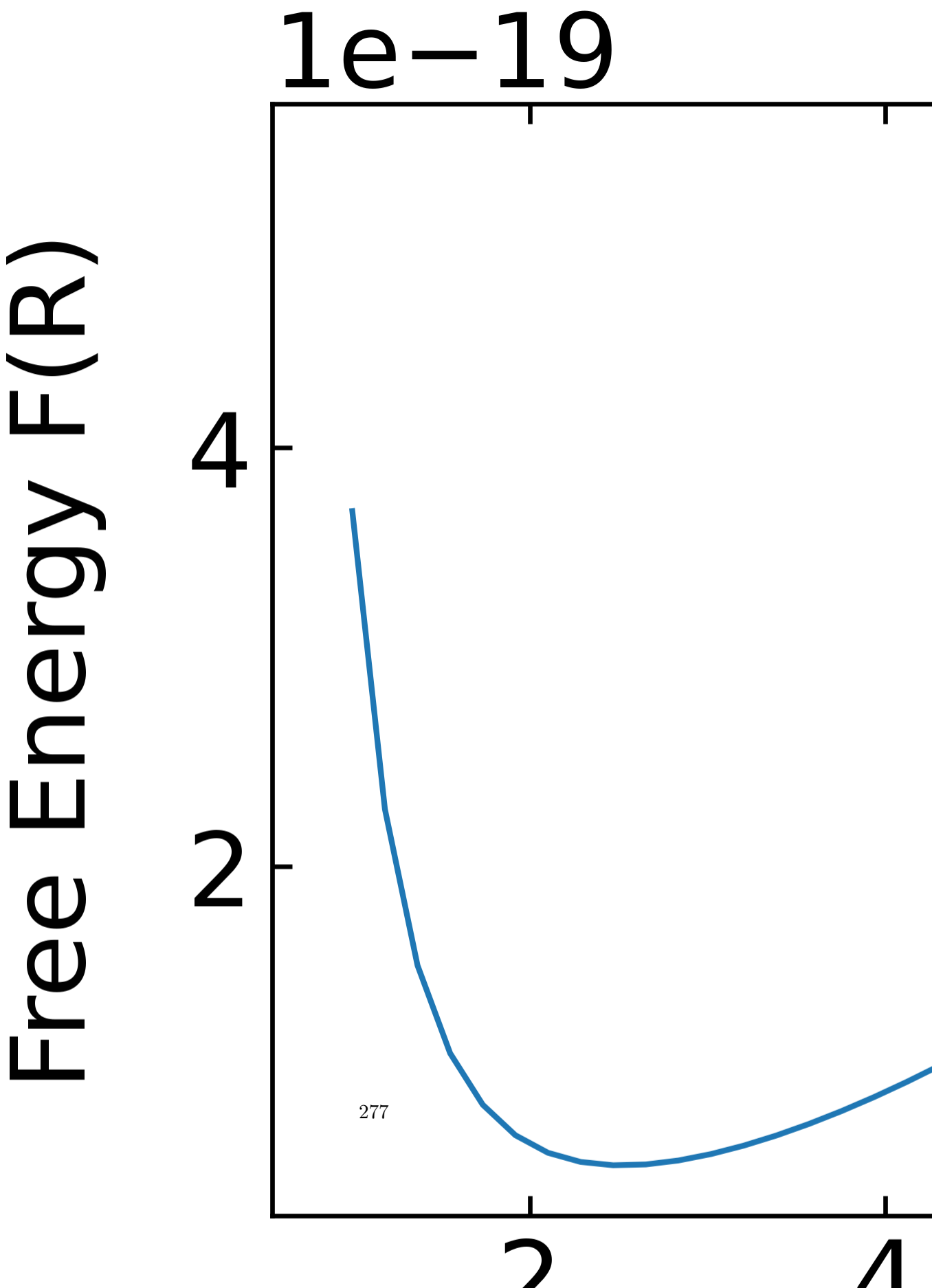
$$F_{\text{entropic}} \approx k_B T \frac{R^2}{Nb^2}$$

which gives a total free energy

$$F \approx k_B T \left(v \frac{N^2}{R^3} + \frac{R^2}{Nb^2} \right)$$

```
def F(R):
    T=293.15
    v=10
    b=0.5
    N=3
    return k*T*(v*N**2/R**3+R**2/(N*b**2))
```

```
R=np.linspace(1, 10)
plt.plot(R, F(R))
plt.xlabel("end to end distance R")
plt.ylabel("Free Energy F(R)")
plt.show()
```



The total free energy as a function of the end to end distance R has two components which either decay with R^{-3} or increase with R^2 . Therefore this function has a minimum, i.e.

$$\left. \frac{\partial F}{\partial R} \right|_{R_F} = 0$$

at a particular end to end distance, which is the so-called Flory radius R_F . From the derivative we find

$$R_F \approx v^{1/5} b^{2/5} N^{3/5}$$

which shows, that the size of a real polymer chain scales with $N^{3/5}$, where $\nu = 3/5 = 0.6$ is the Flory exponent, which has to be compared to $\nu = 1/2$ for an ideal (Gaussian chain). The polymer size thus scales stronger with the number of segments in the polymer, which seems at first glance a small difference, but due to the large numbers involved for N , this could make quite some difference.

insert experimental plot here

The simple approach taken by Flory provides surprisingly good results - more modern theories/calculations provide $R \sim N^{0.588}$. However, the success of the Flory theory is due to a cancellation of errors. The excluded volume contributions are overestimated as correlations between monomers (which decrease the probability of overlap) are not considered. At the same time, the entropic restoring force is also overestimated. Nevertheless, such approaches based on a mean field approximation of density combined with ideal chain conformation-derived entropy can provide quite useful results, for example in the case of an adsorbed chain. The treatment of the case for $v < 0$ in the preceding simple manner leads to an unphysical result for the coil size that minimizes the total free energy. Stabilizing terms need to be considered.

28.5 Flory Theory (in all solvents)

To extend the Flory theory for all kinds of solvents you have to go back to the virial expansion of the free energy density.

$$\frac{F_{int}}{V k_B T} = F_0 + vc^2 + wc^3 + \dots$$

which essentially contains a contribution of the ideal chain, plus the corrections in orders of the segment density c . The ideal chain thereby contributes the entropic part and the real chain correction gives the free volume correction. The main difference now to the good solvent

model is that the entropic part above has to include some additional term to include a repulsive Term

$$F_{\text{entropic}} \approx k_B T \frac{R^2}{Nb^2} + \underbrace{\frac{Nb^2}{R^2}}_{\text{new term}}$$

In this way, the free energy is

$$\frac{F}{k_B T} = \frac{R^2}{Nb^2} + \frac{Nb^2}{R} + v \frac{N^2}{R^3} + w \frac{N^3}{R^6} + \dots$$

Defining now the ratio of the end to end distance of the real chain and the ideal chain gives

$$\alpha^2 = \frac{\langle R^2 \rangle}{\langle R^2 \rangle_0 = \frac{R^2}{Nb^2}}$$

results in

$$\frac{F}{k_B T} = \alpha^2 + \alpha^{-2} + \frac{v N^{1/2}}{b^3} \alpha^{-3} + \frac{w}{b^6} \alpha^{-6}$$

This allows us to see that for

- $\alpha \gg 1$ we have a good solvent with $R_F \propto N^{3/5}$ and an extended polymer conformation
- $\alpha \ll 1$ we find $R_F \propto N^{1/3}$ with a collapsed polymer

28.6 Temperature dependence of the chain size

Using the Mayer f-function we can now also write down some basic ideas about the temperature dependence of the chain size. This is essentially hidden in the Boltzman factor including the potential energy $U(r)$.

If this potential energy is much bigger than the thermal energy, i.e. $U(r) \gg k_B T$, then we are commonly at small distances $r < b$ in the repulsive region. In this region, we can reduce the Mayer f-function to

$$f(r) = \exp\left(\frac{U(r)}{k_B T}\right) - 1 \approx -1$$

essentially to -1 .

If, on the other side the distance is larger than the Kuhn length ($r > b$), the interaction potential is small as compared to $k_B T$ and we may write

$$f(r) = \exp\left(\frac{U(r)}{k_B T}\right) - 1 \approx -\frac{U(r)}{k_B T}$$

Following these approximation we may split the intergral, which yields the excluded volume into two parts

$$v = -4\pi \int_0^\infty f(r)r^2 dr \approx 4\pi \int_0^b r^2 dr + \frac{4\pi}{k_B T} \int_b^\infty U(r)r^2 dr$$

This gives two terms, one the voume of the hard core repulsion and the second a term which comprises all the temperature dependent interaction. The dependencies can then be written as

$$v \approx \left(1 - \frac{\theta}{T}\right) b^3$$

where θ is the theta temperature, which is defined as

$$\theta \approx -\frac{1}{b^3 k_B} \int_B^\infty U(r)r^2 dr$$

According to this simplified formula for the excluded volume we see now the individual effects of solvent

- $T < \theta$ means the free volume is negative and we are in a **poor solvent**
- $T = \theta$ means that we have $v = 0$, and we are in a θ -solvent
- $T > \theta$ means that we have $v > 0$ and a **swelling** (growth) of the polymer
- $T \gg \theta$ means we are in the **athermal** situation such that $v = b^3$

display experimental graph from Colby

Part XXII

Lecture 23

29 Scattering Techniques for Polymer Conformation

The scattering of electromagnetic or matter waves is a commonly used tool to obtain information about the conformation of polymer chains. Light wave, X-rays (SAXS) but also neutrons (SANS) are used to study polymer solutions. While all waves have their own peculiarities, they are all based on the interference of partial waves scattered at different segments of the polymer.

```
import numpy as np
import matplotlib.pyplot as plt
from numpy.linalg import norm
from scipy.constants import c,epsilon_0,e,physical_constants
import json

%config InlineBackend.figure_format = 'retina'

with open('style.json', 'r') as fp:
    style = json.load(fp)

plt.rcParams.update(style)
```

A solution of different polymer chains (assume its dilute) has different length scales involved. There is an average distance between the polymer chains which is large as compared to the polymer size. Waves that interfere when being scattered from different polymers reflect the structure of the solution and is commonly addressed in a scattering quantity, which is the **structure factor**. Waves that are scattered by the same chain and interfere are a measure of the polymer conformation and described by the **form factor**. Yet, this scale separation might not always be possible in dense polymer solutions.

29.1 Form Factor

We would like to consider the form factor only, which gives us information on the polymer conformation. We have an incident plane wave with the wave vector \vec{q}_i which is falling on our polymer chain. The wavevector has a direction and magnitude according to

$$\vec{q}_i = \frac{2\pi}{\lambda} \vec{u}_i$$

where λ is the wavelength. Note that you should take care of the corresponding refractive index n in the case of light scattering ($\lambda = \lambda_0/n$). We will neglect the refractive index in the following, as it does not change the qualitative results.

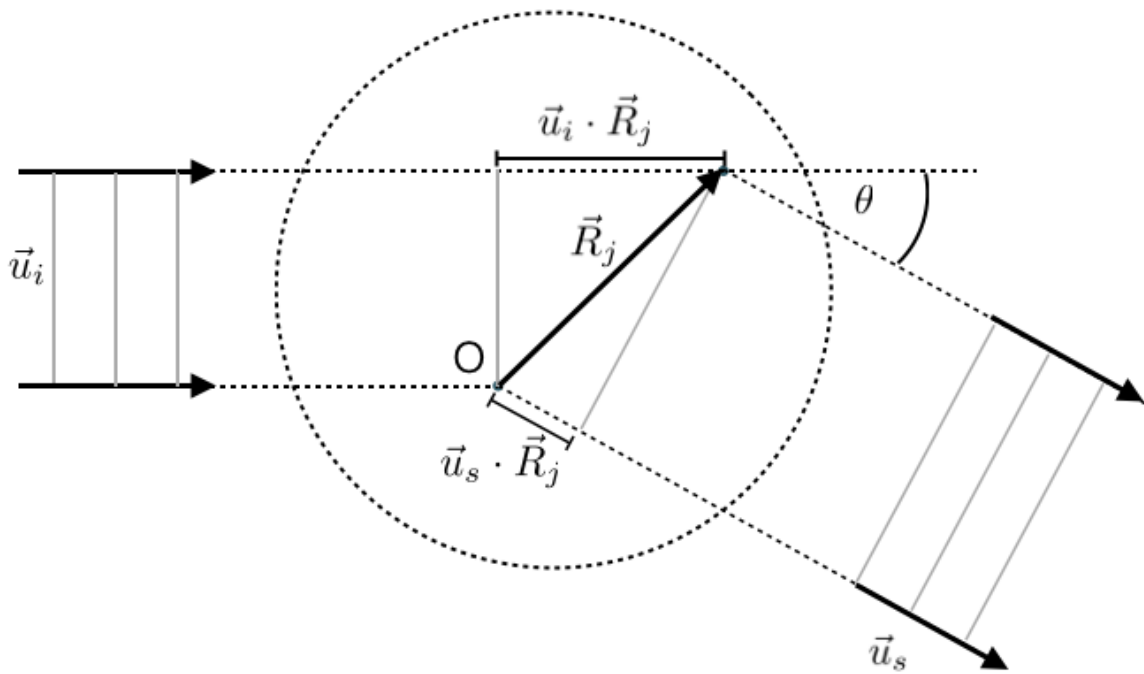


Figure 29.1: Scattering

The scattered light is then observed in a different direction, e.g. along the direction \vec{u}_s , which results in a scattered wavevector \vec{q}_s . Considering now the scattered wave from two segments of the polymer at \vec{R}_i and \vec{R}_j results in a path length difference Δ between the two waves, that is given by the incident wave path difference and the scattered wave path difference.

$$\Delta = \vec{u}_i \cdot \vec{R}_j - \vec{u}_s \cdot \vec{R}_j = (\vec{u}_i - \vec{u}_s) \cdot \vec{R}_j$$

This path difference translates into a phase difference if the waves

$$\varphi_j = \frac{2\pi}{\lambda} (\vec{u}_i - \vec{u}_s) \cdot \vec{R}_j = (\vec{q}_i - \vec{q}_s) \cdot \vec{R}_j = \vec{q} \cdot \vec{R}_j$$

Since the magnitude of the incident and the scattered wavevectors are the same, i.e.

$$|\vec{q}_i| = |\vec{q}_s| = \frac{2\pi}{\lambda}$$

we can express the magnitude of the vector \vec{q} denoting the momentum exchange during scattering, in terms of the scattering angle θ

$$q \equiv |\vec{q}| = 2|\vec{q}_i| \sin\left(\frac{\theta}{2}\right) = \frac{4\pi}{\lambda} \sin\left(\frac{\theta}{2}\right)$$

With the help of the phase angle, we can now find the electric field amplitude of the scattered waves of all segments j with

$$E_s = E_i \sum_{j=1}^N A \cos(2\pi\nu t - \varphi_j)$$

which provides with its magnitude square also the intensity of the scattered wave.

$$\begin{aligned} I_s &= 2I_i A^2 \nu \int_0^{1/\nu} \left[\sum_{j=1}^N \cos(2\pi\nu t - \varphi_j) \right]^2 dt \\ &= 2I_i A^2 \nu \int_0^{1/\nu} \left[\sum_{j=1}^N \sum_{k=1}^N \cos(2\pi\nu t - \varphi_j) \cos(2\pi\nu t - \varphi_k) \right] dt \\ &= I_i A^2 \nu \int_0^{1/\nu} \left[\sum_{j=1}^N \sum_{k=1}^N (\cos(4\pi\nu t - \varphi_j - \varphi_k) + \cos(\varphi_k - \varphi_j)) \right] dt \end{aligned}$$

The first term in the sum turns out to be zero when integrated over time, such that only the difference of the two individual phase angles is important.

$$I_s(\vec{q}) = \underbrace{I_i A^2 N^2}_{I_s(0)} \underbrace{\frac{1}{N^2} \sum_{k=1}^N \sum_{j=1}^N \cos(\varphi_k - \varphi_j)}_{P(\vec{q})}$$

The latter double sum including a prefactor defines the **form factor**

$$P(\vec{q}) \equiv \frac{I_s(\vec{q})}{I_s(0)} \quad (\text{form factor})$$

Inserting the expression for the individual phase angles yields

$$P(\vec{q}) = \frac{1}{N^2} \sum_{i=1}^N \sum_{j=1}^N \cos [\vec{q} \cdot (\vec{R}_i - \vec{R}_j)]$$

We therefore have to calculate the average over the phase angles or exchanged momentum times the position difference between two segments

$$\langle \cos [\vec{q} \cdot (\vec{R}_i - \vec{R}_j)] \rangle = \frac{1}{4\pi} \int_0^{2\pi} \left[\int_0^\pi \cos (qR_{ij} \cos \alpha) \sin \alpha d\alpha \right] d\beta$$

Using

$$\vec{q} \cdot (\vec{R}_i - \vec{R}_j) = qR_{ij} \cos \alpha$$

directly gives us the idea that the averaged cosine results in a sinus cardinalis

$$\langle \cos [\vec{q} \cdot (\vec{R}_i - \vec{R}_j)] \rangle = \frac{1}{2} \int_{-1}^1 \cos (qR_{ij}x) dx = \frac{\sin (qR_{ij})}{qR_{ij}}$$

which is reminiscent of the single slit result or the Fourier transform of the segment distribution in the scattering objects components:

$$P(q) = \frac{1}{N^2} \sum_{i=1}^N \sum_{j=1}^N \frac{\sin (qR_{ij})}{qR_{ij}}$$

29.2 Radius of Gyration

We can relate the latter result directly with properties of the polymer chain, like the radius of gyration. If we consider only values of the sinc argument which are $qR_{ij} < 1$, i.e. we consider **small angle scattering**, we can expand the sinc function into

$$\frac{\sin x}{x} = 1 - \frac{x^2}{3!} + \frac{x^4}{5!} - \dots$$

This yields a form factor

$$P(q) = 1 - \frac{q^2}{6N^2} \sum_{i=1}^N \sum_{j=1}^N R_{ij}^2 + \dots \quad \text{for } qR < 1$$

which gives with the definition of the radius of gyration directly

$$P(q) = 1 - \frac{1}{3}q^2 \langle R_g^2 \rangle + \dots \quad \text{for } qR_g < 1$$

or

$$P(q) = 1 - \frac{16\pi^2 n^2}{3\lambda^2} \langle R_g^2 \rangle \sin^2\left(\frac{\theta}{2}\right) + \dots$$

when inserting q . We will see in the derivation of the Debye function, that this inverse parabola can also be approximated with a Gaussian function

$$P(q) \cong \exp\left(-\frac{q^2 R_g^2}{3}\right) \quad \text{for } qR_g < 1$$

which is termed the **Guinier function**.

29.3 Debye Function

The above consideration is not taking into account that not all distances R_{ij} have the same probability for a polymer chain. This was first taken into account by Pieter Debye in form of the ideal chain. The end-to-end distance distribution we have obtained earlier delivers the probability to find the ending segments of a polymer with N Kuhn segments of length b at a distance R . We can use this expression as well to give a probability density to find two segments i, j at a distance R_{ij} , which is then given by

$$p(R_{ij}; \underbrace{|i-j|}_N) dR_{ij} = \left(\frac{3}{2\pi|i-j|b^2} \right)^{\frac{3}{2}} e^{-3R^2(2|i-j|b^2)} 4\pi R_{ij}^2 dR_{ij}$$

Note that the number of segments takes here the value $N=|i-j|$. Using this density distribution, we have to weight each contribution of the form factor with the corresponding probability density, i.e.

$$P(q) = \frac{1}{N^2} \sum_{i=1}^N \sum_{j=1}^N \int_0^\infty \frac{\sin(qR_{ij})}{qR_{ij}} P(R_{ij}, |i-j|) 4\pi R_{ij}^2 dR_{ij} \quad (29.1)$$

$$= \frac{1}{N^2} \sum_{i=1}^N \sum_{j=1}^N \exp\left(-\frac{q^2 b^2 |i-j|}{6}\right) \quad (29.2)$$

One can transform the double sum above in the case of large segment number into a double integral. The result is the Debye function

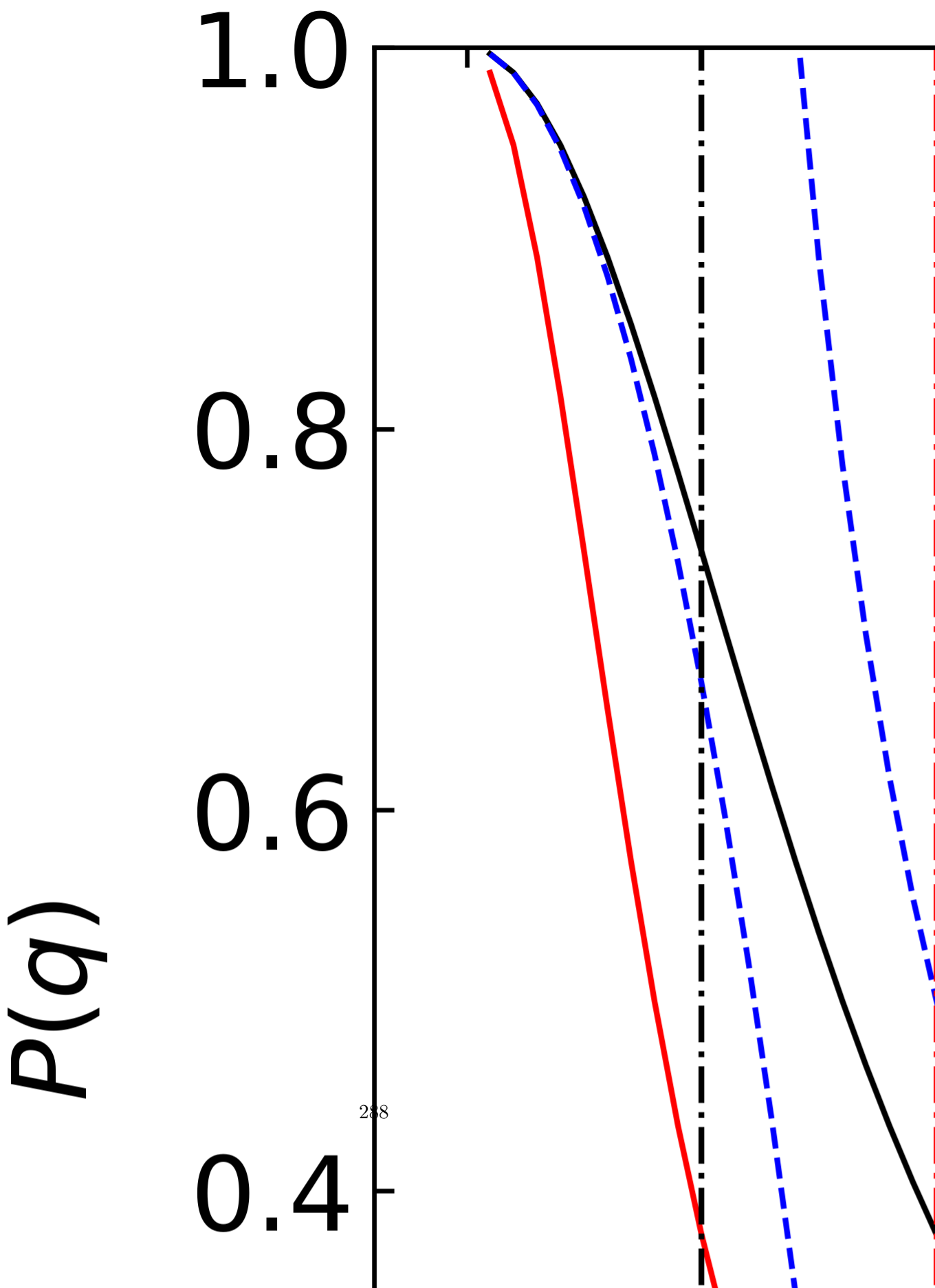
$$P(q) = \frac{2}{(q^2 \langle R_g^2 \rangle)^2} [\exp(-q^2 \langle R_g^2 \rangle) - 1 + q^2 \langle R_g^2 \rangle] \quad (\text{Debye function})$$

describing the scattering of an ideal chain, which is displayed in the graph below for two different radii of gyration.

```
def DebyeFunction(q,R_g):
    return((np.exp(-(q*R_g)**2)-1+(q*R_g)**2)*2/((q*R_g)**2)**2)

q=np.linspace(0.1,10,100)
R_g=1

fig=plt.figure(figsize=(8,6))
plt.ion()
plt.plot(q,DebyeFunction(q,R_g),'k-',label=r"$R_g=1$")
plt.plot(q,1-(q*R_g)**2/3,'b--')
plt.plot(q,2/(q*R_g)**2,'b--')
R_g=2
plt.plot(q,DebyeFunction(q,R_g),'r-',label=r"$R_g=2$")
plt.axvline(x=1,color='k',linestyle='-.')
plt.axvline(x=2,color='r',linestyle='-.')
plt.xlabel(r"$q$")
plt.ylabel(r"$P(q)$")
plt.ylim(0,1)
plt.legend()
plt.savefig("img/tmp1.png")
plt.show()
plt.close(fig)
```



We can have a look at different limits again, e.g. the small angle limit for which we find the same result as in the derivation in the previous section

$$P(q) \cong \left(1 - \frac{q^2 \langle R_g^2 \rangle}{3} + \dots \right) \quad \text{for } q\sqrt{\langle R_g^2 \rangle} < 1$$

Similarly, we find

$$P(q) \cong \frac{2}{q^2 \langle R_g^2 \rangle} \quad \text{for } q\sqrt{\langle R_g^2 \rangle} > 1$$

in the limit of large q , where the form factor decays as $1/q^2$. Both limits are included in the plot above to see their range of validity.

While the Debye function is the result for a simple ideal Gaussian chain, the form factor can also be derived for many other polymer shapes. The table below reports some examples.

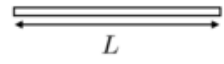
shape		R_g^2	x	$P(q)$
spherical		$\frac{3}{5}R_s^2$	qR_s	$[3x^{-3}(\sin(x) - x \cos(x))]^2$
rodlike		$\frac{L^2}{12}$	$q\frac{L}{2}$	$x^{-1} \int_0^{2x} z^{-1} \sin(z) dz - (x^{-1} \sin(x))^2$
Gaussian		$b^2 \frac{N}{6}$	qR_g	$2x^{-2}[1 - x^{-1}(1 - \exp(-x^2))]$

Figure 29.2: FormFactors

30 Viscoelasticity

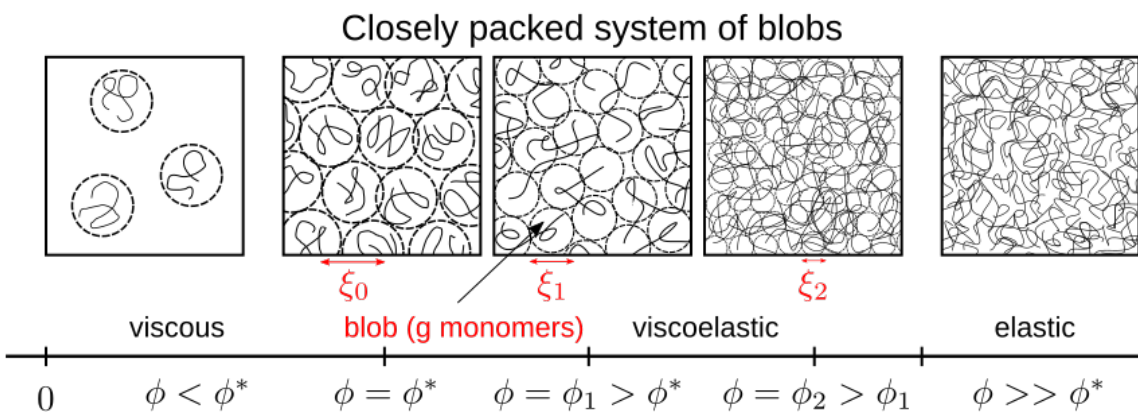


Figure 30.1: Ranges

Viscoelastic behavior is a mixture of viscous behavior, which we know already from simple liquids and elastic behavior, which is typical for solids. Yet, this mixture is not just a simple superposition but often quite complex and depending on the way mechanical deformation is introduced.

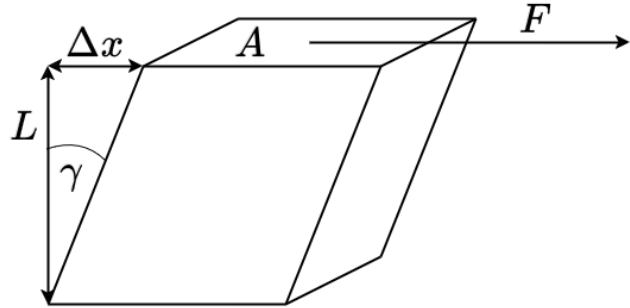


Figure 30.2: mechanical deformation example

As already previously introduced, we can define a **shear stress**

$$\sigma = \frac{F}{A}$$

as the tangential force F to an area A . As a response to such a stress, the material deforms and the deformation is called **shear strain**

$$\gamma = \frac{\Delta x}{L}$$

which corresponds directly to the angle in the above sketch as long as the displacement is small. Within this description all parts of the sample experience the same shear stress and strain if the material is uniform.

A perfectly elastic solid would give a very simple relation between stress and strain, i.e.

$$\sigma = G\gamma$$

where G is the shear modulus. This corresponds to Hooke's law of elasticity, which is valid for small deformations or small strain. In case of a simple liquid with a dynamic viscosity η , a constant strain leads to a zero shear stress. The liquid flow in response to the deformation and all flows have dissipated the initial deformation due to the internal friction of the liquid. Thus for liquids and viscous dissipation the **shear rate** may be of larger importance

$$\dot{\gamma} = \frac{d\gamma}{dt}$$

A constant stress in the liquid thus needs a constant strain rate such that

$$\sigma = \eta \dot{\gamma} \quad (\text{Newton's law of viscosity})$$

The response of an elastic or viscous material to stepwise introduced stress or strain is therefore different and helps to classify the mechanical material response.

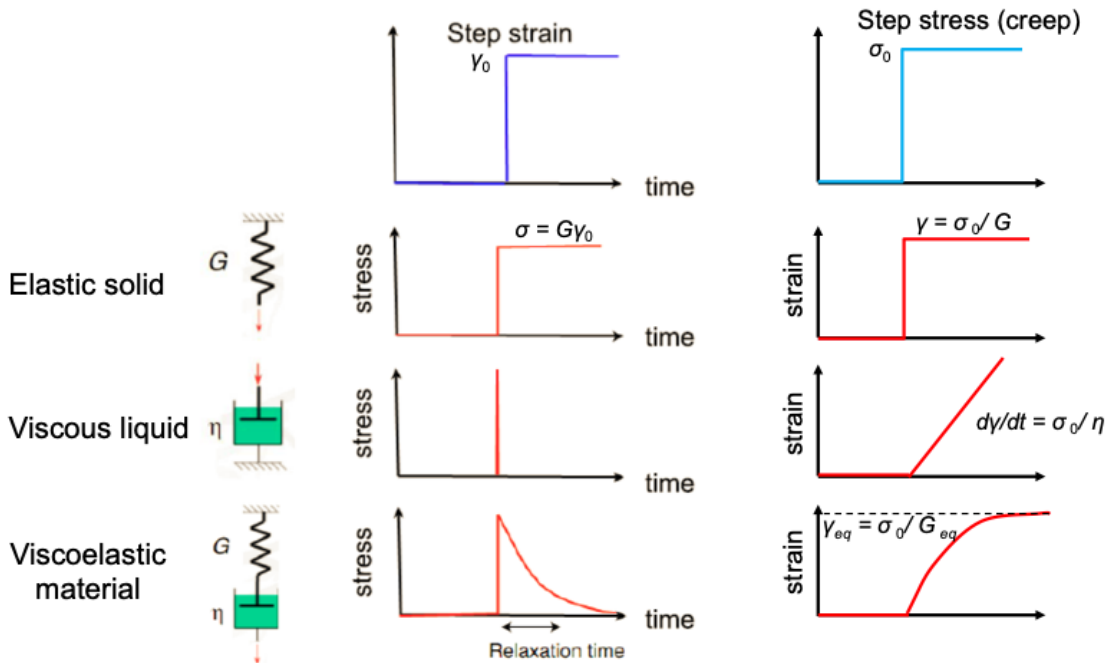


Figure 30.3: Response

According to this picture, and

- **elastic solid** responds with a step stress to a step strain, but also with a step strain to a step stress
- **viscous liquid** responds with a spike in the stress to a step strain and a linear strain to the step stress
- **viscoelastic material** responds with an (exponential) decay to a step strain and an (exponential) increase to a limiting value to a step stress

Viscoelastic materials are thus materials that exhibit both viscous and elastic responses under applied mechanical stress and strain. As these responses are time dependent, viscoelastic materials may show elastic behavior on short timescales but liquid on long timescales. Viscoelastic solids will always reach non-zero values for stress or strain after a certain amount of time, while for a viscoelastic material, the stress always decays to zero but the strain is able to grow without bounds.

30.1 Models for Viscoelastic behavior

30.2 Maxwell Model

A model for a viscoelastic liquid is the Maxwell model being a serial combination of a spring and a dashpot (viscous element).

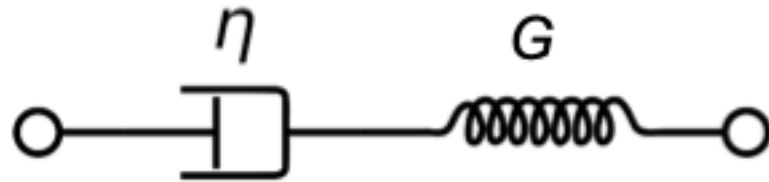


Figure 30.4: Maxwell

30.3 Kelvin-Voigt

The Kelvin-Voigt model is a parallel combination of both elements and can grasp some features of a viscoelastic solid. It can however not describe the behavior for step strain.

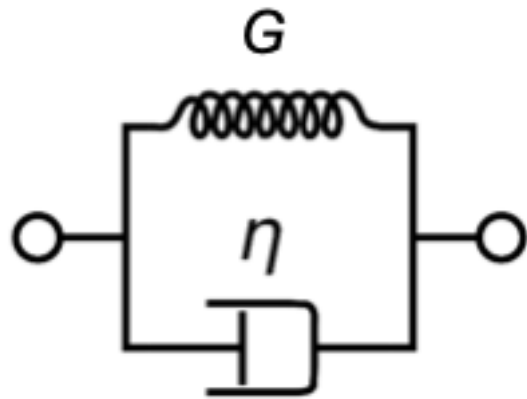


Figure 30.5: Kelvin-Voigt

30.4 Standard Model

A better model for viscoelastic solids is the standard linear solid model comprising three mechanical elements.

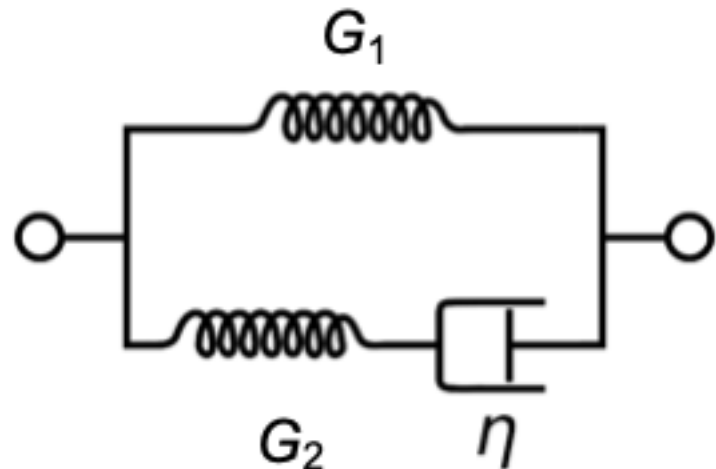


Figure 30.6: Standard

Part XXIII

Lecture 24

31 Viscoelasticity

```
import numpy as np
import matplotlib.pyplot as plt
from numpy.linalg import norm
from scipy.constants import c,epsilon_0,e,physical_constants
import json

%config InlineBackend.figure_format = 'retina'

with open('style.json', 'r') as fp:
    style = json.load(fp)

plt.rcParams.update(style)
```

31.1 Maxwell Model

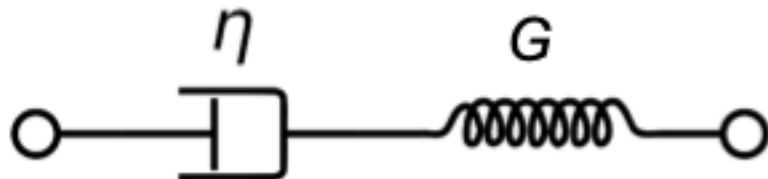


Figure 31.1: Maxwell

Combing back to the Maxwell model, we have a serial combination of viscous and elastic element. Thus both elements feel the same stress σ and the deformation is the sum of the elastic and viscous deformation, i.e. $\gamma = \gamma_e + \gamma_v$.

We therefore find

$$\sigma = G_M \gamma_e = \eta_M \frac{d\gamma}{dt}$$

or

$$\gamma_e = \frac{\eta_M}{G_M} \frac{d\gamma_v}{dt}$$

where η_M/G_M defines a timescale for the viscous relaxation. Such a timescale is always present in viscoelastic materials. In most materials even multiple timescales are relevant.

In the following sections we explore the response of a viscoelastic material to different perturbations. They can be either formed by a **step strain**, a **steady shear** or a **step stress or creep**.

31.2 Stress Relaxation after Step Strain

Here we impose a step strain γ at a time $t = 0$, such that the strain is constant for $t > 0$. Depending on the material we will get a different response. If we have for example an

- **elastic solid** will respond with a jump in the stress according to $G\gamma$ and the stress will stay constant as long as the strain is constant
- **Newtonian liquid** will respond with a stress spike that instantaneously decays to zero
- **viscoelastic system** will respond with some time dependent stress $\sigma(t)$

Due to the time dependence of the stress $\sigma(t)$ for a viscoelastic material we can generalize Hooke's law to

$$G(t) = \frac{\sigma(t)}{\gamma}$$

The plot shows the response of either a viscoelastic liquid or a viscoelastic solid. The latter comprise a general elastic part, which lets the stress converge for infinity time to some constant value

$$G_{\text{eq}} = \lim_{t \rightarrow \infty} G(t)$$

For viscoelastic liquids this residual stress is absent and the stress decays to zero.

```

fig=plt.figure()
plt.ion()
t=np.linspace(0,10,100)
plt.plot(t,np.exp(-t),label="ve-liquid")
plt.plot(t,0.8*np.exp(-t)+0.2,label="ve-solid")
plt.xlabel("time t")
plt.ylabel(r"stress $\sigma(t)$");plt.legend()
plt.tight_layout()
plt.savefig("img/tmp.png")
plt.close(fig)

```

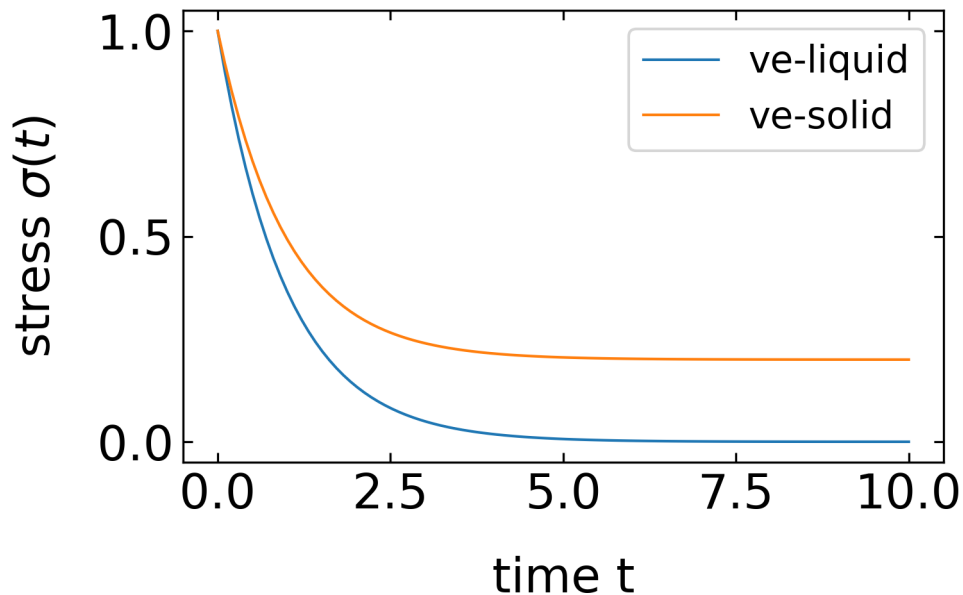


Figure 31.2: TMP

The Maxwell model, which is represented by a viscous dashpot element and an elastic spring represents such a viscoelastic liquid. The elastic strain thereby is

$$\gamma_e = \frac{\eta_M}{G_M} \frac{d\gamma_v}{dt} = \tau_M \frac{d\gamma_v}{dt}$$

Since the two elements are in series the elastic strain is also expressed by

$$\gamma_e = \gamma - \gamma_v(t)$$

Separation off variables leads to

$$\frac{d\gamma_v(t)}{\gamma - \gamma_v(t)} = \frac{dt}{\tau_M}$$

from which we obtain

$$\ln(\gamma - \gamma_v(t)) = \frac{-t}{\tau_M} + C$$

with $C = \ln(\gamma)$ based on the initial condition that $\gamma(t = 0) = \gamma$. As a result we obtain

$$\gamma_e(t) = \gamma - \gamma_v(t) = \gamma \exp\left(-\frac{t}{\tau_M}\right)$$

and for the stress

$$\sigma(t) = G_M \gamma_e(t) = G_M \gamma \exp\left(-\frac{t}{\tau_M}\right)$$

Thus in the Maxwell model, the stress relaxation has a simple exponential decay with the characteristic time constant τ_M . Such a characteristic time constant is characteristic for all viscoelastic materials. Many materials, e.g., polymers have multiple relaxation modes, each with its own time constant τ as we will see later. It turns out, that any stress relaxation modulus can be described by a series of Maxwell elements.

31.2.1 Boltzmann Superposition

The mechanical response of all materials has a region of linear response, where the relaxation modulus is independent of the strain. A manifestation of this linear response is the Boltzmann superposition principle.

Stress from any combination of small step strains is simply the linear combination of stresses resulting from each individual step.

If this individual strain step $\delta\gamma$ is applied at t_i , then the stress at a time t is given by

$$\sigma(t) = \sum_i G(t - t_i) \delta\gamma_i$$

This means that the stress of each individual step is independent of the other steps and the system remembers the deformations that were imposed earlier and continue to relax from earlier deformations as new ones are applied.

The stress relaxation modulus tells then how much stress remains at t past each deformation $\delta\gamma_i$ through $t - t_i$. With

$$\delta\gamma_i = \dot{\gamma}_i \delta t_i$$

we obtain

$$\sigma(t) = \sum_i G(t - t_i) \dot{\gamma}_i \delta t_i$$

or from a smooth history of strains

$$\sigma(t) = \int_{-\infty}^t G(t - t') \dot{\gamma}(t') dt'$$

which tells you that the stress in any material is the result of all past deformations, which is expressed by this convolution. The memory of each past deformation only decays as the relaxation modulus decay over the elapsed time $t - t'$

31.3 Steady Shear

We now switch to a different mode of mechanical perturbation of a material, which is the steady shear deformation. There we already considered the flow profile in the low Reynolds number section.

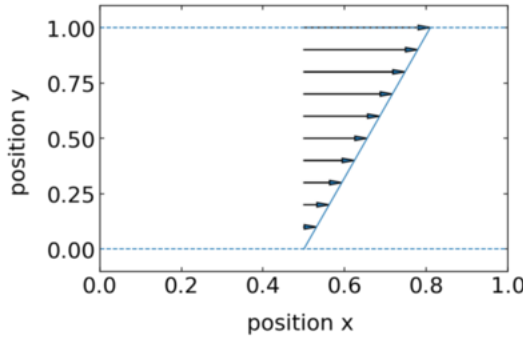


Figure 31.3: Flow

Here, the shear rate is given by the speed of the top surface $\dot{\gamma} = |\vec{v}|/h$, where h is the height of the film. According to our previous considerations the stress follows from

$$\sigma(t) = \dot{\gamma} \int_{-\infty}^t G(t-t')dt' \quad (31.1)$$

$$= \dot{\gamma} \int_0^\infty G(s)dt \quad (31.2)$$

with $s = t - t'$. With Newtons law of viscosity follows that

$$\eta = \int_0^\infty G(t)dt$$

Using the Maxwell model this means that the viscosity is

$$\eta = G \int_0^\infty \exp\left(-\frac{t}{\tau}\right) dt = G\tau = \eta_M$$

which is also the result for a viscoelastic liquid. If the modulus G is not constant, the viscosity can be also approximated by $\eta = G(\tau)\tau$.

For a viscoelastic solid, the moduls $G(t)$ does not decay to zero in time, but stays constant for long times. As a result the integral will diverge, as solids have an infinite viscosity.

If the shear rate becomes very large, the linear response approximation we have asummed for the Boltzmann superposition will not hold and we will observe non-linear effects. This leads for example to a **shear thinning** in polymeric liquids but also to a **shear thickening** for other materials such as the corn starch.

In these nonlinear regions, we can still define an apparent viscosity as the ration of shear stress divided by shear strain. The viscosity we commonly refer to is, however, the viscosity measured in the limit of $\gamma \ll \tau^{-1}$.

Note that all liquids display viscoelasticity even though the range where the viscosity is independent of the shear rate is very wide. For water, for example, the molecular relaxations are fast and the viscoelastic regimes starts at shear rates of about $10^{10} s^{-1}$

31.4 Creep and Creep Recovery

31.4.1 Creep

Another mechanical perturbation is the step stress that can be applied to watch the strain relax. This is called **creep** and switching of a constant stress is called **creep recovery**. For

the study of creep relaxation processes we define a new quantity, which is the inverse of the shear modulus. It is called the **shear creep compliance**

$$J(t) \equiv \frac{\gamma(t)}{\sigma} \quad (\text{Creep Compliance})$$

The relation of modulus and compliance is much like the relation of resistivity and conductivity. We can use again the Maxwell model to gain some insight. There the elastic element responds with an instantaneous strain

$$\gamma_e = \frac{\sigma}{G_M}$$

For the viscous element on the other hand we have

$$\frac{d\gamma_v(t)}{dt} = \frac{\sigma}{\eta_M}$$

which results in a linear growth of the viscous strain with time

$$\gamma_v(t) = \frac{\sigma}{\eta_M} t$$

The creep compliance in the Maxwell model is therefore

$$J(t) = \frac{\gamma_e + \gamma_v(t)}{\sigma} = \frac{1}{G_M} + \frac{t}{\eta_M}$$

which is overall linear in time. At time $t = 0$, the compliance is given by the elastic part $1/G_M$, while the slope at long times is given by $1/\eta$. For viscoelastic liquids we have in general

$$J(t) = J_{eq} + \frac{t}{\eta}$$

where J_{eq} corresponds to the energy stored in the elastic part of the liquid, but the compliance grows linearly with time. For a viscoelastic solid we know, however, that

$$J_{eq} = \lim_{t \rightarrow \infty} = \frac{1}{\sigma} \lim_{t \rightarrow \infty} \gamma(t) = \frac{1}{G_{eq}}$$

We can therefore use a different model to better describe a viscoelastic solid. This is done by the Kelvin Voigt model, where viscous and elastic part are connected in parallel.

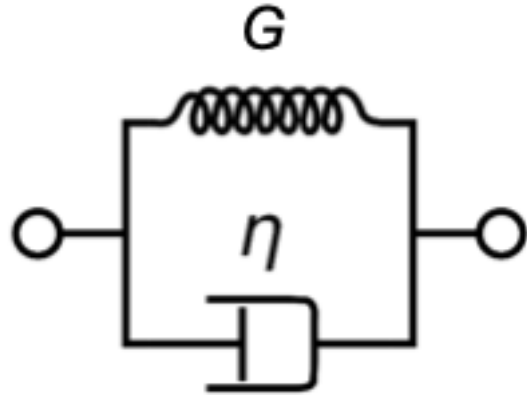


Figure 31.4: Kelvin Voigt

In this case the stresses add up

$$\sigma = \sigma_e(t) + \sigma_v(t) = G\gamma(t) + \eta \frac{d\gamma}{dt}$$

Separation of variables yields

$$\int_0^\gamma \frac{d\gamma(t)}{\frac{\sigma}{G} - \gamma(t)} = \frac{G}{\eta} \int_0^t dt$$

which results in the strain

$$\gamma(t) = \frac{\sigma}{G} (1 - \exp(-t/(\eta/G)))$$

which gives for the creep compliance

$$J(t) = \frac{\gamma(t)}{\sigma} = \frac{1}{G} (1 - \exp(-t/\tau))$$

with $J_{eq} = \lim_{t \rightarrow \infty} J(t)$.

```

fig=plt.figure()
plt.ion()
t=np.linspace(0,10,100)
plt.plot(t,0.2*(1-np.exp(-t)),label="ve-solid")
plt.plot(t,0.2*(1-np.exp(-t))+0.08*t,label="ve-liquid")
plt.ylim(0,1)
plt.xlabel("time t")
plt.ylabel(r"$J(t)$")
plt.legend()
plt.tight_layout()
plt.savefig("img/tmp1.png")
plt.close(fig)

```

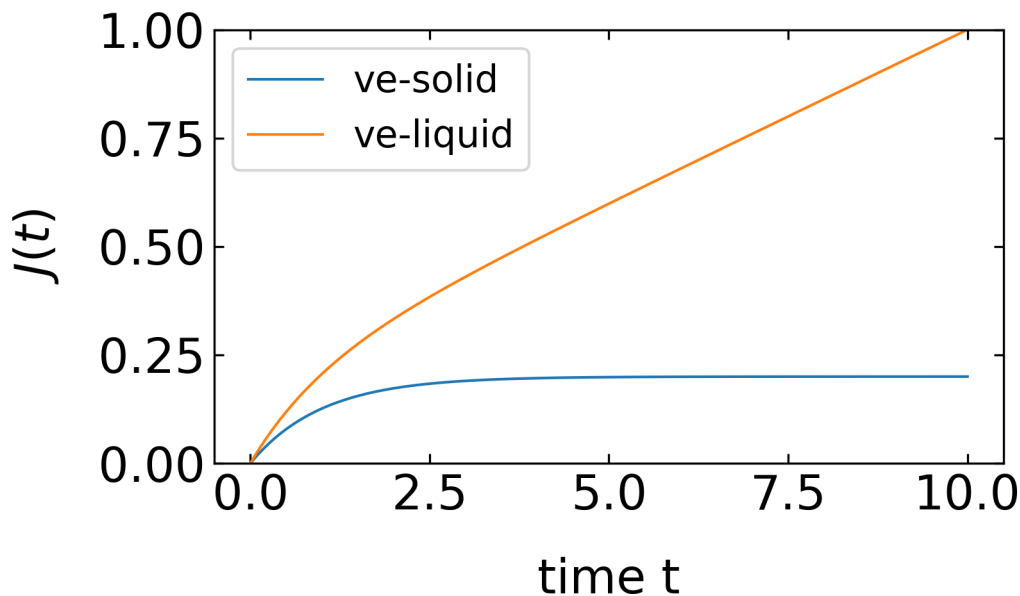


Figure 31.5: test

31.4.2 Creep Recovery

When switching off the stress, the viscoelastic material recovers and we get an elastic recoil. The recovery strain is defined as

$$\gamma_R = \gamma_0 - \gamma(t)$$

where the switch off happens at $t = 0$. The corresponding recovery compliance is then

$$J_R(t) \equiv \frac{\gamma_R(t)}{\sigma}$$

which directly gives

$$J_R(t) = J(t) - \frac{t}{\eta}$$

for a viscoelastic liquid. For a solid, the viscosity is infinite and we obtain

$$J_R(t) = J(t)$$

$$\lim_{t \rightarrow \infty} J_R(t) = \lim_{t \rightarrow \infty} \left[J(t) - \frac{t}{\eta} \right] = J_{eq}$$

31.5 Oscillatory Shear

All the previous consideration were done in the time domain with step-like perturbations. The step-like perturbation responses have an analog in the frequency domain, which is commonly measured by a type of “spectroscopy”, which is termed **rheology**. In rheology you apply an oscillating strain at a frequency ω , which can be written in the complex form as

$$\gamma(t) = \gamma_0 \exp(i\omega t)$$

For a pure elastic solid, the response is instantaneous and the stress reads:

$$\sigma(t) = G\gamma(t) = G\gamma_0 e^{i\omega t}$$

The stress is oscillating in phase with the strain. For a viscous liquid, however, the stress is related to the strain rate and thus

$$\sigma(t) = \eta \frac{d\gamma(t)}{dt} = i\omega \eta \gamma_0 e^{i\omega t}$$

we obtain an out of phase signal, a purely imaginary response, of the stress, which trails the strain as shown in the Figure below.

```
def gamma(t,omega,gamma0):
    return(gamma0*np.exp(1j*omega*t))
```

```
t=np.linspace(0,20,100)
g=gamma(t,1,1);G=1.5;eta=1;omega=1
fig=plt.figure(figsize=(10,4))
plt.ion()
plt.subplot(1,2,1)
plt.plot(t,np.real(g),'k-',label="strain")
plt.plot(t,np.real(g*G),'k--',label="stress")
plt.xlabel("time t")
plt.ylabel(r"stress $\sigma$,strain $\gamma$")
plt.legend()
plt.ylim(-2,2)

plt.subplot(1,2,2)
plt.plot(t,np.real(g),'k-',label="strain")
plt.plot(t,np.real(g*1j*omega*eta),'k--',label="stress")
plt.xlabel("time t")
plt.ylabel(r"stress $\sigma$,strain $\gamma$")
plt.legend()
plt.ylim(-2,2)
plt.tight_layout()
plt.savefig("img/tmp2.png")
plt.close(fig)
```

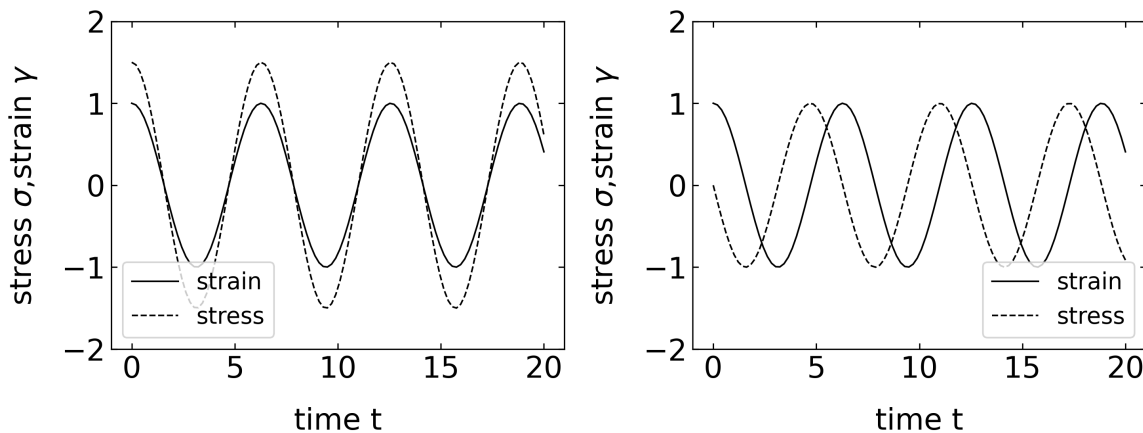


Figure 31.6: tmp

For a viscoelastic material, we have now both responses, which we can summarize in a complex modulus G . The real part is called the **storage modulus** and the imaginary part is called the **loss modulus**

$$G(\omega) = G'(\omega) + iG''(\omega)$$

Therefore, the time dependent stress is also a complex quantity and given by

$$\sigma(t) = \underbrace{G\gamma_0 e^{i\omega t}}_{\sigma_0} = \underbrace{G'\gamma_0 e^{i\omega t}}_{\text{Re } \sigma_0} + i \underbrace{G''\gamma_0 e^{i\omega t}}_{\text{Im } \sigma_0}$$

The phase angle δ is given by the ratio of imaginary and real part

$$\tan \delta = \frac{\text{Im } G}{\text{Re } G} = \frac{G''}{G'}$$

and the tangens of the phase angle is called the **loss tangent**.

$$P = \frac{dW}{dt} = \frac{Fdx}{dt} = \underbrace{\sigma F A}_{\text{F}} \frac{Ld\gamma}{dt}$$

$$\frac{P}{V} = \sigma \left(\frac{d\gamma}{dt} \right)$$

$$\frac{P}{V} = \frac{1}{2} \sigma_0 \left(\frac{d\gamma}{dt} \right)_0^* = \frac{1}{2} (G'\gamma_0 + iG''\gamma_0) (-i\omega\gamma_0) = \frac{1}{2} (\underbrace{G''}_{\substack{\text{active} \\ \text{power}}} - \underbrace{iG'}_{\substack{\text{reactive} \\ \text{power}}}) \gamma_0^2 \omega$$

The last part of the equation shows, that the imaginary part is responsible for the dissipation, while the real part adds some pseudo power much like the ac resistance in electronic circuitry.

31.5.1 Complex shear modulus of the Maxwell model

The elastic part in the Maxwell model is again given by

$$\gamma_e = \frac{\sigma}{G}$$

while the viscous part is determined by the following differential equation

$$\frac{d\gamma_v}{dt} = \frac{\sigma}{\eta} = \frac{\sigma_0}{\eta} e^{i\omega t}$$

which yields

$$\gamma_v = \frac{1}{i} \frac{\sigma_0}{\omega\eta} e^{i\omega t} = -i \frac{\sigma}{\omega\eta}$$

or

$$\sigma = i\omega\eta\gamma_v$$

Thus inserting both in the total strain

$$\underbrace{\gamma_0 e^{i\omega t}}_{\gamma} = \underbrace{\frac{\sigma_0}{G} e^{i\omega t}}_{\gamma_e} - i \underbrace{\frac{\sigma_0}{\omega\eta} e^{i\omega t}}_{\gamma_v}$$

from which we can read the complex modulus

$$G^* = \frac{\sigma_0}{\gamma_0} = \frac{1}{1/G - i/(\omega\eta)} = \frac{\omega\eta}{\omega\eta/G - i} = \frac{\omega\eta(\omega\eta/G + i)}{(\omega\eta/G)^2 + 1} \quad (31.3)$$

$$= \underbrace{G \frac{1}{1 + 1/(\omega\tau)^2}}_{G'} + i \underbrace{G \frac{\omega\tau}{(\omega\tau)^2 + 1}}_{G''} \quad (31.4)$$

The plot below shows the frequency dependence of the real and imaginary part of the modulus for the Maxwell model. The imaginary part has the shape of a Lorentzian, which is corresponding to the Fourier transform of an exponential in the time domain. The wings of G'' increase or decay with ω , while the real part G' shows a steeper increase with ω^2 until it saturates. The saturation and the peak occur at the characteristic timescale $\tau = \eta/G$, indicated by the vertical dashed line.

```

def G(omega,eta,Gm):
    return(1/(1/Gm-1j/(omega*eta)))

om=np.linspace(0.01,100,1000)
fig=plt.figure()
plt.ion()
plt.loglog(om,np.real(G(om,1,1)),lw=2,label=r"$G'{}$")
plt.loglog(om,np.imag(G(om,1,1)),lw=2,label=r"$G''{}$")
plt.axvline(x=1,color='k',ls='--')
plt.xlabel(r"$\omega$")
plt.ylabel(r"$G'{}$, $G''{}$")
plt.legend()
plt.tight_layout()
plt.savefig("img/tmp3.png")
plt.close(fig)

```

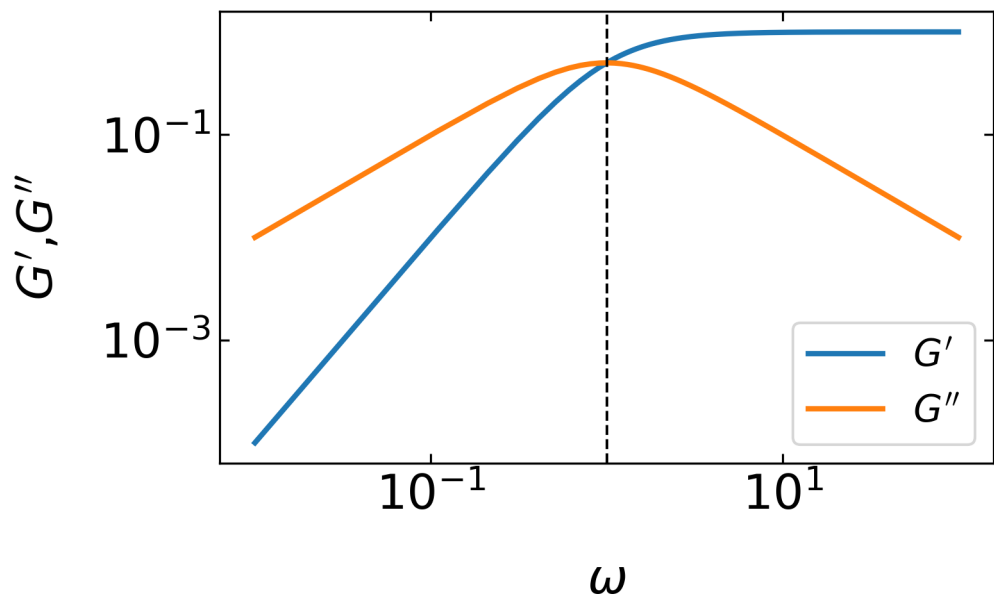


Figure 31.7: tmp3

31.5.2 Complex shear modulus of the Kelvin-Voigt model

$$\underbrace{\sigma_0 e^{i\omega t}}_{\sigma} = \sigma_e + \sigma_v = G\gamma + \eta \frac{d\gamma}{dt} = G\gamma_0 e^{i\omega t} + i\omega\eta\gamma_0 e^{i\omega t}$$

$$G^* = \frac{\sigma_0}{\gamma_0} = G + i\omega\eta = \underbrace{G}_{G'} + i\underbrace{\frac{G\omega\tau}{G''}}_{G''}$$

(Complex modulus Kelvin-Voigt model)

Part XXIV

Lecture 25

32 Dynamics of Polymers

```
import numpy as np
import matplotlib.pyplot as plt
from numpy.linalg import norm
from scipy.constants import c,epsilon_0,e,physical_constants
import json

%config InlineBackend.figure_format = 'retina'

with open('style.json', 'r') as fp:
    style = json.load(fp)

plt.rcParams.update(style)
```

After we have introduced a phenomenological model for the viscoelasticity of materials, we would like to connect this to the dynamics of polymers. This means, that we have to connect the response of a polymer to deformations to the polymer chain in a way.

32.1 Diffusion of a Single Polymer Chain

A first clue on the dynamics is already given by a process of the diffusion of the polymer chain. During diffusion, all segments fluctuate with the position and experience hydrodynamic friction. If the molecule would be a rigid sphere of radius R , the diffusion coefficient would be given by the Stokes-Einstein relation

$$D = \frac{k_B T}{\gamma} = \frac{k_B T}{6\pi\eta R}.$$

Using the mean-squared displacement $\langle r^2 \rangle = 6Dt$, this also means that the particle will diffuse a distance corresponding to its own size in a time

$$\tau = \frac{R^2}{D} = \frac{R^2}{k_B T} \gamma.$$

For a polymer, which is now a flexible entity, this time means that all conformational fluctuations have relaxed at this time and the polymer chain is displaced by its own radius. This, therefore, sets the longest timescale of relaxation. This relaxation timescale can now be obtained with different dynamic approaches, which are the **Rouse model** and the **Zimm model**. Both models differ mainly in how the hydrodynamic coupling of individual segments are considered.

32.1.1 Rouse Model

In the Rouse model, the polymer is approximated by a bead-spring model (Gaussian chain) of N segments:

$$\gamma \frac{d\vec{R}_n}{dt} = k [\vec{R}_{n-1} - \vec{R}_n + \vec{R}_{n+1} - \vec{R}_n] + \vec{f}_n(t),$$

where the force on the segment n at a position \vec{R}_n is given by the forces exerted from the neighboring elements with a spring constant $k = 3k_B T/b^2$ and the thermal noise force $\vec{f}_n(t)$.

Each of the segments is experiencing a friction given by the factor γ . The total friction on the Rouse chain is now assumed to be

$$\gamma_R = N\gamma$$

which needs some short explanation, as this is one key assumption of the Rouse model. Imagine you have 5 different rigid spheres each experiencing the same friction coefficient and they are far apart from each other. The total friction coefficient will be 5γ . Yet if the spheres come closer to each other, the hydrodynamic flow fields around each sphere influence each other until the point when they are in close contact and act as a new body. In this case, the friction coefficient will not be just the sum of all friction coefficients. This means, that the assumption of the Rouse model is now that the individual beads cause only localized flow fields when fluctuating, which are, in turn, not influencing the motion of the other segments.

According to that, we may write down the time to diffuse the size R of the polymer as

$$\tau_R = \frac{R^2}{k_B T} N\gamma$$

which is the Rouse time. At times shorter than the Rouse time, the polymer exhibits viscoelastic relaxation modes. The longest relaxation mode is that of the whole chain, which is the Rouse time τ_R . As the size of the polymer chain is approximately given by $R \approx bN^\nu$ with ν being the fractal dimension (e.g., the Flory exponent) of the chain we obtain for the Rouse time

$$\tau_R = N \underbrace{\frac{\gamma}{k_B T}}_{\tau_0} b^2 N^{2\nu} = \tau_0 N^{2\nu+1},$$

where τ_0 is the relaxation time for a single segment in the chain. Depending if we now consider an ideal or a real chain, we find different scaling of the Rouse time with the number of segments, i.e.:

$$\tau_R \propto \begin{cases} \tau_0 N^2 & \text{for ideal chain } (\nu = 1/2) \\ \tau_0 N^{11/5} & \text{for real chain in good solvent } (\nu \approx 3/5) \end{cases}$$

which is just a simple estimate.

The full calculation by Rouse for an ideal chain shows a similar result, which is

$$\tau_R = \frac{1}{6\pi^2} \frac{\gamma b^2}{k_B T} N^2.$$

To summarize, on time scales smaller than τ_R , we expect to find **viscoelastic modes** of the polymer contributing to the modulus, while for modes larger than τ_R everything should be **diffusive**.

32.1.2 Zimm Model

The Zimm model takes care of the fact that each segment is generating a flow field that decays as $1/r$ and is thus typically long range. Thus segments in the chain volume (the so-called pervaded volume) are coupled by hydrodynamics in solution. This has to be taken into account for the dynamics of the polymer chain and the fact that the Rouse model neglects that restricts its validity essentially to the melt region (a system of polymer chains without solvent) only.

This hydrodynamic coupling in the Zimm model changes the friction coefficient of the chain to

$$\gamma_Z \approx \eta R$$

with R being the root-mean-squared end-to-end distance of the polymer chain as used also in the Rouse model. Thus the Zimm chain behaves hydrodynamically more like a solid sphere rather than a collection of individual beads.

With $R = bN^\nu$ we find for the Zimm relaxation time

$$\tau_Z \approx \frac{R^2}{D_Z} \approx \frac{\gamma_Z}{k_B T} R^2 \approx \frac{\eta}{k_B T} R^3 \approx \frac{\eta b^3}{k_B T} N^{3\nu} = \tau_0 N^{3\nu}$$

while the full calculation by Zimm shows

$$\tau_Z = \frac{1}{2\sqrt{3\pi}} \frac{\eta}{k_B T} R^3. \quad (\text{Zimm time})$$

Using the exponents ν for the ideal and the real chains, we can now make predictions for the scaling of the Zimm relaxation time for both chains, which gives

$$\tau_Z \propto \begin{cases} \tau_0 N^{3/2} & \text{for ideal chain } (\nu = 1/2) \\ \tau_0 N^{9/5} & \text{for real chain in good solvent } (\nu = 3/5) \end{cases}.$$

Thus, the scaling of relaxation times as predicted by the Zimm and the Rouse model are different. Which regime is valid has to be decided based on experimental results. As mentioned before, the Zimm model is rather valid for dilute polymer solutions, while the Rouse model rather applies to the dynamics of polymer chains in the melt.

32.2 Intrinsic viscosity of polymer solutions

In dilute solutions, polymer chains are isolated and deformed in an affine way. In such solutions, polymers linearly increase the viscosity of the solution with increasing concentration. To study the contribution of the polymer chains to the viscosity of the solution we define a specific viscosity

$$\eta_{sp} = \frac{\eta - \eta_s}{\eta_s},$$

where η is the viscosity of the solvent with polymers and η_s is the one of the solvent only. One may also write the same expression as $\eta_{sp} = \eta_r - 1$ where $\eta_r = \eta/\eta_s$ is the reduced viscosity. The contribution of a single polymer chain is then measured by the intrinsic viscosity

$$[\eta] = \lim_{c \rightarrow 0} \frac{\eta_{sp}}{c},$$

where c is the polymer concentration. Note that the intrinsic viscosity now has the unit of an inverse concentration. Using this intrinsic value we may connect now the viscosity to the shear modulus, e.g., by using the result of the Maxwell model:

$$\eta \approx G(\tau) \int \exp(-t/\tau) dt = G(\tau)\tau.$$

32.2.1 Affine Deformation and Entropy

To include the polymer in the shear viscosity, we have to consider an affine deformation of the chain.

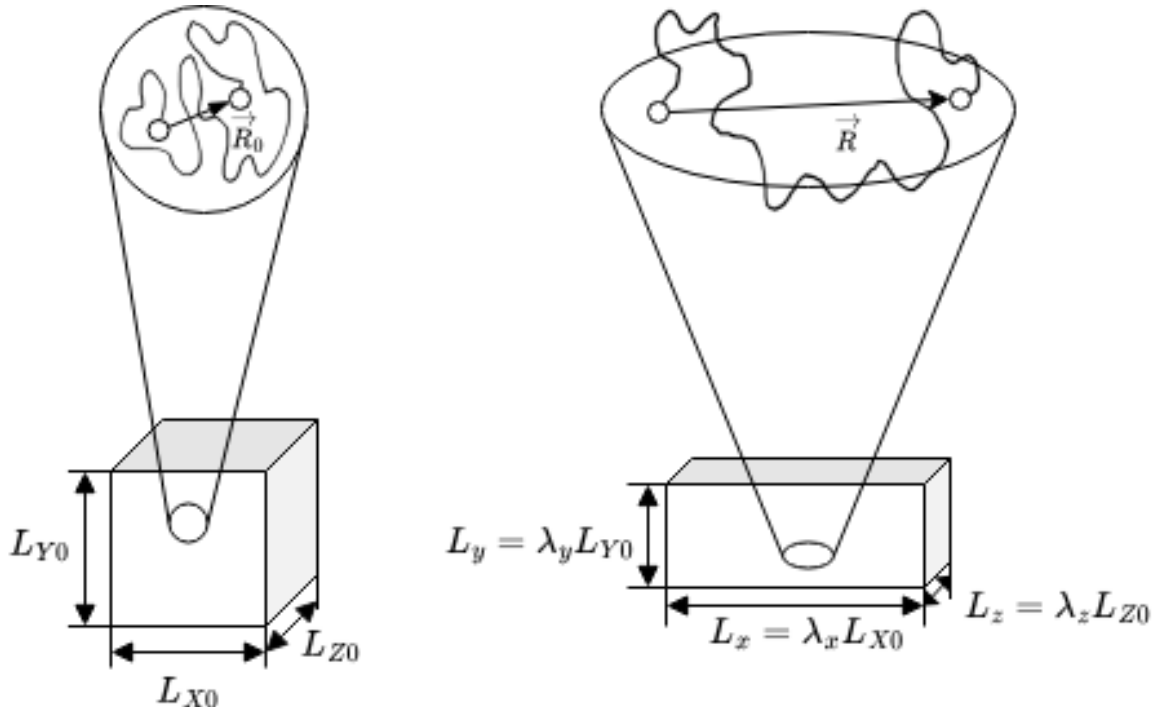


Figure 32.1: affine deformation of chain

As we have discussed earlier, the entropy of a single chain with an end-to-end distance R can be calculated from

$$\begin{aligned} S(R) &= k_B \ln(p(\vec{R}, N)) + \text{const} \\ &= -\frac{3}{2} \frac{k_B R^2}{Nb^2} + \text{const.} \end{aligned}$$

In our lab system the end-to-end vector length R^2 can be expressed by its components such that

$$S(R) = -\frac{3}{2} \frac{k_B(R_x^2 + R_y^2 + R_z^2)}{Nb^2} + \text{const.}$$

If we now introduce a deformation

$$L_x = \lambda_x L_{X0}, L_y = \lambda_y L_{Y0}, L_z = \lambda_z L_{Z0}$$

where the λ are just scaling factors for the volume, we can also assume that the components of the end-to-end vector scale in the same way, i.e.

$$R_x = \lambda_x R_{X0}, R_y = \lambda_y R_{Y0}, R_z = \lambda_z R_{Z0}$$

such that we obtain for the change in entropy upon deformation

$$\Delta S = S(R) - S(R_0) = \frac{3}{2} \frac{k_B}{Nb^2} [(\lambda_x^2 - 1)R_{X0}^2 + (\lambda_y^2 - 1)R_{Y0}^2 + (\lambda_z^2 - 1)R_{Z0}^2]$$

If we have now a system of n -chains in the solution, we have to sum up all squared components of the end-to-end distance

$$\sum_{i=1}^n (R_{X0})_i^2 = n \frac{1}{n} \sum_{i=1}^n (R_{X0})_i^2 = n \langle R_{X0}^2 \rangle = n \frac{Nb^2}{3}$$

using our previous result for the mean squared end-to-end distance. This finally results in

$$\Delta S = -\frac{nk_B}{2} (\lambda_x^2 + \lambda_y^2 + \lambda_z^2 - 3)$$

for the entropy change of all chains. The results lets us calculate the change in free energy $\Delta F = -T\Delta S$, which is

$$\Delta F = -\frac{nk_B T}{2} (\lambda_x^2 + \lambda_y^2 + \lambda_z^2 - 3)$$

If we assume now that the volume is unchanged upon deformation, i.e. $V = \lambda_x \lambda_y \lambda_z V_0$ or $\lambda_x \lambda_y \lambda_z = 1$, we can express a uniaxial deformation along the x-axis as

$$\lambda_x = \lambda, \lambda_y = \lambda_z = \frac{1}{\sqrt{\lambda}}$$

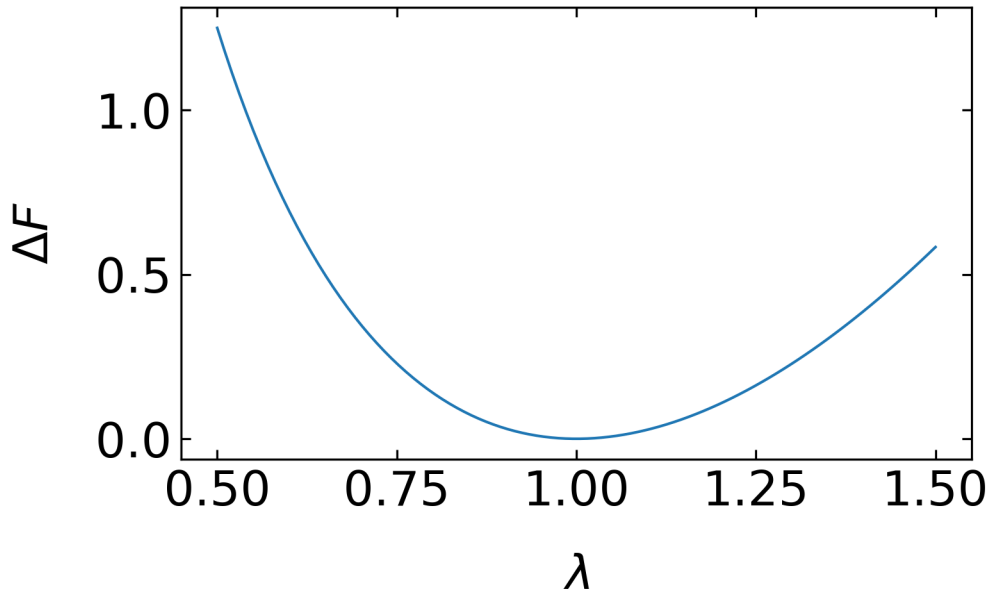
from which we obtain for the deformation

$$\Delta F = \frac{nk_B T}{2} \left(\lambda^2 + \frac{2}{\lambda} - 3 \right)$$

```
def free_energy(lam):
    return(lam**2+2/lam-3)

l=np.linspace(0.5,1.5,100)

fig=plt.figure()
plt.ion()
plt.plot(l,free_energy(l))
plt.xlabel(r"\lambda")
plt.ylabel(r"\Delta F")
plt.tight_layout()
plt.savefig("img/test.png")
plt.close(fig)
```



The corresponding force that has to be applied to stretch the molecules can be calculated from the derivative

$$\begin{aligned} f_x &= \frac{\partial \Delta F}{\partial L_x} = \frac{\partial \Delta F}{\partial \lambda L_{x0}} = \frac{1}{L_{x0}} \frac{\partial \Delta F}{\partial \lambda} \\ &= \frac{n K_B T}{L_{x0}} \left(\lambda - \frac{1}{\lambda^2} \right) \end{aligned}$$

which results in a stress

$$\begin{aligned} \sigma_{xx} &= \frac{f_x}{L_y L_z} = \frac{n K_B T}{L_{x0} L_y L_z} \\ &= \frac{n k_B T}{L_{x0} L_{y0} L_{z0}} \lambda \left(\lambda - \frac{1}{\lambda^2} \right) \\ &= \frac{n}{V} k_B T \left(\lambda^2 - \frac{1}{\lambda} \right) \end{aligned}$$

As the stress is in general the result of a modulus G multiplied with a deformation and the term with the λ denotes the deformation, we have found the modulus to be

$$G = \frac{n}{V} k_B T = \frac{\rho R_M T}{M_s}$$

where R_M is gas constant, ρ the density and M_s the molar mass of a single strand. The stress is this

$$\sigma = G \left(\lambda^2 - \frac{1}{\lambda} \right)$$

Returning to our calculation of the contribution of the polymer chain to the intrinsic viscosity we may write

$$[\eta] = \frac{1}{c} \frac{\eta - \eta_s}{\eta_s} = \frac{1}{c} \frac{G(\tau) \tau}{\eta_s}$$

with

$$G(\tau) = \frac{\rho R_M T}{M_s} = \frac{\rho N_A k_B T}{N M_b}$$

with M_b being the molar mass of the monomer (Kuhn segment). The intrinsic viscosity is therefore

$$[\eta] = \frac{N_A k_B T}{\eta_s N M_b} \tau$$

With the result of Rouse for the Rouse time

$$\tau_R = \frac{1}{6\pi^2} \frac{\gamma b^2}{k_B T} N^{2\nu+1} = N \frac{\eta_s b}{k_B T} b^2 N^{2\nu} \frac{1}{6\pi^2}$$

we find for the **intrinsic viscosity of a Rouse chain**

$$[\eta]_R \approx \frac{N_A b^3}{M_b} N^{2\nu} \propto \begin{cases} N, & \text{ideal chain} \\ N^{6/5}, & \text{real chain in good solvent} \end{cases}$$

A similar calculation can be done using the Zimm relaxation time

$$\tau_Z \approx \frac{\eta b^3}{k_B T} N^{3\nu}$$

which gives for the **intrinsic viscosity of a Zimm chain**

$$[\eta]_Z \approx \frac{N_A b^3}{M_b} N^{3\nu-1} \propto \begin{cases} N^{1/2}, & \text{ideal chain} \\ N^{4/5}, & \text{real chain in good solvent} \end{cases}$$

A more general expression for the intrinsic viscosity of a dilute polymer solution is the **Fox Flory law**

$$[\eta] = \Phi \frac{R^3}{M}$$

with $\Phi = 0.425 N_A \approx 2.5 \times 10^{23} \text{ mol}^{-1}$.

plot some experimental data

32.3 Relaxation Modes of a Polymer

Polymers are self-similar objects, which means that shorter parts of a polymer behave like shorter chains. Thus there must be a spectrum of relaxation modes present for a polymer chain and we considered in the section before just the longest one.

If there are N segments, the

- there are N modes index by $p = 1 \dots N$
- shortest mode $p = N$ with τ_0
- largest mode $p = 1$ with τ_R

32.3.1 Rouse modes

In the Rouse model, we therefore have the Rouse time

$$\tau = \tau_R \approx \tau_0 N^2$$

and for the individual model

$$\tau_p \approx \tau_0 \left(\frac{N}{p} \right)^2 \text{ for } p = 1, 2, \dots, N$$

or

$$p \approx \left(\frac{\tau_p}{\tau_0} \right)^{1/2} N$$

Each of these modes relaxes independently.

On a timescale $\tau = \tau_0$ all of the N modes have not relaxed. At $\tau = \tau_p$ $N - p$ modes have not decayed. Each of these modes contributes $k_B T$ to the energy density as we have seen before. With $N - p$ modes deviated, there is $p k_B T$ still stored in the deformation of the chain. Thus the modulus amplitude for each mode is found to be

$$G(\tau_P) \approx \frac{n}{V} k_B T p$$

and the modulus itself

$$G(t) \approx \frac{n}{V} k_B T \sum_{p=1}^N \exp \left(-\frac{t}{\tau_p} \right)$$

with

$$\tau_p = \frac{\tau_0}{6\pi^2} \frac{N^2}{p^2}$$

For large N we may convert the sum into an integral and obtain for the modulus

$$G(t) = n_p k_B T \int_0^\infty dp \exp(-p^2 t / \tau_R) = \frac{\sqrt{\pi}}{2} n_p k_B T \left(\frac{\tau_R}{t} \right)^{1/2}$$

which gives an inverse square root dependence for the modulus with time. This is valid only for short times, as the chain has a longest relaxation, which is the Rouse time. Including this cut-off at long times we may write

$$G(t) \approx \underbrace{\frac{nNk_B T}{v} \frac{t}{\tau_0}^{-1/2}}_{\tau_0 < t < \tau_R} \underbrace{\exp\left(-\frac{t}{\tau_R}\right)}_{t > \tau_R}$$

```
fig=plt.figure()
t=np.linspace(0.01,100000,1000)
t0=1;N=100;tR=t0*N**2
plt.loglog(t/tR,1/np.sqrt(t/t0)*np.exp(-t/tR))
plt.xlabel(r"$t/\tau_R$")
plt.ylabel(r"$G(t)$")
plt.axvline(x=1,color="k",ls='--')
plt.tight_layout()
plt.savefig("img/tmp4.png")
plt.close(fig)
```

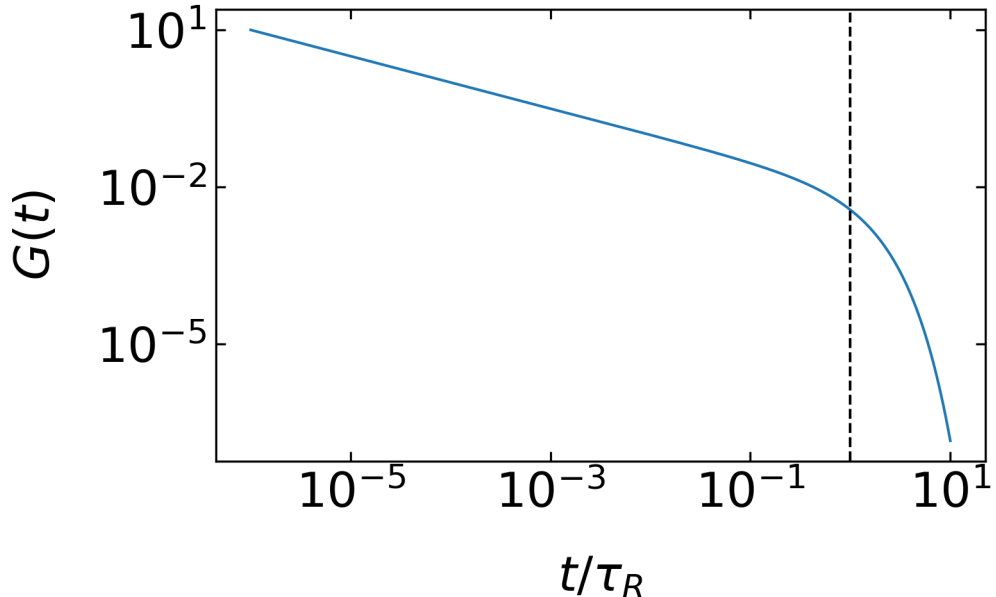


Figure 32.2: tmp4

32.3.1.1 Shear modulus with oscillating deformation

With the calculations done above we may now also determine the frequency dependence of the shear modulus. Both can be obtained by Fourier transforming the time dependent modulus. The storage modulus $G'(\omega)$

$$G'(\omega) = G_{eq} + \omega \int_0^\infty [G(t) - G_e q] \sin(\omega t) dt$$

which gives

$$G'(\omega) \approx \frac{nk_B T}{V} \frac{(\omega \tau_R)^2}{\sqrt{[1 + (\omega \tau_R)^2] \left[\sqrt{1 + (\omega \tau_R)^2} + 1 \right]}} \text{ for } \omega < 1/\tau_0$$

The loss modulus is found by

$$G''(\omega) = \omega \int_0^\infty [G(t) - G_e q] \cos(\omega t) dt$$

resulting in

$$G''(\omega) \approx \frac{n}{V} k_B T \omega \tau_R \sqrt{\frac{\sqrt{1 + (\omega \tau_R)^2} + 1}{1 + (\omega \tau_R)^2}} \text{ for } \omega < 1/\tau_0$$

According to that both the storage and the loss modulus scale in the range $\frac{1}{\tau_R} < \omega < \frac{1}{\tau_0}$ as $G' \propto G'' \propto \omega^{1/2}$, while for $\omega < \frac{1}{\tau_R}$ the storage modulus scales as $G' \sim \omega^2$.

frequency dependence here

```
def rouse_gp(omega,tauR):
    otr=(omega*tauR)**2
    return(otr/np.sqrt((1+otr)*(np.sqrt(1+otr)+1)) )

def rouse_gpp(omega,tauR):
    otr=(omega*tauR)**2
    return(np.sqrt(otr)*np.sqrt((np.sqrt(1+otr)+1)/(1+otr)))
```

```

fig=plt.figure()
plt.ion()
omega=np.linspace(0.001,100,100000)
tauR=10
plt.loglog(omega*tauR,rouse_gp(omega,tauR),label=r"$G^{\prime}$")
plt.loglog(omega*tauR,rouse_gpp(omega,tauR),label=r"$G^{\prime\prime}$")
#plt.loglog(omega*tauR,(omega*tauR)**0.5)
plt.axvline(x=1,color="k",ls="--")
plt.xlabel(r"$\omega \tau_R$")
plt.ylabel(r"$G^{\prime}(\omega), G^{\prime\prime}(\omega)$")
plt.legend()
plt.tight_layout()
plt.savefig("img/tmp6.png")
plt.close(fig)

```

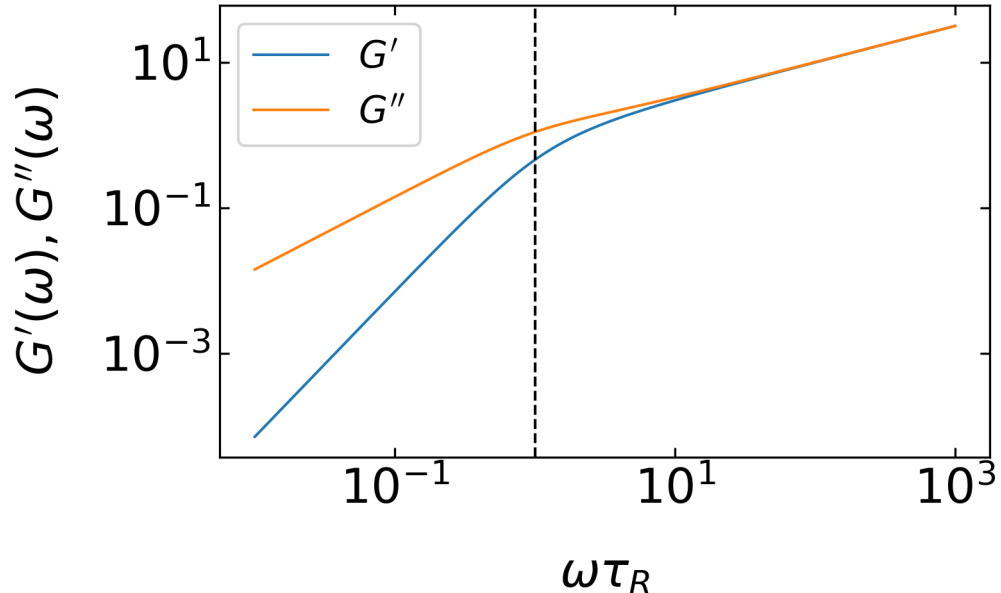


Figure 32.3: tmp6

The viscosity of a dilute Rouse polymer solution is obtained by integrating the time dependent modulus

$$\eta = \int_0^\infty G(t) dt \approx \frac{k_B T}{V} n N \int_0^\infty \left(\frac{t}{\tau_0} \right)^{-1/2} \exp \left(-\frac{t}{\tau_R} \right) dt$$

add part on the diffusion coefficient

32.3.2 Zimm modes

The same calculation as for the Rouse model can be done for the Zimm modes as well. The relaxation times for the Zimm model scale as

$$\tau_p = \tau_0 \left(\frac{N}{p} \right)^{3\nu}$$

and we obtain for the mode index

$$p \approx N \left(\frac{\tau_p}{\tau_0} \right)^{-1/3\nu} = N \left(\frac{t}{\tau_0} \right)^{-1/3\nu}$$

where we make a transition from the mode relaxation times $\tau_p \rightarrow t$. This then leads to the time dependent stress modulus

$$G(t) \approx \underbrace{\frac{n}{V} N k_B T \left(\frac{\tau_0}{t} \right)^{1/3\nu}}_{\tau_0 < t < \tau_Z} \underbrace{\exp \left(-\frac{t}{\tau_Z} \right)}_{t > \tau_Z}$$

```
fig=plt.figure()
t=np.linspace(0.01,10000,1000)
nu=1/2;t0=1;N=100;tZ=t0*N**(3*nu)
plt.loglog(t/tZ,(t0/t)**(1/(3*nu))*np.exp(-t/tZ))
plt.xlabel(r"$t/\tau_Z$")
plt.ylabel(r"$G(t)$")
plt.axvline(x=1,color='k',ls='--')
plt.tight_layout()
plt.savefig("img/tmp5.png")
plt.close(fig)
```

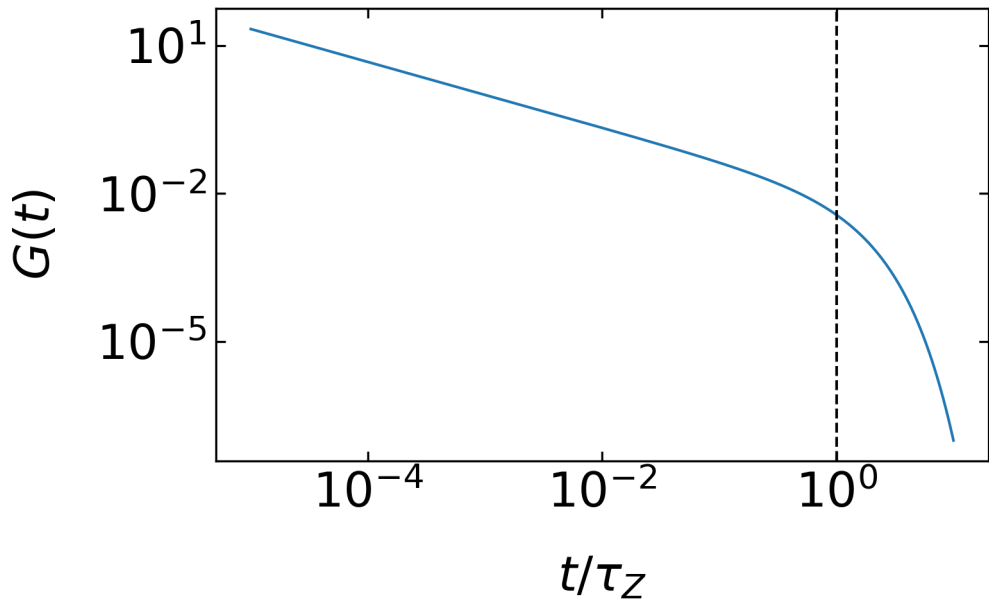


Figure 32.4: tmp5

32.3.2.1 Shear modulus with oscillating deformation

Using this result we may now also obtained the frequency dependent storage and loss modulus of the Zimm chains.

storage modulus

$$G' \approx \frac{n}{V} k_B T \frac{\omega \tau_Z \sin \left[\left(1 - \frac{1}{3\nu}\right) \arctan(\omega \tau_Z) \right]}{\left[1 + (\omega \tau_Z)^2\right]^{(1-1/3\nu)/2}}$$

loss modulus

$$G'' \approx \frac{n}{V} k_B T \frac{\omega \tau_Z \cos \left[\left(1 - \frac{1}{3\nu}\right) \arctan(\omega \tau_Z) \right]}{\left[1 + (\omega \tau_Z)^2\right]^{(1-1/3\nu)/2}}$$

```
def zimm_gp(omega, tauZ, nu):
    otz=(omega*tauZ)
    return(otz*np.sin((1-1/3/nu)*np.arctan(otz))/(1+otz**2)**((1-1/3/nu)/2))

def zimm_gpp(omega, tauZ, nu):
```

```

otz=(omega*tauZ)
return( otz*np.cos((1-1/3/nu)*np.arctan(otz))/(1+otz**2)**((1-1/3/nu)/2))

```

```

fig=plt.figure()
plt.ion()
omega=np.linspace(0.001,100,100000)
tauZ=10
nu=0.5
plt.loglog(omega*tauZ,zimm_gp(omega,tauZ,nu),label=r"$G^{\prime}(\omega)$")
plt.loglog(omega*tauZ,zimm_gpp(omega,tauZ,nu),label=r"$G''(\omega)$")
#plt.loglog(omega*tauR,(omega*tauR))
plt.axvline(x=1,color="k",ls="--")
plt.xlabel(r"$\omega \tau_Z$")
plt.ylabel(r"$G^{\prime}(\omega), G''(\omega)$")
plt.legend()
plt.tight_layout()
plt.savefig("img/tmp7.png")
plt.close(fig)

```

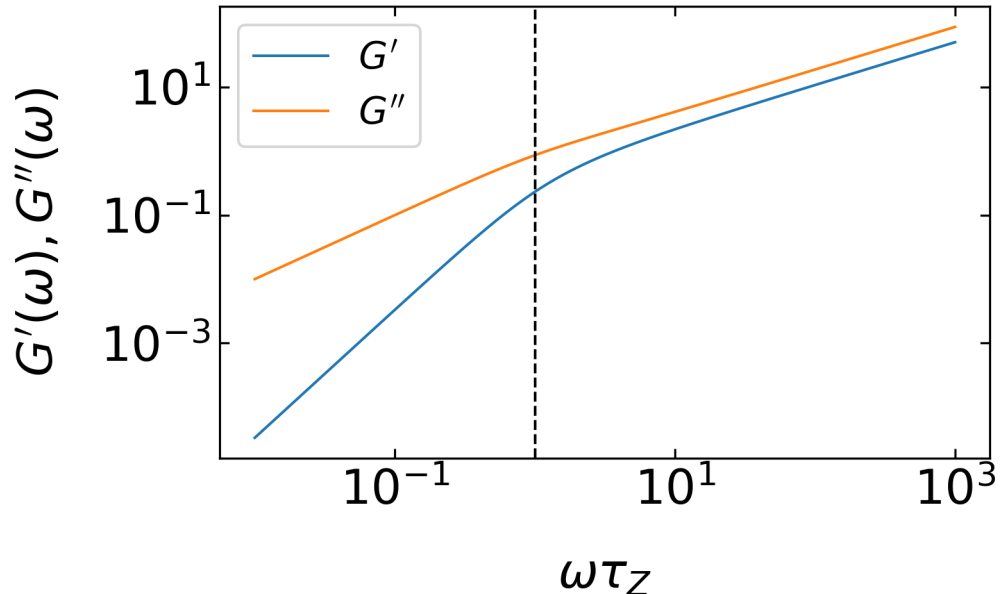


Figure 32.5: tmp7

The viscosity contribution of solution of Zimm chains is then

$$\eta - \eta_s = \int_0^\infty G(t) dt \approx \eta_s \frac{n}{V} N b^3 N^{3\nu-1}$$

We can summarize

- The **Zimm limit** applies to dilute solutions, where the solvent within the pervaded volume of the polymer is hydrodynamically coupled to the polymer. Polymer dynamics are described by the Zimm model in dilute solutions.
- The **Rouse limit** applies to unentangled polymer melts because hydrodynamic interactions are screened in melts (just as excluded volume interactions are screened in melts). Polymer dynamics in the melt state (with no solvent) are described by the Rouse model, for short chains that are not entangled.

Part XXV

Lecture 26

33 Semidilute Polymer Solutions

```
import numpy as np
import matplotlib.pyplot as plt
from numpy.linalg import norm
from scipy.constants import c,epsilon_0,e,k,physical_constants
import json

%config InlineBackend.figure_format = 'retina'

with open('style.json', 'r') as fp:
    style = json.load(fp)

plt.rcParams.update(style)
```

The properties of polymer solutions change when you increase the density of the solution. In the case of dilute solutions, we have already seen that the viscosity changes linearly with the concentration of the polymer. When the chains start to overlap, the neighboring chains impose constraints which influence the relaxation of the chains upon deformation.

To identify, when such a semi-dilute regime is reached, we can have a look at the volume fraction

$$\phi = \frac{nVb^3}{V}$$

where n is the number of polymer chains, V is the sample volume and N is the number of Kuhn segments of length b . If we have now polymer chains of a size R (end-to-end distance), with a volume of R^3 we can then fill our sample volume space filling with n chains such that the sample volume $V = nR^3$. This results in a concentration that is given by

$$\phi^* \approx \frac{Nb^3}{R^3}$$

which is the overlap concentration indicating that the chains start to overlap at this concentration. Since the size R of the chain can be now expressed by

$$R \approx b \left(\frac{v}{b^3} \right)^{2\nu-1} N^\nu$$

according to our consideration of the Flory chain (v free volume, ν fractal dimension/Flory exponent), we find that the overlap concentration scales as

$$\phi^* \approx N^{1-3\nu}$$

with the number of segments in the chain. We therefore have

- a dilute solution for $\phi < \phi^*$
- a semidilute solution for $\phi^* < \phi \ll 1$
- a melt for $\phi = 1$

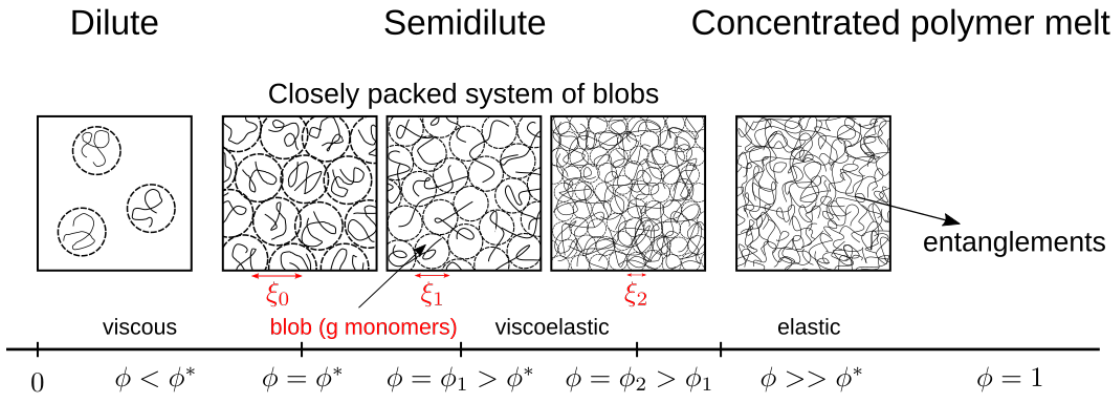


Figure 33.1: polymer states

Due to the overlap of the chains in the semidilute regime, there must be some length scale ξ (called correlation length), such that

- for $r < \xi$ the monomers are just surrounded by solvent mostly or same chain monomers
- for $r > \xi$ the monomer starts to see other chains

This correlation length helps us to subdivide the chain into blobs of a size ξ . This size is determined by the free volume and the chain size again via

$$\xi \approx b \left(\frac{\nu}{b^3} \right)^{2\nu-1} g^\nu$$

with g segments in the blob. The correlation volume is then given by $\phi = gb^3/\xi^3$ such that we can express the blob size as

$$\xi \approx b\phi^{-\frac{\nu}{3\nu-1}} \begin{cases} \phi^{-1} & \text{for } \nu = 1/2 \\ \phi^{-3/4} & \text{for } \nu = 3/5 \end{cases}$$

From this, the number of segments per blob follow to scale as

$$g \approx \phi^{-\frac{1}{3\nu-1}}$$

Since for $r > \xi$ the monomers sees other chains, excluded volume interactions are screened. Thus, a semidilute solution of polymer is like a “melt” of blobs. The blobs are the new segments of a random walk of the size

$$R \approx \xi \left(\frac{N}{g} \right)^{1/2} \approx bN^{1/2}\phi^{-\frac{2\nu-1}{6\nu-2}} \begin{cases} \phi^0 & \text{for } \nu = 1/2 \\ \phi^{-1/8} & \text{for } \nu = 3/5 \end{cases}$$

The polymer size therefore changes only very weakly with the concentration. To understand the dynamics of these polymer solutions, we now need the two models we have referred to already earlier

- **Zimm model** which was valid for a dilute solution where monomers are hydrodynamically coupled
- **Rouse model** which typically is valid in a melt in the absence of entanglements and neglects hydrodynamic coupling

Since there is a characteristic length scale in the structure of the semidilute solutions, the hydrodynamic coupling must also possess a characteristic length scale ξ_h such that

- when $r < \xi_h$ the segments are coupled by hydrodynamics and the Zimm model can be applied
- when $r > \xi_h$ the hydrodynamics is screened and the system is comparable to a melt of blobs

In fact, this hydrodynamic length scale is assumed to be the same as the structural length scale $\xi_h = \xi$ such that we have for the short length scales

Zimm dynamics

Here the chain sections feel the hydrodynamic coupling which leads to a maximum relaxation time

$$\tau_\xi \approx \frac{\eta_s \xi^3}{k_B T} \approx \frac{\eta_s b^3}{k_B T} \phi^{-\frac{3\nu}{3\nu-1}}$$

as already used earlier. Beyond this length scale the dynamics becomes Rouse like and we have the

Rouse dynamics

with the longest relaxation time being for the whole chain of blobs

$$\tau_{chain} \approx \tau_\xi \left(\frac{N}{g} \right)^2 \approx \frac{\eta_s b^3}{k_B T} N^2 \phi^{\frac{2-3\nu}{3\nu-1}}$$

scaling as

$$\tau_{chain} \approx \begin{cases} \phi & \text{for } \nu = 1/2 \\ \phi^{0.31} & \text{for } \nu = 3/5 \end{cases}$$

with the concentration of the chain ϕ . With this longest relaxation time for the chain we can now obtain the diffusion coefficient of a chain in the semi-dilute regime, which is

$$D \approx \frac{R^2}{\tau_{chain}} \approx \frac{k_B T}{\eta_s b N} \phi^{-\frac{1-\nu}{3\nu-1}} \approx D_z \left(\frac{\phi}{\phi^*} \right)^{-\frac{1-\nu}{3\nu-1}}$$

with $D_z = k_B T / \eta_s b N^\nu$. The diffusion coefficient therefore scales as

$$D \approx \begin{cases} \phi^0 & \text{for } \nu = 1/2 \\ \phi^{-0.54} & \text{for } \nu = 3/5 \end{cases}$$

This scaling for the real chain with an exponent of -0.54 is also found in the experiments.

insert experimental image

33.0.1 Stress Relaxation

The stress relaxation now follows the dynamics in the two regimes and can be obtained from the corresponding relaxation time spectrum as we have introduced that also already earlier.

For $\tau_0 < t < \tau_\xi$:

$$G(t) \approx \frac{k_B T}{b^3} \phi \left(\frac{t}{\tau_0} \right)^{-\frac{1}{3\nu}}$$

For $\tau_\xi < t < \tau_{chain}$:

$$G(t) \approx \frac{k_B T}{b^3} \phi^{\frac{3\nu}{3\nu-1}} \left(\frac{t}{\tau_0} \right)^{-\frac{1}{2}}$$

Part XXVI

Lecture 27

34 Liquid Crystals

$$Q_{\alpha\beta}(r) = \frac{1}{N} \sum_i \left(u_\alpha^{(i)} u_\beta^{(i)} - \frac{1}{3} \delta_{\alpha\beta} \right)$$

- $Q_{\alpha\beta} = Q_{\beta\alpha}$ since $u_\alpha^{(i)} u_\beta^{(i)} = u_\beta^{(i)} u_\alpha^{(i)}$
- $\text{Tr } Q_{\alpha\beta} = Q_{xx} + Q_{yy} + Q_{zz} =$
 $= \frac{1}{N} \sum_i \left[\left(u_x^{(i)} \right)^2 + \left(u_y^{(i)} \right)^2 + \left(u_z^{(i)} \right)^2 - 1 \right] = 0$

$$u_x = \sin \theta \cos \phi$$

$$\bullet \quad u_y = \sin \theta \sin \phi$$

$$u_z = \cos \theta$$

$$Q_{\alpha\beta} = \int_0^{2\pi} d\phi \int_0^\pi \sin \theta d\theta f(\theta, \phi) \left(u_\alpha u_\beta - \frac{1}{3} \delta_{\alpha\beta} \right)$$

$$\begin{aligned} Q_{zz} &= \frac{1}{4\pi} \int_0^{2\pi} d\phi \int_0^\pi \sin \theta d\theta \left(\cos^2 \theta - \frac{1}{3} \right) = \\ &= \frac{1}{6} (x^3 - x) \Big|_{-1}^1 = 0. \end{aligned}$$

prolate

$$\mathbf{Q}^{\text{prolate}} = \begin{pmatrix} -1/3 & 0 & 0 \\ 0 & -1/3 & 0 \\ 0 & 0 & 2/3 \end{pmatrix}$$

oblate

$$\mathbf{Q}^{\text{oblate}} = \begin{pmatrix} 1/6 & 0 & 0 \\ 0 & 1/6 & 0 \\ 0 & 0 & -1/3 \end{pmatrix}$$

$$Q_{\alpha \beta} = S \left(n_\alpha n_\beta - \frac{1}{3} \delta_{\alpha \beta} \right)$$

$$Q_{zz}=\frac{2}{3}S,\quad Q_{xx}=Q_{yy}=-\frac{1}{3}S$$

$$S=\int_0^{\pi}\left(1-\frac{3}{2}\sin^2\theta\right)f(\theta)\sin\theta d\theta$$

$$f(\theta)=\int_0^{2\pi} f(\theta,\phi) d\phi$$

Part XXVII

Lecture X

35 Forces and Interactions in Soft Matter

While we have discussed in the previous sections the thermodynamics of systems and the kinetics of phase transitions, we have made as few as possible assumptions on the interactions between the, i.e., liquid components of a mixture to highlight the importance of entropic and other effects. Now, we would like to have a close look at the possible types of interactions and their order of magnitude in soft matter systems. We may classify the interactions in the following way: - covalent interaction (chemical binding) - electrostatic (Coulomb) - dipolar (vdW) - dispersion (vdW) - fluctuation, depletion (entropic)

These interactions deliver the forces that hold soft matter together, even though the phases are characterized by *density*, *free energy* and *entropy*, but not by the forces.

Pairwise interaction energy – Before we go into further details, we may have a look at some general behavior again. Let us assume that the interaction energy between two atoms/molecules is given by

$$w(r) = -\frac{C}{r^n}$$

with C being an interaction specific constant, then the force between the two species at a distance r is given by

$$F(r) = -\frac{dw(r)}{dr} = -\frac{nC}{r^{n+1}}.$$

For a material, which has a number density and thus the total number $\rho 4\pi r^2 dr$ molecules in a shell between $r, r + dr$ around a molecule, we obtain the following total interaction energy per molecule (the standard chemical potential)

$$\mu^0 = \int_{\sigma}^L w(r) \rho 4\pi r^2 dr = \frac{-4\pi C \rho}{(n-3)\sigma^{n-3}} \left[1 - \left(\frac{\sigma}{L}\right)^{n-3} \right].$$

The total interaction energy, and thus also the property of the system will thus depend on the size L of the system, except we assume $n > 3$ and $L \gg \sigma$, where σ is the size of the molecule. This states nothing else, that long range interactions may yield system dependent properties or bulk properties do not depend on the volume size only if objects become small. Obviously Coulomb interactions, or dipolar interactions may not satisfy the above assumptions. We

can find out some general rule about the cohesive energy of molecule with its neighbors in a liquid, when comparing the molar gas and molar liquid volumes. A typical gas molar volume is $22.400 \text{ cm}^3/\text{mol}$, while this is only $20 \text{ cm}^3/\text{mol}$ for a liquid. If liquid and gas coexist at a certain temperature T , then the chemical potential of gas and liquid have to be the same, i.e.,

$$\mu_{\text{gas}}^0 + k_B T \ln(X_{\text{gas}}) = \mu_{\text{liq}}^0 + k_B T \ln(X_{\text{liq}})$$

or

$$\mu_{\text{gas}}^0 - \mu_{\text{liq}}^0 \approx -\mu_{\text{liq}}^0 = k_B T \ln \left(\frac{X_{\text{liq}}}{X_{\text{gas}}} \right) \approx 7k_B T$$

assuming that there is essentially no cohesive energy in the gas phase. At the vaporization temperature, the energy required to release one mole of molecules from its cohesion with its neighboring molecules to the gas phase is thus

$$U_{\text{vap}} = -N_A \mu_{\text{liq}}^0 = 7N_A k_B T.$$

This allows us to estimate the latent heat of vaporization

$$\Delta H_{\text{vap}} = U_{\text{vap}} + pV \approx 7RT_B + RT_B$$

According to that, the ratio of latent heat of vaporization and boiling temperature is $\frac{\Delta H_{\text{vap}}}{T_B} \approx 8R \approx 80 \frac{\text{J}}{\text{K mol}}$ per mole, or $9k_B T$ per molecule. If we assume that each molecule has on average 6 neighbors in a liquid, than we obtain a value of $\frac{3}{2}k_B T$ as energy molecular pair. The about rough rule is called **Troutons rule** and gives only a very rough estimate of the cohesive energy, as it completely neglects the details of the interactions. However, it demonstrates why the thermal energy is important in soft matter.

35.0.1 Coulomb forces, charge–charge interactions

The simplest form but at the same time, also one of the most important types of interaction is the electrostatic interaction, e.g., of simple charges. This type of interaction is important not only due to its relevance in biological systems, but the electrostatic interaction is in principle the only one delivering a long range repulsive forces.

Charge–charge interactions Charge–charge interactions are mediated by the electric fields. Assume that we have a charge Q_1 that creates an electric field

$$E_1 = \frac{Q_1}{4\pi\epsilon_0\epsilon r^2}.$$

We neglect the vectorial character of the electric field to avoid further complications. The electric field is creating a force on a second charge Q_2

$$F(r) = Q_2 E_1 = \frac{Q_1 Q_2}{4\pi\epsilon_0\epsilon r^2}.$$

In this charge assembly at a distance r an energy is stored, which is the potential energy of assembling these two charges from infinity. The free energy of the two charges thus reads

$$w(r) = \int_{\infty}^r -F(r) dr = - \int_{\infty}^r \frac{Q_1 Q_2}{4\pi\epsilon_0\epsilon r^2} dr = \frac{Q_1 Q_2}{4\pi\epsilon_0\epsilon r}.$$

If we evaluate this energy, for example, for a sodium and a chlorine ion at a distance of $r = 0.276$ nm we find a free energy of interaction of $w = -8.4 \cdot 10^{-19}$ J, which corresponds to about $200 k_B T$ at 300 K temperature. This is on the same order of magnitude than covalent interactions. It requires about 3 nN to break this bond and the long range character of electrostatics becomes clear when evaluating the distance at which this interaction becomes comparable to $k_B T(r = 56$ nm). This is only considering a pair of ions. In a NaCl crystal, multiple neighbors contribute to the interaction energy of one sodium ion with its surrounding. One sodium ion has 6 Cl⁻ neighbors at a distance of $r = 0.276$ nm, 12 Na⁺ neighbors at $\sqrt{2}r$, and further 8 Cl⁻ neighbors at $\sqrt{3}r$ and so on. We have to sum up all the interaction energies for the total cohesive energy of the sodium ion in the crystal

$$\mu^0 = -\frac{e^2}{4\pi\epsilon_0 r} \left[6 - \frac{12}{\sqrt{2}} + \frac{8}{\sqrt{3}} - \frac{6}{2} + \dots \right] = -1.748 \frac{e^2}{4\pi\epsilon_0 r}.$$

The factor in front of the Coulomb term (the one in the square brackets) is termed Madelung constant and is known from solid state physics. It is characteristic for specific lattice types such as a simple cubic lattice in this case. Note that the cohesive energy of one sodium ion therefore is about $350 k_B T$ and is thus much larger than the thermal energy keeping the NaCl crystal stable. Yet it can be dissolved in water very easily.

Born energy of solvation The Born energy of solvation calculates the free energy of assembling a charge inside a dielectric medium of dielectric constant ϵ . Let us shortly reconsider the free energy

$$\begin{aligned} dU &= dQ + dW \\ dU &= TdS + dW \\ dW &= dU - TdS \end{aligned}$$

which leads to

$$dF = dU - TdS = dW.$$

Therefore, the free energy change is related to the energy to assemble a charge

$$\Delta F = \frac{\epsilon\epsilon_0}{2} \int_V E^2 dV.$$

To find the free energy we, therefore, integrate the square of the electric field over the volume (this is actually the same as adding tiny charge elements against previously assembled parts of the charge). According to that, the free energy of a charge in a medium with dielectric constant ϵ is

$$\mu^0 = \frac{z^2 e^2}{8\pi\epsilon\epsilon_0 a}$$

if the charge has a radius a . If we look now at the difference of assembling the charge in vacuum (with $\epsilon = 1$) and in a medium with ϵ , we find the following difference in the chemical potential (free energy)

$$\Delta\mu^0 = \frac{z^2 e^2}{8\pi\epsilon_0 a} \left(\frac{1}{\epsilon} - 1 \right) = -\frac{28z^2}{a} \left(\frac{1}{\epsilon} - 1 \right).$$

This is the Born free energy of solvation of a single ion. The molar free energy is then obtained by multiplication with the Avogadro number N_A

$$\Delta G = N_A \Delta\mu^0 = -\frac{69z^2}{a} \left(\frac{1}{\epsilon} - 1 \right)$$

$$\Delta\mu^0 \approx \frac{e^2}{4\pi\epsilon_0\epsilon(a_+ + a_-)}$$

The mole fraction that is dissolved in water is then found by the Boltzmann factor

$$X_s = e^{-\frac{\Delta\mu^0}{k_B T}}$$

which is a measure for the solubility of the ions. Inserting the formula for the chemical potential delivers the proportionality $X_s \propto \exp(-\text{const}/\epsilon)$. This dependency on the dielectric constant of the solvent is indeed observed in the experiment, even though this is only a trend and there are solvents with marked deviations. The reason for that is essentially that the theory just

assumes 1) continuous changes in the interactions, despite the fact that there is a near order and 2) that additional interactions like hydrogen bonds exist.

Interactions involving polar molecules

Many molecules exhibit dipole or even higher moments due to the fact that the charges are not evenly distributed over the molecular structure. Some of the atoms exhibit a stronger tendency to accept charges than others. This is typically measured by electronegativity and provides an idea of whether atoms rather donate or accept a charge when binding to other atoms. While homo-atomic bonds therefore do not have dipole moments heteroatomic bonds do (see table).

Bond	Dipole moment
C-C	0
C-N	0.22

The dipole moment of a molecule is measured by the displacement of two charges $\pm q$ from each other

$$\vec{u} = q\vec{l}.$$

Its direction is from the negative to the positive side. It creates an electric field that is given by

$$\vec{E} = \frac{3(\vec{u} \cdot \hat{r})\hat{r} - \vec{u}}{4\pi\epsilon_0\epsilon r^3}.$$

The dipole self-energy, i.e., the energy to create the dipole in a solvent is given by

$$\mu^0 = \frac{1}{4\pi\epsilon_0\epsilon} \left[\frac{q^2}{2a} + \frac{q^2}{2a} - \frac{q^2}{l} \right].$$

If $l = 2a$ this yields $\mu^0 = q^2/(8\pi\epsilon_0\epsilon a) = u^2/(4\pi\epsilon_0\epsilon l^3)$ and thus yields a similar dependence of the chemical potential on the dielectric function ϵ as in the case of a single charge. The result is a similar dependence of the solubility on the dielectric function.

Ion–dipole interaction

The interaction energy of a dipole with a charge can be calculated by

$$w(r) = -\frac{qQ}{4\pi\epsilon_0\epsilon} \left[\frac{1}{r - \frac{1}{2}l \cos(\theta)} - \frac{1}{r + \frac{1}{2}l \cos(\theta)} \right] = -\frac{qQ}{4\pi\epsilon_0\epsilon r^2} \cos(\theta) = -uE \cos(\theta),$$

{#eqn:energy}

where the last two equations are assuming that the distance between both objects r is much larger than the extent of the dipole l itself. From equation @ref(eqn:energy), we see that the interaction can be either attractive or repulsive. An angle $\theta = 0^\circ$ results in an attractive interaction, while $\theta = 180^\circ$ yields repulsive interaction. Using a single chargee(Na⁺ ion) and a dipole of $u = 1.85 \text{ D}$ (water molecule) results in an interaction energy of about $39 k_{\text{B}}T$. Ions align and bind polar molecules like water, for example. For arbitrary polar molecules this is called solvation, while for water the term hydration is used. The strength of the hydration can effect the mobility of ions in solution as it makes them effectively charges and is of interest, for example, for the study of ion transport through ion channels, as this requires stripping the hydration shell.

Dipole–dipole interactions

The interactions of two dipoles (u_1, u_2) in the solution can be also calculated following the above scheme

$$w(r, \theta_1, \theta_2, \phi) = -\frac{u_1 u_2}{4\pi\epsilon_0\epsilon r^3} [2 \cos(\theta_1) \cos(\theta_2) - \sin(\theta_1) \sin(\theta_2) \cos(\phi)]. \quad (35.1)$$

Also in this case the dipole–dipole interaction yields an orientation dependence with either repulsive or attractive interactions. The figure below shows the distance dependence for two configurations where the dipoles are arranged parallel but either along the connecting line or perpendicular to it.

Rotating dipoles, angle averaged Potential

35.0.2 van der Waals interactions

35.0.3 Depletion Forces

Depletion force between two plates

Depletion force between two spheres – To describe the depletion interaction between two spheres (radius R) in a solution of smaller spheres (radius $\sigma/2$), we may use the same approach of assuming an isotropic osmotic pressure of the smaller spheres. The smaller spheres can actually not approach a spherical shell of thickness $\sigma/2$ around the larger spheres or a total volume of $4\pi(R + \sigma/2)^3/3$. The pressure on the large spheres has no consequences except in the case where the two spheres approach closer than $r \leq 2(R + \sigma/2) = 2R_d$. In this case the two excluded volumes around each sphere overlap to a lens-like volume. Due to this overall, the forces which create the pressure on the spherical surface up to an angle θ_0 are unbalanced from the other side of the surface (see image) and result in an attractive interaction.

The total force is then calculated from the osmotic pressure times the surface area of the spherical cap by just taking into account the force components along the connecting line. This the read

$$F(r) = -2nk_B T \pi (R + \sigma/2)^2 \int_0^{\theta_0} \sin(\theta) \cos(\theta) d\theta$$

resulting in

$$F(r) = -nk_B T \pi (R_d)^2 \left[1 + \left(\frac{r}{2R_d} \right)^2 \right]$$

which is valid if the distance between the centers of the large spheres is $r < 2(R + \sigma/2)$. For $r \geq 2(R + \sigma/2)$ there is no depletion of the smaller spheres from the region between the larger spheres and the force is zero, i.e., $F(r) = 0$.

General description – A more general description of the depletion interaction may be obtained based on our introduction into statistical physics at the beginning of the course. There we stated that the probability of finding a system in a stet of energy E is

$$p(E) = \frac{e^{-\beta E}}{Z},$$

where $\beta = 1/k_B T$ and the partition function Z is

$$Z = \sum_i e^{-\beta E_i}$$

for a system with a discrete number of states numbered by the indexi. For a single particle with a continuous number of energies the energy may look like

$$E = \frac{p^2}{2m} + U(q),$$

where q is some general coordinate. The classical partition function for a system of N particles is then

$$Z = \frac{1}{N!h^{3N}} \int d^3p^N \int d^3q^N \exp \left(-\beta \left[\sum_i \frac{p_i^2}{2m} + U(q^N) \right] \right),$$

where we use the notation p^N and q^N to denote the whole set of variables. The prefactor is appropriate for indistinguishable particles and the phase space normalization factor h (Planck's constant) for every pair of p and q . Since there is no issue of the non-commutation of positions and momenta we can perform the momentum integrals exactly, yielding

$$Z = \frac{1}{N!} \frac{1}{\Lambda^{3N}} \int d^3 q^N \exp(-\beta U(q^N)),$$

where the thermal de Broglie wavelength Σ is

$$\Lambda = \frac{h}{\sqrt{2\pi m k_B T}}.$$

In the case of two interacting large spheres in a solution of small spheres with all spheres being hard spheres, the integration over the exponential function yields

$$Z = \frac{V_A^N}{N! \Lambda^{3N}}$$

with V_A being the volume available to the small spheres, i.e., $V_A = V - V_E$ for $r < D + d$ and $V_A = V - V'_E$ for $r > D + d$ with $V_E = \pi(D + d)^3/3$ and $V'_E = V_E - (2\pi l^2)/3[3(D+d)/2 - l]$ and $l = (D+d)/2 - r/2$. The calculation then yields the free energy

$$G = -k_B T \ln(Z) = -k_B T \ln \left(\frac{V_A^N}{N! \Lambda^{3N}} \right).$$

Using Stirling's formula again this can be turned into

$$G = G_{\text{ideal}} - N k_B \ln \left(\frac{V_A}{V} \right).$$

The ideal contribution to the free energy is constant with the separation of the large sphere, so it does not contribute to the depletion force. It reads

$$G_{\text{ideal}} = -N k_B T \left(1 - \ln \left(\frac{N \Lambda^3}{V} \right) \right).$$

The distance-dependent part still contains the logarithm which we can approximate by

$$\ln \left(\frac{V_A}{V} \right) \approx -\frac{V_E}{V} + \frac{\pi}{6V} (D + d - r)^2 (D + d + r/2)$$

for the case of the overlapping excluded volumes. This gives then finally a force

$$F = -\frac{N}{4V}k_B T \pi (D + d - r)(D + d + r)$$

for $r < d + D$. For all other distances of the two centers of the spheres, the depletion force is zero.

36 Flows and Transport in Liquids

36.0.1 Diffusion and Brownian Motion

- particles are moving in soft materials all the time → thermal fluctuations, Brownian motion
- in addition flows, friction → hydrodynamics, mechanical properties
- elasticity, rheology

a) Continuity

flux $\vec{j} = \rho \vec{n}$ Consider a volume surrounded by a surface S flow through surface:

$$\int_S \vec{j} \cdot \vec{n} dS \quad (36.1)$$

material in volume, e.g., particle density:

$$\int_V f dV \frac{d}{dt} \int f dV = \int_V \frac{df}{dt} dV \quad (36.2)$$

conservation of matter:

$$\int_S \vec{j} \cdot \vec{n} dS = - \int_V \frac{df}{dt} dV \quad (36.3)$$

Due to Gauss's law

$$\int_S \vec{j} \cdot \vec{n} dS = \int_V \operatorname{div} \vec{j} dV \quad (36.4)$$

and thus

$$\int_V \left(\frac{df}{dt} + \vec{\nabla} \cdot \vec{j} \right) dV = 0 \quad (36.5)$$

This yields the continuity equation

$$\frac{df}{dt} + \vec{\nabla} \cdot \vec{j} = 0. \quad (36.6)$$

For the density $n = f$, $\vec{j} = n \cdot \vec{v}$

$$\frac{\partial n}{\partial t} + \vec{\nabla} \cdot (n \vec{v}) = 0$$

for $n = \text{const.}$ it is $\vec{\nabla} \cdot \vec{V} = 0$, $\vec{\nabla} \cdot \vec{j} = 0$ incompressible

Diffusion

$N(x)$, $N(x + \Delta x)$, $0.5 \cdot N(x)$ to the right, $0.5 \cdot N(x + \Delta x)$ to the left net number $-1/2(N(x + \Delta x) - N(x))$ thus

$$j = \frac{-\frac{1}{2}(N(x + \Delta x) - N(x))}{A \tau}$$

With the number density of particles $n(x) \equiv N(x) / A \tau$ one obtains

$$j = -\frac{1}{2} \frac{n(x + \Delta x) A \Delta x - n(x) A \Delta x}{A \tau} = -\frac{1}{2} \frac{(\Delta x)^2}{\tau} \frac{n(x + \Delta x) - n(x)}{\Delta x} \quad (36.7)$$

For $\Delta x \rightarrow 0$ it is

$$j = -D \frac{\partial n}{\partial x} \quad (36.8)$$

with $D = (\Delta x)^2 / 2\tau$. In 3d, this is

$$\vec{j} = -D \vec{\nabla} n \quad (36.9)$$

This is Fick's first law (1855, Fick, empirical). flux from a gradient is due to fluctuations in the velocity, diffusion max. entropy to vanish the gradient

Combination with the continuity equation

in 1d:

$$\frac{dn}{dt} = -\frac{\partial j}{\partial x} \frac{\partial j}{\partial x} = -D \frac{\partial^2 n}{\partial x^2} = -\frac{\partial n}{\partial t} \quad (36.10)$$

Fick's second law:

$$\frac{\partial n}{\partial t} = D \nabla^2 n \quad (36.11)$$

$n f$ could be different quantities

flux	transport property	gradient
particles	diffusivity	particle density
charge	conductivity	potential
liquid	permeability	pressure
momentum	viscosity	momentum density
energy	heat conductivity	temperature

36.0.2 Smoluchowski-diffusion in an external potential

Smoluchowski-diffusion in an external potential

$$F = -\frac{dU}{dx} \quad (36.12)$$

velocity of the particle

$$v = -\frac{1}{\xi} \frac{\partial U}{\partial x} \quad (36.13)$$

ξ is the friction coefficient. For a sphere $\xi = 6\pi\eta R$. flux due to flow with $v, j_v = nv$

$$j = -D \frac{\partial n}{\partial x} - \frac{n}{\xi} \frac{\partial U}{\partial x} \quad (36.14)$$

in steady state $j = 0$ and

$$n = n_0 \exp\left(-\frac{U}{k_B T}\right) \quad 0 = -D \frac{d}{dx} \left(n_0 \exp\left(-\frac{U}{k_B T}\right) \right) - \frac{1}{\xi} \frac{dU}{dx} n_0 \exp\left(-\frac{U}{k_B T}\right) + \frac{D}{k_B T} \frac{dU}{dx} n_0 \exp\left(-\frac{U}{k_B T}\right) = -\frac{1}{\xi} \frac{dU}{dx} n_0 \exp\left(-\frac{U}{k_B T}\right) \quad (36.15)$$

With the diffusion coefficient $D = k_B T / \xi$ one has

$$j = -\frac{1}{\xi} \left(k_B T \frac{\partial n}{\partial x} + n \frac{\partial U}{\partial x} \right) = -\frac{1}{\xi} n \frac{\partial}{\partial x} (k_B T \cdot \ln(n) + U), \quad (36.16)$$

since

$$\frac{d}{dx} \ln(n(x)) = \frac{1}{n} \frac{du}{dx} \quad (36.17)$$

and thus

$$\frac{du}{dx} = n \cdot \ln(n). \quad (36.18)$$

Here, $k_B T \cdot \ln n + U$ is the chemical potential.

$$j = -\frac{1}{\xi} n \frac{\partial \mu}{\partial x} \quad (36.19)$$

The chemical potential is constant in equilibrium, extend potential for ?? $\mu = \text{const}$.

$$U = -k_B T \ln(n(x)) + \text{const.} \quad (36.20)$$

With Fick's second law

$$\frac{\partial n}{\partial t} = -\frac{\partial j}{\partial x} = \frac{1}{\xi} \frac{\partial}{\partial x} \left(k_B T \frac{\partial U}{\partial x} + n \frac{\partial U}{\partial x} \right) \frac{\partial n}{\partial t} = \vec{\nabla} \left(D \vec{\nabla} n + \frac{\vec{F}_{\text{ext}}}{\xi} n \right) \quad (36.21)$$

This is the Smoluchowski equation. More general: Fokker—Planck equation

$$\frac{\partial p(x, t)}{\partial t} = -\frac{\partial}{\partial x} \left[\frac{1}{\xi(x, t)} p(x, t) \right] + \frac{\partial^2}{\partial x^2} [D(x, t)p(x, t)] \quad (36.22)$$

$D = k_B T / \xi$ gives a connection between thermal position fluctuations and viscous friction (fluctuation—dissipation) $D = k_B T / 6\pi\eta R$ for sphere, e.g., protein: $R \equiv 3 \text{ nm}$, $D = 100 \text{ m}^2/\text{s}$, $\eta = 0.7 \text{ mPas}$. Solution of the diffusion equation

$$\frac{\partial}{\partial t} n(\vec{r}, t | \vec{r}_0, t_0) = D \nabla^2 n(\vec{r}, t | \vec{r}_0, t_0) \quad (36.23)$$

initial condition $n(\vec{r}, t \rightarrow t_0 | \vec{r}_0, t_0) = \delta(\vec{r} - \vec{r}_0)$

solution:

$$n(\vec{r}, t | \vec{r}_0, t_0) = \frac{1}{(4\pi D(t - t_0))^{\frac{3}{2}}} \exp \left(-\frac{(\vec{r} - \vec{r}_0)^2}{4D(t - t_0)} \right) \quad (36.24)$$

This is the Green's function for the diffusion equation for the given boundary conditions. It propagates the initial conditions through the ??? space. solution for any initial condition can be found

$$n(\vec{r}, t \rightarrow 0) = f(\vec{r}_0) n(\vec{r}, t) = \int d^3 r_0 n(\vec{r}, t | \vec{r}_0, t_0) f(\vec{r}_0) \quad (36.25)$$

properties: e.g., particle initially at x_0 in 1D, initial distribution $\delta(x_0)$

$$\langle x \rangle = \int_{-\infty}^{\infty} x \frac{1}{\sqrt{4\pi D(t-t_0)}} \exp\left(-\frac{(x-x_0)^2}{4D(t-t_0)}\right) dx \quad (36.26)$$

$\langle x \rangle = x_0$, does not depend on time, particles do not change their initial position on average

$$\langle (x - x_0)^2 \rangle = \int_{-\infty}^{\infty} (x - x_0)^2 n(x, t) dx \quad (36.27)$$

$$\langle (x - x_0)^2 \rangle = 2Dt \text{ in 1D}$$

$$\langle r^2 \rangle = 6Dt \text{ in 3D}$$

mean squared displacement = width of the probability distribution increases linearly in time

$\langle r^2 \rangle = 2dDt$, d is the dimension in more complex diffusion scenarios: $\langle r^2 \rangle = cDt^\alpha$ with $\alpha < 1$ for subdiffusion and $\alpha > 1$ for superdiffusion Application: fluorescence recovery after photobleaching Molecules are photophysically/chemically bleached in a spatial region with high intensity layer. Diffusion causes fluorescent molecules to diffuse in again, ?? bleached come out The “hole” is filling up and the dynamics is determined by the diffusion coefficient. initial distribution after the bleach is $w(x, t_0)$

$$n(x, t_0) = \Theta(-a - x) + \Theta(x - a) \quad (36.28)$$

Heaviside step function

$$\Theta(x) = \begin{cases} 0 & x < 0 \\ 1 & x \geq 0 \end{cases} \quad (36.29)$$

$$\frac{\partial n(x, t)}{\partial t} = D \frac{\partial^2}{\partial x^2} n(x, t) \quad (36.30)$$

boundary condition $\lim_{x \rightarrow \infty} n(x, t) = 0$ solution with Green's function

$$n(x, t | x_0, t_0) = \frac{1}{\sqrt{4\pi D(t-t_0)}} \exp\left(-\frac{(x-x_0)^2}{4D(t-t_0)}\right) \quad (36.31)$$

$$\begin{aligned}
n(x, t) &= \int_{-\infty}^{\infty} dx_0 n(x, t|x_0, t_0) [\Theta(-a - x) + \Theta(x - a)] \\
&= \int_{-\infty}^{-a} dx_0 \frac{1}{\sqrt{4\pi D(t - t_0)}} \exp\left(-\frac{(x - x_0)^2}{4D(t - t_0)}\right) + \int_a^{\infty} dx_0 \frac{1}{\sqrt{4\pi D(t - t_0)}} \exp\left(-\frac{(x - x_0)^2}{4D(t - t_0)}\right)
\end{aligned} \tag{36.32}$$

$$\operatorname{erf}(x) = \frac{1}{\sqrt{\pi}} \int_{-x}^x \exp(-t^2) dt = \frac{2}{\sqrt{\pi}} \int_0^x \exp(-t^2) dt \tag{36.33}$$

solution:

$$n(x, t) = 1 + \frac{1}{2} \left(\operatorname{erf}\left[\frac{x + a}{2\sqrt{D(t - t_0)}}\right] - \operatorname{erf}\left[\frac{x - a}{2\sqrt{D(t - t_0)}}\right] \right) N(t, t_0) = c_0 \int_{-a}^a dx n(x, t) \tag{36.34}$$

if there is a concentration of c_0 fluorescent molecules

$$N(t, t_0) = \frac{\sqrt{D(t - t_0)}}{a\sqrt{\pi}} \left(\exp\left[-\frac{a^2}{D(t - t_0)}\right] - 1 \right) + 1 + \operatorname{erf}\left[\frac{a}{\sqrt{D(t - t_0)}}\right] \tag{36.35}$$

Extension

Diffusion can also occur on a spherical surface ?? to a point ?? surface is ?? doing rotational diffusion

$$\frac{\partial n(\vec{r}, t|\vec{r}_0, t_0)}{\partial t} = D \nabla^2 n(\vec{r}, t|\vec{r}_0, t_0) \tag{36.36}$$

with $|\vec{r}_0| = |\vec{r}| = 1$ so no radial ??

$$\frac{\partial n(\Omega, t|\Omega_0, t_0)}{\partial t} = D_{\text{rot}} \left[\frac{1}{\sin \vartheta} \frac{\partial}{\partial \vartheta} \left(\sin \vartheta \frac{\partial}{\partial \vartheta} \right) + \frac{1}{\sin^2 \vartheta} \frac{\partial^2}{\partial \varphi^2} \right] n(\Omega, t, \Omega_0, t_0) \tag{36.37}$$

The eigenfunctions of the operator on the right are spherical harmonics and the solution may be expressed in terms of Y_l^m .

$$Y_l^m = N \exp(im\varphi) P_l^m(\cos \theta) p(\Omega, t|\Omega_0, t_0) = \sum_{l=0}^{\infty} \sum_{m=-l}^{+l} A_{lm}(t, \Omega_0, t_0) Y_l^m(\Omega) \tag{36.38}$$

insert into diffusion equation

$$\sum_{l=0}^{\infty} \sum_{m=-l}^{+l} \frac{\partial A_{lm}}{\partial t} Y_l^m = - \sum_{l=0}^{\infty} \sum_{m=-l}^l l(l+1) \frac{1}{\tau_R} A_{lm} Y_l^m \quad (36.39)$$

with orthonormality

$$\frac{\partial A_{lm}}{\partial t} = -l(l+1) \tau_R^{-1} A_{lm} A_{lm}(t|\Omega_0, t_0) = \exp\left(-l(l+1) \frac{t-t_0}{\tau_R}\right) a_{lm}(\Omega_0) p(\Omega, t|\Omega_0, t_0) = \sum_{l=0}^{\infty} \sum_{m=-l}^l \exp\left(-l(l+1) \frac{t-t_0}{\tau_R}\right) a_{lm}(\Omega_0) Y_l^m(\Omega) \quad (36.40)$$

a_{lm} from $p(\Omega, t_0|\Omega_0, t_0) = \delta(\Omega - \Omega_0)$ and

$$\delta(\Omega - \Omega_0) = \sum_{l=0}^{\infty} \sum_{m=-l}^l Y_l^m(\Omega_0) Y_l^m(\Omega) \quad (36.41)$$

$$a_{lm}(\Omega_0) = Y_{lm}^*(\Omega_0) p(\Omega, t|\Omega_0, t_0) = \sum_{l=0}^{\infty} \sum_{m=-l}^l \exp\left(-\frac{l(l+1)}{\tau_R}\right) Y_{lm}^*(\Omega_0) Y_{lm}(\Omega) \quad (36.42)$$

for example projection on z-direction (NMR/diel.)

$$P_3 = P_0 \cos(\theta), l = 1 \langle P_3 \rangle = \frac{1}{4\pi} \int d\Omega P_0 \cos(\theta) \rightarrow 0 \quad (36.43)$$

?? correlation:

$$\begin{aligned} \langle P_3(t) P_3^*(t_0) \rangle &= P_0^2 \int d\Omega \int d\Omega_0 \cos(\theta) \cos(\theta_0) p(\Omega, t|\Omega_0, t_0) p_0(\Omega_0) \\ &= \frac{4\pi}{3} P_0^2 \sum_{m=-l}^l \exp\left(-l(l+1) \frac{t-t_0}{\tau_r}\right) |C_{10lm}|^2 \end{aligned} \quad (36.44)$$

$$C_{10lm} = \int d\Omega Y_{10}^*(\Omega) Y_{lm}(\Omega) = \delta_{l1} \delta_{m0} \langle P_3(t) P_3^*(t_0) \rangle = \frac{4\pi}{3} P_0^2 \exp\left(-\frac{2(t-t_0)}{\tau_r}\right) \quad (36.45)$$

application in dielectric spectroscopy or NMR for example, $A_l m \rightarrow C_l m \exp(-t/\tau_l)$ rotational diffusion of Janus particles

$$P_3 = P_0 \cos(\vartheta) \quad (36.46)$$

$l = 1$, Legendre projection on z-axis, NMR, DS

$$\langle P_3(t)P_3^*(t_0) \rangle = \frac{4\pi}{3} P_0^2 \exp\left(-\frac{2(t-t_0)}{\tau_r}\right) \tau_l = \frac{D_1}{D_{\text{rot}} l(l+1)} n(\vartheta, \varphi, t) = \sum_{l=0}^{\infty} \sum_{m=-l}^l C_{lm} Y_l^m(\vartheta, \varphi) \exp\left(-\frac{t}{\tau_l}\right) \quad (36.47)$$

quadratic angular displacement

$$\langle |\hat{u}(t) - \hat{u}_0|^2 \rangle = 2 - 2\langle \cos(\theta) \rangle \quad (36.48)$$

\hat{u} is a unit vector

$$\frac{d}{dt} p(\theta, t) = D_r \nabla^2 p(\theta, t) 2\pi \int_0^\pi p(\theta, t) \sin(\theta) d\theta = 1 \langle \cos(\theta) \rangle = 2\pi \int_0^\pi p \sin(\theta) \cos(\theta) d\theta \quad (36.49)$$

$$\begin{aligned} \frac{d}{dt} \langle \cos(\theta) \rangle &= 2\pi \int_0^\pi \frac{\partial p}{\partial t} \sin(\theta) \cos(\theta) d\theta \\ &= 2\pi D_r \int_0^\pi \frac{1}{\sin(\theta)} \left[\frac{\partial}{\partial t} \left(\sin(\theta) \frac{\partial p}{\partial \theta} \right) \right] \sin(\theta) \cos(\theta) d\theta \end{aligned} \quad (36.50)$$

36.0.3 Hydrodynamics

37